UNIVERSIDADE DE LISBOA, FACULDADE DE FARMÁCIA

SEARCH FOR BIOACTIVE COMPOUNDS FROM MEDICINAL PLANTS USED AS ANTIMALARIALS

The study of Momordica balsamina L.

Cátia Beatriz Almeida Ramalhete

DOUTORAMENTO EM FARMÁCIA

(QUÍMICA FARMACÊUTICA E TERAPÊUTICA)

2010

Universidade de Lisboa, Faculdade de Farmácia

SEARCH FOR BIOACTIVE COMPOUNDS FROM MEDICINAL PLANTS USED AS ANTIMALARIALS

The study of Momordica balsamina L.

Cátia Beatriz Almeida Ramalhete

Tese orientada por:

Orientador: Professora Doutora Maria José Umbelino Ferreira

Co-orientador: Professor Doutor Virgílio Estólio do Rosário

Dissertação apresentada à Faculdade de Farmácia, Universidade de Lisboa, com vista à obtenção do grau de Doutor em Farmácia (Química Farmacêutica e Terapêutica)

2010

This thesis was conducted at the Medicinal Chemistry Group of the Research Institute for Medicines and Pharmaceutical Sciences (iMed.UL), Faculdade de Farmácia, Universidade de Lisboa. The financial support was provided by Fundação para a Ciência e a Tecnologia (SFH/BD/22321/2005).

Dedicated to my Parents

Francisco and Otelinda

ABSTRACT

The main goal of this dissertation was to search for new antimalarial compounds from plants used in traditional medicine. For the purpose, the claimed antimalarial properties of fifty eight extracts from fifteen plants, used in traditional medicine against malaria and/or fever, mainly in Mozambique, were evaluated against the 3D7 *Plasmodium falciparum* strain. The highest activity was shown by *Momordica balsamina* L. (Cucurbitaceae), which was selected for further studies. Bioassay-guided fractionation of the methanol extract of *M. balsamina* led to the isolation of fourteen new cucurbitane-type triterpenoids, along with five known cucurbitacins and one megastigmane-type *nor*-isoprenoid. In order to obtain a higher homologous series of compounds required for structure-activity relationships, karavilagenin C and balsaminol F were esterified using several acylating agents, yielding twenty new derivatives, named karavoates A - R, triacetylbalsaminol F and tribenzoylbalsaminol F, respectively. The chemical structures of compounds were deduced from their physical and spectroscopic data (IR, UV, MS, HRMS, ^{1}H and ^{13}C NMR and 2D NMR experiments - COSY, HMQC, HMBC and NOESY experiments). Some of the new compounds feature unusual oxidation patterns, reported for the first time in cucurbitane triterpenoids from plant sources, such as at C-29 (balsaminagenins A, B, balsaminols A - D, and balsaminapentaol) and C-12 (cucurbalsaminols A, B, and C). Moreover, balsaminapentaol has a 23,24-diol system coupled with an exocyclic double bond in the side chain, never found before in cucurbitane-type triterpenoids.

Compounds were evaluated for their antimalarial activity against the chloroquine-sensitive (3D7) and chloroquine-resistant (Dd2) *P. falciparum* strains. Most of them displayed antimalarial activity. Among the natural compounds, the glycoside derivatives and karavilagenin E revealed the highest activity against both strains of *P. falciparum* tested, displaying $IC_{50} < 9$ μM. A strong increase in the activity was found for the majority of alkanoyl ester derivatives of karavilagenin C and balsaminol F. Triacetylbalsaminol F, and karavoates B, D, and E displayed IC_{50} values similar to those obtained with chloroquine, particularly against the resistant strain ($IC_{50} \leq 0.6$ μM). However, a significant decrease of activity was observed when both positions, C-3 and C-23 of the parent compounds, were esterified with aroyl or cinnamoyl chlorides, highlighting the influence of molecular esteric effects on the antimalarial activity. Moreover, the substitution pattern of ring B seems also to play an important role in the antiplasmodial activity of compounds. The preliminary toxicity toward human cells of compounds was also investigated on breast cancer cell line, and the selectivity index was calculated.

Compounds were also evaluated for their ability as MDR reversers in both cancer cells and resistant bacteria strains. In cancer cells, the anti-MDR activity was carried out in human *MDR1* gene-transfected mouse lymphoma cells, by flow cytometry. Most of the compounds exhibited a strong activity when compared with the one of the positive control, verapamil, in a non-toxic concentration. Karavilagenin C showed the strongest activity, at a low concentration. Structure-activity relationships will be discussed. The presence of free hydroxyl groups at C-3 and C-23 seems to be crucial for the reversing activity. Moreover, in the checkerboard model of combination chemotherapy, the interaction between doxorubicin and most of the compounds synergistically enhanced the effect of the anticancer drug. Some of the results obtained by flow cytometry were corroborated by using a real-time fluorometric method that employs ethidium bromide. Some of the compounds were also able to inhibit, significantly, the efflux of ethidium bromide by methicillin-resistant *Staphylococcus aureus* highly resistant to oxacillin (MRSA COL_{oxa}), and *Enterococcus faecalis* ATCC29212 strains. A good correlation between MRSA COL_{oxa} reversal activity and the topological polar surface area of compounds was found.

Keywords: *Momordica balsamina*; Cucurbitane-type triterpenoids; Antimalarial activity; *Plasmodium falciparum*; Multidrug resistance; P-glycoprotein; MDR modulators.

RESUMO

Esta dissertação teve como principal objectivo o isolamento de compostos com actividade antimalárica a partir de plantas usadas na medicina tradicional. Nesse sentido, foram avaliadas as propriedades antimaláricas de cinquenta e oito extractos provenientes de quinze plantas, usadas na sua maioria em Moçambique para o tratamento da malaria e/ou febres associadas, usando a estirpe sensível 3D7 de *Plasmodium falciparum*. A espécie Africana *Momordica balsamina* L. (Cucurbitaceae) demonstrou a melhor actividade, sendo escolhida para estudos posteriores.

Do fraccionamento bio-guiado do extracto metanólico da espécie *M. balsamina* resultaram catorze novos compostos com o esqueleto do cucurbitano, juntamente com cinco compostos conhecidos com o mesmo esqueleto e um *nor*-isoprenóide com o esqueleto do megastigmano. De modo a obter um número de compostos que possibilitasse a realização de estudos de relação estrutura-actividade, os compostos karavilagenina C e balsaminol F, isolados em maiores quantidades da planta, foram esterificados. Do balsaminol F, por acilação em C-3/C-7/C-23 com anidrido acético ou cloreto de benzoílo, obtiveram-se os derivados triacilados, designados por triacetilbalsaminol F e tribenzoilbalsaminol F, respectivamente. Do mesmo modo, a karavilagenina C foi esterificada com vários anidridos/cloretos de ácido, originando dezoito novos compostos (monoésteres em C-23 e diésteres em C-3/C-23) designados de karavoatos A - R.

Os compostos foram isolados utilizando técnicas cromatográficas (cromatografia em coluna, cromatografia preparativa em camada fina e cromatografia líquida de alta resolução). A caracterização estrutural foi estabelecida com base nas suas características físicas e dados espectroscópicos (IV, UV, MS, HRMS e RMN unidimensional- ^{1}H, ^{13}C, DEPT e bidimensional- COSY, HMQC, HMBC e NOESY).

Alguns dos compostos apresentaram particularidades estruturais identificadas pela primeira vez em compostos com o esqueleto do cucurbitano, isolados a partir de plantas, nomeadamente no padrão de oxidação em C-29 (balsaminageninas A, B; balsaminois A - D e balsaminapentaol) e em C-12 (cucurbalsaminois A - C). O composto balsaminapentaol apresentou igualmente, na cadeia lateral, um sistema 23,24-diol *vicinal* a uma dupla ligação exocíclica, identificado pela primeira vez em compostos com o esqueleto do cucurbitano.

A actividade antimalárica dos compostos obtidos foi avaliada, *in vitro*, em dois clones de *P. falciparum*, um sensível 3D7 e um resistente Dd2. A maioria dos compostos demonstrou actividade antimalárica. Dos compostos isolados, as melhores actividades foram observadas para os derivados glicosilados e karavilagenina E ($IC_{50} < 9$ μM). No que diz respeito aos ésteres, verificou-se um aumento pronunciado da actividade antimalárica para a maioria dos ésteres alifáticos da karavilagenina C e triacetilbalsaminol F. Com efeito, os derivados triacetilbalsaminol F e karavoatos B, D e E demonstraram uma actividade antimalárica ($IC_{50} \leq 0.6$ μM) comparável à obtida com a

cloroquina, principalmente na estirpe resistente de *P. falciparum*. Contudo, verificou-se que, quando ambas as posições C-3 e C-23 da karavilagenina C são substituídas por grupos aroílo ou cinamoílo, é observada uma diminuição significativa da actividade antimalárica. O mesmo sucedeu no caso do derivado tribenzoílado do balsaminol F. Estes resultados evidenciam a importância de efeitos estéreos na actividade antimalárica deste grupo de compostos. É também de salientar que o padrão de substituição no anel B parece influenciar a actividade. Foi realizado um ensaio preliminar de citotoxicidade em células humanas tumorais de mama (MCF-7). Os valores de IC_{50} obtidos neste ensaio permitiram o cálculo do índice de selectividade (razão entre a citotoxicidade e a actividade antimalárica) para todos os compostos.

Os compostos foram também avaliados no que diz respeito à sua capacidade como reversores de multirresistência em células cancerígenas. Alguns compostos foram também testados em estirpes bacterianas resistentes.

Deste modo, estudou-se a actividade anti-MDR em células de linfoma de rato transfectadas com o gene humano *MDR1*. Neste ensaio avaliou-se, por citometria de fluxo, a acumulação intracelular de rodamina-123, um substrato fluorescente análogo da doxorrubicina. A maioria dos compostos, numa concentração não citotóxica, demonstrou uma potente capacidade inibitória da actividade da glicoproteína-P quando comparada com a do verapamil, usado como controlo positivo. Dos compostos avaliados, a karavilagenina C demonstrou ser o mais activo, quando testado em concentrações baixas. O estudo realizado permitiu retirar algumas conclusões sobre a relação estrutura-actividade dos compostos. É de salientar a importância da presença de grupos hidroxilo livres nas posições C-3 e C-23 para a actividade. A lipofilia e a presença de grupos funcionais com capacidade para estabelecer ligações de hidrogénio foram também evidenciadas como características fundamentais para a actividade reversora da glicoproteína-P. Foram também avaliados os efeitos antiproliferativos *in vitro* de alguns destes triterpenos em combinação com a doxorrubicina. Todos os compostos, à excepção da balsaminagenina C que mostrou um efeito aditivo, demonstraram um efeito sinérgico sobre a actividade da doxorrubicina. Alguns dos resultados de actividade anti-MDR obtidos no ensaio com a rodamina-123 foram confirmados, utilizando um método fluorimétrico em tempo real que analisa a acumulação de brometo de etídio, um substrato fluorescente.

A avaliação de alguns compostos como modeladores de resistência de estirpes bacterianas Gram-positivas e Gram-negativas foi igualmente realizada. Dos compostos testados, o balsaminol E, o balsaminosido A e a karavilagenina C inibiram significativamente o efluxo de brometo de etídio na estirpe de *Staphylococcus aureus* resistente à meticilina e adaptada à oxaciclina (MRSA COL_{oxa}) e na de *Enterococcus faecalis* ATCC29212. É de salientar a correlação obtida entre a actividade reversora da estirpe MRSA COL_{oxa} e a área de superfície polar dos compostos testados.

Palavras-chave: *Momordica balsamina*; Triterpenos; Cucurbitano; Actividade antimalárica; *Plasmodium falciparum*, Multirresistência, Glicoproteína-P; Modeladores de multirresistência.

ACKNOWLEDGMENTS

I would like to express my gratitude to Professor Maria José U. Ferreira, my supervisor, for the support, scientific guidance and enthusiasm always demonstrated. I am very grateful for her careful revision of all my work, and first of all because she always believes that I can do everything! I also would like to say how thankful I am for her friendship.

I would like to thank Professor Virgílio do Rosário, my co-supervisor, from Centro de Malária e outras Doenças Tropicais (CMDT), Instituto de Higiene e Medicina Tropical de Lisboa, for all the knowledge transmitted. I would also like to thank his teamwork, particularly Dr. Dinora Lopes, who was critical in the performing of the antimalarial assays.

I also wish to thank Professor József Molnár, at the University of Szeged, Hungary, for his friendship, always welcoming me as a member of his laboratory and making possible all the activity measurements, namely in the assay of MDR-reversing activity by flow cytometry, and also the cytotoxicity assay on human breast cancer cells. I would also like to thank his teamwork, especially Julianna Serly, who made my life in the laboratory much easier, helping me in all the translations needed, among other things.
I would like also to thank Anikó Váradi for her precious technical contribution with the tissue cultures, and Imre Ocsovszki for the flow cytometry measurements, during my stay in Hungary.

My thanks go also to Professor Leonard Amaral from Instituto de Higiene e Medicina Tropical de Lisboa, and all his teamwork, particularly Gabriella Spengler and Ana Martins for all the collaboration and knowledge transmitted during the studies performed in the Rotor-Gene (ethidium bromide accumulation assays).

I would like also to thank Dr. Silva Mulhovo from Mozambique, for the collection and identification of some plants.

My thanks also go to Dr. Teresa Vasconcelos from Instituto Superior de Agronomia, Universidade de Lisboa, Portugal, for the taxonomic work on some plants material, as well as the Head of Jardim Garcia da Horta, where some species were collected.

I would like to thank Dr. Catarina Arruda, from the Portuguese Embassy in Mozambique, as well as the Portuguese Office of International Affairs for plant transport.

I would like to thank Professor José Ascenso from Instituto Superior Técnico, for his help getting NMR data from a particular compound.

I would like to thank the ungraduated students for their collaboration in the phytochemical study of *Momordica balsamina*.

I also wish to thank Dr. Isabel Joglar, from Faculdade de Farmácia, Universidade de Lisboa, for her support and technical help during some equipment problems with HPLC, and also for her help with ESIMS spectra analyses.

I would like to thank Professor Rui Moreira as Coordinator of Medicinal Chemistry Group, where the majority of this work was carried out.

I wish to express my gratefulness to Francisco Carvalho and Helena Brito for their technical support in the laboratory and their friendship.

I would like to thank my friends and colleagues from the laboratory, particularly Patricia Rijo, Ana Sofia Newton, Rita Capela, João Lavrado, Tiago Rodrigues, Nuno Candeias, and Paulo Glória for their friendship and all their technical and emotional support in the bad and good moments.

I wish also to thank all the professors from the Medicial Chemistry Group, namely Dr. Noélia Duarte, Dr. Ana Margarida Madureira and Dr. Emilia Valente for their friendship and principally for the help and knowledge transmitted during all my work. I would like to reaffirm my appreciation to Dr. Noélia Duarte, my big teacher at the laboratory and who was always there when I needed.

I deeply appreciate and thank my friends Maria João Catalão and Ana Martins who, like me, are finishing their dissertations. I wish to thank all their patience to listen and support me in all the critical moments. A big, big THANK YOU!!!

Finally, I wish to express my profound gratitude to my family for the support they provided me, in particular, to my parents, Francisco and Otelinda, my sister Ana, and her husband Sérgio. Without all their love, encouragement, assistance and patience, I would not have finished this long and arduous task.

LIST OF PUBLICATIONS

Most of the results described in this dissertation were presented in various scientific meetings, published in peer-reviewed journals or sent for publication.

A. Papers

1. **Ramalhete, C.**, Molnar, J., Mulhovo, S., Rosário, V.E. and Ferreira, M.J.U., 2009. New potent P-glycoprotein modulators with the cucurbitane scaffold and their synergistic interaction with doxorubicin on resistant cancer cells. Bioorganic & Medicinal Chemistry 17, 6942-6951.

2. **Ramalhete, C.**, Mansoor, T.A., Mulhovo, S., Molnar, J. and Ferreira, M.J.U., 2009. Cucurbitane-type triterpenoids from the African plant *Momordica balsamina*. Journal of Natural Products 72, 2009-2013.

3. Spengler, G., **Ramalhete, C.**, Martins, M., Martins, A., Serly, J., Viveiros, M., Molnar, J., Duarte, N., Mulhovo, S., Ferreira, M.J.U. and Amaral, L., 2009. Evaluation of cucurbitane-type triterpenoids from *Momordica balsamina* on P-glycoprotein (ABCB1) by flow cytometry and real-time fluorometry. Anticancer Research 29, 3989-3993.

4. **Ramalhete, C.**, Lopes, D., Mulhovo, S., Rosário, V. and Ferreira, M.J.U., 2010. New antimalarials with a triterpenic scaffold from *Momordica balsamina*. Bioorganic & Medicinal Chemistry. Doi: 10.1016/j.bmc.2010.05.054.

5. **Ramalhete, C.**, Lopes, D., Mulhovo, S., Rosário, V. and Ferreira, M.J.U., 2010. Karavilagenin C derivatives as antimalarials. *Submitted*

B. Proceedings

1. **Ramalhete, C.**, Lopes, D., Mulhovo, S., Rosário, V. E., Ferreira, M. J. U. 2008. Antimalarial activity of some plants traditionally used in Mozambique. In: Workshop Plantas Medicinais e práticas fitoterapêuticas nos trópicos, IICT/CCCM, Lisbon, Portugal. *Available in: http://www2.iict.pt/archive/doc/C_Ramalhete_wrkshp_plts_medic.pdf.*

C. Communications in Scientific Meetings

1. **Ramalhete, C.**, Duarte, A., Mulhovo, S., Ferreira, M.J.U. Screening for antimicrobial activity of plants used in the traditional medicine. October 2006, Medicinal Chemistry in the 21st Century, Lisbon, Portugal. (Poster)

2. **Ramalhete, C.**, Lopes, D., Mulhovo, S., Rosário, V., Ferreira, M.J.U., 2008. Screening for antimalarial activity of crude extracts from African medicinal plants. 7th Joint Meeting of AFERP, ASP, GA, PSE & SIF, 3rd- 8th August 2008, Athens, Greece. Planta Medica 74, 1140-1140. (Poster)

3. **Ramalhete, C.**, Lopes, D., Mulhovo, S., Rosário, V., Ferreira, M.J.U. Actividade antimalárica de plantas usadas na medicina tradicional Moçambicana, Workshop Plantas Medicinais e Práticas Fitoterapêuticas nos Trópicos, IICT/CCCM, 29th-31st October 2008, Lisbon, Portugal. (Oral communication)

4. **Ramalhete, C.**, Lopes, D., Mulhovo, S., Rosário, V. E., Ferreira, M.J.U. Medicinal plants as a source of antiplasmodial compounds**,** First National Meeting on Medicinal Chemistry of "Building Scientific Bridges", 13th -15th November 2008, Porto, Portugal. (Poster)

5. **Ramalhete, C.**, Spengler, G., Serly, J., Amaral, L., Molnar, J., Mulhovo, S., Ferreira, M.J.U., 2009. Efflux modulators from *Momordica balsamina* L. in multidrug resistant bacterial strains. 57th International Congress and Annual Meeting of the Society for Medicinal-Plant-Research and Natural Product Research**,** 16-20th August 2009, Geneva, Switzerland. Planta Medica 75, 896-896. (Oral communication)

6. **Ramalhete, C.**, Duarte, N., Capucha, V., Molnar, J., Mulhovo, S., Rosario, V., Ferreira, M.J.U., 2009. Inhibition of P-glycoprotein activity by cucurbitane-type triterpenes and their interaction with doxorubicin on resistant cancer cells. 57th International Congress and Annual Meeting of the Society for Medicinal-Plant-Research and Natural Product Research**,** 16-20th August 2009, Geneva, Switzerland. Planta Medica 75, 976-976. (Poster)

7. **Ramalhete, C.**, Spengler, G., Serly, J., Duarte, N., Viveiros, M., Amaral, L., Molnar, J., Mulhovo, S., Ferreira, M.J.U. New efflux pump inhibitors for Gram positive bacteria strains and cancer cells from an African medicinal plant**.** 2º Congresso Iberoamericano de Fitoterapia, Lisboa, Portugal, 15th-18th de Outubro 2009**.** Revista de Fitoterapia 9 (S1), 92-92. (Poster)

ABBREVIATIONS AND SYMBOLS

Ac	Acetyl
ABC	ATP Binding Cassette
ABCB	ATP Binding Cassette Superfamily type B
ADP	Adenosine diphosphate
ATCC	American Type Culture Collection
ATP	Adenosine triphosphate
ax	Axial
br s	Broad singlet
br d	Broad doublet
BRCP	Breast cancer resistance protein
Bu	Butanoyl
Bz	Benzoyl
c	Concentration
^{13}C NMR	^{13}C Nuclear Magnetic Resonance
calcd.	Calculated
$CDCl_3$	Deuterated chloroform
CD_3COCD_3	Deuterated acetone
Cin	Cinnamoyl
CIP	Ciprofloxacin
COSY	COrrelation SpectrometrY
d	Doublet
dd	Doublet of doublets
ddd	Doublet of doublet of doublets
DEPT	Distortionless Enhancement by Polarization Transfer
DMAPP	Dimethylallyl diphosphate
DMSO	Dimethylsulphoxide
DNA	Deoxyribonucleic acid
DXP	Deoxy-xylulose phosphate pathway
EB	Ethidium bromide
EDTA	Ethylenediaminetetraacetic acid
EIMS	Electronic Impact Mass Spectrometry
EP	Efflux pump
EPI	Efflux pump inhibitor

eq	Equatorial
ESIMS	ElectroSpray Mass Spectrometry
et al,	And others
EtOAc	Ethyl acetate
eV	Electron volt
FAR	Fluorescence activity ratio
FIX	Fractional inhibitory concentration index
FL	Fluorescence activity
FPP	Farnesyl diphosphate
FSC	Forward scatter
GPP	Geranyl diphosphate
GGPP	Geranyl geranyl diphosphate
^{1}H NMR	^{1}H Nuclear Magnetic Resonance
HIV	Human Immunodeficiency Virus
HMBC	Heteronuclear Multiple Bond Correlation
HMQC	Heteronuclear Multiple Quantum Correlation
HPLC	High Performance Liquid Chromatography
HR-EIMS	High Resolution Electronic Impact Mass Spectrometry
HR-ESITOFMS	High Resolution Electrospray Ionization Time-Of-Flight Mass Spectrometry
HR-CIMS	High Resolution Chemical Ionization Mass Spectrometry
IC_{50}	Sample concentration causing 50% inhibition
IPP	Isopentenyl diphosphate
IR	InfraRed
J	Coupling constant
$^{2}J_{C\text{-}H}$	C-H coupling through two bonds (*geminal* coupling)
$^{3}J_{C\text{-}H}$	C-H coupling through three bonds (*vicinal* coupling)
log *P*	Octanol/water partition coefficient
m	Multiplet
m.p.	Melting point
m/z	Ratio of mass to charge
max	Maximum
MDR	Multidrug resistance
Me	Methyl
Me_2CO	Acetone
MeCN	Acetonitrile

MeOD	Deuterated methanol
MeOH	Methanol
MEP	Methylerythritol phosphate pathway
MFS	Major facilitator superfamily
MIC	Minimum inhibitory concentration
*m*RNA	Messenger ribonucleic acid
MRP	Multidrug resistance associated protein
MRSA	Methicillin resistant *Staphylococcus aureus*
MTT	3-(4,5-dimethylthiazol-2-yl)-2,5-diphenyltetrazolium bromide
MVA	Mevalonoic acid
MW	Molecular weight
n.d.	Not described or not determined
NADH	Nicotinamide adenine nucleotide
NBD	Nucleotide binding domain
NMR	Nuclear Magnetic Resonance
NO	Nitric oxide
NOE	Nuclear Overhauser Effect
NOESY	Nuclear Overhauser Enhancement Spectroscopy
OD	Optical density
PAR	Parental cells
PBS	Phosphate buffer saline
Pgh-1	P-glycoprotein homologue
P-gp	P-glycoprotein
PMF	Proton motive force
ppm	Parts per million
QSAR	Quantitative structure-activity relationship
Rel. int.	Relative intensity
R_f	Retention fraction
RFF	Relative final fluorescence
RNA	Ribonucleic acid
RND	Resistance nodulation division
rpm	Rotations per minute
RPMI	Roswell Park Memorial Institute medium
R_t	Retention time
s	Singlet

SAR	Structure-activity relationship
SDS	Sodium dodecyl sulfate
SSC	Side scatter
Suc	Succinoyl
t	Triplet
td	Triplet of doublets
TLC	Thin Layer Chromatography
TMD	Transmembrane domain
TMS	Tetramethylsilane
UV	Ultraviolet
WHO	World Health Organization
δ	Chemical shift
δ_C	Carbon chemical shift
δ_H	Proton chemical shift
$\Delta^{x,y}$	Unsaturated bond between carbons X and Y
λ_{max}	Maximum wave length
$[\alpha]_D^{26}$	Specific rotation
ν_{max}	Maximum wave number
$[M]^+$	Molecular ion

GENERAL INDEX

Page

ABSTRACT i
RESUMO iii
ACKNOWLEDGMENTS v
LIST OF PUBLICATIONS vii
ABBREVIATIONS AND SYMBOLS ix
GENERAL INDEX xiii
INDEX OF FIGURES xvi
INDEX OF SCHEMES xviii
INDEX OF TABLES xix

CHAPTER 1 1

Introduction

1. *MOMORDICA* GENUS 5
   1.1. General considerations 5
   1.2. *Momordica balsamina* L. 6
   1.3. Terpenoids: biogenetic generalities 8
      1.2.1. Cucurbitane-type triterpenoids 12
   1.4. Literature review 15
   1.5. Biological activity of cucurbitane-type triterpenoids 26
2. MALARIA 28
   2.1. Life cycle of the parasite 30
   2.2. Currently available antimalarials 32
      2.2.1. Quinolines 32
      2.2.2. Antifolates 34
      2.2.3. Artemisinin and its derivatives 35
   2.3. Natural products as antimalarials 37
3. MULTIDRUG RESISTANCE 38
   3.1. Multidrug resistance in cancer cells 39
      3.3.1. The human P-glycoprotein 40
      3.1.2. Other ABC-transporters 43
   3.2. Multidrug resistance in malaria parasite 43
   3.3. Multidrug resistance in bacteria 45
   3.4. Multidrug resistance reversal agents 47
      3.4.1. Modulators in cancer cells 47
      3.4.2. Malaria parasite modulators 51
      3.4.3. Bacterial modulators 52

CHAPTER 2 53

Results and Discussion: Phytochemical study of Momordica balsamina

1. STRUCTURAL ELUCIDATION OF CUCURBITANE-TYPE TRITERPENOIDS 55
   1.1. Balsaminapentaol [cucurbita-5,25-diene-3β,7β,23(*R*),24(*R*),29-pentaol] 57
   1.2. Balsaminagenin A [cucurbita-5,23(*E*)-diene-3β,7β,25,29-tetraol] 61
   1.3. Balsaminagenin B [25-methoxycucurbita-5,23(*E*)-diene-3β,7β,29-triol] 64
   1.4. Balsaminol A [cucurbita-5,24-diene-3β,7β,23(*R*),29-tetraol] 65

1.5. Balsaminol B [7β-methoxycucurbita-5,24-diene-3β,23(*R*),29-triol] 67
1.6. Balsaminol C [cucurbita-5,24-diene-7,23-dione-3β,29-diol] 69
1.7. Balsaminol D [25,26,27-*trinor*-cucurbit-5-ene-7,23-dione-3β,29-diol] 72
1.8. Balsaminol E [cucurbita-5,24-dien-7-one-3β,23(*R*)-diol] 73
1.9. Balsaminol F [cucurbita-5,24-diene-3β,7β,23(*R*)-triol] 75
1.10. Acylated derivatives of balsaminol F 76
1.10.1. Triacetylbalsaminol F 76
1.10.2. Tribenzoylbalsaminol F 77
1.11. Karavilagenin C [7β-methoxycucurbita-5,24-diene-3β,23(*R*)-diol] 80
1.12. Acylated derivatives of karavilagenin C 81
1.12.1. Alkanoyl esters 81
1.12.1. Aroyl and cinnamoyl esters 86
1.13. Cucurbalsaminol A [cucurbita-5,23(*E*)-diene-3β,7β,12β,25-tetraol] 94
1.14. Cucurbalsaminol B [7β-methoxycucurbita-5,23(*E*)-diene-3β,12β,25-triol] 95
1.15. Cucurbalsaminol C [7β-methoxycucurbita-5,24-diene-3β,12β,23(*R*)-triol] 96
1.16. Balsaminoside A [25-methoxycucurbita-5,23(*E*)-dien-3β-ol-7-O-β-D-allopyranoside] 99
1.17. Balsaminoside B [cucurbita-5,24-diene-3β,23(*R*)-diol-7-O-β-D-allopyranoside] ... 100
1.18. Balsaminoside C [cucurbita-5,24-diene-3β,23(*R*)-diol-7-O-β-D-glucopyranoside]. 101
1.19. Kuguaglycoside A [7β-methoxycucurbita-5,24-dien-3β-ol-23-O-β-D-glucopyranoside] 104
1.20. Balsaminagenin C [cucurbita-5,23(*E*)-diene-3β,7β,25-triol] 106
1.21. Karavilagenin E [5β,19β-epoxycucurbita-6,24-diene-3β,23(*R*)-diol] 107
1.22. (+)-Dehydrovomifoliol 109

CHAPTER 3 113

Results and Discussion: Biological studies

1. ANTIMALARIAL ACTIVITY 115
1.1. Screening for antimalarial activity of selected plants 115
1.2. Antimalarial activity of *Momordica balsamina* constituents 116
1.2.1. Cucurbitane-type triterpenoids activity 117
1.2.2. Acyl derivatives activity 119
1.2.3. Cytotoxic activity of isolated compounds and derivatives 125
1.2.4. Structure-activity relationships 125
2. REVERSAL OF MULTIDRUG RESISTANCE IN CANCER CELLS 129
2.1. Evaluation of the inhibition of P-gp transport activity by flow cytometry 129
2.2. Evaluation of the inhibition of P-gp transport activity by real-time fluorometry 148
3. EVALUATION OF THE INHIBITION OF BACTERIAL EFFLUX PUMPS 151

CHAPTER 4 157

Experimental Section

Phytochemical study 159

1. GENERAL EXPERIMENTAL PROCEDURES 159
2. SELECTION OF PLANTS 160
2.1. Preparation of extracts 160
3. STUDY OF *MOMORDICA BALSAMINA* 163
3.1. Extraction and isolation 163
3.2. Study of fraction M2 163
3.2.1. Derivatization of karavilagenin C 170

3.2.2. Derivatization of balsaminol F 189
3.3. Study of fraction M3 191
3.3.1. Study of fraction M3C 192
3.3.2. Study of fraction M3D 194
3.3.3. Study of fraction M3E 195
3.3.4. Study of fraction M3G 195
3.3.5. Study of fraction M3H 197
3.4. Study of fraction M4 200
3.4.1. Study of fraction M4C 201
3.4.2. Study of fraction M4D 203
3.5. Study of fraction M5 208
3.5.1. Study of fraction M5B 209
3.5.2. Study of fraction M5C 211
3.6. Study of fraction M6 212
3.6.1. Study of fraction M6B 214

Biological assays 217

1. ANTIMALARIAL ACTIVITY 217
1.1. *In vitro* culture of *Plasmodium falciparum* 217
1.2. Antimalarial activity assay 217
2. CYTOTOXIC ACTIVITY 218
2.1. Cell culture, medium, and growth conditions 218
2.2. Cytotoxicity assay 218
3. REVERSAL OF MULTIDRUG RESISTANCE ON L5178 MOUSE T-LYMPHOMA CELLS 219
3.1. Cell culture, medium and growth conditions 219
3.2. Antiproliferative assay 220
3.3. Rhodamine-123 accumulation assay 220
3.4. Ethidium bromide accumulation assay 221
3.5. Checkerboard microplate method 222
4. REVERSAL OF MULTIDRUG RESISTANCE ON BACTERIAL STRAINS 222
4.1. Bacterial strains 222
4.2. Growth conditions 223
4.3. Determination of minimal inhibitory concentration (MIC) values 223
4.4. Ethidium bromide accumulation assay 224

CHAPTER 5 225

Conclusion

References 235

INDEX OF FIGURES

Figure 1.1. The most important Cucurbitaceae crops: **A.** Watermelon (*Citrullus lanatus*), **B.** Cucumber (*Cucumis sativus*) and **C.** Melon (*Cucumis melo*)..... 5

Figure 1.2. A. Flower of *M. balsamina*; **B.** Immature fruits of *M. balsamina*; **C.** Mature fruits of *M. balsamina*; **D.** *M. charantia*; **E.** Fruits of *M. grosvenorii*; **F.** *M. foetida*. 7

Figure 1.3. Chemical structures of some cucurbitacins. 26

Figure 1.4. Malaria transmission map (Adapted from: WHO, 2008). 28

Figure 1.5. A. *P. falciparum* (1. immature form- trophozoite; 2. mature form- schizont with merozoites); **B.** *P. vivax* (1. immature form- trophozoite; 2. mature form- schizont with merozoites); **C.** *Anopheles* sp..... 29

Figure 1.6. Life cycle of *Plasmodium falciparum* (Adapted from: Wirth, 2002). 31

Figure 1.7. Haem detoxification mechanism (Adapted from: Rathore, 2006)..... 32

Figure 1.8. Chemical structures of quinoline-containing antimalarial drugs (chloroquine, quinine, mefloquine, amodiaquine, halofantrine and primaquine) and atovaquone. 34

Figure 1.9. Chemical structures of antifolate compounds..... 35

Figure 1.10. Chemical structures of artemisinin and derivatives. 36

Figure 1.11. The most accepted mode of action of artemisinins against the malarial parasite. - Inhibition of sarco-endoplasmic reticulum Ca^{2+}-ATPase (SERCA) of the parasite, and consequently its growth (Adapted from: Gershenzon and Dudareva, 2007; Ridley, 2003). 37

Figure 1.12. Biochemical mechanisms that cause drug resistance in cancer cells (Adapted from: Gottesman et al., 2002). 39

Figure 1.13. Structures of ABC transporters known to confer drug resistance to cancer cells (Adapted from: Gottesman et al, 2002). 40

Figure 1.14. Chemical structures of some substrates of P-gp. 41

Figure 1.15. Models to explain the mechanism of drug efflux by P-gp (Adapted from: Varma et al., 2003)..... 42

Figure 1.16. The Pgh-1 protein of *P. falciparum*. Polymorphic amino acids are indicated (Adapted from: Duraisingh and Cowman, 2005)..... 44

Figure 1.17. Some examples of the first generation P-gp inhibitors..... 48

Figure 2.1. Key ^{1}H-^{1}H COSY and HMBC correlations of compound **36**. 59

Figure 2.2. Key NOESY correlations of compound **36**. 60

Figure 2.3. Energy-minimized 3D structure of compound **36**. 61

Figure 2.4. Main ^{1}H-^{1}H COSY and HMBC correlations of compound **34**. 62

Figure 2.5. Energy-minimized 3D structure of compound **35**. 66

Figure 2.6. ^{1}H-spin systems (A - D) of compound **29** assigned by the HMQC and COSY experiments (▬) and their connection by the principal heteronuclear $^{2}J_{C\text{-}H}$ and $^{3}J_{C\text{-}H}$ correlations displayed in the HMBC spectrum (→). 71

Figure 2.7. Isomerization of the side chain of karavoate G (**11**). 88

Figure 2.8. Energy-minimized 3D structure of compound **32**. 95

Figure 2.9. Main HMBC correlations of compound **4**. 108

Figure 2.10. Key COSY and HMBC correlations of compound **25**. 111

Figure 3.1. Chemical structure of rhodamine-123 (**1**) and verapamil (**2**). 130

Figure 3.2. Histogram of the amount of rhodamine accumulated in MDR (black) and parental (red) cells and in MDR cell line treated with 1 μM (blue) and 2 μM (green) of karavilagenin C (**1**). 138

Figure 3.3. Effects of balsaminol A (**35**), (concentrations between 0 and 83.3 μM), in combination with doxorubicin on human *MDR1* gene-transfected mouse lymphoma cell line. 142

Figure 3.4. Effects of balsaminols B (**27**), C (**29**) and E (**26**), (concentrations between 0 and 83.3 μM), in combination with doxorubicin on human *MDR1* gene-transfected mouse lymphoma cell line. 143

Figure 3.5. Effects of balsaminol F (**3**) and balsaminagenin B (**33**), (concentrations between 0 and 41.6 μM), and balsaminagenin A (**34**), (concentrations between 0 and 83.3 μM), in combination with doxorubicin on human *MDR1* gene-transfected mouse lymphoma cell line. 144

Figure 3.6. Effect of balsaminagenin C (**2**), and balsaminosides A (**40**), B (**38**), (concentrations between 0 and 83.3 μM), in combination with doxorubicin on human *MDR1* gene-transfected mouse lymphoma cell line. 145

Figure 3.7. Effects of cucurbalsaminols A (**32**), B (**28**) and C (**30**), (concentrations between 0 and 83.3 μM), in combination with doxorubicin on human *MDR1* gene-transfected mouse lymphoma cell line. 146

Figure 3.8. Effects of karavilagenin C (**1**) (concentrations between 0 and 41.6 μM), and karavilagenin E (**4**) and karavoate A (**5**), (concentrations between 0 and 83.3 μM), in

combination with doxorubicin on human *MDR1* gene-transfected mouse lymphoma cell line..... 147

Figure 3.9. Effects of kuguaglycoside A (**37**), (concentrations between 0 and 83.3 μM), in combination with doxorubicin on human *MDR1* gene-transfected mouse lymphoma cell line..... 148

Figure 3.10. Accumulation of EB (1 μg/mL) by MDR mouse limphoma cells in the presence of balsaminagenin A (**34**) and karavilagenin C (**1**). ◆ DMSO control, ▲ 3 μM, • 30 μM. 150

Figure 3.11. Effects of compounds **1**, **3**, and **40** on the accumulation of EB (1 μg/ mL) by MRSA COL_{OXA}. ◆ DMSO control, ▲ 3 μM, • 30 μM. 153

Figure 3.12. Effects of compounds **3**, **33**, and **35** on the accumulation of EB (0.5 μg/ mL) by *E. faecalis*. ◆ DMSO control, ▲ 3 μM, • 30 μM. 154

Figure 3.13. Relative final fluorescence (RFF), express as log (1/RFF), in MRSA COL_{OXA} strain versus the topological polar surface area, expressed as log (TPSA). 156

INDEX OF SCHEMES

Scheme 1.1. Schematic illustration of isoprenoid biosynthetic pathways (Adapted from: Kirby and Keasling, 2009). 9

Scheme 1.2. Suggested pathways for the biosynthesis of monoterpenes, sesquiterpenes, diterpenes, triterpenes and tetraterpenes (Adapted from: Roberts, 2007)..... 10

Scheme 1.3. Biosynthesis of 2,3-squalene epoxide (Adapted from: Rowe, 1989). 13

Scheme 1.4. Biosynthesis of cucurbitacins (Adapted from: Shibuya et al., 2004). 14

Scheme 2.1. Alkanoyl esters of karavilagenin C (**1**). 82

Scheme 2.2. Aroyl and cinnamoyl esters of karavilagenin C (**1**). 87

Scheme 3.1. Screening for antimalarial activity: extraction methodology..... 162

Scheme 3.2. Study of *Momordica balsamina*: extraction, fractionation procedures, and compounds isolated from fraction M2. 165

Scheme 3.3. Acylation of karavilagenin C (**1**) with alkanoyl anhydrides. 170

Scheme 3.4. Acylation of karavilagenin C (**1**) with different benzoyl chlorides. 177

Scheme 3.5. Study of fraction M3. 192

Scheme 3.6. Study of fraction M4C. 202

Scheme 3.7. Study of fraction M4D. 204

INDEX OF TABLES

Table 1.1. New cucurbitane-type triterpenoids isolated from *Momordica* species. 16

Table 1.2. Other compounds isolated from *Momordica* species. 25

Table 2.1. Compounds isolated from *Momordica balsamina*. 55

Table 2.2. Derivatives obtained from balsaminol F (**3**) and karavilagenin C (**1**). 56

Table 2.3. NMR data of balsaminapentaol (**36**), (MeOD, ^{1}H 500 MHz, ^{13}C 100.61 MHz; δ in ppm, J in Hz). 58

Table 2.4. NMR data of balsaminagenin A (**34**), (MeOD, ^{1}H 400 MHz, ^{13}C 100.61 MHz; δ in ppm, J in Hz). 63

Table 2.5. NMR data of balsaminagenin B (**33**), (MeOD, ^{1}H 400 MHz, ^{13}C 100.61 MHz; δ in ppm, J in Hz). 65

Table 2.6. NMR data of balsaminols A and B, (MeOD, ^{1}H 400 MHz, ^{13}C 100.61 MHz; δ in ppm, J in Hz). 68

Table 2.7. NMR data of balsaminol C (**29**), (MeOD, ^{1}H 400 MHz, ^{13}C 100.61 MHz; δ in ppm, J in Hz). 70

Table 2.8. NMR data of balsaminol D (**31**), (MeOD, ^{1}H 400 MHz, ^{13}C 100.61 MHz; δ in ppm, J in Hz). 73

Table 2.9. NMR data of balsaminol E (**26**), (MeOD, ^{1}H 400 MHz, ^{13}C 100.61 MHz; δ in ppm, J in Hz). 74

Table 2.10. NMR data of balsaminol F (**3**), (MeOD, ^{1}H 400 MHz, ^{13}C 100.61 MHz; δ in ppm, J in Hz). 76

Table 2.11. ^{1}H NMR data of balsaminol F (**3**), triacetylbalsaminol F (**23**) and tribenzoylbalsaminol F (**24**) (400 MHz, MeOD^{a}, CD_3COCD_3^{b}, δ in ppm, J in Hz). 78

Table 2.12. ^{13}C NMR data of balsaminol F (**3**), triacetylbalsaminol F (**23**) and tribenzoylbalsaminol F (**24**) (100.61 MHz, MeOD^{a}, CD_3COCD_3^{b}, δ in ppm). 79

Table 2.13. NMR data of karavilagenin C (**1**), ($CDCl_3$, ^1H 400 MHz, ^{13}C 100.61 MHz; δ in ppm, *J* in Hz)..... 81

Table 2.14. ^1H NMR data of karavilagenin C (**1**) and karavoates A - F (**5** - **10**), ($CDCl_3$ [a], CD_3COCD_3[b], 400 MHz; δ in ppm, *J* in Hz)..... 83

Table 2.15. ^1H NMR data of karavoates Q (**21**) and R (**22**), ($CDCl_3$[a], MeOD[b], 400 MHz, δ in ppm, *J* in Hz)..... 84

Table 2.16. ^{13}C NMR data of karavilagenin C (**1**), and karavoates A - F (**5** - **10**), and Q (**21**) ($CDCl_3$[a], CD_3COCD_3[b], MeOD[c], 100.61 MHz, δ in ppm)..... 85

Table 2.17. ^1H NMR data of karavilagenin C (**1**), and karavoates G - L (**11** - **16**), ($CDCl_3$[a], CD_3COCD_3[b] , 400 MHz, δ in ppm, *J* in Hz). 89

Table 2.18. ^1H NMR data of karavoates M (**17**) and N (**18**), ($CDCl_3$[a], CD_3COCD_3[b], 400 MHz, δ in ppm, *J* in Hz)..... 90

Table 2.19. ^{13}C NMR data of karavilagenin C (**1**) and karavoates G - N (**11** - **18**), ($CDCl_3$[a], CD_3COCD_3[b], 100.61 MHz, δ in ppm). 91

Table 2.20. ^1H NMR data of karavoates O (**19**), and P (**20**) (CD_3COCD_3, 400 MHz, δ in ppm, *J* in Hz)..... 92

Table 2.21. ^{13}C NMR data of karavoates O (**19**) and P (**20**) (CD_3COCD_3, 100.61 MHz, δ in ppm). 93

Table 2.22. NMR data of cucurbalsaminol A (**32**), (MeOD, ^1H 400 MHz, ^{13}C 100.61 MHz; δ in ppm, *J* in Hz)..... 97

Table 2.23. NMR data of cucurbalsaminols B (**28**) and C (**30**), (MeOD, ^1H 400 MHz, ^{13}C 100.61 MHz; δ in ppm, *J* in Hz). 98

Table 2.24. ^1H NMR data of balsaminosides A (**40**), B (**38**), and C (**39**), (MeOD[a], C_5H_5N[b], 400 MHz, δ in ppm, *J* in Hz). 102

Table 2.25. ^{13}C NMR data of balsaminosides A (**40**), B (**38**), and C (**39**), (MeOD[a], C_5H_5N[b], 100.61 MHz, δ in ppm). 103

Table 2.26. NMR data of kuguaglycoside A (**37**), (MeOD, ^1H 400 MHz, ^{13}C 100.61 MHz; δ in ppm, *J* in Hz)..... 105

Table 2.27. NMR data of cucurbita-5,23(*E*)-diene-3β,7β,25-triol (**2**), (MeOD, ^1H 400 MHz, ^{13}C 100.61 MHz; δ in ppm, *J* in Hz). 107

Table 2.28. NMR data of karavilagenin E (**4**), (MeOD, ^1H 400 MHz, ^{13}C 100.61 MHz; δ in ppm, *J* in Hz)..... 109

Table 2.29. NMR data of dehydrovomifoliol (**25**), (MeOD, ^1H 400 MHz, ^{13}C 100.61 MHz; δ in ppm, *J* in Hz)..... 110

Table 3.1. *In vitro* antimalarial activity (IC_{50} values, μg/mL) of selected plants against *Plasmodium falciparum* 3D7 strain. 116

Table 3.2. Antimalarial activity, cytotoxicity and selectivity index of compounds **1** - **4** and **26** - **40**. 121

Table 3.3. Antimalarial activity, cytotoxicity and selectivity index of balsaminol F (**3**) and its derivatives, triacetylbalsaminol F (**23**) and tribenzoylbalsaminol F (**24**). 122

Table 3.4. Antimalarial activity, cytotoxicity and selectivity index of the alkanoyl derivatives **5** - **10** of karavilagenin C (**1**). 123

Table 3.5. Antimalarial activity, cytotoxicity and selectivity index of the aroyl (**11** - **18**) and cinnamoyl derivatives **19** and **20** of karavilagenin C (**1**). 124

Table 3.6. Physico-chemical properties of compounds **1** - **4** and **26** - **40** (topological polar surface area, number of hydrogen bond acceptors and donors, molecular weight, octanol/water partition coefficient, and volume)[a]. 127

Table 3.7. Physico-chemical properties of esters **5** - **20** of karavilagenin C, and **23** and **24** of balsaminol F (**3**) (topological polar surface area, number of hydrogen bond acceptors and donors, molecular weight, octanol/water partition coefficient, and volume)[a]. 128

Table 3.8. Effects of balsaminols A - F (**35**, **27**, **29**, **31**, **26**, **3**), balsaminagenins A - C (**34**, **33**, **2**) on the reversal of MDR in human *MDR1* gene-transfected mouse lymphoma cells. 132

Table 3.9. Effects of balsaminapentaol (**36**), balsaminosides A - C (**40**, **38**, **39**), cucurbalsaminols A - C (**32**, **28**, **30**), karavilagenins C (**1**), E (**4**) and kuguaglycoside A (**37**) on the reversal of MDR in human *MDR1* gene-transfected mouse lymphoma cells. 133

Table 3.10. Effects of the esters **5** - **10** and **21** - **23** on the reversal of MDR in human *MDR1* gene-transfected mouse lymphoma cells. 134

Table 3.11. Effects of esters **11** - **20** and **24** on the reversal of MDR in human *MDR*1 gene-transfected mouse lymphoma cells. 135

Table 3.12. Antiproliferative effects of compounds **1** - **4** and **26** - **40**. 136

Table 3.13. Antiproliferative effects of esters **5** - **24**. 137

Table 3.14. Comparison of MDR modulator activities with physico-chemical properties of natural compounds **1** - **4** and **26** - **40** (topological polar surface area, number of hydrogen bond acceptors and donors, molecular weight, and octanol/water partition coefficient)[a]. 140

Table 3.15. Comparison of MDR modulator activities with physico-chemical properties of esters **5** - **24** (topological polar surface area, number of hydrogen bond acceptors and donors, molecular weight, and octanol/water partition coefficient)[a]. 141

Table 3.16. *In vitro* effects of some selected compounds (**1**, **2**, **4**, **5**, **26** - **30**, **32** - **35**, **38** and **40**) in combination with doxorubicin on human MDR1 gene-transfected mouse lymphoma cell line. 142

Table 3.17. Effects of balsaminagenins A (**34**), B (**33**), balsaminoside (**40**), and karavilagenin C (**1**) on the activity of MDR efflux pump of mouse lymphoma cells transfected with human ABCB1 gene by the real-time fluorometric method after 60 minutes. 149

Table 3.18. Minimum inhibitory concentration (MIC) values of compounds **1**, **3**, **33** - **35**, and **40** on Gram-negative and Gram-positive bacteria strains**.** 151

Table 3.19. Effects of compounds **1**, **33** - **35**, and **40** on the accumulation of EB by the Gram-positive MRSA COL_{OXA} (1μg/mL), and *E. faecalis* (0.5 μg/mL) strains. 152

Table 3.20. Effects of compounds **1**, **33** - **35**, and **40** on the accumulation of EB by the *E. coli* and *S. enteriditis* strains tested. 155

Table 4.1. Plant material data. 161

Table 4.2. Column chromatography of the EtOAc extract 164

Table 4.3. Column chromatography of the fraction M2 164

Table 4.4. Column chromatography of the fraction M3 193

Table 4.5. Column chromatography of the fraction M4 201

Table 4.6. Column chromatography of the fraction M4C. 201

Table 4.7. Column chromatography of the fraction M5 209

Table 4.8. Column chromatography of the fraction M5B. 209

CHAPTER 1

Introduction

The main goal of this project was to search for bioactive compounds from plants used in traditional medicine against malaria, and to contribute to the scientific validation of their use. Another objective was to evaluate the effect of some isolated compounds as drug resistance modulators.

Based on an ethnobotanical or a quimiotaxonomic approach, initially the work focused on the selection of some plants, and on the investigation of their claimed antimalarial properties. To achieve this goal, plant parts used in traditional medicine were sequentially extracted with apolar and polar solvents and the extracts were analyzed for their *in vitro* antimalarial activity against a chloroquine sensitive *Plasmodium falciparum* strain.

Momordica balsamina showed the best antimalarial activity, and for this reason was selected for the bio-guided fractionation in order to isolate the effective compounds. The compounds were analysed for their activity against two different *P. falciparum* strains. Moreover, the effect of some isolated compounds as drug resistance modulators was also evaluated using both eukaryotic (human *MDR1* gene-transfected mouse lymphoma cells) and prokaryotic (bacterial strains) systems.

Therefore, this dissertation is divided into five chapters. The first one, Introduction, will focus on *Momordica balsamina*, and in the biological models used to test the activity of its constituents. A literature review of the chemical constituents of *Momordica* genus and the principal findings in malaria and multidrug resistance will be focused on this section. Some biogenetic generalities about terpenoids will be also discussed. In the second chapter, it will be described and discussed the physical and spectroscopic data that have allowed the structural elucidation of all the compounds obtained from *M. balsamina*. The third chapter is dedicated to the results and discussion of the biological assays, and is subdivided as follows: i) evaluation of the antimalarial activity of extracts and pure compounds; ii) evaluation of the MDR reversal activity of pure compounds in cancer cells; and iii) modulation of antibiotic resistance in some resistant bacterial strains by some compounds. The fourth chapter summarizes the methodologies used, and finally, in the fifth chapter, the main conclusions will be presented.

1. *MOMORDICA* GENUS

1.1. General considerations

Momordica genus belongs to the Cucurbitaceae family, commonly referred to as the cucumber, gourd, melon, or pumpkin family. It comprises about 118 genera and more than 800 species (Bates, 1990; Wang, 2007). Most of the plants of this family are climbing or prostate, annual or perennial herbs, less often woody lianas, and rarely erect herbs without tendrils. They are native in most of the world, especially in the tropical and subtropical regions, with warm temperature (Bates, 1990)[1].

Some members of the Cucurbitaceae family have a huge economical importance due to their edible fruits, flowers, and seeds. In terms of world's total production, the most economically important Cucurbitaceae crops (Figure 1.1) are watermelon (*Citrullus lanatus* (Thunb.) Matsum. & Nakai), cucumber (*Cucumis sativus var. sativus* L.) and melon (*Cucumis melo* L.), (Neuwinger, 1996; Rosengarten, 2004).

Figure 1.1. The most important Cucurbitaceae crops: **A.** Watermelon (*Citrullus lanatus*), **B.** Cucumber (*Cucumis sativus*) and **C.** Melon (*Cucumis melo*).[2]

[1] Adapted from the web site (02-02-2010): http://www.cucurbit.org/family.html.

[2] Adapted from the web site (24-03-2010): A. http://velvetfont.wordpress.com/2008/04/30/watermelon-fruit-or-vegatable/; B. http://en.wikipedia.org/wiki/File:ARS_cucumber.jpg; C. http://www.agroatlas.ru/en/content/cultural/Cucumis_melo_K/

1.2. *Momordica balsamina* L.

Momordica balsamina L. (Figure 1.2), also referred to as the balsam apple, Southern balsam pear, or African pumpkin, is one of the 47 species of the *Momordica* genus. This is a tendril-bearing herb native in tropical regions of Africa. *M. balsamina* is also indigenous to tropical Asia, Arabia, India and Australia (Thakur et al., 2009). The meaning of the Latin word *Momordica* is "to bite", and it refers to the jagged edges of the leaf, which appear to have been bitten (Rios, 2005). Some other species (Figure 1.2) of this genus are *M. charantia*, *M. foetida*, *M. grosvenorii*, *M. cochinchinensis* and *M. kirkii*. In the same way, as *M. balsamina*, they are known due to their nutritional value and pharmacological properties, being extensively used in the traditional medicine in many countries. In Mozambique, the fruits and leaves of *M. balsamina* are cooked and used as relish. In Botswana, and in other Southern African countries, leaves and fruits of *M. balsamina* are served as porridge with the main meal. The leaves and green fruits of this plant can also be cooked with crushed ground nuts and used as gravy (Flyman and Afolayan, 2007; Thakur et al., 2009). The fruits from the close related species *M. charantia* (Bitter melon) are fried and stuffed with potatoes, in Pakistani traditional cuisine (Ansari et al., 2005).

Concerning the pharmacological uses, the leaves, fruits, seeds, and barks of *Momordica* species are important traditional medicines. In fact, they are used as antihelmintic, vermifuge, cathartic, aphrodisiac, and also for the treatment of fever, malaria, burns, bilious disorders, diabetes, cataract, hypertension, leprosy, jaundice, snake bite, haemorrhoids, and piles, not only in South Africa and other African regions but also in other tropical parts of the world (Joseph and Antony, 2008; Neuwinger, 2000). In a recent review, the main medicinal properties of *M. balsamina* were described (Thakur et al., 2009). In this way, in Mozambique, its leaves are used to treat fever symptoms associated with malaria disease (Bandeira et al., 2001). In South Africa, the roots are used to treat fever, stomach ulcers and stomach pains (Van Wyk et al., 2008), and the stems and flowers are used to treat diabetes (van de Venter et al., 2008). Besides the recognized antiplasmodial activity, extracts of various parts of this plant have shown the following properties: antiviral (Bot et al., 2007; Detommasi et al., 1995), anti-inflammatory, analgesic (Karumi, 2003), shigellocidal (Iwalokun et al., 2001), anti-diarrhoeal (Kainyemi, 2005), antimicrobial, and antidiabetic properties (Otimenyin, 2008).

The antidiabetic property is one of the most emphasised and investigated characteristic of *M. charantia* (Basch et al., 2003; Garau, 2003; Menan et al., 2006). As a matter of fact, the

use of this plant to treat diabetes is known in almost all African countries and also in some countries of Central and South America. Some other medicinal properties of *M. charantia* are pointed in two recent reviews (Beloin et al., 2005; Grover and Yadav, 2004) and in a book section (Ross, 2003). Similarly to *M. balsamina*, this plant is also used to treat malaria symptoms (Amorim et al., 1991; Hout et al., 2006; Kaou et al., 2008; Menan et al., 2006; Muñoz, 2000).

M. foetida is used in East and Central Africa, namely in Uganda, to treat a number of ailments, especially symptoms of malaria (Froelich, 2007; Tabuti, 2008; Waako et al., 2005).

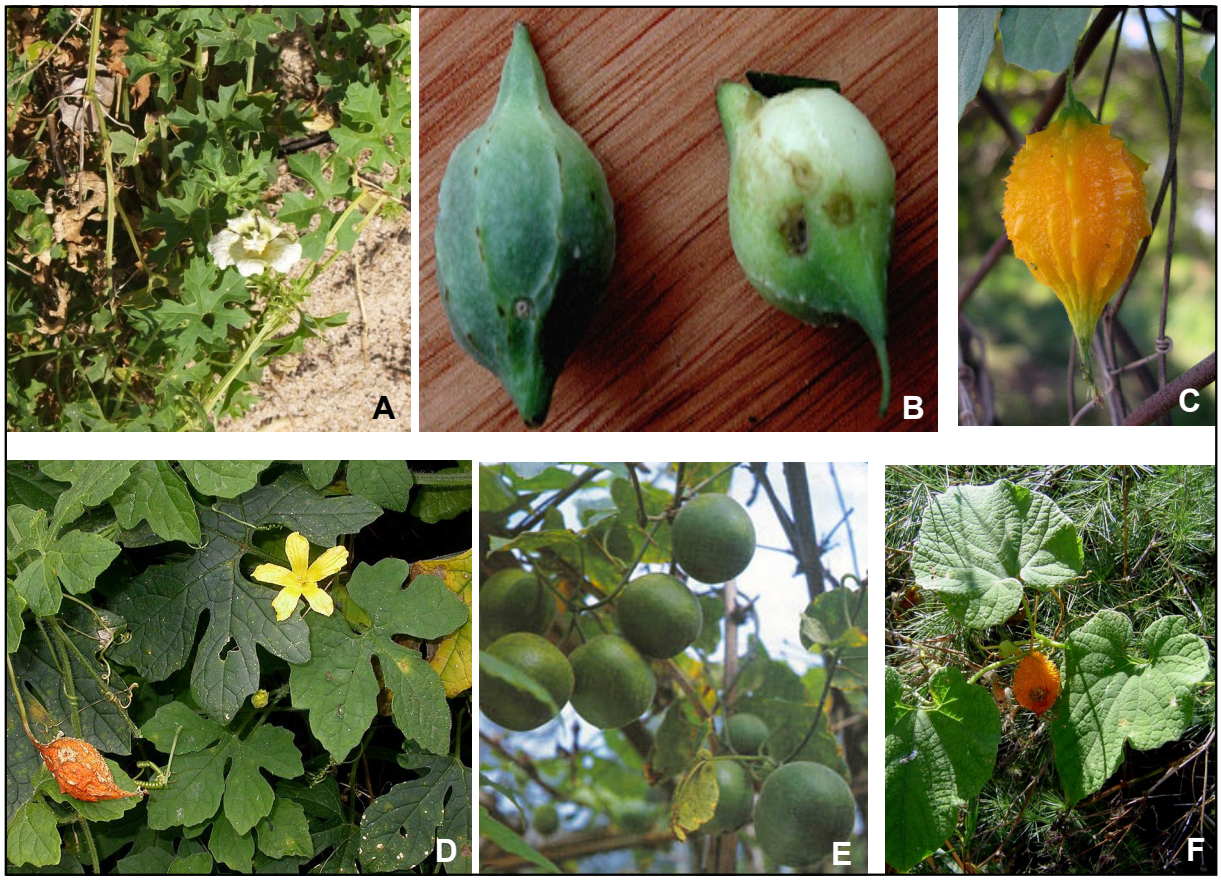

Figure 1.2. A. Flower of *M. balsamina*; **B.** Immature fruits of *M. balsamina*; **C.** Mature fruit of *M. balsamina*; **D.** *M. charantia*; **E.** Fruits of *M. grosvenorii*; **F.** *M. foetida*.[3]

[3] A and B pictures taken by the author, C - F adapted from the web site (24-03-2010): C. http://www.flickr.com/photos/shyzaboy/3168341948/; D. http://www.metafro.be/prelude/view_reference?ri=VN%2015 ; E. http://www.horizonherbs.com/product.asp?specific=1507; F. http://www.zimbabweflora.co.zw/speciesdata/image-display.php?species_id=157210&image_id=1

1.3. Terpenoids: biogenetic generalities

Terpenoids are perhaps the most diverse family of natural compounds, which are widely distributed in nature and abundantly in higher plants. Over 40.000 different terpenoids have been isolated not only from plants but also from fungi, marine organisms (an abundant source of unusual terpenoids), and from insects (in pheromones and in defence secretions). Plant terpenoids include primary metabolites (gibberellins, carotenoids and sterols) necessary for cellular function and maintenance; and secondary metabolites that are not involved in growth and development. The latter are often commercially attractive because of their uses as flavours and colour enhancers, agricultural chemicals, and medicines. In fact, a huge number of terpenoids have been used against human ailments, such as cancer, malaria, and others (Bohlmann and Keeling, 2008; Roberts, 2007).

Structurally, they are derived from the branched C_5 carbon skeleton of isoprene. Each isoprenoid is constructed using a different number of repetitions of isoprene motifs, cyclization reactions, rearrangements, and further oxidation of the carbon skeleton (Rohmer, 1999; Torssell, 1997).

The terpenoid biosynthesis can be divided into two main stages:

1. The first one includes the synthesis of the two universal C_5 building blocks, the isoprene unit: isopentenyl diphosphate (IPP) and its allylic isomer dimethylallyldiphosphate (DMAPP). These universal precursors are synthesized ubiquitously among prokaryotes and eukaryotes. In higher plants they can be produced by either of two routes: the mevalonate pathway (MVA) or the 1-deoxy-D-xylulose-5-phosphate pathway (DXP), (Scheme 1.1), (Rohmer, 1999).

2. In the second phase of terpene biosynthesis, IPP and DMAPP are used by prenyltransferases in head-to-tail condensation reactions to produce geranyl diphosphate (GPP), farnesyl diphosphate (FPP) and geranyl geranyl diphosphate (GGPP). These compounds are the immediate precursors of monoterpenes (C_{10}), sesquiterpenes (C_{15}) and diterpenes (C_{20}). Higher order terpenoids, like triterpenoids (C_{30}), derive from the triterpenoid squalene (C_{30}), (Scheme 1.2). Squalene contains six isoprene units, as a result of the condensation tail-to-tail of two FPP molecules. After the formation of the acyclic terpenoid structural building blocks (e.g. GPP, FPP, GGPP), terpene synthases (cyclases) act to generate the different terpene carbon skeletons. These can also suffer additional transformations, such as oxidation, reduction, isomerization, and conjugation that are responsible for the production of thousands of different terpenoid metabolites (Bohlmann et al., 1998).

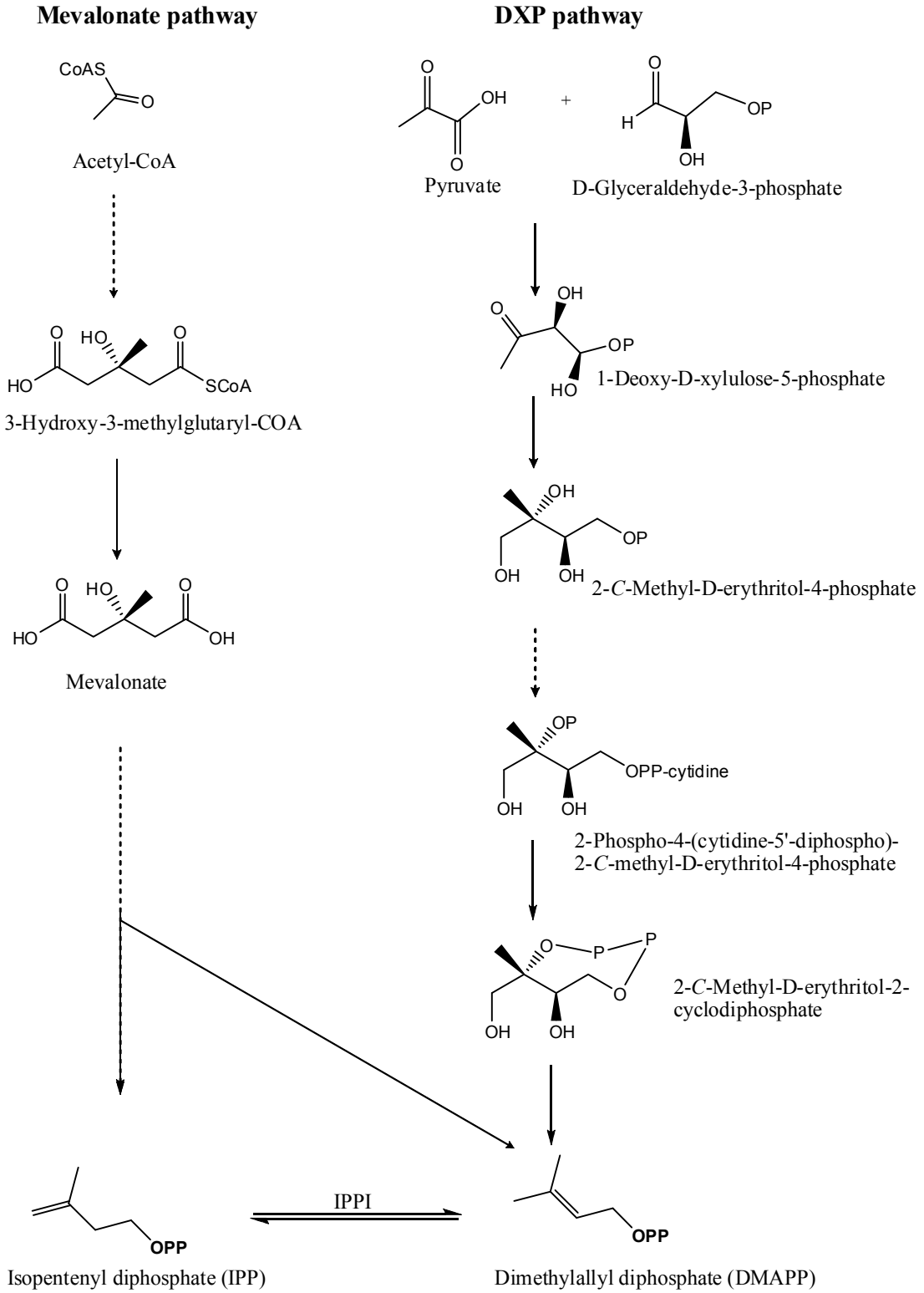

Scheme 1.1. Schematic illustration of isoprenoid biosynthetic pathways (Adapted from: Kirby and Keasling, 2009).

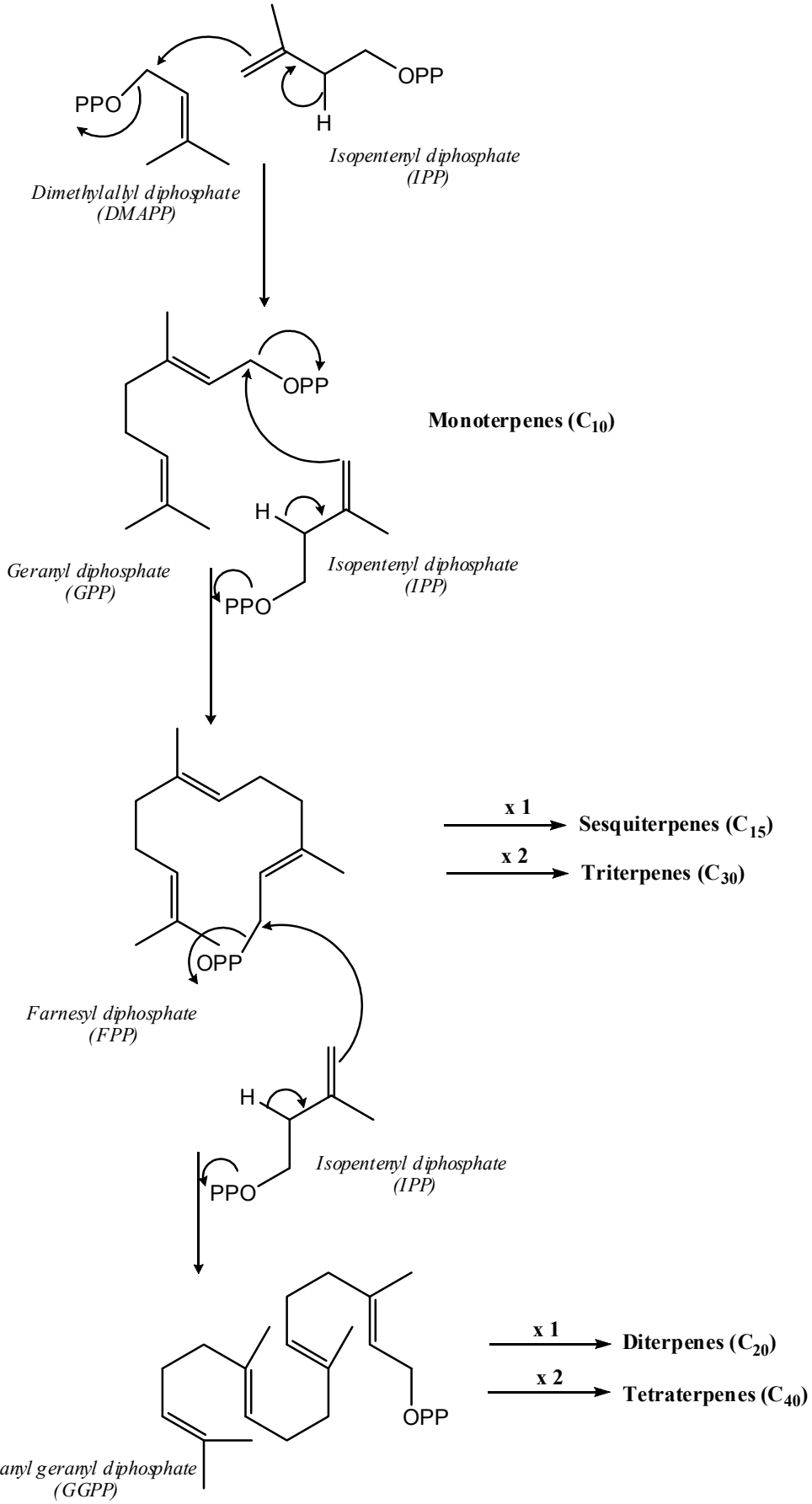

Scheme 1.2. Suggested pathways for the biosynthesis of monoterpenes, sesquiterpenes, diterpenes, triterpenes and tetraterpenes (Adapted from: Roberts, 2007).

As it can be observed in Scheme 1.2, the two universal precursors, IPP and its allylic isomer DMAPP, are the central intermediates in the biosynthesis of terpenoids. These are synthesized by two distinct pathways (Scheme 1.1): the mevalonate (MVA) pathway and the 1-deoxy-D-xylulose-5-phosphate pathway (DXP).

Mevalonate pathway

The mevalonate pathway discovered in the 1950s, takes place in cytosol of bacteria, plants, animals and fungi, and it is a supply of precursors for the production of sesquiterpenes and triterpenes. MVA has a branched chain C_6-skeleton that undergoes phosphorylation to mevalonic acid pyrophosphate, followed by further phosphorylation and descarboxylation to form the essential C_5-intermediates: IPP and its isomer DMAPP (Thomas, 2004). For a long time this pathway has been the only biosynthetic scheme known for the biosynthesis of all isoprenoids in whole of the living organisms. However, several experimental results had been reported to be inconsistent with this route (Kuzuyama and Seto, 2003; Rohmer, 1999), and had been showed that this was much less prominent in secondary metabolism than the mevalonate-independent pathway *via* deoxy-xylulose phosphate, also called MEP or Rohmer's-pathway.

Mevalonate-independent pathway via deoxy-xylulose phosphate

The mevalonate-independent pathway *via* deoxy-xylulose phosphate was discovered in 1988 and only characterized few years ago (Ajikumar et al., 2008). There are several terminologies in use for this pathway, namely, mevalonate-independent pathway, non-mevalonate pathway, glyceraldehyde-3-phosphate/pyruvate pathway, deoxy-xylulose phosphate pathway (DXP or DOXP) and methylerythritol phosphate pathway (MEP), (Dewick, 2002). This is known to supply the precursors from the isoprenoids (especially monoterpenoids, diterpenoids and tetraterpenoids) of apicomplexan protozoa and of many eubacteria, as well as for the majority of isoprenoids of plants (Eisenreich et al., 2004; Rohmer, 1999). It appears to be started with the formation of 1-deoxy-D-xylulose-5-phosphate (DXP) by condensation of D-glyceraldehyde-3-phosphate and pyruvate by DXP synthase (Kuzuyama and Seto, 2003), (Scheme 1.1). The precursors IPP and DMAPP are

obtained *via* 2-methyl-D-erythritol-4-phosphate, 2-methyl-D-erythritol-2,4-cyclodiphosphate and 1-hydroxy-2-methyl-2(*E*)-butenyl-4-diphosphate. In higher plants, both MVA and MEP pathways are used. In this way, the mevalonate pathway, whose enzymes are localized in cytosol, provides cytosolic metabolites (triterpenoids, steroids, and also some sesquiterpenoids). The DXP pathway, whose enzymes are located in a plastid organelle, supplies the plastid-related metabolites such as, monoterpenes, diterpenes, some sesquiterpenes, tetraterpenes (carotenoids), and the prenyl-side chains of chlorophyll and plastoquinones. There are examples of cooperation between the cytosolic and plastidial pathways, mainly in the biosynthesis of stress metabolites (Dewick, 2002; Rohmer, 1999).

1.2.1. Cucurbitane-type triterpenoids

Triterpenoids are a large and structurally diverse group of natural compounds, widely distributed through the plant kingdom. According to the isoprene biogenetic rule, triterpenes derive from all-*trans* squalene or related acyclic 30-carbon precursors. Squalene is formed by the linkage tail-to-tail of two farnesyl diphosphate units (FPP) that is catalyzed by a membrane-bound enzyme (Scheme 1.3), (Rowe, 1989). Generally, its cyclization occurs by oxidation first to squalene-2,3-epoxide, in which the configuration at C-3 is usually *S* (Rowe, 1989). Most triterpenoids are C_6-C_6-C_6-C_5 tetracyclic, C_6-C_6-C_6-C_6-C_5 pentacyclic, or C_6-C_6-C_6-C_6-C_6 pentacyclic, but there are also acyclic, monocyclic, bicyclic, and hexacyclic triterpenoids. Indeed, more than 200 distinct skeletons are known (Xu et al., 2004). The polycyclic structure adopted from squalene depends on the conformation in which squalene chain can be folded on the enzyme surface: into a chair, or boat conformation. The cyclization is usually initiated by acid-catalyzed ring opening of the squalene epoxide, and probably occurs through a series of carbocationic intermediates (Rowe, 1989).

If the mode of cyclization is chair-boat-chair-boat-unfolded the resulting triterpenes are the lanostane, protostane, and cycloartane groups and also the steroids (Rowe, 1989).

For a long time cucurbitacins, due to their tetracyclic skeleton similar to steroids, have been assumed to be synthesized *via* lanosterol, cycloartenol or parkeol (Scheme 1.4). As illustrated in Scheme 1.4, the cleavage of the cyclopropane ring of cycloartenol, followed by the hydride shift (from C-5 to C-10), and proton elimination from C-6 could give 10α-cucurbita-5,24-dien-3β-ol. In the same way, cucurbitadienol can be obtained by addition of a proton to the double bond $\triangle^{8,9}$ of lanosterol with 1,2-shifts of methyl (from C-10 to C-9) and

hydride, and proton elimination. From parkeol, followed the same migrations as in lanosterol, and the protonation of the double bound ($\triangle^{9,11}$), cucurbitadienol is also obtained. However, due to experimental evidences (Balliano et al., 1983a; b), a distinct biosynthesis route for cucurbitacins after oxidosqualene formation was proposed. A recent work clarified the presence of a specific enzyme responsible for the oxidosqualene cyclization step and consequently for the formation of cucurbitadienol, the simplest tetracyclic triterpene with a cucurbitane skeleton, without intermediary steps (Shibuya et al., 2004).

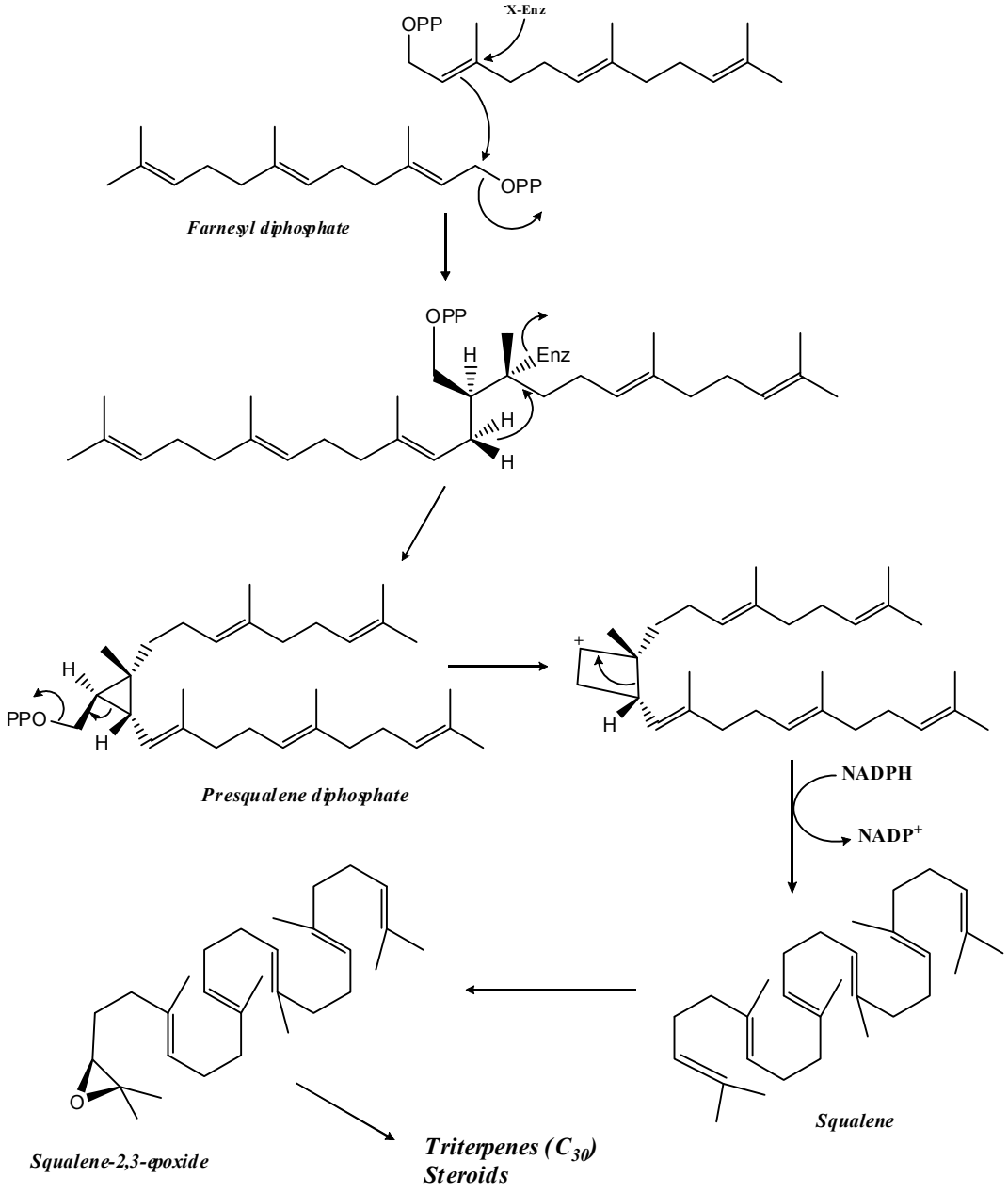

Scheme 1.3. Biosynthesis of 2,3-squalene epoxide (Adapted from: Rowe, 1989).

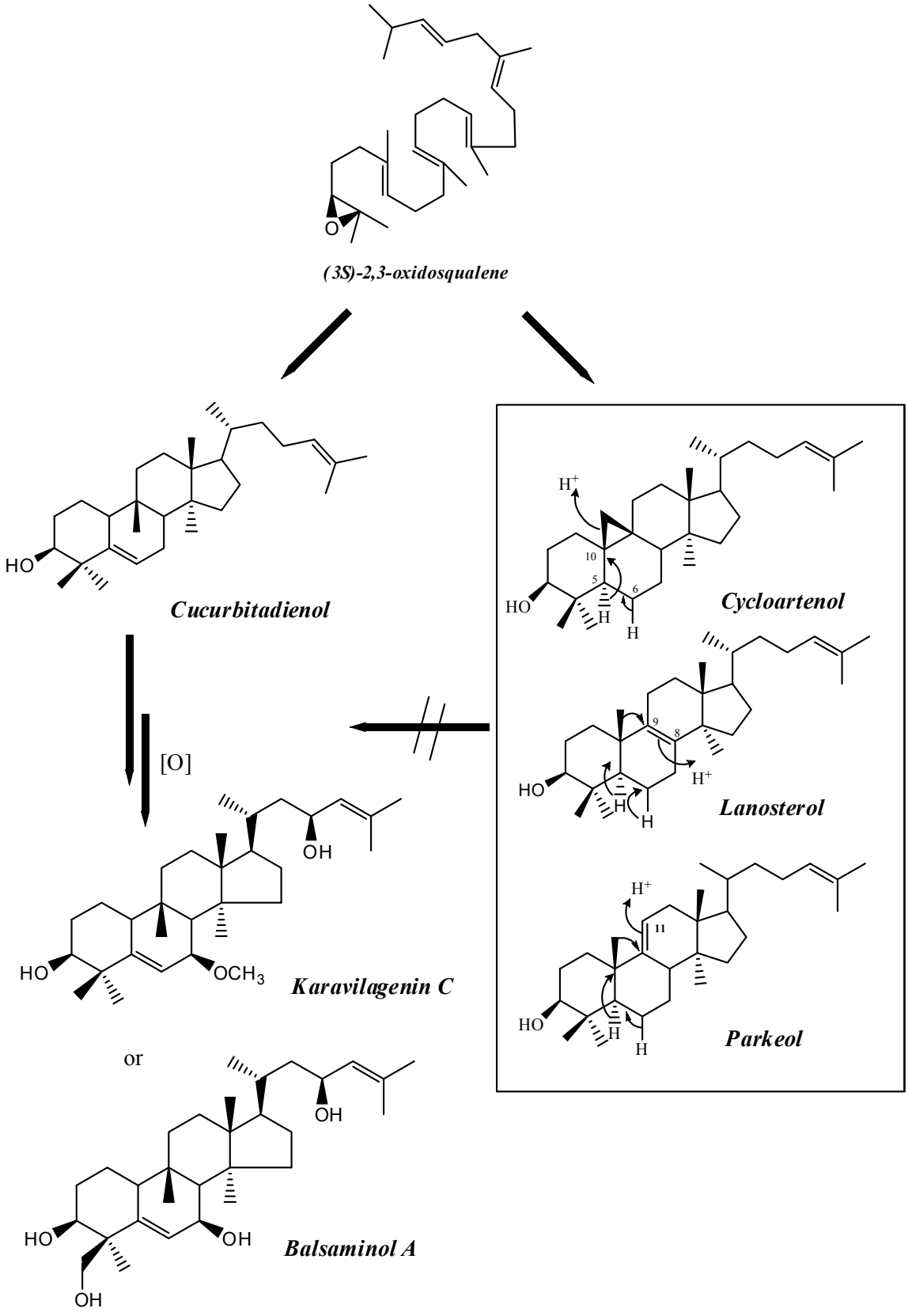

Scheme 1.4. Biosynthesis of cucurbitacins (Adapted from: Shibuya et al., 2004).

1.4. Literature review

Plants of *Momordica* genus are known to have a bitter taste due to cucurbitacins (Rios, 2005). Structurally, cucurbitacins are characterized by the tetracyclic cucurbitane skeleton, 19-(10→9β)-*abeo*-10α-lanost-5-ene, also known as 9β-methyl-19-*nor*-lanost-5-ene, with a variety of oxygen functions in different positions that can be present either non-glycosylated or glycosylated. They are predominantly found in the Cucurbitaceae family, but they are also present in several families, like Brassicaceae, Scrophulariaceae, Begoniaceae, Elaeocarpaceae, Datiscaceae, Desfontainiaceae, Polemoniaceae, Primulaceae, Rubiaceae, Sterculiaceae, Rosaceae, and Thymelaeaceae. Some cucurbitacins were also isolated from mushrooms of *Russula* and *Hebeloma* genus, and from shell-less marine molluscs (dorid nudibranchs), (Rios, 2005).

Besides cucurbitane-type triterpenoids, other compounds have been isolated from species of *Momordica* genus, such as pentacyclic triterpenes, steroids, diterpenes, alkaloids, flavonois, phenolic acids, and some monoterpenes (Detommasi et al., 1991; Detommasi et al., 1995; Froelich, 2007; Grover and Yadav, 2004).

Cucurbitane-type triterpenoids

In this section, a literature review between September 2004 and March 2010 is presented, in respect to the new cucurbitane-type triterpenoids isolated from *Momordica* genus. A review with all cucurbitane-type triterpenoids isolated from 1980 to August 2004 was recently published (Chen et al., 2005).

As shown in Table 1.1, between 2004 and 2010 most of the new cucurbitacins were isolated from *Momordica charantia.* The most studied parts of the plant were the fruits, and stems. Some new cucurbitane-type triterpenoid glycosides were also isolated from *Momordica grosvenorii* Swingle.[4]

[4] *Momordica grosvenorii* Swingle is the synonymy of *Siraitia grosvenorii* (Swingle) C. Jeffrey ex. A. M. Lu & Zhi Y. Zhang.

Table 1.1. New cucurbitane-type triterpenoids isolated from *Momordica* species.

Species	***Analysed part***	***Extract (fraction)***	***Compounds***	***References***
Momordica charantia	**Fresh leaves**	Methanol (*n*-BuOH fr.)	**1.01 – 1.02**	(Mekuria DB, 2005)
		Methanol	**1.03 – 1.04**	(Kashiwagi et al., 2007; Mekuria et al., 2006)
	Dried leaves and vines	Ethanol 95 % (EtOAc fr.)	**1.05 – 1.18**	(Chen et al., 2009b)
	Dried stems	Methanol (EtOAc fr.)	**1.19 – 1.23**	(Chang et al., 2006)
			1.24 – 1.27	(Chang et al., 2008)
			1.28 – 1.31	(Chang et al., 2010)
		Methanol ($CHCl_3$ fr.)	**1.32 – 1.33**	(Liu et al., 2010)
	Fresh fruits	Ethanol 95% (*n*-BuOH fr.)	**1.34**	(Li et al., 2007c)
		Ethanol 95% (Water fr.)	**1.35 – 1.37**	(Li et al., 2007b)
		Ethanol 80 % (*n*-BuOH fr.)	**1.38 – 1.41**	(Tan et al., 2008a)
	Dried fruits	Methanol (*n*-Hexane fr.)	**1.42 – 1.44**	(Kimura et al., 2005)
		Methanol (Ether fr., EtOAc fr.)	**1.45 – 1.62**	(Harinantenaina et al., 2006; Matsuda et al., 2007; Nakamura et al., 2006)
		Methanol ($MeOH/H_2O$ fr.)	**1.63 – 1.70**	(Akihisa et al., 2007b)
		Methanol ($CHCl_3$ fr.)	**1.71 – 1.73**	(Nhiem, 2010)
		Methanol (EtOAc fr.)	**1.74 – 1.75**	(Liu et al., 2008c)
		Methanol (*n*-BuOH fr.)	**1.76 – 1.78**	(Liu, 2010)

Table 1.1. (cont.).

Species	***Analysed part***	***Extract (fraction)***	***Compounds***	***References***
Momordica charantia	**Dried roots**	Methanol (*n*-BuOH fr.)	**1.79 – 1.86**	(Chen et al., 2008a)
		Methanol (EtOAc fr.)	**1.87 – 1.91**	(Chen et al., 2008b)
Momordica grosvenorii	**Dried fruits**	Ethanol 80 %	**1.92**	(Si et al., 2005)
		Ethanol 99 % (*n*-BuOH fr. and Water fr.)	**1.93 – 1.97**	(Akihisa et al., 2007a)
	Fresh fruits	Methanol	**1.98 – 1.99** **1.100 – 1.102**	(Li et al., 2006a) (Li et al., 2007a)
	Dried roots	Methanol	**1.103 – 1.104**	(Li et al., 2009)

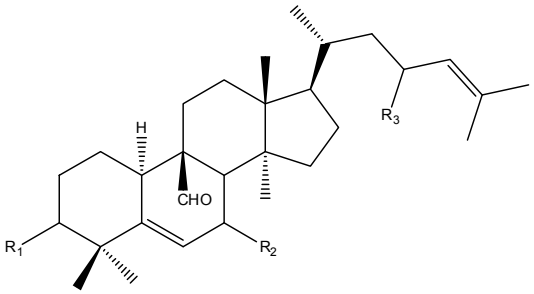

	R_1	R_2	R_3
1.01	β-OH	β-OH	ξ-OH
1.02	β-$OCOCH_2COOH$	β-OH	ξ-OH
1.03	β-OH	β-Oglu	ξ-OH
1.04	β-$OCOCH_2COOH$	β-OH	β-Oglu
1.05	β-OH	β-OH	= O
1.06	= O	= O	= O

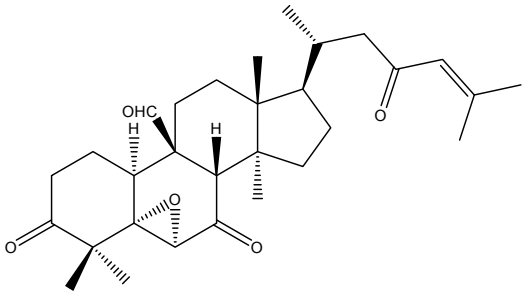

1.07

glu=

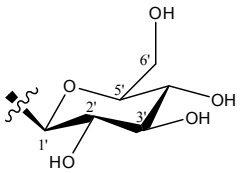

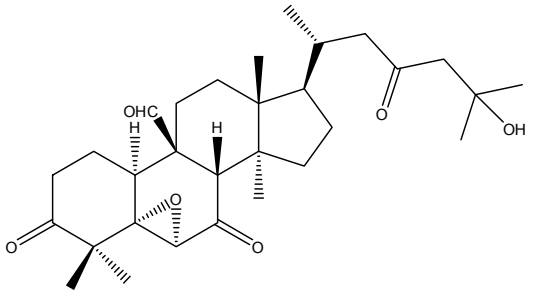

1.08

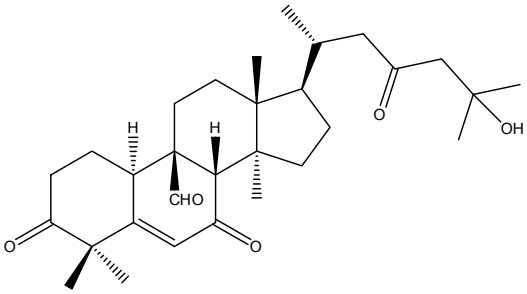

1.09

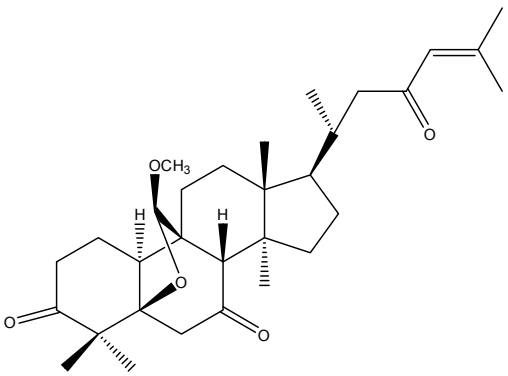

1.10

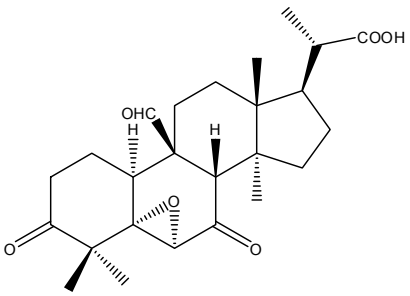

1.11

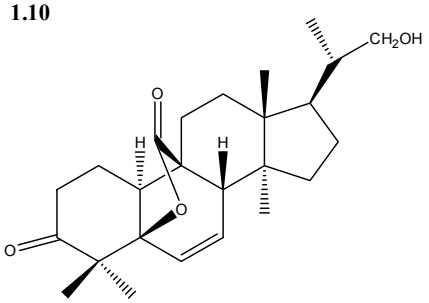

1.12

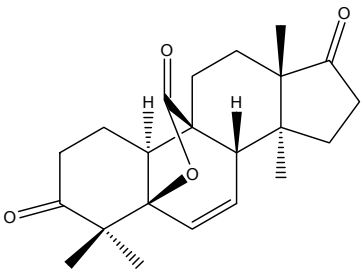

1.13

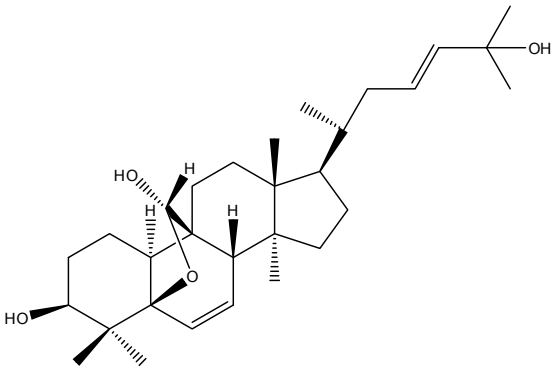

1.14

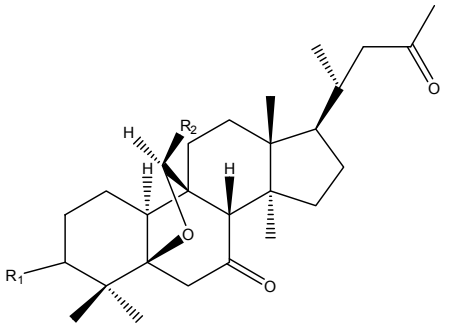

	R_1	R_2
1.15	= O	H
1.16	= O	OEt
1.91	β-OH	H

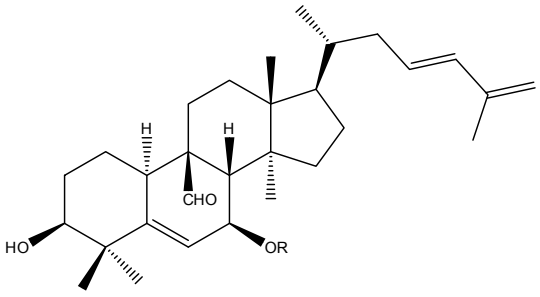

	R
1.17	H
1.43	CH_3
1.86	glu

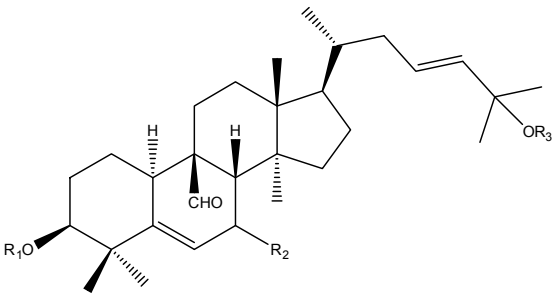

	R_1	R_2	R_3
1.18	= O	= O	H
1.44	H	β-OCH_3	CH_3
1.45	all	β-OH	H
1.70	glu	β-OCH_3	CH_3
1.74	all	β-OCH_3	CH_3
1.87	H	= O	H

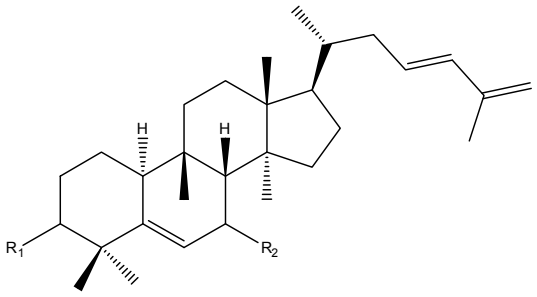

	R_1	R_2
1.19	β-OH	β-OH
1.20	= O	= O

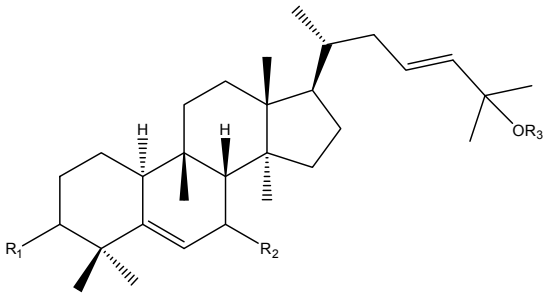

	R_1	R_2	R_3
1.21	β-OH	β-OH	CH_3
1.22	= O	= O	H
1.24	β-OH	β-OH	H
1.25	β-OAc	β-OCH_3	H
1.46	β-OH	β-OCH_3	CH_3
1.47	β-OH	β-OCH_3	H
1.48	β-Oglc	β-OCH_3	CH_3
1.49	β-Oall	β-OCH_3	CH_3
1.50	β-Oall	β-OCH_3	H
1.83	β-OH	β-OGlc	CH_3
1.88	β-OH	= O	H

glu=

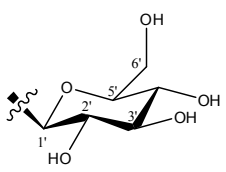

all=

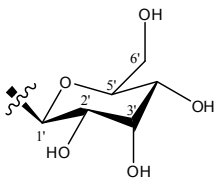

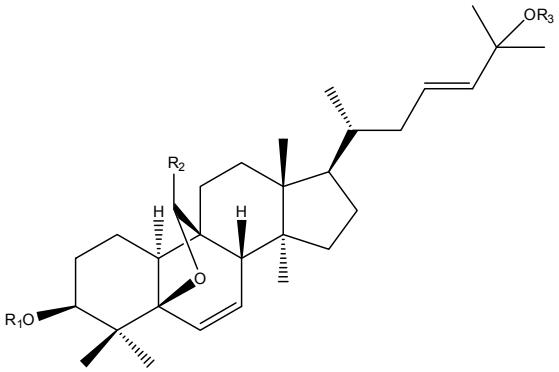

	R_1	R_2	R_3
1.23	H	H	H
1.34	all	OH	H
1.54	H	= O	H
1.55	glc	= O	CH_3
1.73	glu	OH	H
1.76	glu	OBu	H

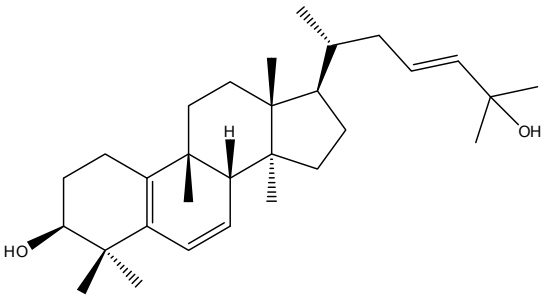

1.26

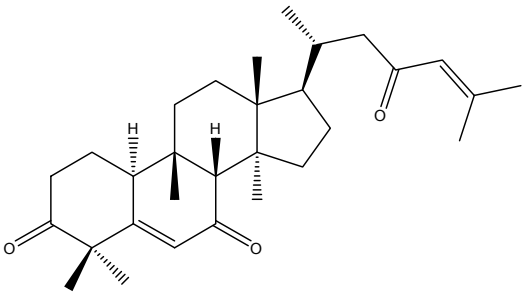

1.27

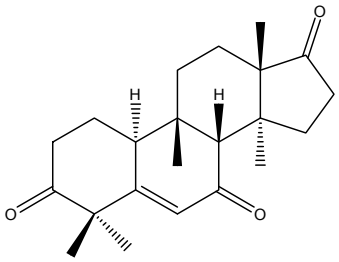

1.28

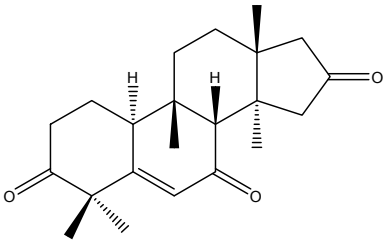

1.29

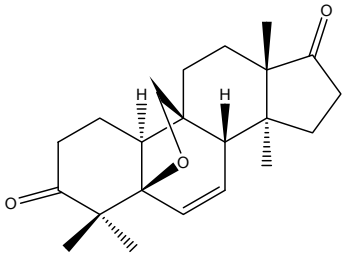

1.30

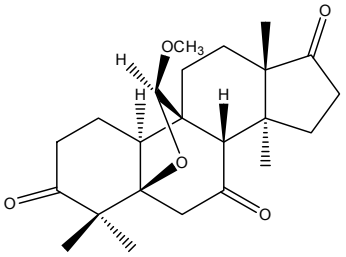

1.31

glc=

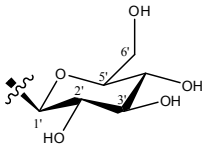

all=

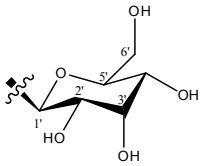

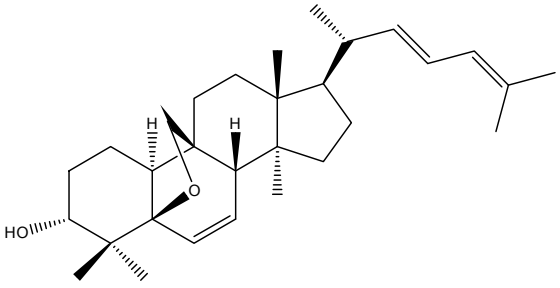

1.32

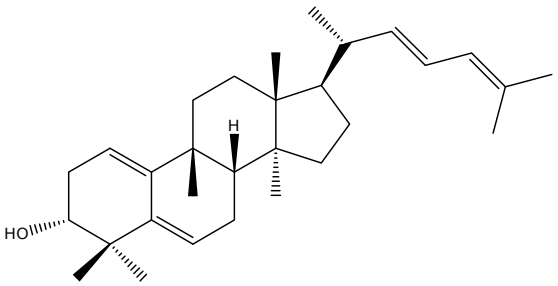

1.33

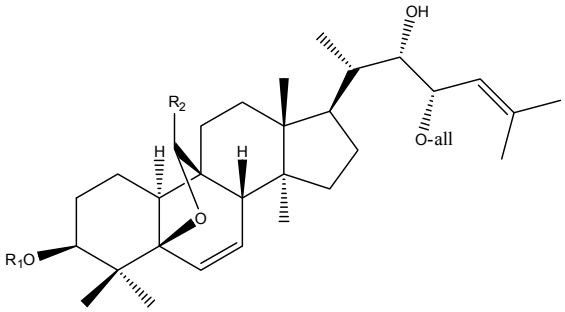

	R_1	R_2
1.35	glc	H
1.36	all	H
1.37	all	OH

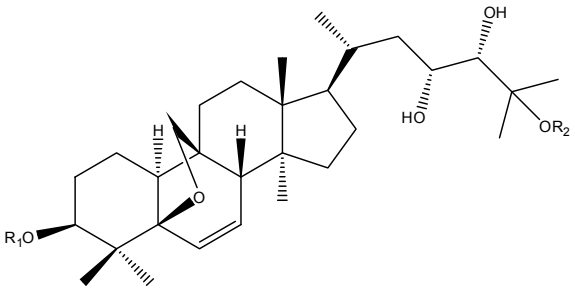

	R_1	R_2
1.38	glc	H
1.39	all	glc

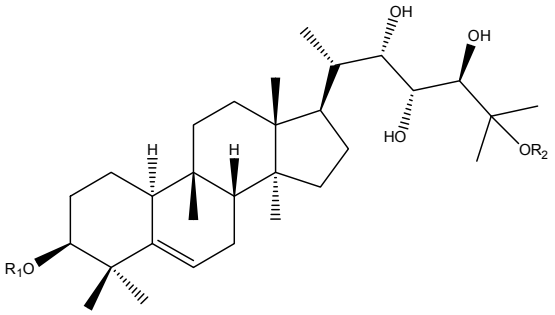

	R_1	R_2
1.40	glc(1→6)glc	glc
1.41	xyl(1→4)-glc(1→6)glc	glc

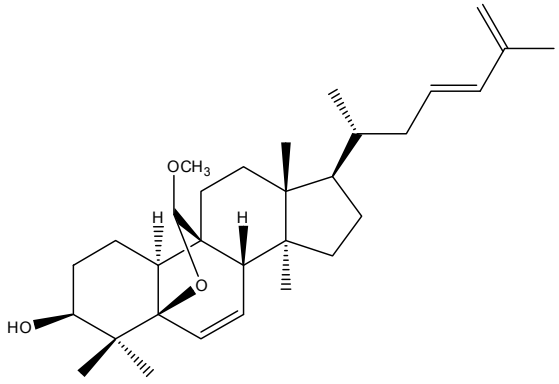

1.42

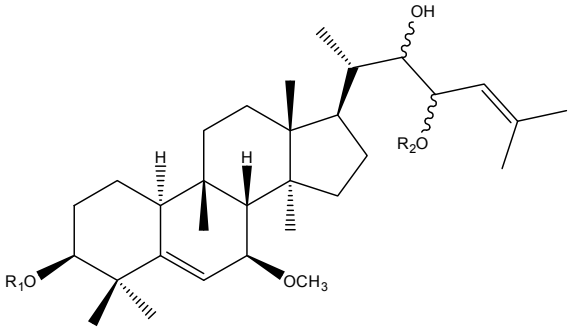

	R_1	R_2
1.51	H	glc
1.52	all	all

glc=

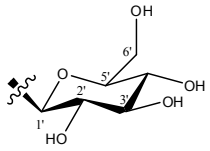

all=

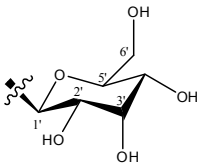

xyl=

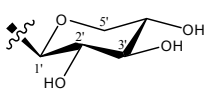

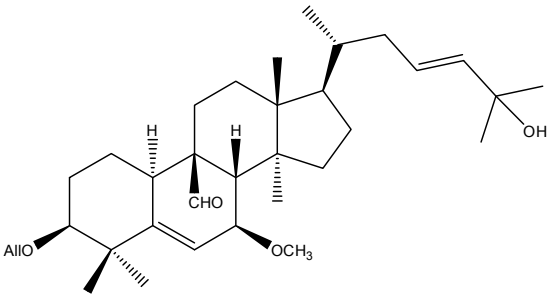

1.53

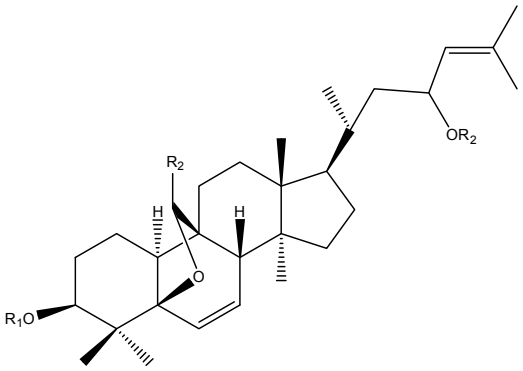

	R_1	R_2
1.56	H	H
1.57	glc	CH_3

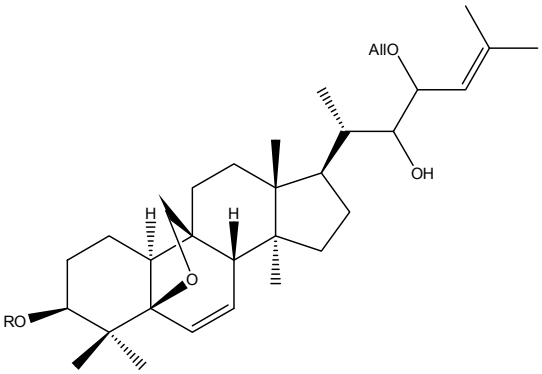

	R_1
1.58	H
1.59	glc
1.60	all

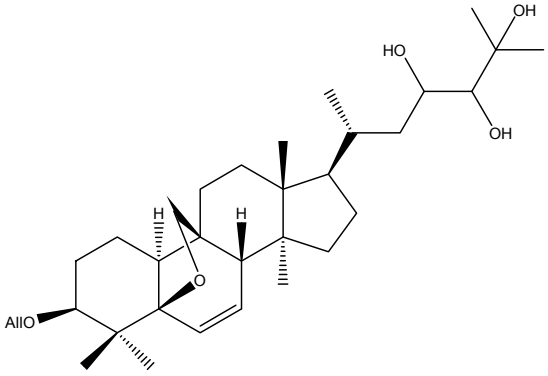

1.61

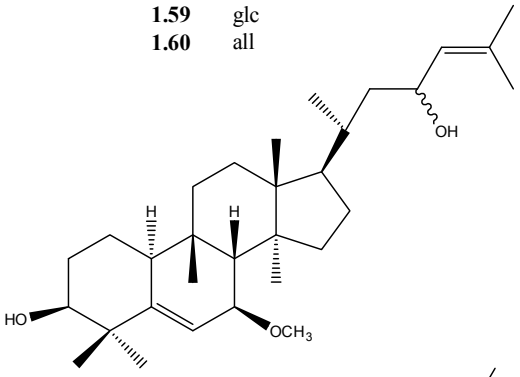

1.62

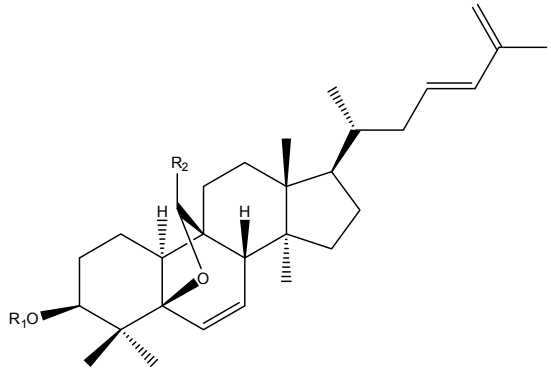

	R_1	R_2
1.63	glc	OCH_3
1.64	glc	H
1.65	all	H
1.66	glc	= O

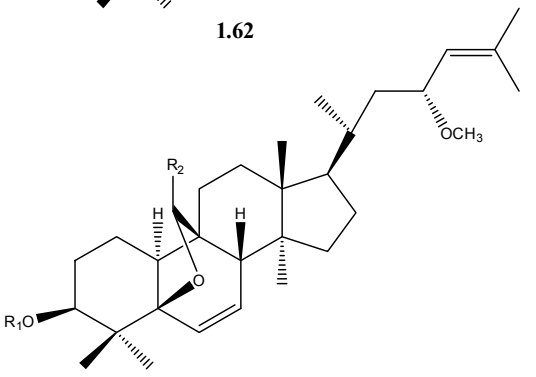

	R_1	R_2
1.67	all	OCH_3
1.68	glc	H

glc=

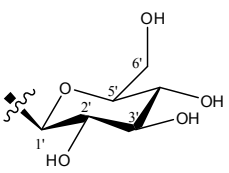

all=

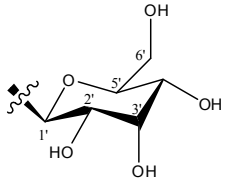

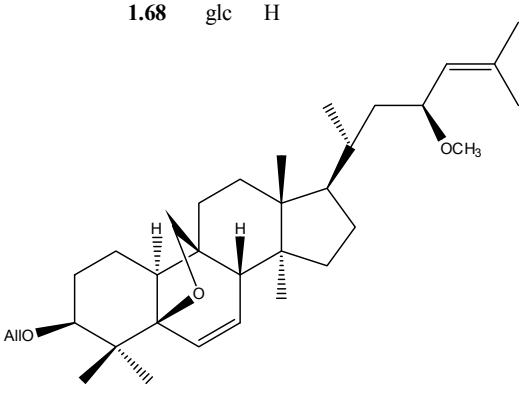

1.69

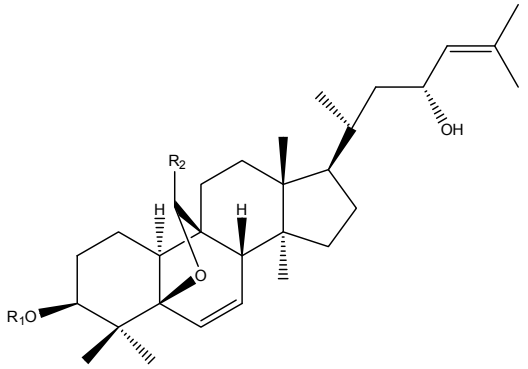

	R_1	R_2
1.71	all	OCH_3
1.72	all	H

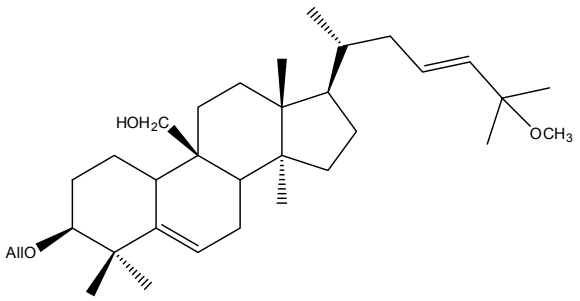

1.75

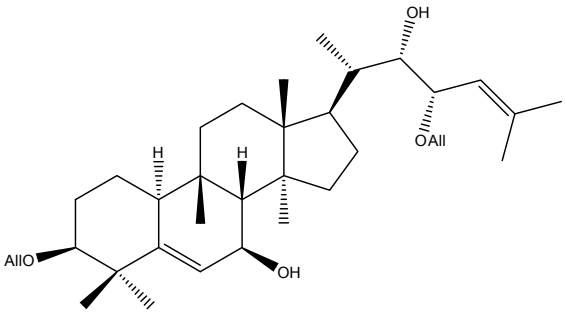

1.77

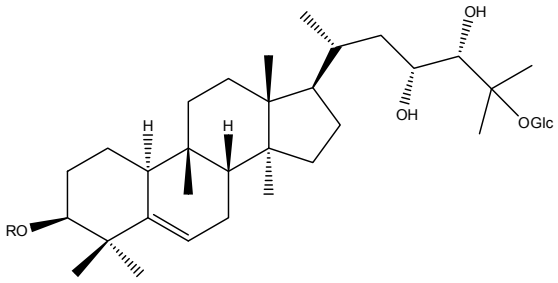

R: glc(6→1)glc

1.78

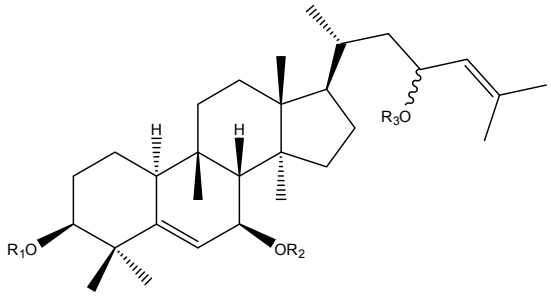

	R_1	R_2	R_3
1.79	H	CH_3	glc
1.80	all	CH_3	glc
1.81	H	glc	glc
1.82	H	glc	glc(1→2)glc

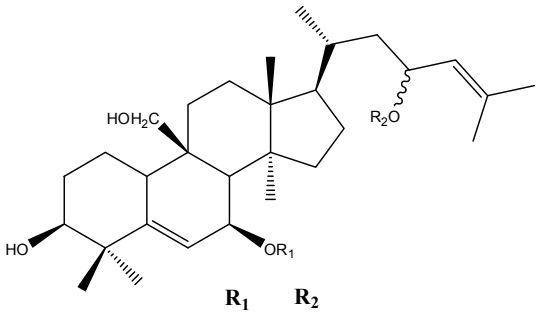

	R_1	R_2
1.84	glc	H
1.85	glc	glc

glc=

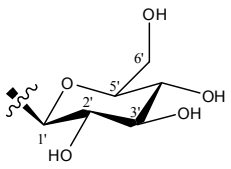

all=

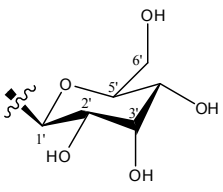

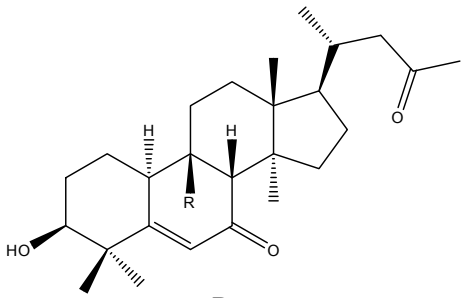

R

1.89 CH_3
1.90 CHO

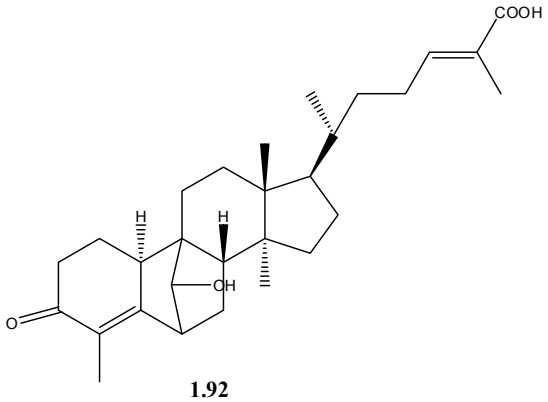

1.92

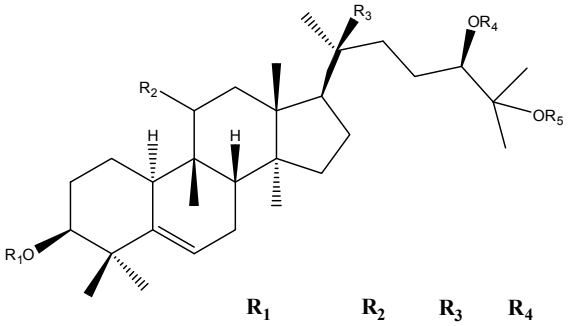

	R_1	R_2	R_3	R_4	R_5
1.93	glc	α-OH	H	H	glc
1.94	glc	H	H	glc(1→6)glc	H
1.95	H	= O	H	glc(1→6)glc	H
1.98	H	= O	OH	glc	H
1.99	glc	= O	H	glc	H
1.100	glc	= O	H	glc	H
1.101	glc	β-OH	H	glc	H
1.102	glc(1→6)glc	= O	H	glc(1→6)glc	H

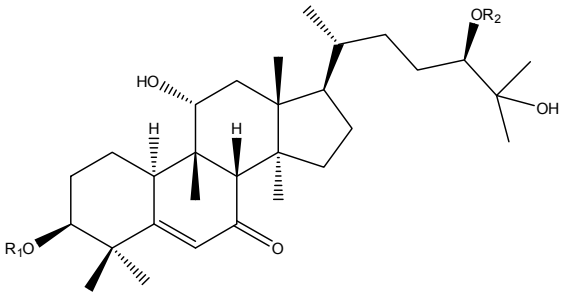

	R_1	R_2
1.96	glc	glc
1.97	glc(1→6)glc	glc(1→6)-glc(1→2)glc

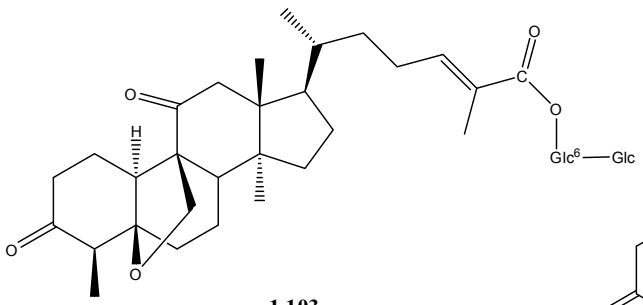

1.103

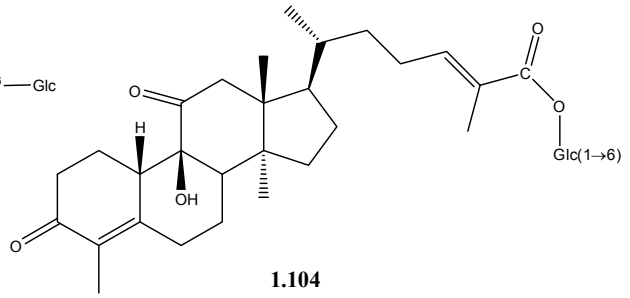

1.104

glc=

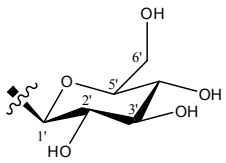

Other compounds

Besides cucurbitane-type triterpenoids, in the last years, some compounds from other classes were also isolated from *Momordica* species, as illustrated in Table 1.2.

Table 1.2. Other compounds isolated from *Momordica* species.

***Momordica* sp.**	***Analysed part***	***Class***	***Compounds***	***References***
M. charantia	Dried fruits	steroid	**1.105**	(Liu, 2010)
	Stems	triterpenoid	**1.106**	(Liu et al., 2010)
M. grosvenorii	Fresh fruits	flavonoid	**1.107 - 1.108**	(Li et al., 2006b)
M. foetida	Dried leaves	flavonoid	**1.109 - 1.112**	(Froelich, 2007)

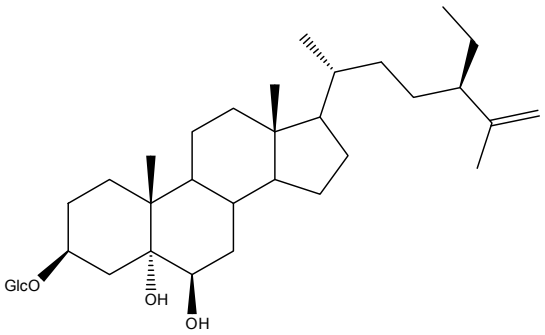

1.105

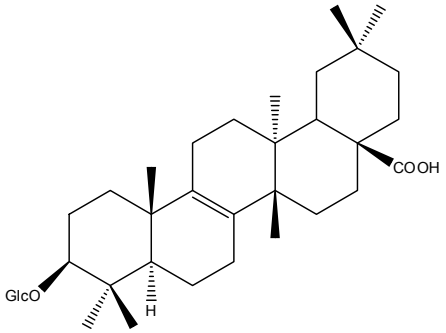

1.106

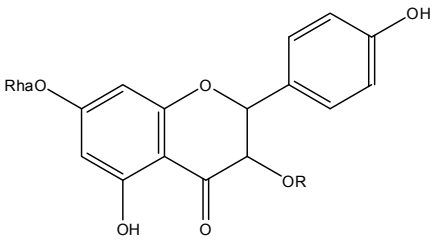

1.107 **R** = H
1.108 **R** = Rha

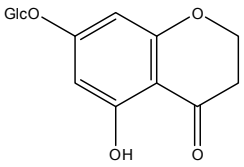

1.109

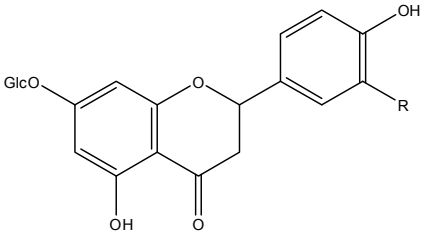

1.110 **R** = H
1.111 **R** = OH

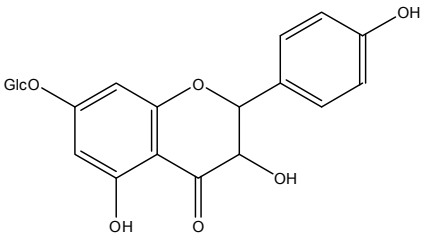

1.112

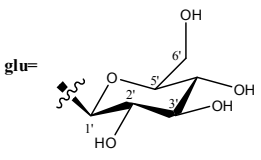

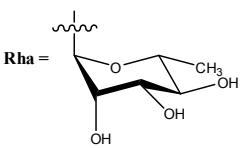

1.5. Biological activity of cucurbitane-type triterpenoids

Cucurbitane-type triterpenoids are a group of compounds with a broad range of potent biological activities namely, cytotoxic, hepatoprotective, anti-inflammatory, cardiovascular, antidiabetic and antiparasitic (Chen et al., 2005; Rios, 2005).

The cytotoxic and antiproliferative activities of cucurbitacin B (Liu et al., 2008a; Wakimoto et al., 2008; Zhang et al., 2009), cucurbitacin D (Rodriguez et al., 2003; Takahashi et al., 2009), cucurbitacin E , cucurbitacin I (Su et al., 2008), cucurbitacin Q (Figure 1.3) and some of their glycoside derivatives (Takasaki et al., 2003; Tannin-Spitz et al., 2007), have been widely studied in the last years, on several cancer cell lines. Moreover, the cytotoxic activity of recently isolated cucurbitane-type triterpenoids from *M. charantia* and *Cucumis melo*, was also studied (Akihisa et al., 2007b; Chen et al., 2009a; Chen et al., 2008b). It is important to note that synergic effect was demonstrated by some cucurbitacins when co-administer with current anticancer drugs, like doxorubicin (Liu et al., 2008a; Liu et al., 2008b; Sadzuka et al., 2010). This effect was also observed with the ethanol extract of leaves of *M. charantia* (Limtrakul et al., 2004).

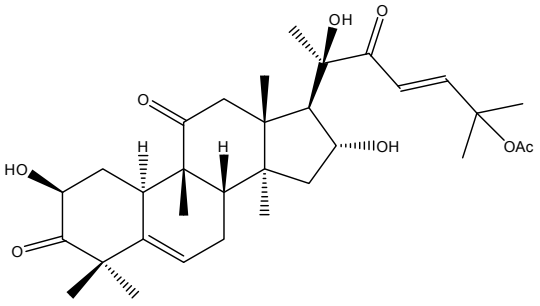

Cucurbitacin B

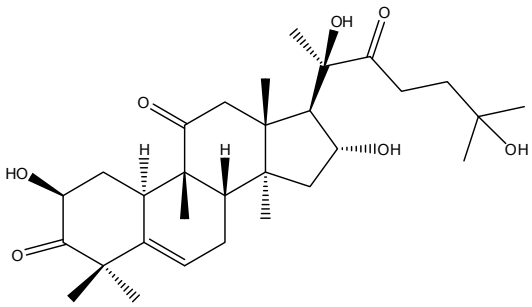

Cucurbitacin D: $\Delta^{23,24}$
Cucurbitacin R

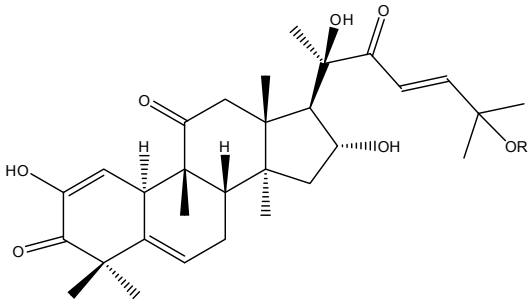

Cucurbitacin E: R = Ac
Cucurbitacin I: R = H

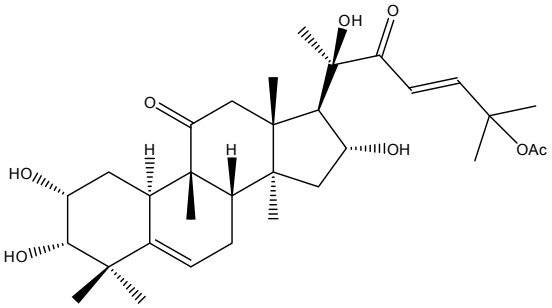

Cucurbitacin Q

Figure 1.3. Chemical structures of some cucurbitacins.

Concerning the anti-inflammatory effects, some studies demonstrated the activity of cucurbitacins R and B in the cycloxygenase (COX) enzymes and reactive oxygen species (ROS) systems (Escandell et al., 2007; Recio et al., 2004; Siqueira et al., 2007). In addition, hepatoprotective and hepatocurative effects were associated to the action of cucurbitacin B (Agil et al., 1999). Recently, it was demonstrated that the octanorcucurbitane triterpenoid **1.13**, isolated from *M. charantia*, had an hepatoprotective effect by acting on *tert*-butyl hydroperoxide (*t*-BHP)-induced hepatotoxicity and cytotoxic activities against human hepatoma HepG2 cells (Chang et al., 2010). From *M. grosvenorii*, two cucurbitane type triterpenoids have shown significant inhibitory effects on reactive oxygen species (O_2^-, H_2O_2 and, $^{\cdot}OH$) and on DNA oxidative damage (Chen et al., 2007).

Regarding the antidiabetic effects, a recent work showed that some cucurbitane-type constituents of *M. charantia*, namely compounds **1.40** and **1.61**, and their aglycones may provide leads for a new class of therapeutics for diabetes and obesity (Harinantenaina et al., 2006; Tan et al., 2008a; Tan et al., 2008b).

A recent work on the antiplasmodial activity of some cucurbitacins showed that cucurbitacins B (1.6 µg/mL) and D (4.0 µg/mL) were active against *Plasmodium falciparum* FcM29 strain (Banzouzi et al., 2008). A patent, filed in 2007, for a preparation containing cucurbitacins B and E, which are active against liver stages of *P. falciparum*, indicates that these compounds are of therapeutic interest and have a potential application in the malaria treatment (Hallwirth, 2007).

The anti-HIV-1 activity of some cucurbitane-type triterpenoids isolated from *M. charantia* (**1.09** and **1.16**) was also reported (Chen et al., 2008b).

2. MALARIA

Malaria is one of the most widespread infectious diseases in tropical and subtropical regions, including Central and South America, Asia and sub-Saharan Africa (Figure 1.4). Half of the world's population is at risk of malaria. In 2008, 247 million people became severely ill due to malaria infection, and nearly one to two millions of people die each year. Malaria is endemic in 108 countries (WHO, 2010a).

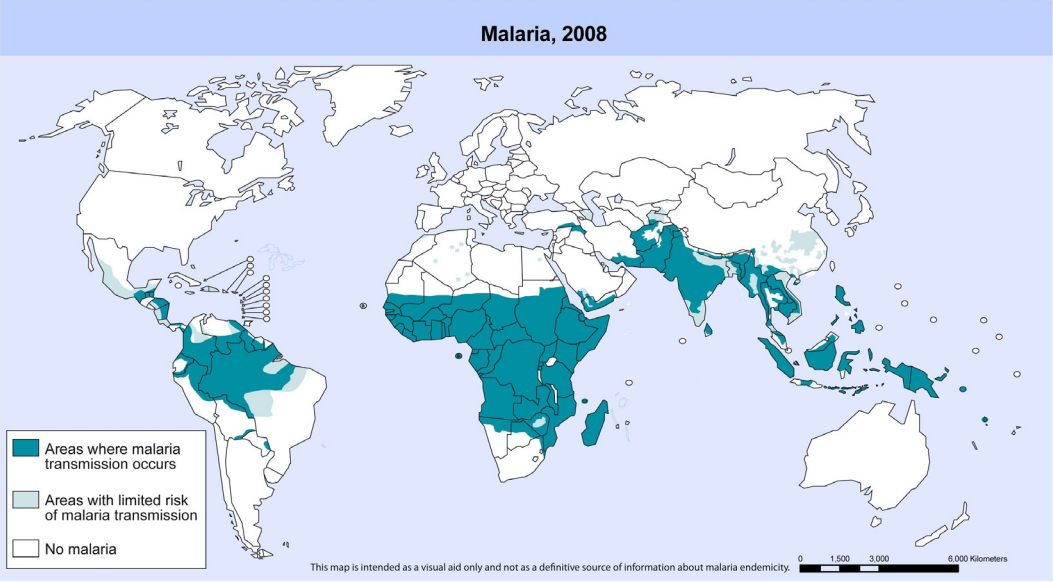

Figure 1.4. Malaria transmission map (Adapted from: WHO, 2008).[5]

The human malaria is caused by five species of protozoan parasites from the *Plasmodium* genus, namely: *Plasmodium falciparum*, *P. vivax*, *P. ovale*, *P. malariae*, and *P. knowlesi*. Among these, *P. falciparum*, found throughout tropical Africa, Asia, and in almost all the regions, is the most dangerous parasite to human health, due to its high pathogenicity and resistance to current drugs (Wells et al., 2009). *P. falciparum* together with *P. vivax* (Figure 1.5) are responsible for the majority of the malaria infections. *P. vivax* causes 25 - 40% of the overall malaria cases, particularly in South and Southeast Asia, and in Central and South America. This is less virulent than *P. falcipar*um; however, as reported in Papua (Indonesia), similar number of deaths were observed in children infected with *P. falciparum* and *P. vivax* (Poespoprodjo et al., 2009). The other two main species are *P. ovale*, confined to

[5] Adapted from web site (02-02-2010): http://www.emvi.org/malaria+vaccines/the+malaria+burden

tropical West Africa region, and *P. malariae*, worldwide distributed without a specific location (Kumar et al., 2003). These parasites are transmitted to humans through the bite of infected female *Anopheles* mosquitoes (Figure 1.5). The intensity of malaria transmission is influenced by ecological factors, such as, rainfall patterns (mosquitoes breed under wet conditions), presence of a determined mosquito species in the region and the proximity of mosquito breeding sites to human settlements (WHO, 2008b).

On the other hand, *P. knowlesi*, the primate malaria parasite is now recognized as the fifth species of *Plasmodium* that infects humans (Schottelius et al., 2010). Its distribution is mainly confined to Southeast Asian countries, with a tendency to widespread. There are some references to severe human cases of malaria attributed to *P. knowlesi* infections (Cox-Singh et al., 2010).

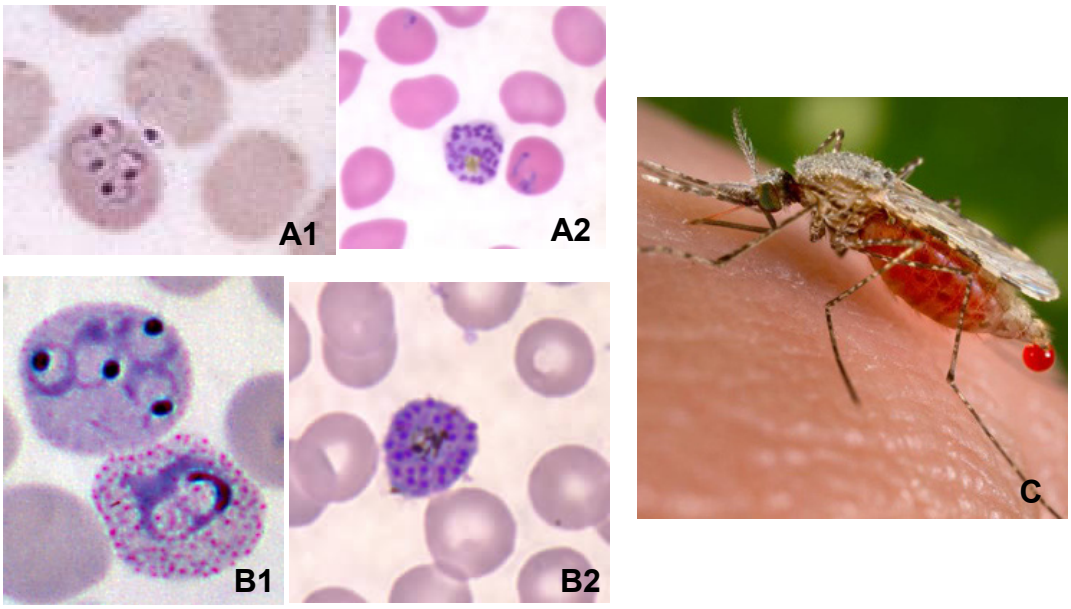

Figure 1.5. A. *P. falciparum* (1. immature form- trophozoite; 2. mature form- schizont with merozoites); **B.** *P. vivax* (1. immature form- trophozoite; 2. mature form- schizont with merozoites)[6]; **C.** *Anopheles* sp..[7]

As illustrated above, the major cause behind the re-emergence and severity of malaria throughout the world is the increasing resistance of malaria parasites, principally *P. falciparum*, to available drugs. This has stimulated investigators to search for novel antimalarial drugs. The development of new antimalarial drugs can be carried out by different strategies, ranging from minor modifications of existing agents to the design of novel agents

[6] Adapted from web site (27-03-2010): http://www.investigalog.com/biologia_y_ciencias_de_la_salud/queraltoa/malaria-segunda-parte-plasmodium-spp-vision-microscopica/?lang=pt
[7] Adapted from web site (02-02-2010): http://en.academic.ru/pictures/enwiki/65/Anopheles_stephensi.jpeg

that can act against new targets (Rosenthal, 2003). However, the success of malaria chemotherapy is closely related to the complete understanding of the interactions between the three major intervenients: human host, antimalarial drugs and malaria parasites (Na-Bangchang and Karbwang, 2009). Therefore, the understanding of the parasite's life cycle is a critical step.

2.1. Life cycle of the parasite

The human malaria parasite has a complex life cycle (Figure 1.6) that requires both a human host (carrier) and an insect host. In the mosquito, the parasite reproduces sexually (by combining sex cells). In the humans, the parasite reproduces asexually (by cell division), first in liver cells and then, repeatedly, in red blood cells. The infection begins with the bite of an infected female *Anopheles* mosquito. The mosquito salivary glands contain the infectious sporozoites that are introduced into the human blood during the blood feeding by the mosquito. The sporozoites, once released in the bloodstream, rapidly invade the hepatocytes, and begin the liver-stage cycle that ends with the disruption of the infected liver cells. Merozoites are released into the bloodstream and rapidly invade red cells and begin the asexual erythrocytic-stage cycle. Alternatively, some sporozoites of *P. vivax* and *P. ovale* turn into hypnozoites, a form that can remain dormant in the liver, for months or years. In the red blood cells, the parasite multiplies rapidly, and depending on the *Plasmodium* species, a single infected red cell gives rise to 48 - 32 asexual blood-form merozoites in 48 - 72 hours. Subsequently, the parasite lyses the infected red cells and the cycle is repeated. Some of these merozoites develop into female and male gametocytes that are essential for the transmission of the disease through the female *Anopheles* mosquito (Sharma, 2005). When the mosquito takes a bloodmeal of an infected person, gametocytes may be ingested. In the midgut of the insect, sexual recombination of the gametocytes takes place and the resulting sporozoites migrate into the salivary glands where the cycle begins again (Rathore et al., 2005; Turschner and Efferth, 2009).

Malaria main clinical symptoms are associated with the rupture of infected red cells, and production of tumor necrosis factors and other cytokines. Some of the most characteristic clinical manifestations include: headache, periodically recurrent fever (every 48 to 42 h), chills, myalgia, sudoresis, hepato- and splenomegalia, and the presence of high anaemia in children and pregnants with severe malaria. Severe *P. falciparum* human malaria can happen

principally due to its ability to adhere to capillary walls. Major complications include acute renal failure, acute pulmonary oedema, liver dysfunction, and cerebral malaria, and if not properly treated, they can lead to coma and death (Cooke et al., 2000; Newton et al., 2000). This disease occurs mostly in populations that are immune compromised, such as young children and travellers (Kumar et al., 2003; Rathore et al., 2005). For what concerns *P. falciparum* infections, a parasitaemia of 10% or more is observed and 1% or less for other species.

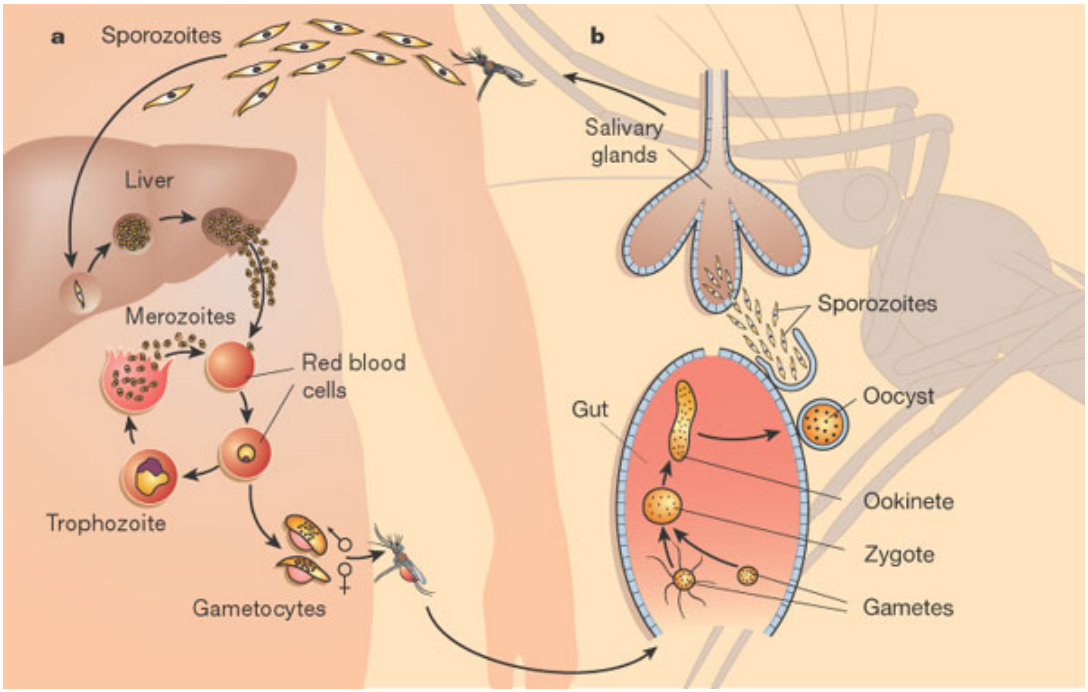

Figure 1.6. Life cycle of *Plasmodium falciparum* (Adapted from: Wirth, 2002).

During the trophozoite stage, a high metabolic activity is observed inside the red blood cell, with glycolysis of large amounts of imported glucose, ingestion of the host cell cytoplasm and proteolysis of haemoglobin into constituent amino acids. *P. falciparum* digests between 60 and 80% of the available haemoglobin inside the acidic food vacuole. The toxic product released during the digestion of the host haemoglobin, the haem, cannot be degraded by malaria parasites and therefore, is stored in their food vacuole in a polymerised non-toxic form called hemozoin (malaria pigment). The detoxification mechanism (Figure 1.7) has been widely studied as a useful target against malaria parasite (Egan, 2008; Hempelmann, 2007), specially due to its parasite specificity (Sharma, 2005).

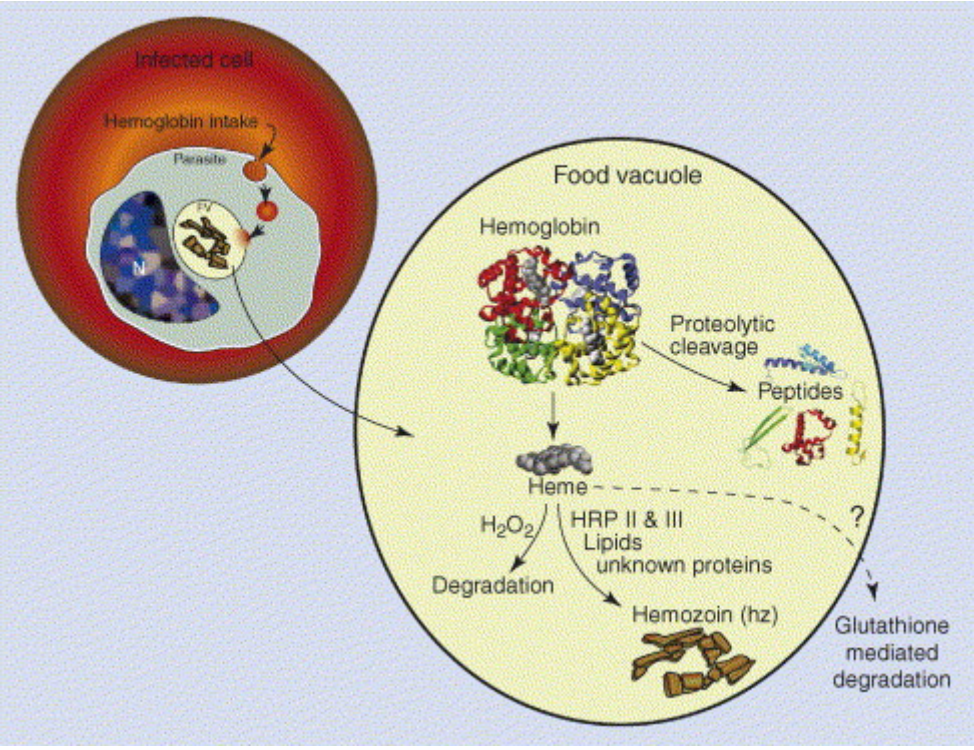

Figure 1.7. Haem detoxification mechanism (Adapted from: Rathore, 2006).

2.2. Currently available antimalarials

Nowadays, the prevention and treatment of malaria is done by a relatively small number of drugs. The most important are quinolines (e.g. chloroquine, primaquine, and quinine), folates (e.g. pyrimethamine and sulfadoxine), as well as atovaquone and the natural sesquiterpene lactone artemisinin, and its derivatives (Figures 1.08 - 1.10).

2.2.1. Quinolines

Quinoline-containing antimalarials have long been used to combat malaria. It was in 1940 that the 4-aminoquinoline, chloroquine (CQ), was introduced and proved to be during a long time, the drug of choice to treat malaria due to its efficacy, and reduced price. However, the spread of CQ resistant strains of *P. falciparum* has limited its use for the treatment of *P. vivax*, *P. ovale*, *P. malariae* and for uncomplicated *P. falciparum* malaria. To overcome this resistance, a number of compounds based on CQ scaffold were synthesized, producing firstly the active quinoline analogue amodiaquine. Amodiaquine has a better activity than CQ, and it

remains a common second-line drug in several malaria control programmes in Africa (Na-Bangchang and Karbwang, 2009). Primaquine, an 8-aminoquinoline, is extremely effective against hypnozoites, a latent form of liver-stage usually seen in *P. vivax* infection. This drug is also active against the sexual stages of the parasite and has been successfully used for the eradication of malaria in some islands of the Southwest Pacific (Rathore et al., 2005). Recent studies demonstrated that primaquine can be used as a CQ resistance reversal agent in *P. falciparum* resistant strains (Turschner and Efferth, 2009). However, administration of primaquine is associated with some adverse events, the most important of which is the one related to methaemoglobinaemia and haemolysis in glucose-6-phosphate dehydrogenase (G6PD)-deficient persons (Cappellini and Fiorelli, 2008).

Quinolinemethanol compounds are another class of quinoline antimalarials synthesized on the basis of CQ scaffold. They comprise the 4-quinolinemethanols, represented by mefloquine, and a group in which the quinoline portion of the 4-quinolinemethanols was replaced by a different aromatic ring system to form the aryl(amino)carbinols, represented by halofantrine. Both drugs proved to be effective against CQ-resistant malaria; however, there are problems with their cost and tolerability. The use of halofantrine is also restricted due to its potential to induce heart arrhythmia (Rathore et al., 2005).

Quinine, a quinolinemethanol compound, was the first drug used as an antimalarial. It is a natural compound obtained from the bitter bark of the Cinchona tree, native of South America. This drug has been the mainstay of treatment of severe malaria since the introduction of Cinchona bark in European medicine in the 1630s. There is evidence of a decline in the efficacy of quinine in Southeast Asia in terms of parasite and fever clearance in uncomplicated malaria, and coma recovery times in severe malaria. However, not any indication of a corresponding rise in mortality was observed (Faiz et al., 2005).

The mechanism of action of quinoline-containing antimalarial drugs is not yet completely understood. Nevertheless, it is generally accepted that the weak base selectively accumulates in the acidic food vacuole of the parasite and there exerts its antimalarial activity by interfering with the polymerization of toxic haem moieties, the products of haemoglobin digestion in the blood stage of the parasite (Foley and Tilley, 1998; Ginsburg et al., 1999; Martinelli et al., 2008).

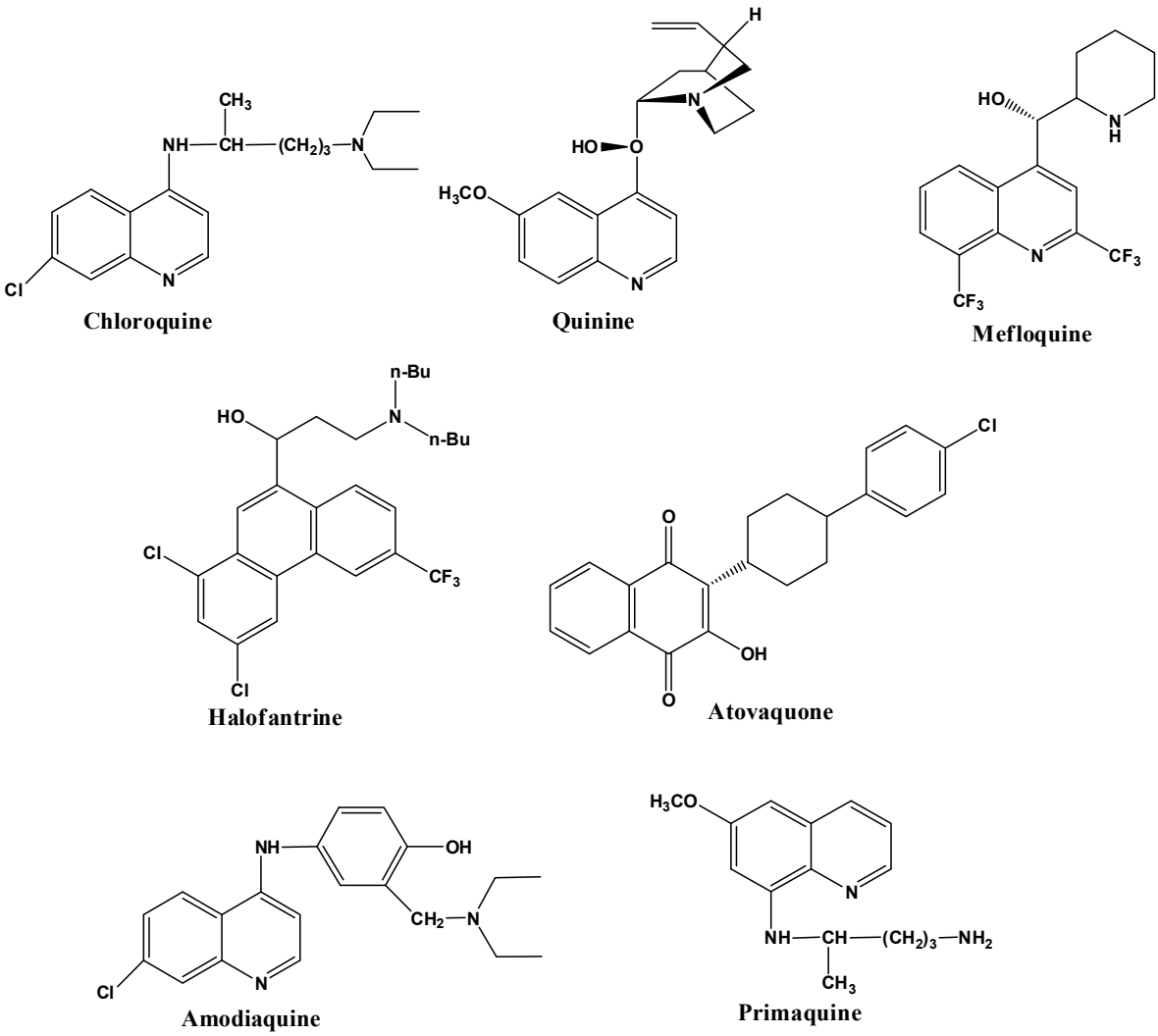

Figure 1.8. Chemical structures of quinoline-containing antimalarial drugs (chloroquine, quinine, mefloquine, amodiaquine, halofantrine and primaquine) and atovaquone.

2.2.2. Antifolates

The main antifolate drugs (Figure 1.9) include pyrimethamine, proguanil, a pro-drug metabolized to the active form cycloguanil, and the so-called sulfa drugs like sulfadoxine, as well as dapsone. They are administrated in combination to reduce the risk of drug resistance development. The most popular combination was pyrimethamine-sulfadoxine, used as the first-line alternative to CQ. However, due to loss of efficacy and development of resistance, new antifolate drugs and drug combinations are now in development and use, including atovaquone-proguanil (Malarone®) (Krudsood et al., 2007), chlorproguanil (Lapudrine)-dapsone (LapDaP®) (Lang and Greenwood, 2003) and combinations of a close analog of proguanil, PS-15 (N-(3-(2,4,5-trichlorophenoxy)propyloxy)-N'-(1-methylethyl)-midocarbonimidodiamide hydrochloride), (Edstein et al., 1997; Kinyanjui et al., 1999). The

mode of action of the antifolates is well known. These drugs interact with the folate pathway of the parasite by inhibiting essential enzymes. In this way, sulfadoxine inhibit the dihydropteroate synthetase, and pyrimethamine and cycloguanil interfere with dihydrofolate reductase. Resistance to these drugs arises from point mutations of the target genes *dhfr* and *dhps* (Martinelli et al., 2008).

The above cited drug, atovaquone, is a hydroxynaphtoquinone that acts on the parasite's mitochondrial electron transport by the inhibition of membrane depolarization. It was the rapid development of resistance, resulting from mutations in the cytochrome *b* gene, when administrated in monotherapy, which led to the formulation of a combination with proguanil (Turschner and Efferth, 2009).

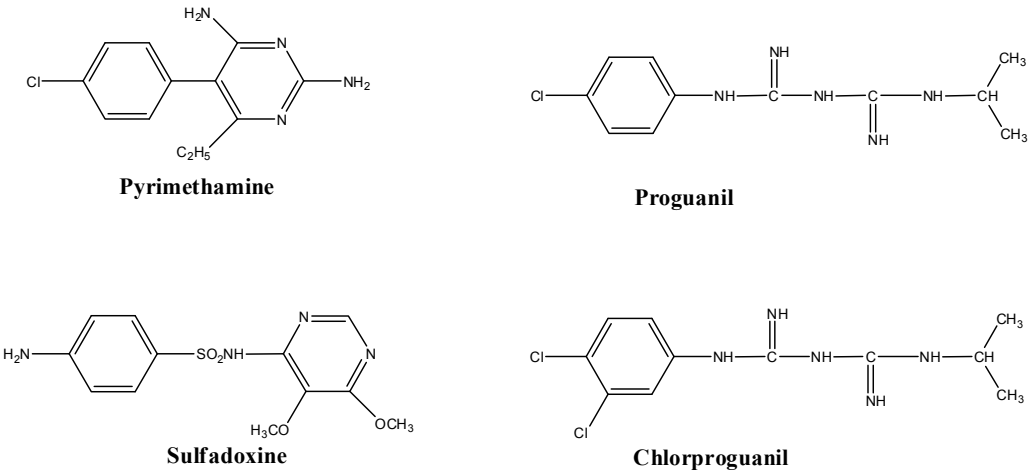

Figure 1.9. Chemical structures of antifolate compounds.

2.2.3. Artemisinin and its derivatives

Artemisinin or Quinghaosu, an endoperoxide-containing sesquiterpene lactone isolated from the plant *Artemisia annua*, is one of the most potent antimalarial drugs currently available. Artemisinin has been used, for more than 2000 years, in Chinese traditional medicine to treat fever resulting from malaria. Despite promising biological activity, difficulties in the formulation of artemisinin due to limited bioavailability and poor solubility led to the synthesis of several derivatives (Figure 1.10). Artemether, arteether and sodium artenusate are metabolized to dihydroartemisinin (Haynes, 2006), which is highly effective and can rapidly reduce parasitaemia. Artemisinins kill nearly all the asexual stages of parasite development in the blood and also delay the development of early sexual stages (gametocytes) of *P. falciparum*, which are transmitted during the bloodmeal by mosquitoes (White, 2008).

Nevertheless, these compounds do not affect pre-erythrocytic stage or the hypnozoite (latent stages) stage of *P. vivax* and *P. ovale* in the liver (White, 2008).

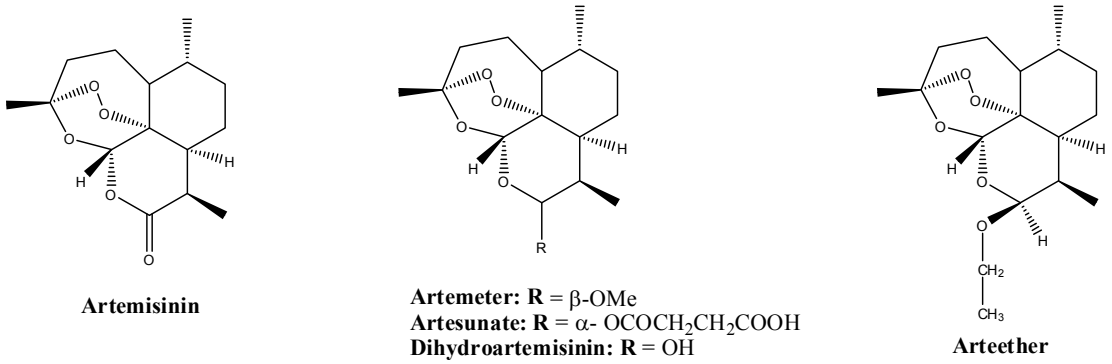

Figure 1.10. Chemical structures of artemisinin and derivatives.

Artemisinin drugs have a very short plasma half-life in the body and thus, a multiple dose regimen of seven days is required to achieve an acceptable cure rate. Normally, when artemisinins are used in monotherapy, recrudescence of parasites is observed (Woodrow et al., 2005). In order to circumvent this problem and minimize the development of resistance, artemisinins are used mainly in combination with other antimalarials, such as mefloquine, lumefantrine, piperaquine, amodiaquine and sulfadoxine-pyrimethamine, which operate on longer time scales. These combinations are named artemisinin combination therapies (ACTs). Although some cases of reduced-efficacy of artemisinin-based combination therapy (ACT) have been previously reported, these combinations are now being recommended by the WHO as the first-line treatment for *P. falciparum* infections in malaria endemic countries (WHO, 2010b). Nowadays, there are five fixed-dose ATCs available, and one is artemether-lumefantrine (Wells et al., 2009; WHO, 2010b). There are some evidences that resistance to this ATC, may be developing in some areas of East Africa (Denis et al., 2006). Artemisinins together with quinine are the only classes of drugs useful to treat cases of severe malaria presenting resistance to CQ; however, quinine has more clinical limitations (Krishna et al., 2004). The exact mechanism of action of artemisinin and its derivatives is still unclear. The peroxide within the 1,2,3-trioxane system seems to be essential for the antiparasitic activity (Krishna et al., 2008). The endoperoxide bridge of artemisinins is activated by ferrous iron generating free radicals, which subsequently alkylate haem, proteins and other molecules of the parasite (Asawamahasakda et al., 1994; Krishna et al., 2004). However, some studies showed that artemisinins are activated by nonhaem Fe^{2+} in the parasite cytoplasm, inhibiting

the parasite sarcoplasmic and endoplasmic reticulum Ca^{2+} ATPase (SERCA), as shown in Figure 1.11 (Eckstein-Ludwig et al., 2003; Fidock et al., 2008; Muraleedharan and Avery, 2009). The latter mechanism is supported by the isolation of some parasites, from French Guiana where artemisinins were used without control, that present mutations at SERCA, and consequently a reduced susceptibility to artemether (Gershenzon and Dudareva, 2007; Jambou et al., 2005; Ridley, 2003; Zhang et al., 2008).

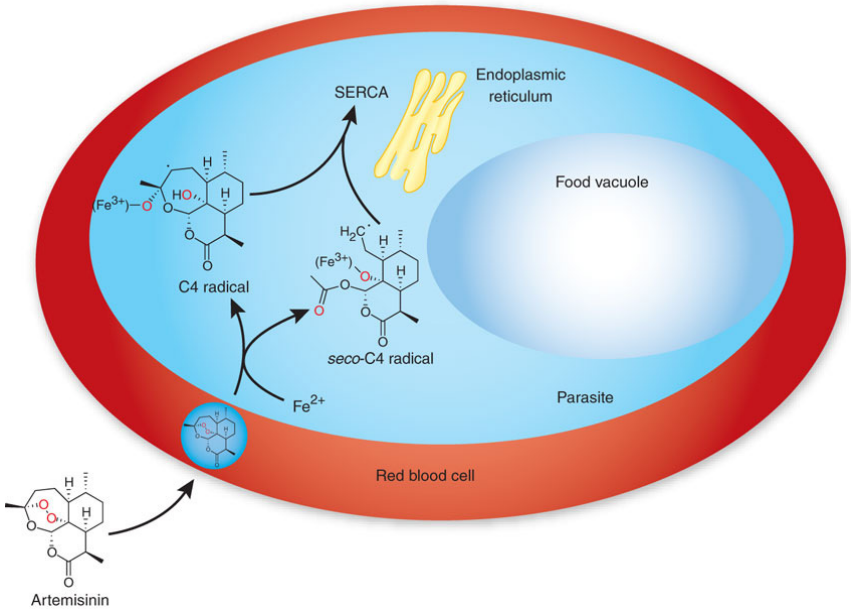

Figure 1.11. The most accepted mode of action of artemisinins against the malarial parasite. - Inhibition of sarco-endoplasmic reticulum Ca^{2+}-ATPase (SERCA) of the parasite, and consequently its growth (Adapted from: Gershenzon and Dudareva, 2007; Ridley, 2003).

2.3. Natural products as antimalarials

As illustrated above, natural products are one of the most important sources of antimalarials. In fact, quinine and artemisinin have demonstrated the enormous potential of natural compounds. They have provided powerful lead structures, which served as templates for the development of structurally simpler analogues, and they are also intrinsic effective antimalarials. As a matter of fact, plants have for many years formed the basis of traditional medicine systems, and continued to be used in countries where malaria is endemic, playing an essential role in health care. In Africa, up to 80% of the population uses traditional medicines as a source of primary health care (WHO, 2008a). In the last years, several screenings of different natural sources, especially plants used locally to treat malaria, and marine organisms, yielded some potential new antimalarial agents, with novel structures and a possible distinct

mode of action. These compounds have been extensively reviewed in the literature (Batista et al., 2009; Ioset, 2008; Kaur et al., 2009; Kumar et al., 2003; Oliveira et al., 2009; Saxena et al., 2003; Turschner and Efferth, 2009). Several classes of natural compounds displayed antimalarial activity, but alkaloids and some terpenes, mostly quassinoids and sesquiterpene lactones, have demonstrated the best results (Saxena et al., 2003). Indeed, for instance, the indoloquinoline cryptolepine from the West African plant *Crysptolepsis sanguinolenta*, used traditionally against malaria and other infectious diseases, has been identified as a lead to new antimalarial drugs (Wright, 2007; Wright et al., 2001). On the other hand, bruceantin, the quassinoid with the highest reported antimalarial activity, was also selected as a lead in the design of new antimalarials (Guo, 2005).

3. MULTIDRUG RESISTANCE

Resistance is defined as the temporary or permanent ability of an organism to remain viable and/or multiply under conditions that would destroy or inhibit other members from the same strain (Savjani et al., 2009). The development of resistance to multiple drugs is a major problem in the treatment of cancer and infections by pathogenic microorganisms. Multidrug resistance (MDR) is defined as the intrinsic or acquired simultaneous resistance of cells to the action of multiple classes of structurally dissimilar and functionally divergent drugs commonly used (Li et al., 2010). Several biochemical mechanisms (Figure 1.12) can be involved in MDR (such as, enzymatic inactivation of drugs, target modification, or reduction of accumulation within the cell); however, overexpression of membrane proteins, which mediate the active extrusion of drugs through the cellular membrane of human cells and microorganisms is one of the most studied (Savjani et al., 2009; Teodori et al., 2006; Wiese and Pajeva, 2001).

Membrane transporters can be classified as passive or active transporters. According to the mechanism of energy coupling, the active transporters are divided into primary- or secondary-active transporters. The ATP-binding cassette (ABC) transporters are primary-active transporters that use the energy derived from the hydrolysis of ATP to ADP by inherent ATPase activity to export substrates from the cell against a chemical gradient (Perez-Tomas, 2006). The ATP-binding cassette (ABC) proteins are ubiquitous among all the organisms, and

can carry a high variety of substrates across membranes, ranging from small molecules such as ions, sugars or amino acids to larger compounds such as antibiotics, anticancer drugs, lipids and oligopeptides (Perez-Tomas, 2006; Teodori et al., 2006). These transporters also take part in the uptake of nutrients or secretion of toxins in bacteria. The most critical problem in treatment failures occurs when ABC transporters are overexpressed, which leads to a decrease in intracellular drug concentration (Sauvage et al., 2009).

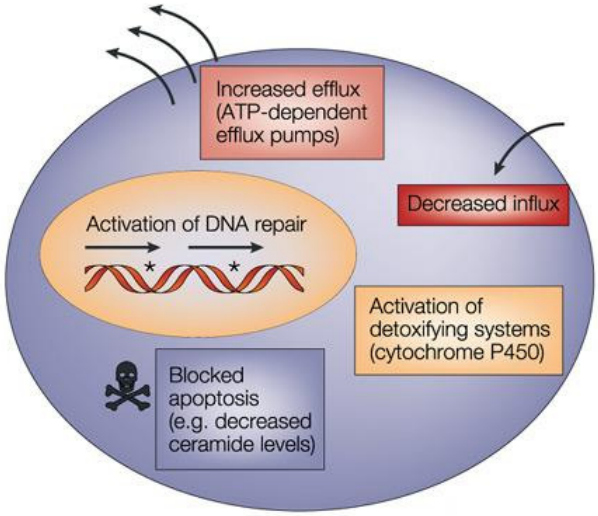

Figure 1.12. Biochemical mechanisms that cause drug resistance in cancer cells (Adapted from: Gottesman et al., 2002).

3.1. Multidrug resistance in cancer cells

Cancer is the second main cause of mortality in the developed countries, after the cardiovascular diseases. According to WHO, 7.9 million of people died from this pathology in 2007 (WHO, 2009). The conventional cancer chemotherapy is seriously limited by MDR. This phenotype is commonly exhibited by tumour cells, to which has been attributed the failure of treatment in over 90% of patients with metastatic cancer (Longley and Johnston, 2005). Human tumours can be intrinsically resistant to a number of chemotherapeutic drugs or develop such resistance after one treatment. As already mentioned, a major cause of cancer MDR is the overexpression of efflux pumps from the ABC (ATP-binding cassette) superfamily. In mammalian cells, three major groups of ABC transporters (Figure 1.13) are involved: the classical P-glycoprotein (P-gp) encoded by the *mdr1* gene, the multidrug resistance associated protein (MRP1) encoded by the *mrp1* gene, and the BCRP protein, an ABC half-protein (Gottesman et al., 2002; Perez-Tomas, 2006).

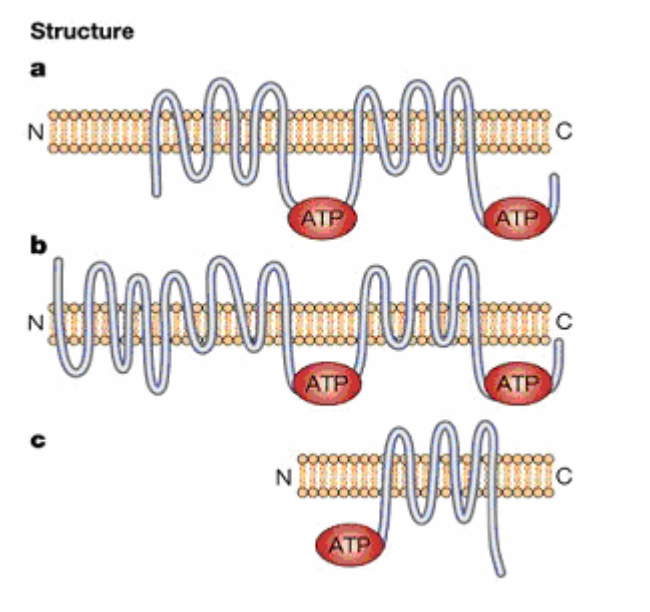

Figure 1.13. Structures of ABC transporters known to confer drug resistance to cancer cells (Adapted from: Gottesman et al, 2002). **a.** MDR1; **b.** MRP1; **c.** BCRP.

3.3.1. The human P-glycoprotein

The human P-glycoprotein (P-gp) was the first human ABC transporter to be cloned and characterized due to its ability to confer a multidrug resistance phenotype to cancer cells. This is an integral membrane polypeptide with 170-kDa, consisting of 1280 amino acids organized in two homologous halves of 610 amino acids joined by a linker region. Each half contains six putative transmembrane domains (TMD) and short hydrophilic N- and C-terminal segments. The C-terminal of each half, contains the sequence for a nucleotide binding site or domain (NBD), responsible for ATP-binding and hydrolysis (Aller et al., 2009; Yuan et al., 2008). Crystal structures of the ABC domains of several ABC transporters indicate that a functional ATP site is formed by the interaction of residues from both halves. Moreover, the structure of NBDs shows that the two NBDs form a "nucleotide-sandwich dimmer" with ATP bound along the dimmer interface (Chang and Roth, 2001; Schmitt, 2002; Shilling et al., 2003). Concerning the drug-substrate binding sites, it was demonstrated that they are localized within the hydrophobic transmembrane segments (Aller et al., 2009). In a recent work, Globisch and co-workers proposed that P-gp has multiple binding sites and multiple pathways for drug transport (Aller et al., 2009; Globisch et al., 2008). The existence of various substrate binding sites and different affinities of the substrate to these binding sites, explains the broad substrate diversity of P-gp, that includes a large variety of natural anticancer drugs such as doxorubicin and daunorubicin, vinblastine and vincristine,

colchicine, etoposide, teniposide and paclitaxel (Figure 1.14), (Avendano and Menendez, 2002; Gottesman et al., 2002; Ozben, 2006; Zhou et al., 2008). Recently, different computational methods and models were reviewed to predict ABC transporter substrate properties of drug-like compounds. However, no consensus was achieved (Demel et al., 2009).

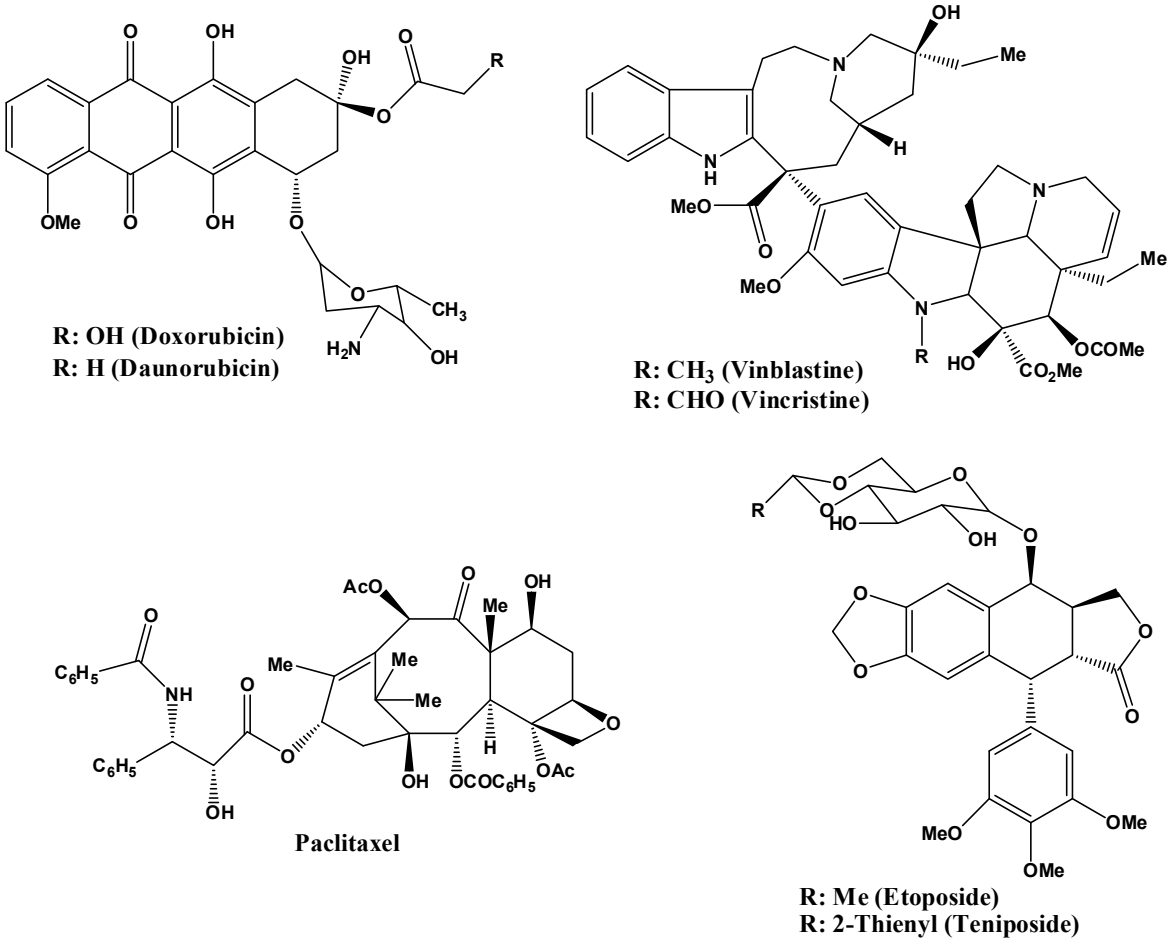

Figure 1.14. Chemical structures of some substrates of P-gp.

The mechanism of action of P-gp

The mechanism of P-gp efflux is not yet completely understood. There are several models (Figure 1.15) that try to explain the P-gp mechanism of action, namely, "hydrophobic vacuum cleaner", "flippase", and "aqueous pore". Among them, the "flippase" and "hydrophobic vacuum cleaner" are the most accepted (Varma et al., 2003). The "hydrophobic vacuum cleaner" mechanism suggests that P-gp recognizes hydrophobic substrates from either the inner or the outer leaflet of the lipid bilayer and translocates them through a central

channel (Varma et al., 2003). In other way, according to the "flippase" model, P-gp acts as a translocase or flippase. Firstly, the amphoteric drug inserts in the lipid bilayer, and only then interacts with the glycoprotein transporter which does the translocation to the outer leaflet of the bilayer from which they passively diffuse into extracellular fluid (Varma et al., 2003; Yuan et al., 2008). In all of these processes ATP binding and hydrolysis was found to be essential for the functioning of P-gp (Sauna et al., 2001).

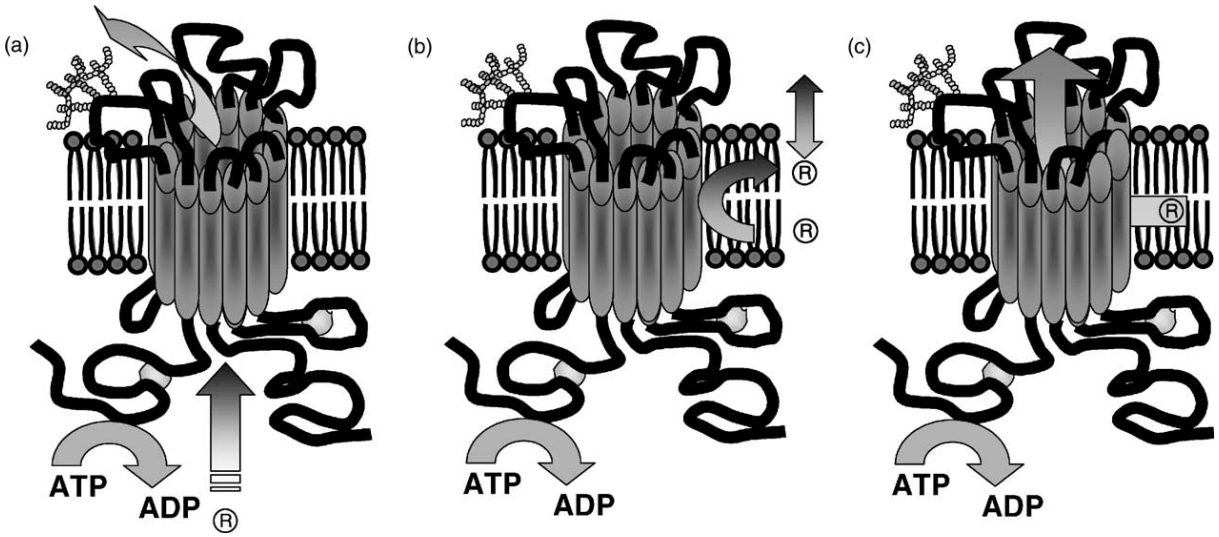

Figure 1.15. Models to explain the mechanism of drug efflux by P-gp (Adapted from: Varma et al., 2003). (**a**) Pore model; (**b**) flippase model and (**c**) hydrophobic vacuum cleaner model.

Cellular distribution of P-gp

It is well accepted that expression of P-gp is usually highest in tumours that are derived from tissues which normally expressed P-gp, like the liver, the kidney, the intestine, and the blood-brain and blood-placenta barriers. Its physiological function is still not completely clear, but its localization on mucosal epithelium is indicative of its implication in detoxification and disposition of lipophilic endogenous chemicals and xenobiotics. Once a xenobiotic has reached the systemic blood circulation, P-gp limits its penetration into the sensitive tissue (e.g. into the brain, testis and fetal circulation) and also into lymphocytes. There are evidences suggesting that P-gp may be involved in the transport and regulation of endogenous molecules such as hormones and phospholipids (Avendano and Menendez, 2002; Fusi et al., 2006; Varma et al., 2003).

3.1.2. Other ABC-transporters

Although P-gp has a widespread expression in many human cancers, some like lung cancers were found to rarely express it. In this type of cancer was found the overexpression of a 190 KDa protein that was identified as a member of the multidrug-resistance-associated proteins (MRP). MRP1 was the first to be discovered; it has a structure similar to P-gp, with the exception of an amino-terminal extension that contains five-membrane-spanning domains attached to a P-gp-like core (Figure 1.13). MRP1 and all members of this family induce resistance to anthracyclines, vinca alkaloids, epipodophyllotoxins, camptothecins, and methotrexate but not to taxanes (Zhou et al., 2008). They can transport negatively charged natural product drugs, such as glutathione (GSH), glucuronate, and other drug conjugates. MRP1 is also widely expressed in many human tissues and cancers (Perez-Tomas, 2006; Zhou et al., 2008).

The breast cancer resistance protein (BCRP) is another member of the ABC family, and is responsible for the transport of mitoxantrone, topotecan, irinotecan and methotrexate. Unlike MDR1 and the MRP family members, it only has one region with six transmembrane domains (Figure 1.13) and a single ATP-binding cassette, but it is presumed to function as a dimmer (Perez-Tomas, 2006).

3.2. Multidrug resistance in malaria parasite

Chloroquine (CQ), as already mentioned, is the selected drug for treating malaria. However, resistance to CQ is widespread in every geographic regions in which malaria is endemic. Resistance to CQ in malaria parasites shares several phenotypic features with MDR of human cancer cells, like the reduced accumulation of the drug and the reversing of resistance in the presence of verapamil. In fact, the work developed by Foote and Wilson led to the discovery of two genes encoding P-glycoprotein homologues of the human P-gp in *P. falciparum* - *pfmdr1* and *pfmdr2*, (Foote et al., 1989; Wilson et al., 1989).

P-glycoprotein homologue 1 (Pgh-1) is the protein product of *pfmdr1* gene located on chromosome 5 of *P. falciparum* (Figure 1.16). This is a 160 kDa protein predominantly located in the digestive vacuole membrane of the parasite, and associated with the regulation of intracellular CQ concentration. However, it was demonstrated that Pgh-1 expression levels are not always associated with chloroquine resistance, since equal amounts have been

detected in both chloroquine sensitive (CQS) and chloroquine resistant (CQR) strains tested (Cowman et al., 1991). In fact, it is now clear that the primary determinant for chloroquine resistance is not P-gh1 but, instead, another digestive vacuole membrane transport protein – the "*Plasmodium falciparum* Chloroquine Resistance Transporter" (*Pf*CRT), encoded by the *pfcrt* gene located on chromosome 7 of *P. falciparum*. It was demonstrated that *pfcrt* polymorphisms are more strongly associated with chloroquine-resistance than are *pfmdr1* polymorphisms. However, a combination of *pfcrt* and *pfmdr1* polymorphisms together results in higher levels of chloroquine-resistance (Cruz et al., 2009). *Pf*CRT is a 48 kDa protein localized in the digestive vacuole membrane in erythrocytic stage parasites, containing 424 amino acids, and 10 predicted transmembrane-spanning domains (Cooper et al., 2002; Fidock et al., 2000). The function and substrate or substrates of *Pf*CRT remain unknown. Several studies suggested that *Pf*CRT interacts directly with quinoline-based drugs, as well as chemosensitizing agents like verapamil (Cooper et al., 2005). Two possible mechanisms have been considered for the increased CQ efflux in resistant parasites. One is a channel model, in which deprotonated CQ passively leaks out of the food vacuole through mutated *Pf*CRT down along an electrochemical gradient. The other is a transporter model, in which *Pf*CRT is assumed to pump CQ out of the food vacuole in an energy-dependent manner (Mita et al., 2009)

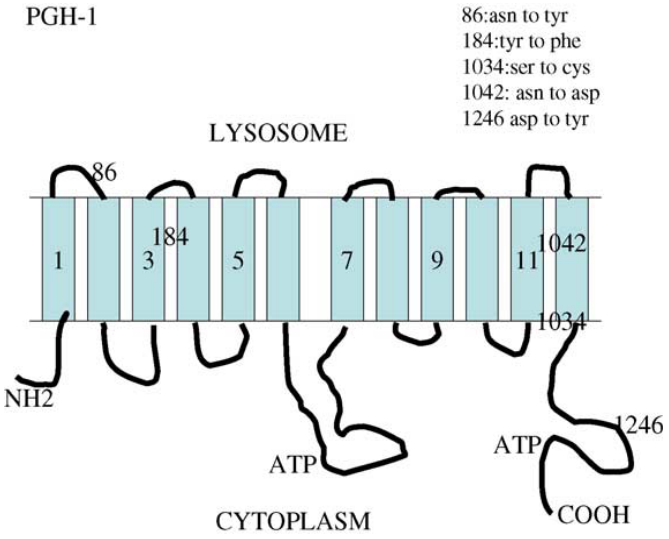

Figure 1.16. The Pgh-1 protein of *P. falciparum*. Polymorphic amino acids are indicated (Adapted from: Duraisingh and Cowman, 2005).

Regarding Pgh-1 substrate or substrates and its mechanism of action, they are not fully known. The most acceptable explanation is the one proposed for protein homologues in other

organisms (Hennessy and Spiers, 2007). According to this mechanism, Pgh-1 plays the role of clearing toxins from the cell cytosol, pumping them into the parasite's internal digestive vacuole, and if the protein is located on the parasite plasma membrane, these substances will be pumped out of the parasite (Hennessy and Spiers, 2007). Nowadays, it is known that Pgh-1 modulates the degree of chloroquine resistance in parasites that are resistant to this drug and its amplification, overexpression and/or mutations influence the susceptibility to other drugs such as, mefloquine, quinine and halofantrine; it also decreases the sensitivity to artemisinins (Sidhu et al., 2006).

3.3. Multidrug resistance in bacteria

Infectious diseases caused by bacteria are becoming more challenging to treat, as a result of the emergence of MDR pathogenic bacteria. The MDR phenotype is increasingly prevalent in bacteria strains, especially in Gram-positive pathogens such as *Staphylococcus aureus*, *Streptococcus pneumoniae* and *Enterococcus* spp. (Marquez, 2005). MDR is also prevalent in key Gram-negative clinical bacteria strains, such as *Escherichia coli*, *Salmonella* spp., *Klebsiella* spp., *Pseudomonas* spp., and *Enterobacter* spp. (Pages et al., 2008). The most frequent mechanisms by which bacteria become resistant to antibiotics include: antibiotic inactivation, target modification, and alteration of intracellular antibiotic concentration. The latter mechanism can occur by either decreasing permeability to an antibiotic or increasing the activities of a wide variety of efflux pumps (Savjani et al., 2009). Permeability plays a role in Gram-negative bacteria due to the presence of an outer membrane that does not exist in Gram-positive bacteria. This outer membrane is highly hydrophobic, providing these organisms with a permeability barrier and thus, a first line of defence against mainly hydrophilic compounds, such as macrolide antibiotics like erythromycin (Pages et al., 2008). Regarding efflux of antibiotics through membranes, this is a clinically significant general resistance mechanism in bacteria. Active drug efflux mechanisms can be specific for a given drug or class of drugs, the so-called single-drug resistance transporters, or can have a broad substrate specificity, covering a wide range of toxic compounds that are structurally and functionally unrelated, the so-called multidrug efflux (Savjani et al., 2009).

Based on bioenergetic criteria, transporters contributing to MDR can be classified into two main groups, namely, proton motive force (PMF) and ATP-dependent transporters. Within the proton gradient energy-driven class are included: the major facilitator superfamily

(MFS), the resistance nodulation cell division family (RND), the small multidrug resistance family (SMR), and the multidrug and toxic compound extrusion family (MATE). Within the ATP hydrolysis-driven energy class there are the so-called ABC-transporters, which are functionally related to the eukaryotic P-gp. Although, members from ATP transport system are usually involved in the resistance to only one drug (Single Drug Resistance - SDR transporters) (Marquez, 2005), some are known to be responsible for MDR phenotype in bacteria strains (Van Bambeke et al., 2000).

In this way, the first ABC-type transporter described in prokaryotic cells was the LmrA, a protein encoded by the *lmrA* gene present in *Lactococcus lactis*, a non-pathogenic bacterium. LmrA is responsible for the resistance to a large number of antibiotics, such as aminoglycosides, lincosamides, macrolides, quinolones, streptagramins, tetracyclines (van Veen et al., 2000; van Veen et al., 1999; VanVeen et al., 1996). The *L. lactis* genome contains many other genes that specify putative MDR systems (LmrC, and LmrD), (Lubelski et al., 2006; Lubelski et al., 2007). The presence of a bacterial ABC exporter homologous to LmrA, the Sav 1866, was also reported in *S. aureus*. This protein transporter is activated by typical MDR substrates (Dawson and Locher, 2006). Another example of bacterial ABC transporters is present in *E. faecalis*. The work developed by Lee and collaborators, suggested that in *E. faecalis* genome there are genes that encoded to EfrA and EfrB, two membrane proteins with similar structure that when in a heterodimer active form act as a multidrug efflux pump, which is structurally related to human P-gp (Lee et al., 2003).

In Gram-negative bacteria only a few number of ABC-type transporters have been reported to be involved in drug resistance. For instance, *E. coli* contains five putative ABC-type MDR-like transporters. The investigation of these transporters showed that none provided an appreciable drug resistance for *E. coli*, except the membrane protein YbjYZ, which confers resistance to erythromycin (Nishino and Yamaguchi, 2001).

However, it is well known that in prokaryotic organisms, MDR is mainly associated with secondary efflux transporters where energy required to pump a drug out the cell comes from the PMF class of transporters. In this way, in Gram-positive bacteria, this efflux is mediated mainly by single proteins from MFS efflux system. The most studied proteins from this group are the NorA pump from *S. auereus* (Markham et al., 1999), and its homologues in *B. subtilis*, the Bmr and Blt pumps (Neyfakh, 1992).

On the other hand, Gram-negative bacteria contain MDR transporters mostly members of the RND system. Comparing with efflux pumps of Gram-positive bacteria, these are more

complex due to the presence of an outer membrane. In this way, they form a tripartite protein channel, which requires a protein that crosses the periplasm, the membrane fusion protein (MFP) and an outer membrane efflux protein (OEP), together with the cytoplasmatic membrane-located transporter from RND family (Pietras et al., 2008). These multi-protein systems transport a wide variety of substrates including antibiotics, dyes, detergents and host derived molecules from the periplasm to the extra-cellular space. ACrA-AcrB-TolC from *E. coli* and MexA-MexB-OprM from *Pseudomonas aeruginosa*, are the two most studied tripartite systems (Murakami, 2008; Murakami et al., 2002; Sennhauser et al., 2009; Yu et al., 2003a; Yu et al., 2003b).

3.4. Multidrug resistance reversal agents

Many strategies for the overcoming of MDR have been proposed. The development of compounds able to restore the activity of the currently used drugs (MDR modulators, chemosensitizers, reversers), when administered in combination with the latter, is one of the most accepted (Ozben, 2006).

3.4.1. Modulators in cancer cells

So far, three generations of agents that act as P-gp inhibitors have been developed. The first generation of P-gp inhibitors (Figure 1.17) comprises drugs already used in clinical treatment for other pathologies. Verapamil, a calcium channel blocker, was the first compound able to modulate P-gp and enhance the cellular concentration of some anticancer drugs, such as vincristine, vinblastine, doxorubicin, and daunorubicin. Other chemosensitizers from the first generation are quinine, cyclosporine A, tamoxifene and nifedipine. These compounds had other pharmacological activities and were not specifically developed for inhibiting MDR pumps. They were themselves substrates for P-gp and competed with the cytotoxic drugs for efflux by the MDR pumps. Therefore, high serum concentrations of the chemosensitizers were needed to produce sufficient intracellular concentrations. These limitations prompted the development of new modulators that were more potent, less toxic and selective for the P-gp and other ABC transporters (Ozben, 2006; Yuan et al., 2008).

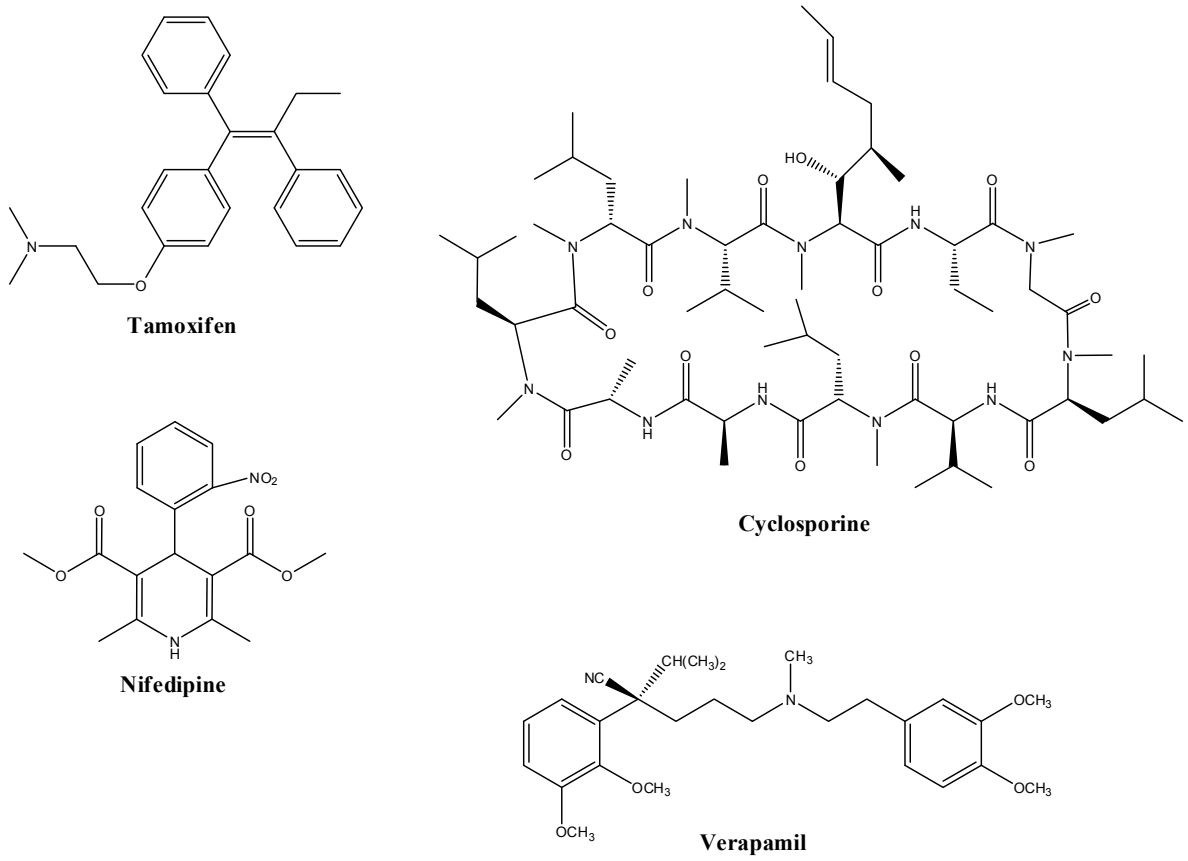

Figure 1.17. Some examples of the first generation P-gp inhibitors.

A second generation of P-gp inhibitors was designed to reduce the side effects of the first generation drugs. These compounds have a better pharmacologic profile and lower toxicity than the first generation compounds; however, they retain some characteristics that limit their clinical use. Some of them are also inhibitors of other ABC transporters or substrates of cytochrome P-450 that may result in pharmacokinetic interactions and increased host toxicity due to overexposure to cytotoxic drug. Typical examples are PSC-833, an analog of cyclosporine without the immunosuppressive effect, and dexverapamil, a chiral isomer of verapamil without its cardiac effect (Nobili et al., 2006; Ozben, 2006; Varma et al., 2003).

The third generation of P-gp inhibitors is characterized by a high affinity to P-gp or to other MDR transporters, mainly benefited from the progresses of structure-activity relationship (SAR) studies and combinatorial chemistry methods. Recently, the SAR studies of tariquidar and its analogs were reviewed. Tariquidar is one of the most promising chemosensitizers of the third generation (Pajeva and Wiese, 2009).

To address the lack of a clinical potent P-gp reverser in the medical practise, in the last years, there is an increasing interest in studying natural resources, such as compounds from

marine organisms and terpenoids from plants (Molnar et al., 2006). Therefore, a large number of compounds capable of reversing MDR phenotype have been found (Lee, 2010). Some of the most studied classes of compounds are the phenols, exemplified by curcumin and its derivatives that have shown to inhibit the function of the three major ABC transporters (Limtrakul, 2007). Macrocyclic diterpenes with jatrophane and lathyrane skeletons, isolated from *Euphorbia* species were found to be strong MDR modulators in tumor cells, by inhibiting the efflux-pump activity, mediated by P-gp (Corea et al., 2009; Duarte et al., 2006; Duarte et al., 2008; Duarte et al., 2007; Engi et al., 2007).

Mechanisms of action of MDR modulators

Different mechanisms of action of MDR modulators in cancer cells have been proposed. The most accepted one presumes that the modulating agent binds to P-gp thus, inhibiting competitively or noncompetitively the protein, decreasing in this way the drug efflux (Pajeva et al., 2005). Nevertheless, other mechanisms, such as modification of physico-chemical properties of the membrane or the disturbance of the lipid environment of P-gp by drugs that interact with cellular membrane, and the modulation of P-gp expression or interference with ATP hydrolysis are also possible ways to inhibit P-gp (Limtrakul, 2007; Varma et al., 2003).

Structure-activity relationships in MDR modulators

As illustrated above, although a large number of compounds have been found to be able to reverse MDR, so far no effective reversal agent has been approved for therapy. This seems to be associated with different features, namely, poor specificity for and low affinity of the inhibitor with the binding site, and also its interference with the pharmacokinetics of the anticancer drug administered (Mayur et al., 2009). And, due to the poor specificity, the *in vivo* plasma concentration required to inhibit P-gp of these compounds is too high and results in severe toxic side effects (Nobili et al., 2006).

The high heterogeneous chemical structure of molecules recognized and transported by P-gp has been considered a big challenge in drug modulators design. This situation is mainly associated with difficulties in establishing the right target sites on P-gp. Furthermore,

p-gp is a membrane protein strongly embedded in the lipid phase of plasma membranes, which cannot be purified at a sufficient level for crystallization studies. Consequently, until now any high-resolution 3D structure of P-gp was not obtained (Mayur et al., 2009).

Nevertheless, some general structural features have been associated with P-gp inhibitory activity, such as the amphiphilic nature of the molecules, the presence of aromatic rings, and a positive charge at neutral pH. Moreover, a diversity of P-pg modulators share specific recognition patterns, namely the presence of H-bond acceptor (or electron donor) groups (e.g. carbonyl, ether, hydroxyl, or halide groups) with a precise spatial separation. Taking into account these characteristics, it was suggested that P-gp modulation was based on the number and strength of electron donor groups separated by fixed distance in relation to the formation of hydrogen bonds. In this way, a high potential to form hydrogen bonds would be correlated with a high P-gp inhibitory property. Conversely, a low potential to form these bonds would correspond to a weaker inhibitory P-gp effect (Mayur et al., 2009). Although these general physicochemical properties have been recognized to play a role in MDR modulation, the exact structural parameters required for an effective modulator are still unknown.

Due to the limited knowledge about 3D structure of P-gp, different approaches have been used to analyse the chemical features involved in P-gp modulation properties. In quantitative structure-activity relationship (QSAR) studies, several molecular descriptors have been applied, and the one most studied is lipophilicity, often measured as the partition log *P* in the octanol/water system. In this way, high hydrophilic compounds were found to be inactive, emphasizing the importance of a required minimal lipophilic value. Other important descriptors are the molecular weight (MW) and also polar surface area (Prasanna and Doerksen, 2009; Srinivas et al., 2006).

The use of three dimensional quantitative structure-activity relationship models (3D QSAR), combined with pharmacophore modelling and docking, has also led to some general features for a P-gp pharmacophore (Mayur et al., 2009; Pajeva et al., 2005; Pajeva et al., 2009).

Moreover, the recently published high-resolution 3D structure of murine P-gp, which shows 87% sequence homology, might provide a new and promising starting point for docking and virtual screening (Aller et al., 2009), and contribute to design new drugs with the desired inhibitor properties.

3.4.2. Malaria parasite modulators

Regarding malaria parasite, quinoline resistance in *P. falciparum* is frequently compared to multidrug resistance in mammalian cells. As a matter of fact, the *in vitro P. falciparum* CQ resistance can be reversed by several known P-glycoprotein substrates, such as the calcium channel drug, verapamil, the antidepressant drug, promethazine, and also chlorpromazine, chlorpheniramine, and citalopram (Evans et al., 1998; Taylor et al., 2000). Verapamil was the first compound that demonstrated to reverse chloroquine resistance. However, the resistance reversal effects of verapamil cannot explain the global CQ accumulation; it results from a multiple gene modulation. In fact, CQ resistant strains can be either fully or partially sensitive to verapamil, and recent reports suggested that verapamil reversing activity was more pronounced in clones that express recombinant *Pf*CRT (Henry et al., 2008). On the other hand, the reversal of quinine resistant strains is made by the same type of chloroquine inhibitors (Henry et al., 2008). Resistance to quinine is determined by mutations in both Pgh-1 (Reed et al., 2000) and also in *Pf*CRT (Cooper et al., 2002). Conversely, molecules known to modulate mefloquine resistance activity are different from those used to modulate resistance to chloroquine and quinine. Some studies have shown that mefloquine efflux from resistant parasites was blocked by penfluridol (calmodulin inhibitors), but not by verapamil. Some other chemosensitizers included in this group are the synthetic surfactant NP30, and natural alkaloids like malagashanine (Henry et al., 2008). Moreover, some antifungal drugs like ketoconazole and also the quinine derivative, quinidine, reverse the resistance to mefloquine, but not by interacting with proteins involved in mefloquine efflux. Ketoconazole and quinidine are cytochrome P450 inhibitors, which act as inhibitors of hepatic microssomal CYP450, the human enzyme that metabolizes mefloquine. In this way, ketoconazole seems to regulate and slow down the rate of mefloquine biotransformation to carboxymefloquine (inactive), and thus helps to maintain higher concentrations of mefloquine. The activity of these inhibitors of hepatic microssomal CYP450 in one CYP-like enzyme in *P. falciparum* is not clearly known (Na-Bangchang et al., 2007; Wisedpanichkij et al., 2009).

Some natural compounds have also shown to modulate resistance in malaria parasite. An example is the already referred to malagashanine, an alkaloid isolated from the medicinal plant *Strychnos myrtoides* used traditionally in combination with CQ in the treatment of chronic malaria. Malagashanine showed to selectively enhance the *in vitro* antimalarial activity of quinolines (CQ, quinine and mefloquine), and halofantrine against chloroquine

resistant strains (Rafatro et al., 2000). A recent study has demonstrated that this alkaloid potentiates chloroquine antimalarial activity in the drug resistant *P. falciparum* strains (Ramanitrahasimbola et al., 2006).

3.4.3. Bacterial modulators

In bacteria, the main targets are the pumps from MFS efflux systems, including NorA, Tet(K) and Msr(A) transporters present in Gram-positive bacteria and the RND efflux systems present in Gram-negative bacteria, namely the tripartite AcrAB-TolC (*E. coli*) and MexAB-OprM (*P. aeruginosa*). For instance, several inhibitors have been developed to restore levofloxacin susceptibility in various *P. aeruginosa* clinical strains. The first efflux pump inhibitor (EPI) identified was MC-207 110 or phenylalanyl-arginyl-β-naphthylamide (PAβN), which not only showed effect on levofloxacin activity but also restored the activity of other antibiotic classes, including chloramphenicol and macrolides (Lomovskaya and Bostian, 2006).

Plants also provide a rich source of EPIs, and several compounds have been identified as potent inhibitors (Gibbons, 2003; 2004; 2008; Stavri et al., 2007). These compounds may act by inhibition of efflux pumps, e.g. inhibition of NorA efflux pump, from methicillin resistant *Staphylococcus aureus* (MRSA), by a chalcone isolated from *Dalea versicolor* (Fabaceae), or by synergistic effect via an uncharacterized mechanism (Belofsky et al., 2004). Examples of the first situation are also some natural phenolic compounds, such as epicatechin-gallate and epigallocatechin-gallate that showed to reverse not only the human P-gp, but also the MRSA strains (Gibbons et al., 2004; Hamilton-Miller and Shah, 2000; Jodoin et al., 2002). Moreover, carnosic acid and isopimarane derivatives isolated from *Rosmanirus officinalis* and *Lycopus europaeus*, respectively, showed to potentiate the activity of erythromycin against a macrolide-resistant *S. aureus* strain with the ABC transporter MsrA (Gibbons et al., 2003; Oluwatuyi et al., 2004). As a matter of fact, a recent study demonstrated that carnosic acid is a potent agent for reversing the down-regulation of *mdr1* *m*RNA and human P-gp expression in human leukaemia cell lines (Yuan et al., 2008).

CHAPTER 2

Results and Discussion

Phytochemical study of Momordica balsamina

1. STRUCTURAL ELUCIDATION OF CUCURBITANE-TYPE TRITERPENOIDS

Previous studies on *Momordica balsamina* reported the isolation of two phenylpropanoid esters, rosmarinic acid and five pimarane diterpenes (Detommasi et al., 1991; Detommasi et al., 1995).

In this work, the bioassay-guided fractionation of the methanol extract of *M. balsamina* led to the isolation of fourteen new cucurbitane-type triterpenoids, along with five known cucurbitacins and one megastigmane-type *nor*-isoprenoid (Table 2.1). Two of the cucurbitane triterpenoids were isolated in major quantities and were esterified to afford several esters (Table 2.2). Here, the physical and spectroscopic data that allowed the structural elucidation of the isolated compounds will be described and discussed.

Table 2.1. Compounds isolated from *Momordica balsamina*.

Compounds	Number
Balsaminapentaol, cucurbita-5,25-diene-3β,7β,23(*R*),24(*R*),29-pentaol	**36**
Balsaminagenin A, cucurbita-5,23(*E*)-diene-3β,7β,25,29-tetraol	**33**
Balsaminagenin B, 25-methoxycucurbita-5,23(*E*)-diene-3β,7β,29-triol	**34**
Balsaminagenin C, cucurbita-5,23(*E*)-diene-3β,7β,25-triol	**2**
Balsaminol A, cucurbita-5,24-diene-3β,7β,23(*R*),29-tetraol	**35**
Balsaminol B, 7β-methoxycucurbita-5,24-diene-3β,23(*R*),29-triol	**27**
Balsaminol C, cucurbita-5,24-diene-7,23-dione-3β,29-diol	**29**
Balsaminol D, 25,26,27-*trinor*-cucurbit-5-ene-7,23-dione-3β,29-diol	**31**
Balsaminol E, cucurbita-5,24-dien-7-one-3β,23(*R*)-diol	**26**
Balsaminol F, cucurbita-5,24-diene-3β,7β,23(*R*)-triol	**3**
Balsaminoside A, 25-methoxycucurbita-5,23(*E*)-dien-3β-ol-7-O-β-D-allopyranoside	**40**
Balsaminoside B, cucurbita-5,24-diene-3β,23(*R*)-diol-7-O-β-D-allopyranoside	**38**
Balsaminoside C, cucurbita-5,24-diene-3β,23(*R*)-diol-7-O-β-D-glucopyranoside	**39**
Cucurbalsaminol A, cucurbita-5,23(*E*)-diene-3β,7β,12β,25-tetraol	**32**
Cucurbalsaminol B, 7β-methoxycucurbita-5,23(*E*)-diene-3β,12β,25-triol	**28**
Cucurbalsaminol C, 7β-methoxycucurbita-5,24-diene-3β,12β,23(*R*)-triol	**30**
Karavilagenin C, 7β-methoxycucurbita-5,24-diene-3β,23(*R*)-diol	**1**
Karavilagenin E, 5β,19β-epoxycucurbita-6,24-diene-3β,23(*R*)-diol	**4**
Kuguaglycoside A, 7β-methoxycucurbita-5,24-dien-3β-ol-23-O-β-D-glucopyranoside	**37**
(+)-Dehydrovomifoliol, 4-cyclohexene-3-one-6-hydroxy-1,1,5-trimethyl-6-(3-oxo-1-butenyl)	**25**

Table 2.2. Derivatives obtained from balsaminol F (**3**) and karavilagenin C (**1**).

Compounds	**Nº**
Triacetylbalsaminol F, 3β,7β,23(*R*)-triacetoxycucurbita-5,24-diene	**23**
Tribenzoylbalsaminol F, 3β,7β,23(*R*)-tribenzoyloxycucurbita-5,24-diene	**24**
Karavoate A, 23(*R*)-acetoxy-7β-methoxycucurbita-5,24-dien-3*β*-ol	**5**
Karavoate B, 3β,23(*R*)-diacetoxy-7β-methoxycucurbita-5,24-diene	**6**
Karavoate C, 23(*R*)-propanoyloxy-7β-methoxycucurbita-5,24-dien-3*β*-ol	**7**
Karavoate D, 3β,23(*R*)-dipropanoyloxy-7β-methoxycucurbita-5,24-diene	**8**
Karavoate E, 23(*R*)-butanoyloxy-7β-methoxycucurbita-5,24-dien-3*β*-ol	**9**
Karavoate F, 3β,23(*R*)-dibutanoyloxy-7β-methoxycucurbita-5,24-diene	**10**
Karavoate G, 3β-benzoyloxy-7β-methoxycucurbita-5,23(*E*)-dien-25-ol	**11**
Karavoate H, 3β,23(*R*)-dibenzoyloxy-7β-methoxycucurbita-5,24-diene	**12**
Karavoate I, 23(*R*)-(*p*-nitrobenzoyloxy)-7β-methoxycucurbita-5,24-dien-3*β*-ol	**13**
Karavoate J, 3β,23(*R*)-di-(*p*-nitrobenzoyloxy)-7β-methoxycucurbita-5,24-diene	**14**
Karavoate K, 23(*R*)-(*p*-chlorobenzoyloxy)-7β-methoxycucurbita-5,24-dien-3*β*-ol	**15**
Karavoate L, 3β,23(*R*)-di-(*p*-chlorobenzoyloxy)-7β-methoxycucurbita-5,24-diene	**16**
Karavoate M, 23(*R*)-(*p*-methoxybenzoyloxy)-7β-methoxycucurbita-5,24-dien-3*β*-ol	**17**
Karavoate N, 3β,23(*R*)-di-(*p*-methoxybenzoyloxy)-7β-methoxycucurbita-5,24-diene	**18**
Karavoate O, 23(*R*)-cinnamoyloxy-7β-methoxycucurbita-5,24-dien-3*β*-ol	**19**
Karavoate P, 3β,23(*R*)-cinnamoyloxy-7β-methoxycucurbita-5,24-diene	**20**
Karavoate Q, 23(*R*)-succinoyloxy-7β-methoxycucurbita-5,24-dien-3*β*-ol	**21**
Karavoate R, 3β,23(*R*)-disuccinoyloxy-7β-methoxycucurbita-5,24-diene	**22**

1.1. Balsaminapentaol [cucurbita-5,25-diene-3β,7β,23(*R*),24(*R*),29-pentaol]

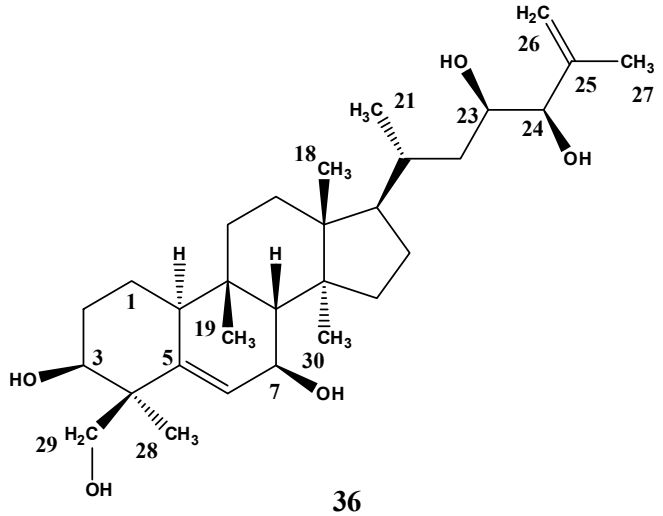

36

Compound **36**, named balsaminapentaol, is a new compound that was obtained as an amorphous powder with $[\alpha]_D^{26}$ + 85 (*c* 0.11, MeOH). Its IR spectrum showed the presence of hydroxyl groups (3408 cm^{-1}) and an exocyclic double bond (1651 cm^{-1}). The low resolution ESIMS spectrum of compound **36** exhibited a pseudomolecular ion at *m/z* 513 $[M + Na]^+$. The molecular formula was deduced as $C_{30}H_{50}O_5$, from its HR-ESITOFMS spectrum, which showed a pseudomolecular $[M + Na]^+$ ion at *m/z* 513.3553 (calcd. for $C_{30}H_{50}O_5Na$: 513.3550), indicating the presence of six degrees of unsaturation. The ^1H NMR spectrum of **36** displayed signals due to six methyl groups: four singlets corresponding to tertiary methyls (δ_H 0.76; 0.96, 2 ×; 1.05), a doublet of a secondary methyl at δ_H 0.92 (d, J = 6.5 Hz), and one vinylic methyl group (δ_H 1.70). The ^1H NMR spectrum also showed signals assignable to one diastereotopic methylene group [δ_H 3.65 (d, J = 11.0 Hz) and 3.95 (d, J = 11.0 Hz)], and four oxymethine protons [δ_H 3.63 (ddd, J = 10.8, 7.0, 1.86 Hz); 3.74 (d, J = 7.0 Hz); 3.82 (br s); 3.94 (br s)]. Furthermore, vinylic NMR signals of a trisubstituted double bond at δ_H 5.74 (d, J = 4.6 Hz) and a terminal double bond at δ_H 4.78 (br s) and 4.84 (br s) were also observed. The ^{13}C NMR and DEPT spectra displayed thirty carbon signals corresponding to six methyl groups, nine methylenes (including an oxygenated at δ_C 69.5, and one sp^2 carbon at δ_C 114.1), nine methines (four oxygenated at δ_C 68.5, 70.9, 75.3, and 81.6, and one sp^2 at δ_C 123.2), and six quaternary carbons (two olefinic carbons at δ_C 145.2, and 146.7). The data indicated a tetracyclic triterpenic scaffold for **36** with a hydroxyl group at one of the *geminal* methyl groups of ring A. This feature, which was consistent with the changes expected for the introduction of a hydroxyl group at C-29, was evidenced by the relative downfield signals of

H-3 (δ_H 3.82) and C-4 (δ_C 45.3) and upfield of Me-28 (δ_H 0.96) that usually resonate at $\delta_H \cong$ 3.50, $\delta_C \cong$ 42.3, and $\delta_H \cong$ 1.00, respectively (Mahato and Kundu, 1994). Moreover, the clear deshielding of H-3 (δ_H 3.82), probably due to intramolecular hydrogen bonding between the hydroxyl groups at C-29 and C-3, also corroborates the existence of a free hydroxyl group at the former carbon. Further structural details were obtained by two-dimensional NMR experiments (COSY, HMQC, and HMBC), which coupled with literature data allowed the unambiguous assignment of all carbon signals (Table 2.3).

Table 2.3. NMR data of balsaminapentaol (**36**), (MeOD, ^{1}H 500 MHz, ^{13}C 100.61 MHz; δ in ppm, J in Hz).

Position	^{1}H	^{13}C	DEPT	Position	^{1}H	^{13}C	DEPT
1	1.57 *m*; 1.70 *m*	22.0	CH_2	**16**	1.37 *m*; 1.89 *m*	28.9	CH_2
2	1.73 *m*; 1.85 *m*	30.1	CH_2	**17**	1.40 *m*	52.4	CH
3	3.82 *br s*	75.3	CH	**18**	0.96 *s*	16.0	CH_3
4	–	45.3	C	**19**	1.05 *s*	29.7	CH_3
5	–	145.2	C	**20**	1.71 *m*	33.5	CH
6	5.74 *d* (4.6)	123.2	CH	**21**	0.92 *d* (6.5)	19.0	CH_3
7	3.94 *br s*	68.5	CH	**22**	0.89 *m*; 1.49 *m*	41.0	CH_2
8	1.98 *br s*	53.9	CH	**23**	3.63 *ddd* (10.8, 7.0, 1.86)	70.9	CH
9	–	35.0	C	**24**	3.74 *d* (7.0)	81.6	CH
10	2.33 *dd* (12.0, 1.9)	39.9	CH	**25**	–	146.7	C
11	1.49 *m*; 1.69 *m*	33.7	CH_2	**26**	4.78 *br s* 4.84 *br s*	114.1	CH_2
12	1.54 *m*; 1.74 *m*	31.5	CH_2	**27**	1.70 *s*	18.0	CH_3
13	–	47.3	C	**28**	0.96 *s*	23.7	CH_3
14	–	49.2	C	**29**	3.65 *d* (11.0) 3.95 *d* (11.0)	69.5	CH_2
15	1.32 *m*; 1.40 *m*	35.6	CH_2	**30**	0.76 *s*	18.6	CH_3

The ^{1}H-^{1}H COSY (^2J, ^3J and ^4J couplings) and HMQC experiments revealed the following key fragments: –CH_2–CH(OH)– (A); –CH–C=CH–CH(OH)–CH– (B); –CH_2–CH(OH)–CH(OH)– (C); –C(CH_3)=CH_2– (D), (Figure 2.1). The heteronuclear $^2J_{C\text{-}H}$ and $^3J_{C\text{-}H}$ correlations displayed in the HMBC spectrum of **36**, indicated the location of the hydroxyl groups and the double bonds. In this way, HMBC correlations between C-3 (δ_C 75.3) and the

signals of the diastereotopic protons at δ_H 3.65 and δ_H 3.95 and Me-28 (δ_H 0.96), and between C-29 (δ_C 69.5) and Me-28 and H-3, placed the hydroxyl groups at C-29 and C-3. The hydroxyl group at the allylic carbon (C-7) was supported by the correlations between the olefinic carbons C-5 (δ_C 145.2) and C-6 (δ_C 123.2) and the oxymethine proton H-7 (δ_H 3.94). The presence of a diol system at C-23 and C-24 was indicated by the ^{1}H-^{1}H COSY coupling between H-23 (δ_H 3.63) and H-24 (δ_H 3.74), and was supported by the heteronuclear HMBC correlations observed between C-24 (δ_C 81.6) and H-23 and between C-26 (δ_C 114.1) and C-27 (δ_C 18.0) and H-24. Furthermore, long-range correlations between C-27 and the olefinic protons were also observed (Figure 2.1).

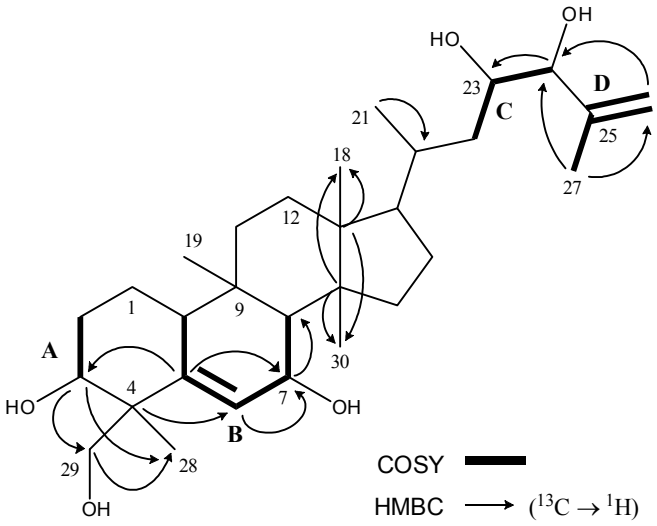

Figure 2.1. Key ^{1}H-^{1}H COSY and HMBC correlations of compound **36**.

The relative configuration of the tetracyclic system of **36** was determined using a NOESY experiment (Figure 2.2), taking into account cucurbitacins biogenesis (Xu et al., 2004) and by comparison of the coupling constants pattern with that reported in literature for similar compounds. The cross-peaks observed between H-10/Me-28, Me-28/H-3 and H-7/Me-30 supported the β-orientation of the hydroxymethyl group at C-4 and the hydroxyl groups at C-3 and C-7. Moreover, NOE correlations between Me-19/H-8, and H-8/Me-18 corroborated the β-orientation of these protons. In the side chain, the configuration at C-23 and C-24 was deduced as *R,R* by comparing the coupling constants of H-23 (J = 10.8, 7.0, 1.86 Hz) and H-24 (J = 7.0 Hz) of compound **36** with those reported in literature for a cycloartenol derivative with the same side chain [H-23 (J = 10.7, 6.5, 1.7 Hz) and H-24 (J = 6.5 Hz)] (Mohamad et

al., 1997). Similar values were also reported for alisol derivatives (Nakajima et al., 1994; Yoshikawa et al., 1993). In spite of the flexibility of the side chain, the NOESY spectrum showed strong correlations between Me-21/H-23, H-24/H-26, H-23/Me-27, which corroborated the *R* configuration of both H-23 and H-24. The energy minimization of the 3D structure of compound **36** was calculated for the four possible configurations, and the *R,R* model showed a good agreement with the experimental data (Figure 2.3), suggesting a preferred conformation for the side chain in spite of its possible free rotation. The minimization was carried out with the MMFF99x forcefield and a root mean square gradient at 0.00001, using MOE (Molecular Operating Environment).[8] The pictures of the referred models of **36** were visualized by using PyMOL[9]. Thus, **36** was determined to be cucurbita-5,25-diene-3β,7β,23(*R*),24(*R*),29-pentaol. To the best of our knowledge, this is the first occurrence of a cucurbitane-type triterpenoid with a 23,24-diol system coupled to an exocyclic double bound.

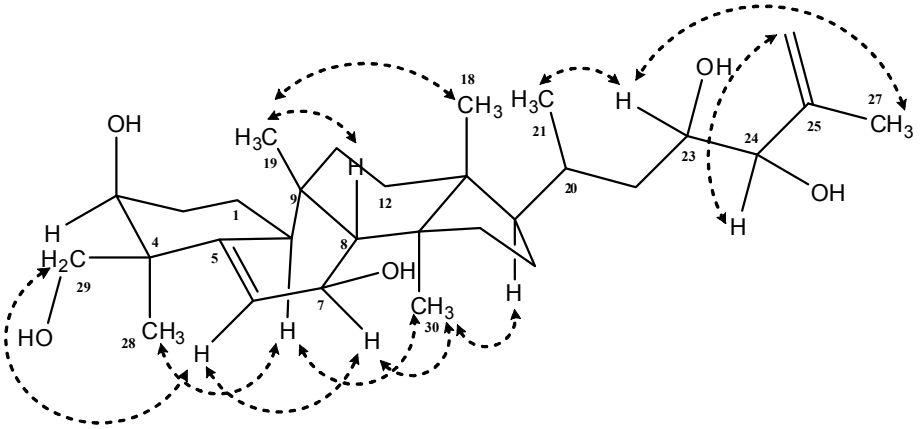

Figure 2.2. Key NOESY correlations of compound **36**.

[8] *Chemical Computing Group Inc. MOE v 2008. 1010 Montreal, Quebec, Canada, 2008.*

[9] *Warren L. DeLano 'The PyMOL Molecular Graphics System.' DeLano Scientific LLC, San Carlos, CA, USA. http://www.pymol.org.*

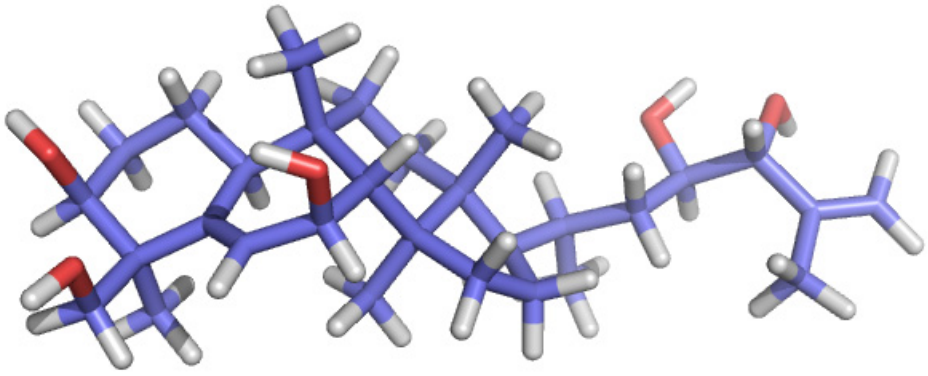

Figure 2.3. Energy-minimized 3D structure of compound **36**.

1.2. Balsaminagenin A [cucurbita-5,23(*E*)-diene-3β,7β,25,29-tetraol]

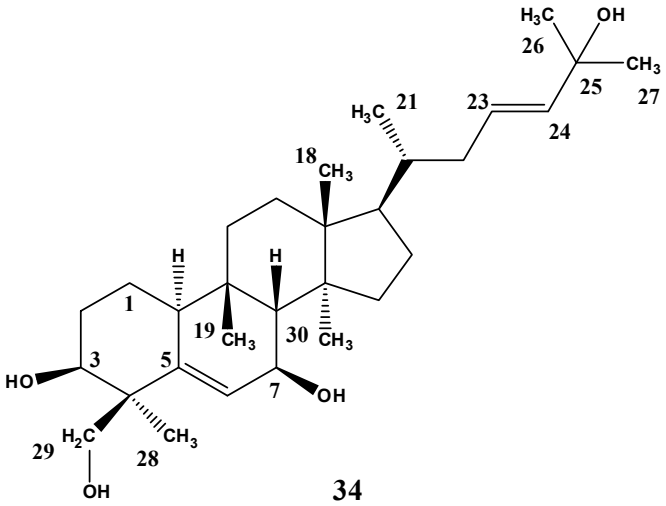

34

Compound **34**, named balsaminagenin A, is a new compound that was obtained as a white powder with positive optical rotation. The low resolution ESIMS spectrum of **34** exhibited pseudomolecular ions at *m/z* 513 $[M + K]^+$, 498 $[M + Na + H]^+$ and 497 $[M + Na]^+$. The molecular formula of **34** was determined as $C_{30}H_{50}O_4$ by HR-ESITOFMS, which showed a pseudomolecular ion at *m/z* 497.3612 (calcd. for $C_{30}H_{50}O_4Na$: 497.3601), indicating the presence of six degrees of unsaturation. The IR spectrum of **34** showed a strong absorption band at 3399 cm^{-1}, providing evidence for the presence of hydroxyl groups. Comparison of the NMR data of **34** (Table 2.4) with those of **36** (Table 2.3) showed that both compounds shared the same triterpenic nucleus, having different side chains. Compound **34** exhibited the

following ^{1}H and ^{13}C NMR signals for the side chain: two tertiary methyls (δ_H 1.25, 2 ×; δ_C 30.1, 30.0), a secondary methyl (δ_H 0.92, J = 5.8 Hz; δ_C 19.2), two olefinic protons (δ_H 5.57, 2 ×; δ_C 126.0, 140.8), as well as a quaternary carbon bounded to oxygen (δ_C 71.4). All the above data were consistent with the presence of a disubstituted double bound and a tertiary hydroxyl group at the side chain. The presence of the double bound was supported by analysis of the HMQC and COSY experiments, which identified the proton spin-system –CH_2–CH=CH–, (Figure 2.4). Its location at C-23 (δ_C 126.0) was deduced from long-range correlations, displayed in the HMBC spectrum, between C-22 (δ_C 40.3) and H-23/H-24 (δ_H 5.57), C-24 (δ_C 140.8) and the two methyl groups at δ_H 1.25 (Me-26, Me-27), and also between C-25 (δ_H 71.4) and the vinylic protons H-23/H-24. Moreover, the marked downfield resonances of the two geminal methyl groups at δ_H 1.25 (Me-26, Me-27) indicated that an hydroxyl group was attached to the allylic position C-25.

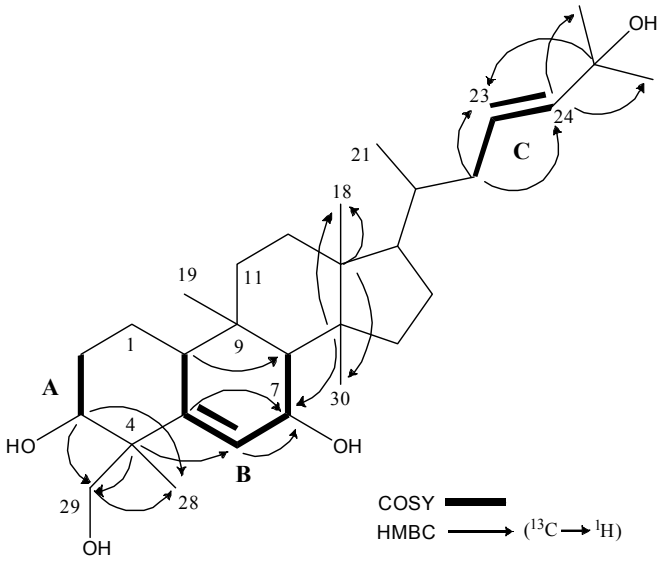

Figure 2.4. Main ^{1}H-^{1}H COSY and HMBC correlations of compound **34**.

The relative configuration of compound **34** was determined from the coupling constants and a NOESY experiment assuming an α orientation for the angular H-10, characteristic of cucurbitacins (Xu et al., 2004). The stereochemistry of the tetrahedral stereocenters of the triterpenic nucleus was found to be identical with that of balsaminapentaol (**36**). The configuration of the disubstituted double bound at C-23 could not be determined by the *vicinal* coupling constant values of the olefinic signals, due to their

overlapping. However, a detailed comparison of the ^{13}C NMR chemical shifts of the side chain carbons of **34,** with those of both *E*/*Z*-isomers of cycloart-23-ene-3β,25-diol (Takahashi et al., 2007), allowed the unequivocally assignment of an *E* geometry to that double bond. From the above data, the structure of **34** was deduced to be cucurbita-5,23(*E*)-diene-3β,7β,25,29-tetraol.

Table 2.4. NMR data of balsaminagenin A (**34**), (MeOD, ^{1}H 400 MHz, ^{13}C 100.61 MHz; δ in ppm, *J* in Hz).

Position	^{1}H	^{13}C	DEPT	Position	^{1}H	^{13}C	DEPT
1	1.58 *m*; 1.70 *m*	22.0	CH_2	**17**	1.53 *m*	51.2	CH
2	1.73 *m*; 1.90 *m*	30.1	CH_2	**18**	0.94 *s*	16.0	CH_3
3	3.83 *br s*	75.3	CH	**19**	1.05 *s*	29.7	CH_3
4	–	45.3	C	**20**	1.53 *m*	37.7	CH
5	–	145.2	C	**21**	0.92 *d* (5.8)	19.2	CH_3
6	5.74 *d* (4.5)	123.1	CH	**22**	1.76 *m*; 2.16 *d* (12.8)	40.3	CH_2
7	3.94 *br s*	68.6	CH	**23**	5.57 *m*[a]	126.0	CH
8	1.97 *br s*	53.9	CH	**24**	5.57 *m*[a]	140.8	CH
9	–	35.0	C	**25**	–	71.4	C
10	2.32 *br d* (10.2)	39.9	CH	**26**	1.25 *s*	30.1[b]	CH_3
11	1.48 *m;* 1.70 *m*	33.7	CH_2	**27**	1.25 *s*	30.0[b]	CH_3
12	1.50 *m*; 1.68 *m*	31.3	CH_2	**28**	0.97 *s*	23.6	CH_3
13	–	47.1	C	**29**	3.95 *d* (10.8)	69.5	CH_2
14	–	49.0	C		3.65 *d* (10.8)	–	–
15	1.31 *m* ;1.38 *m*	35.7	CH_2	**30**	0.76 *s*	18.6	CH_3
16	1.38 *m*; 1.96 *m*	28.8	CH_2				

[a] Overlapped signals.

[b] Interchangeable assignments.

1.3. Balsaminagenin B [25-methoxycucurbita-5,23(*E*)-diene-3β,7β,29-triol]

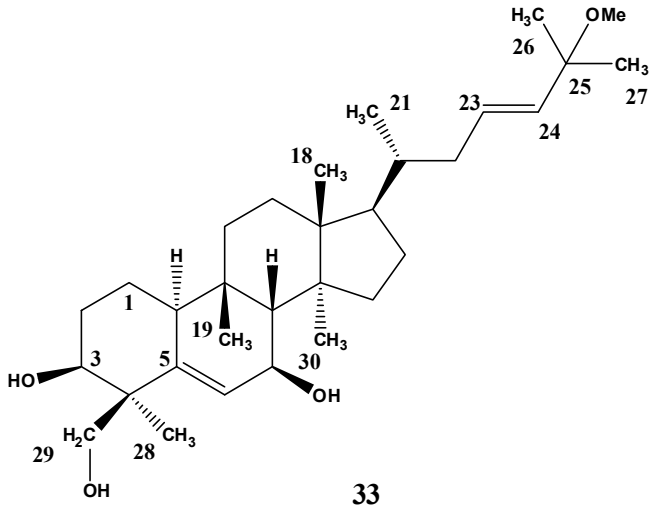

33

Compound **33**, named balsaminagenin B, is a new compound, which was obtained as white needles of m.p. 110 - 112 ºC and $[\alpha]_D^{20}$ + 101 (MeOH, *c* 0.10). Its HR-ESITOFMS showed a pseudomolecular ion at *m/z* 511.3758 $[M + Na]^+$ (calcd. for $C_{31}H_{52}O_4Na$: 511.3758), indicating the molecular formula $C_{31}H_{52}O_4$. The ^{13}C and ^1H NMR data (Table 2.5) of compound **33** were very similar to those of compound **34** (Table 2.4), excepting signals corresponding to the branched C_8 side chain at C-17. When comparing their ^{13}C NMR spectra, compound **33** showed paramagnetic effects at C-23 (+ 4.1 ppm; γ-carbon) and C-25 (+ 5.3 ppm; α-carbon) and diamagnetic effects at C-24 (– 3.2 ppm; β-carbon), C-26 (– 3.6 ppm; β-carbon) and C-27 (– 3.5 ppm; β-carbon). Besides, a downfield singlet corresponding to a methoxyl group appeared in the ^1H NMR spectrum of **33** (δ_H 3.13), which showed a ^{13}C resonance at δ_C 50.6. Moreover, in compound **33**, the stereochemistry of the disubstituted double bound at C-23 could be clearly determined as *E* by the large *vicinal* coupling constant values of the olefinic proton signals at δ_H 5.38 (d, J = 15.6 Hz) and δ_H 5.58 (ddd, J = 15.6, 8.8, 6.0 Hz), which were isochronous in compound **34**. The mentioned features indicated that compounds **33** and **34** differ in the substituent at C-25, having compound **33** a methoxyl group at that location instead a hydroxyl group. The position of the methoxyl group was corroborated by the long-range correlation observed in HMBC spectrum, between C-25 and the protons of the methoxyl group. The COSY and HMQC experiments allowed the unambiguous assignment of all the carbon signals (Table 2.5) and the establishment of the structure of **33** as 25-methoxycucurbita-5,23(*E*)-diene-3β,7β,29-triol.

Table 2.5. NMR data of balsaminagenin B (**33**), (MeOD, ^{1}H 400 MHz, ^{13}C 100.61 MHz; δ in ppm, *J* in Hz).

Position	^{1}H	^{13}C	DEPT	Position	^{1}H	^{13}C	DEPT
1	1.55 *m*; 1.70 *m*	22.0	CH_2	**17**	1.53 *m*	51.2	CH
2	1.70 *m*; 1.89 *m*	30.1	CH_2	**18**	0.95 *s*	16.0	CH_3
3	3.83 *br s*	75.3	CH	**19**	1.05 *s*	29.7	CH_3
4	–	45.3	C	**20**	1.54 *m*	37.6	CH
5	–	145.1	C	**21**	0.94 *d* (6.4)	19.3	CH_3
6	5.74 *d* (4.7)	123.1	CH	**22**	1.81 *m*; 2.18 *m*	40.5	CH_2
7	3.94 *br s*	68.5	CH	**23**	5.58 *ddd* (15.6, 8.8, 6.0)	130.1	CH
8	1.98 *br s*	53.9	CH	**24**	5.38 *d* (15.6)	137.6	CH
9	–	35.0	C	**25**	–	76.5	C
10	2.32 *br d* (9.2)	39.9	CH	**26**	1.24 *s*	26.2[a]	CH_3
11	1.46 *m*; 1.70 *m*	33.7	CH_2	**27**	1.24 *s*	26.5[a]	CH_3
12	1.51 *m*; 1.72 *m*	31.3	CH_2	**28**	0.97 *s*	23.6	CH_3
13	–	47.1	C	**29**	3.95 *d* (10.8)	69.5	CH_2
14	–	49.2	C		3.65 *d* (10.8)	–	–
15	1.33 *m*; 1.40 *m*	35.7	CH_2	**30**	0.75 *s*	18.6	CH_3
16	1.40 *m*; 1.95 *m*	28.8	CH_2	**25-OMe**	3.13 s	50.6	CH_3

[a] Interchangeable assignments.

1.4. Balsaminol A [cucurbita-5,24-diene-3β,7β,23(*R*),29-tetraol]

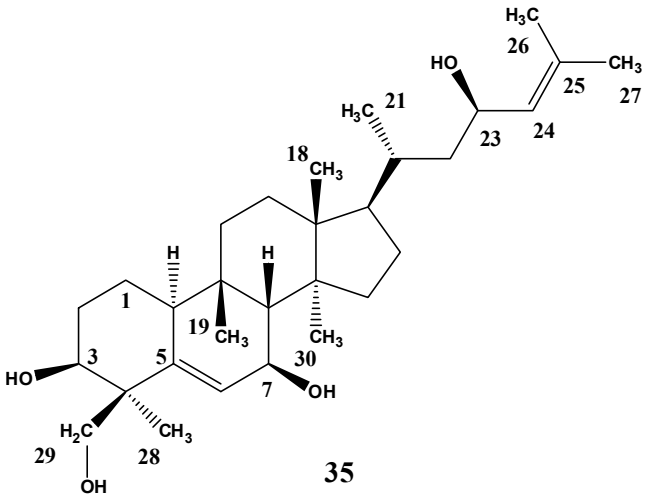

35

Compound **35**, named balsaminol A, is a new compound that revealed a pseudomolecular ion peak at *m/z* 497.3601 $[M + Na]^+$ (calcd. for $C_{30}H_{50}O_4Na$: 497.3601) in

its HR-ESITOFMS, corresponding to the molecular formula $C_{30}H_{50}O_4$, indicating six double bond equivalents. The NMR data of compound **35** (Table 2.6) clearly resembles those found for compounds **33**, **34**, and **36**, differing only in signals assignable to the side chain. Therefore, to the side chain, the ^{1}H and ^{13}C NMR spectra of **35** showed resonances for two allylic methyl groups (δ_H 1.66 and 1.70; δ_C 18.1 and 26.0), one secondary methyl group (δ_H 0.96, d, J = 6.3 Hz; δ_C 19.3), one oxygenated methine (δ_H 4.41, td, J = 9.5, 3.1 Hz; δ_C 66.6], and one olefinic proton of a trisubstituted double bound (δ_H 5.16, d, J = 8.5 Hz; δ_C 130.5). ^{3}J and ^{4}J couplings in the ^{1}H-^{1}H COSY spectrum supported the following substructure for the side chain –$CH(CH_3)CH_2CH(OH)CH=C(CH_3)_2$–, which was corroborated by the HMBC correlations observed between C-26 and C-27 with the olefinic proton at δ_H 5.16.

The stereochemical aspects of balsaminol A (**35**) were investigated by means of a NOESY experiment. The configuration of the tetrahedral stereocenters of the tetracyclic skeleton was found to be identical to that of compounds **33**, **34**, and **36**. Regarding the side chain, the configuration at C-23 was assigned as *R*, by comparison of the ^{13}C NMR data of the side chain carbons of **35** with those reported for the lanostane derivative 23(*R*)-3-oxolanosta-8,24-dien-23-ol, which structure was determine by X-ray crystallography, and for a cycloartane with 23(*S*) *c*onfiguration (Cantrell et al., 1996; Horgen et al., 2000). This assignment was corroborated by a strong NOE effect observed, in the NOESY spectrum, between Me-21 and the proton H-23. This experimental data was supported by the energy minimization of the 3D structure of compound **35** (Figure 2.5).[10,11] Consequently, the structure of **35** was determined to be cucurbita-5,24-diene-3β,7β,23(*R*),29-tetraol.

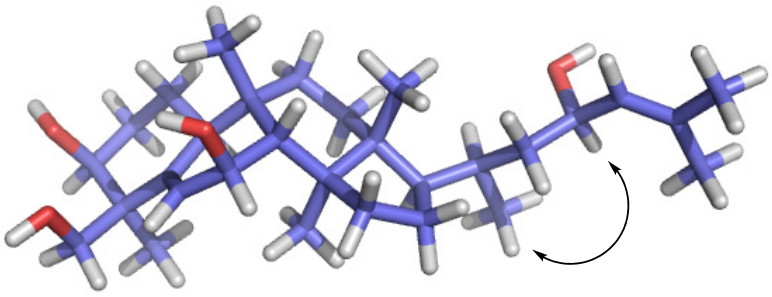

Figure 2.5. Energy-minimized 3D structure of compound **35**.

[10] *Chemical Computing Group Inc. MOE v 2008. 1010 Montreal, Quebec, Canada, 2008.*

[11] *Warren L. DeLano 'The PyMOL Molecular Graphics System.' DeLano Scientific LLC, San Carlos, CA, USA. http://www.pymol.org*

1.5. Balsaminol B [7β-methoxycucurbita-5,24-diene-3β,23(*R*),29-triol]

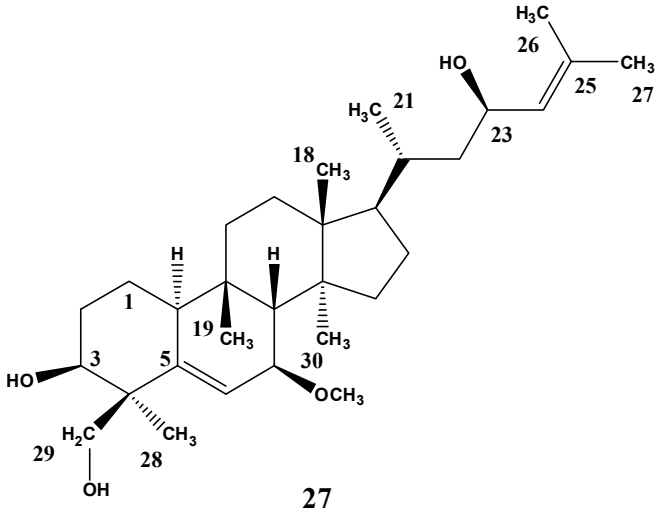

27

Compound **27**, named balsaminol B, is a new compound, which gave a pseudomolecular ion peak at *m/z* 511.3757 $[M + Na]^+$ (calcd. for $C_{31}H_{52}O_4Na$: 511.3758) in its HR-ESITOFMS spectrum, corresponding to the molecular formula $C_{31}H_{52}O_4$. The ^1H NMR and ^{13}C NMR data, of compound **27** (Table 2.6), were quite similar to those of compound **35** (Table 2.6), except for signals of ring B. When comparing their ^{13}C NMR spectra, compound **27** showed paramagnetic effects at C-5 ($\Delta\delta_C$ = + 1.2 ppm, γ-carbon) and C-7 ($\Delta\delta_C$ = + 10.2 ppm, α-carbon) and diamagnetic effects at C-6 and C-8 ($\Delta\delta_C$ = – 2.1 and – 4.8 ppm, respectively, β carbons), suggesting the presence of a methoxyl group at C-7, instead a hydroxyl group. This information was corroborated by the presence of a singlet corresponding to a methoxyl group at δ_H 3.33 in the ^1H NMR spectrum with a corresponding ^{13}C NMR resonance at δ_C 56.5. Its placement at C-7 was corroborated by the heteronuclear $^2J_{C\text{-}H}$ correlation of C-7 with H-8 and $^3J_{C\text{-}H}$ correlation between C-7 and the methoxyl group. The β-configuration of the 7-methoxyl group was assigned based on the Nuclear Overhauser Effect of H-7 (δ_H 3.49) and OCH3 (δ_H 3.33) with the biogenetically α-oriented Me-30 (δ_H 0.77) and the β-oriented H-8 (δ_H 2.06), respectively. From the above evidence, the structure of **27** was determined to be the new cucurbitacin 7β-methoxycucurbita-5,24-diene-3β,23(*R*),29-triol.

Table 2.6. NMR data of balsaminols A and B, (MeOD, ^{1}H 400 MHz, ^{13}C 100.61 MHz; δ in ppm, J in Hz).

Position	35			27		
	^{1}H	^{13}C	DEPT	^{1}H	^{13}C	DEPT
1	1.56 *m*; 1.70 *m*	22.0	CH_2	1.54 *m*; 1.70 *m*	22.0	CH_2
2	1.73 *m*; 1.89 *m*	30.1	CH_2	1.73 *m*; 1.85 *m*	30.1	CH_2
3	3.83 *br s*	75.3	CH	3.82 *br s*	75.4	CH
4	–	45.3	C	–	45.5	C
5	–	145.2	C	–	146.2	C
6	5.74 *d* (4.4)	123.2	CH	5.80 *d* (4.8)	121.1	CH
7	3.95 *br s*	68.5	CH	3.49 *br d* (3.7)	78.7	CH
8	1.98 *br s*	53.9	CH	2.06 *br s*	49.1	CH
9	–	35.0	C	–	35.1	C
10	2.33 *br d* (10.4)	39.9	CH	2.33 *br d* (10.4)	40.1	CH
11	1.47 *m*; 1.70 *m*	33.7	CH_2	1.49 *m*; 1.70 *m*	33.7	CH_2
12	1.55 *m*; 1.73 *m*	31.5	CH_2	1.54 *m*; 1.75 *m*	31.4	CH_2
13	–	47.2	C	–	47.4	C
14	–	49.1	C	–	49.2	C
15	1.32 *m*; 1.40 *m*	35.7	CH_2	1.34 *m*; 1.38 *m*	35.8	CH_2
16	1.39 *m*; 1.90 *m*	28.9	CH_2	1.38 *m*; 1.90 *m*	28.8	CH_2
17	1.46 *m*	52.1	CH	1.48 *m*	52.2	CH
18	0.97 *s*	16.0	CH_3	0.97 *s*[a]	15.9	CH_3
19	1.05 *s*	29.7	CH_3	0.98 *s*	29.3	CH_3
20	1.48 *m*	33.8	CH	1.48 *m*	33.8	CH
21	0.96 *d* (6.3)	19.3	CH_3	0.97[a]	19.3	CH_3
22	0.95 *m*; 1.63 *m*	45.6	CH_2	0.95 *m*; 1.63 *m*	45.6	CH_2
23	4.41 *td* (9.5, 3.1)	66.6	CH	4.41 *td* (9.6, 2.8)	66.6	CH
24	5.16 *d* (8.5)	130.5	CH	5.16 *d* (8.8)	130.5	CH
25	–	133.4	C	–	133.4	C
26	1.66 *s*	18.1	CH_3	1.66 *s*	18.1	CH_3
27	1.70 *s*	26.0	CH_3	1.69 *s*	26.0	CH_3
28	0.97 *s*	23.6	CH_3	0.96 *s*	23.6	CH_3
29	3.65 *d* (11.0)	69.5	CH_2	3.65 *d* (10.8)	69.6	CH_2
	3.95 *d* (11.0)	–	–	3.95 *d* (10.9)	–	–
30	0.76 *s*	18.6	CH_3	0.77 *s*	18.8	CH_3
7-OMe	–	–	–	3.33 *s*	56.5	CH_3

[a] overlapped signals.

1.6. Balsaminol C [cucurbita-5,24-diene-7,23-dione-3β,29-diol]

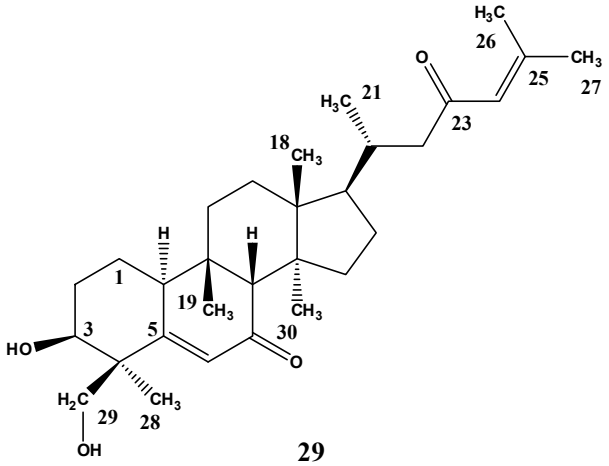

29

Compound **29**, named balsaminol C, is a new compound, which was obtained as an amorphous white powder. Its molecular formula was assigned as $C_{30}H_{46}O_4$ by HR-CIMS, which showed a pseudomolecular ion at *m/z* 471.3466 $[M + 1]^+$ (calcd. for $C_{30}H_{47}O_4$: 471.3474). The IR spectrum of **29** showed absorption bands at 3384 and 1641 cm^{-1}, a characteristic of the hydroxyl function and conjugated carbonyl groups, respectively. The UV spectrum exhibited an absorption maximum at 255 nm, corroborating the presence of α,β-unsaturated ketone groups. In the ^{13}C NMR spectrum, the existence of two relatively high-field carbonyl signals (δ_C 205.5 and 203.9), due to mesomeric effects, together with two remarkable downfield sp^2 carbons (δ_C 170.6 and 157.1), was consistent with the mentioned unsaturated systems. The ^1H NMR spectrum of **29** (Table 2.7) displayed signals for four tertiary methyl groups (δ_H 0.91, 0.96, 0.98, and 1.11), two vinylic methyls (δ_H 1.91, and 2.12), one secondary methyl group at δ_H 0.92 (d, J = 7.0 Hz), and one diastereotopic methylene group bounded to an oxygen at δ_H 3.72 (d, J = 10.9 Hz) and 3.90 (d, J = 10.9 Hz). In addition, a broad singlet of an oxygenated methine proton at δ_H 3.92, assignable to H-3 with an equatorial configuration, and signals for two trisubstituted double bonds (δ_H 6.10 and 6.18) were also found. The ^{13}C NMR spectrum displayed 30 carbon resonances discriminated by a DEPT experiment as seven methyl groups, eight methylenes (one carbon bearing oxygen at δ_C 68.7), seven methines (including an oxygenated sp^3 carbon at δ_C 75.5 and two sp^2 carbons at δ_C 126.9, and 125.3) and eight quaternary carbons (two sp^2 at δ_C 170.6, 157.1, and the carbonyl signals at δ_C 205.5 and 203.9). According to the molecular formula $C_{30}H_{46}O_4$, compound **29** contains eight degrees of unsaturation and therefore a tetracyclic triterpenoid

scaffold, having two hydroxyl groups and two enone systems is proposed. Besides the characteristic hydroxyl at C-3, the location of an unusual hydroxyl group at C-29 was also indicated by the changes observed in NMR data for carbons and protons of ring A, which were similar to those previously referred to for compounds **27**, and **33 - 36** (Tables 2.3 - 2.6).

The ^{1}H-^{1}H COSY and HMQC experiments revealed the structure of the following spin-systems (Figure 2.6): –CH_2–CH(OH)– (A); –CH_2–CH–C=CH– (B); –CH(CH_3)–CH_2– (C) and –CH=C(CH_3)$_2$– (D).

Table 2.7. NMR data of balsaminol C (**29**), (MeOD, ^{1}H 400 MHz, ^{13}C 100.61 MHz; δ in ppm, J in Hz).

Position	^{1}H	^{13}C	DEPT	Position	^{1}H	^{13}C	DEPT
1	1.77 *m*; 1.88 *m*	22.0	CH_2	**17**	1.57 *m*	51.3	CH
2	1.75 *m*; 1.99 *m*	29.8	CH_2	**18**	0.96 *s*	15.9	CH_3
3	3.92 *br s*	75.5	CH	**19**	0.98 *s*	28.2	CH_3
4	–	47.2	C	**20**	2.04 *m*	34.9	CH
5	–	170.6	C	**21**	0.92 *d* (7.0)	20.2	CH_3
6	6.10 *s*	126.9	CH	**22**	2.10 *m*; 2.54 *m*	52.7	CH_2
7	–	205.5	C	**23**	–	203.9	C
8	2.39 *s*	61.1	CH	**24**	6.18 *s*	125.3	CH
9	–	37.0	C	**25**	–	157.1	C
10	2.84 *br d* (11.3)	41.7	CH	**26**	1.91 *s*	20.9	CH_3
11	1.47 *m*; 1.89 *m*	32.2	CH_2	**27**	2.12 *s*	27.7	CH_3
12	1.28 *m*; 1.63 *m*	30.9	CH_2	**28**	1.11 *s*	23.3	CH_3
13	–	47.0	C	**29**	3.72 *d* (10.9)	68.7	CH_2
14	–	49.7	C		3.90 *d* (10.9)	–	–
15	1.03 *m*; 1.56 *m*	35.8	CH_2	**30**	0.91 *s*	18.8	CH_3
16	1.36 *m*; 1.99 *m*	29.0	CH_2				

The connection of these structural fragments and the location of the functional groups were determined on the basis of key long-range correlations, displayed in the HMBC spectrum (Figure 2.6). The α,β-unsaturated carbonyl carbon at C-7 was supported by the $^{2}J_{C\text{-}H}$ correlation between the carbonyl signal (δ_C 205.5) and H-8 (δ_H 2.39). On the other hand, the

presence of an enone system at the side chain was supported by the HMBC long-range hetero-correlations between the carbons of the vinylic methyls (δ_C 20.9, 27.7), and also the carbonyl group (δ_C 203.9) with the vinylic proton H-24 (δ_H 6.18). The ion at m/z 345 [M – side chain]$^+$, displayed by the EIMS, together with the ion at *m/z* 373 [M – $CH_2COCHC(CH_3)_2$]$^+$, arising from cleavage of the C-20–C-22 bound, confirmed the proposed structural feature for the side chain.

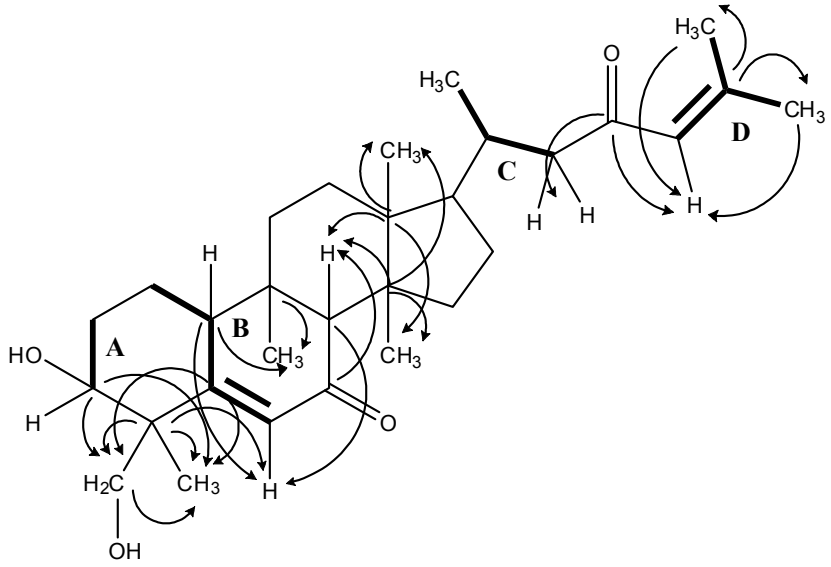

Figure 2.6. ^{1}H-spin systems (A - D) of compound **29** assigned by the HMQC and COSY experiments (**—**) and their connection by the principal heteronuclear $^2J_{C\text{-}H}$ and $^3J_{C\text{-}H}$ correlations displayed in the HMBC spectrum (→).

The relative configuration of compound **29** was characterized by a NOESY experiment, taking into account the coupling constants pattern and assuming an α orientation for H-10 (Xu et al., 2004); It was found to be identical to those of the previously reported compounds. These findings and comparison of ^{1}H NMR and ^{13}C NMR spectra of **29** with those of already known compounds (Chen et al., 2009b; Chen et al., 2008b), led to formulate the structure of balsaminol C as cucurbita-5,24-diene-7,23-dione-3β,29-diol.

1.7. **Balsaminol D** [25,26,27-*trinor*-cucurbit-5-ene-7,23-dione-3β,29-diol]

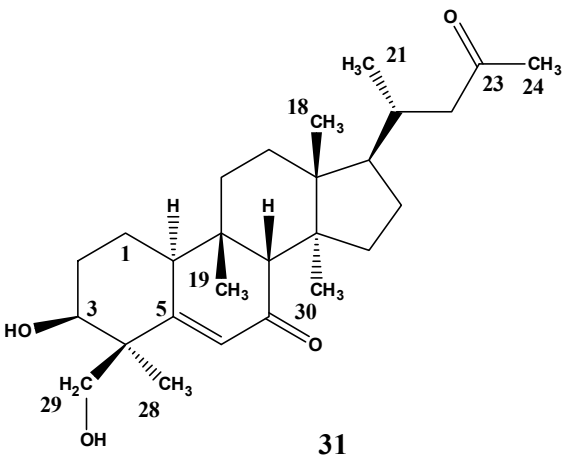

31

Compound **31**, named balsaminol D, is a new compound that was obtained as an amorphous white powder. In the low-resolution ESIMS data, a pseudomolecular ion $[M + Na]^+$ at *m/z* 453 was observed. Its molecular formula was determined as $C_{27}H_{42}O_4$, on the basis of the HR-ESITOFMS spectrum, which exhibited a pseudomolecular $[M + H]^+$ ion peak at *m/z* 431.3153 (calcd. for $C_{27}H_{43}O_4$: 431.3156), indicating seven double bond equivalents. The IR spectrum showed absorption bands for hydroxyl groups (3375 cm^{-1}), an isolated ketone (1707 cm^{-1}), and a conjugated carbonyl group (1645 cm^{-1}), being the latter corroborated by the UV spectrum (λ_{max} = 252 nm). Comparison of NMR data of **31** (Table 2.8) with those of **29** (Table 2.7), revealed that both compounds shared the same triterpenic nucleus with the same α,β-unsaturated carbonyl system at ring B, and the additional hydroxyl group at C-29. Analysis of NMR data revealed that compound **31** has a *trinor*-cucurbit-5-ene-7,23-dione skeleton, without signals for C-25, C-26, and C-27. In this way, the ^1H and ^{13}C NMR data of the side chain of **31** showed resonances for one tertiary methyl group particularly deshielded (δ_H 2.11; δ_C 30.6), one secondary methyl group (δ_H 0.91, d, J = 7.0 Hz; δ_C 20.2), and a carbonyl group at δ_C 212.2. The placement of a carbonyl group at C-23 was supported by the $^2J_{C\text{-}H}$ correlation, observed in the HMBC spectrum, of C-23 (δ_C 212.2) with Me-24 (δ_H 2.11), and the $^3J_{C\text{-}H}$ correlation between C-22 (δ_C 51.8) and Me-24. The relative configuration of **31**, determined by a NOESY experiment, was found to be identical with that of the compounds previously described. Therefore, compound **31** was elucidated as 25,26,27-*trinor*-cucurbit-5-ene-7,23-dione-3β,29-diol. Although highly oxidized cucurbitacins have been isolated from plants, compounds **28**, **29**, **31**, **33**, **34**, and **36** are the first reported occurrence of related derivatives hydroxylated at C-29.

Table 2.8. NMR data of balsaminol D (**31**), (MeOD, ^{1}H 400 MHz, ^{13}C 100.61 MHz; δ in ppm, J in Hz).

Position	^{1}H	^{13}C	DEPT	Position	^{1}H	^{13}C	DEPT
1	1.77 *m*; 1.88 *m*	22.0	CH_2	**15**	1.03 *m*; 1.37 *m*	35.8	CH_2
2	1.75 *m*; 2.00 *m*	29.8	CH_2	**16**	1.33 *m*; 1.97 *m*	28.9	CH_2
3	3.91 *br s*	75.5	CH	**17**	1.55 *m*	51.1	CH
4	–	47.2	C	**18**	0.95 *s*	15.8	CH_3
5	–	170.6	C	**19**	0.98 *s*	28.2	CH_3
6	6.09 *s*	126.9	CH	**20**	2.04 *m*	34.1	CH
7	–	205.5	C	**21**	0.91 *d* (7.0)	20.2	CH_3
8	2.38 *s*	61.1	CH	**22**	2.19 *m*; 2.55 *m*	51.8	CH_2
9	–	36.9	C	**23**	–	212.2	C
10	2.84 *dd* (11.3, 2.7)	41.7	CH	**24**	2.11 *s*	30.6	CH_3
11	1.52 *m*; 1.89 *m*	32.2	CH_2	**28**	1.11 *s*	23.3	CH_3
12	1.30 *m*; 1.63 *m*	30.9	CH_2	**29**	3.72 *d* (10.9)	68.7	CH_2
13	–	47.0	C		3.90 *d* (10.9)	–	–
14	–	49.7	C	**30**	0.90 *s*	18.8	CH_3

1.8. Balsaminol E [cucurbita-5,24-dien-7-one-3β,23(*R*)-diol]

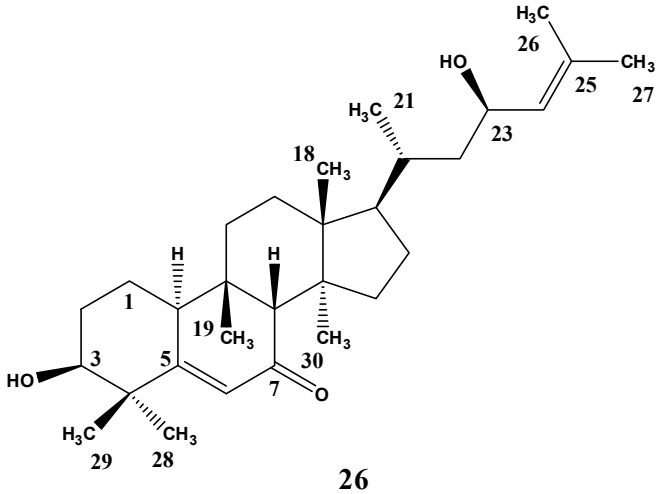

26

Compound **26**, named balsaminol E, is a new compound, which was obtained as an amorphous white powder. Its molecular formula was assigned as $C_{30}H_{48}O_3$ based on the molecular ion at *m/z* 456.3606, exhibited by the HR-EIMS data (calcd. for $C_{30}H_{48}O_3$: 456.3603). The IR and the UV data were similar to those of compounds **29** and **31**. Therefore,

these data, together with the NMR spectra (Table 2.9), were indicative of a tetracyclic triterpenoid bearing a hydroxyl group at C-3 and an α,β-unsaturated carbonyl group at ring B, also found in those compounds. The ^{1}H and ^{13}C NMR data of **26** only differed from those of compounds **29** and **31** in the signals of ring A and the side chain. When comparing the ^{1}H NMR of compounds **26** and **29**, the presence of an extra singlet (δ_H 1.17) in the aliphatic region of the ^{1}H NMR spectrum of **26**, and the paramagnetic effects observed at C-3, C-5, and C-28 ($\Delta\delta_C \cong +2.0, +3.5, +5.3$ ppm, γ-carbons) and the diamagnetic effect at C-4 ($\Delta\delta_C \cong -3.1$ ppm, β-carbon), and C-29 ($\Delta\delta_C \cong -42.0$ ppm, α-carbon), indicated that the hydroxyl group at C-29 was absent. Regarding the side chain, the spectroscopic data indicated the presence of a hydroxyl instead of a carbonyl group at C-23 previously also found in balsaminols A and B. The base peak in the low resolution EIMS spectrum at m/z 357 [M – $CH_2CHOHCHC(CH_3)_2]^+$, together with the fragment ion at *m/z* 329 [M – side chain]$^+$ corroborated the structure of the side chain. The configuration at C-23 was found to be identical to that of balsaminols A (**35**) and B (**27**). Hence, the structure of **26** was formulated as cucurbita-5,24-dien-7-one-3β,23(*R*)-diol.

Table 2.9. NMR data of balsaminol E (**26**), (MeOD, ^{1}H 400 MHz, ^{13}C 100.61 MHz; δ in ppm, *J* in Hz).

Position	^{1}H	^{13}C	DEPT	Position	^{1}H	^{13}C	DEPT
1	1.79 *m*; 1.87 *m*	22.3	CH_2	**17**	1.52 *m*	51.7	CH
2	1.76 *m*; 2.02 *m*	29.8	CH_2	**18**	0.95 *s*	15.9	CH_3
3	3.62 *br s*	77.5	CH	**19**	0.98 *s*	28.3	CH_3
4	–	44.1	C	**20**	1.56 *m*	33.9	CH
5	–	174.1	C	**21**	1.01 *d* (7.0)	19.4	CH_3
6	6.06 *s*	126.9	CH	**22**	0.98 *m*; 1.66 *m*	45.6	CH_2
7	–	205.8	C	**23**	4.42 *td* (9.6, 3.2)	66.6	CH
8	2.39 *s*	61.4	CH	**24**	5.17 *d* (8.2)	130.5	CH
9	–	36.9	C	**25**	–	133.5	C
10	2.84 *br d* (9.8)	41.9	CH	**26**	1.68 *s*	18.2	CH_3
11	1.51 *m*; 1.89 *m*	32.3	CH_2	**27**	1.71 *s*	25.6	CH_3
12	1.65 *m*; 1.86 *m*	31.1	CH_2	**28**	1.24 *s*	28.6	CH_3
13	–	47.0	C	**29**	1.17 *s*	26.0	CH_2
14	–	49.8	C	**30**	0.91 *s*	18.8	CH_3
15	1.03 *m*; 1.56 *m*	35.8	CH_2				
16	1.29 *m*; 1.90 *m*	29.0	CH_2				

1.9. Balsaminol F [cucurbita-5,24-diene-3β,7β,23(*R*)-triol]

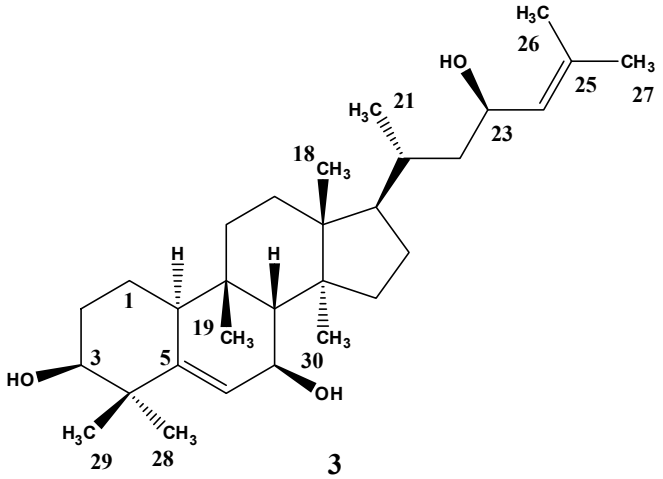

3

Compound **3**, named balsaminol F, is a new compound, which was obtained as a white amorphous powder. Its molecular formula ($C_{30}H_{50}O_3$) was established by HR-ESITOFMS, which showed a pseudomolecular ion at *m/z* 481.3649 $[M + Na]^+$ (calcd. for $C_{30}H_{50}O_3Na$: 481.3652), indicating six degrees of unsaturation. The IR, MS and NMR data (Table 2.10) of compound **3** clearly resemble those found for balsaminol A (**35**). The upfield shifts of 41.5 ppm for C-29 (α-carbon), and 3 ppm for C-4 (β-carbon), and the downfield shifts of 2.2, 3.1, and 5.2 for C-3, C-5, and Me-28 (γ-carbons), respectively, observed in the ^{13}C NMR of compound **3** relatively to balsaminol A (**35**), explain the replacement of the hydroxymethyl at C-4 by a methyl group. All structural features were corroborated by two-dimensional NMR experiments (COSY, HMQC and HMBC), and by comparison with data of compounds **26**, and **35**, allowing the unambiguous assignment of all carbon signals of compound **3**. The stereochemistry of all tetrahedral stereocenters was found to be identical to that of compounds **26**, **27**, and **35**. Therefore, the structure of **3** was elucidated as cucurbita-5,24-diene-3β,7β,23(*R*)-triol.

Table 2.10. NMR data of balsaminol F (**3**), (MeOD, ^{1}H 400 MHz, ^{13}C 100.61 MHz; δ in ppm, J in Hz).

Position	^{1}H	^{13}C	DEPT	Position	^{1}H	^{13}C	DEPT
1	1.57 *m*; 1.70 *m*	22.4	CH_2	**16**	1.39 *m*; 1.70 *m*	28.9	CH_2
2	1.71 *m*; 1.96 *m*	30.1	CH_2	**17**	1.46 *m*	52.1	CH
3	3.50 *br s*	77.5	CH	**18**	0.96 *s*	15.9	CH_3
4	–	42.3	C	**19**	1.04 *s*	29.8	CH_3
5	–	148.3	C	**20**	1.48 *m*	33.8	CH
6	5.74 *d* (5.1)	122.5	CH	**21**	0.97 *d* (6.4)	19.3	CH_3
7	3.93 *br d* (5.2)	68.8	CH	**22**	0.95 *m*; 1.63 *m*	45.6	CH_2
8	1.98 *br s*	54.1	CH	**23**	4.41 *td* (9.6, 3.2)	66.6	CH
9	–	35.0	C	**24**	5.16 *d* (8.5)	130.5	CH
10	2.32 *br d* (7.0)	40.1	CH	**25**	–	133.4	C
11	1.51 *m*; 1.89 *m*	33.9	CH_2	**26**	1.66 *s*	18.1	CH_3
12	1.54 *m*; 1.88 *m*	31.5	CH_2	**27**	1.69 *s*	26.0	CH_3
13	–	47.2	C	**28**	1.03 *s*	28.8	CH_3
14	–	49.5	C	**29**	1.18 *s*	26.1	CH_3
15	1.31 *m*; 1.40 *m*	35.7	CH_2	**30**	0.74 *s*	18.7	CH_3

1.10. Acylated derivatives of balsaminol F

1.10.1. Triacetylbalsaminol F

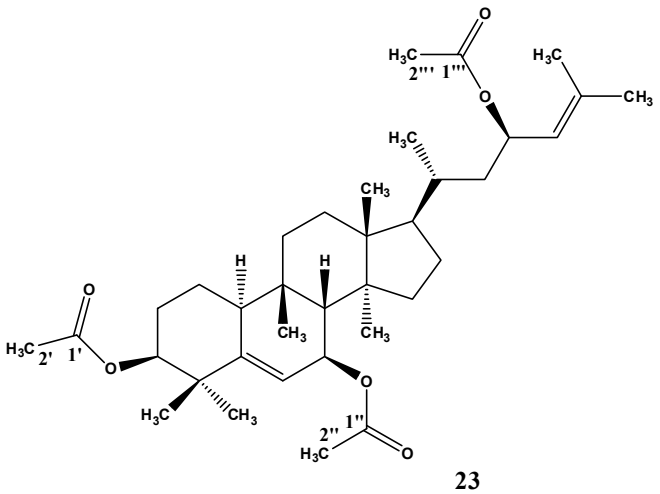

23

Acetylation of balsaminol F (**3**) with acetic anhydride and pyridine afforded the corresponding new triacetate derivative, named triacetylbalsaminol F (**23**). Its EIMS spectrum

showed a molecular ion at *m/z* 584 $[M]^+$. In addition, ions at *m/z* 524 $[M - CH_3COOH]^+$, 464 $[M - 2 \times CH_3COOH]^+$, and 404 $[M - 3 \times CH_3COOH]^+$, resulting from the sequential loss of three acetyl groups, were also observed. Its IR spectrum displayed absorption bands for ester carbonyl groups at 1729 and 1240 cm^{-1}. These structural features were also confirmed by the NMR data of compound **23** (Table 2.11 and 2.12), which revealed the presence of signals for three additional acetyl groups [δ_H 1.98 (6H, s), 1.96 (3H, s), Me-2', Me-2'', Me-2'''); δ_C 170.5 (CO), 170.4 (CO), 170.3 (CO), 21.4, 21.2, and 21.1]. Moreover, when comparing the ^1H NMR spectrum of compound **23** with the one of compound **3**, the chemical shifts of the oxymethine protons H-3, H-7, and H-23 were shifted downfield by 1.22, 1.19 and 1.22 ppm, respectively. Significant differences were also observed in the signals of ^{13}C NMR spectrum, namely paramagnetic effects at C-3, C-7, and C-23 ($\Delta\delta_C \cong + 1.5, + 2.0 + 2.8$ ppm, α-carbons, respectively), and C-5, C-25 ($\Delta\delta_C \cong + 1.7, + 2.3$ ppm, γ carbons), as expected for the acylation of hydroxyl groups (Mahato and Kundu, 1994). Furthermore, diamagnetic effects at C-2, C-4, C-6, C-8, C-22, and C-24 ($\Delta\delta_C \cong - 3.1, -1.5, - 4.0, - 2.7, - 2.9, - 2.3$ ppm, β-carbons, respectively) corroborated the presence of acetyl groups at C-3, C-7, and C-25.

1.10.2. Tribenzoylbalsaminol F

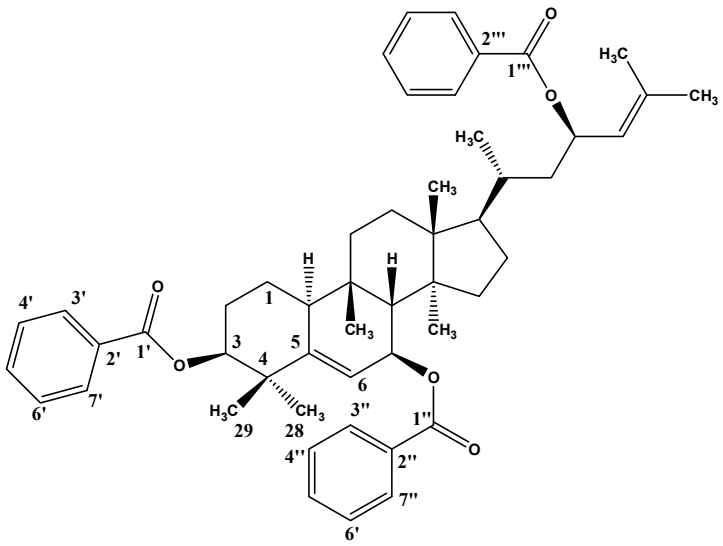

24

Acylation of balsaminol F (**3**) with benzoyl chloride afforded the new derivative tribenzoylbalsaminol F (**24**). Its EIMS spectrum showed a molecular ion at *m/z* 770 $[M]^+$. Comparison of the ^1H and ^{13}C NMR spectra (Tables 2.11 and 2.12) of compound **24** with

those of **3**, showed the presence of additional signals for the three benzoyl ester residues in the spectra of **24**. As expected, when comparing the ^{1}H NMR data of compound **24** with that of the acetyl derivative (**23**), the most remarkable differences were found for the signals of the protons *geminal* to the new ester functions, namely H-3 (δ_H 5.02), H-7 (δ_H 5.50) and H-23 (δ_H 5.92), which were shifted downfield. Moreover, differences were also observed in signals of ^{13}C NMR, as expected for the benzoylation of hydroxyl groups. Among all the effects, the paramagnetic effects at C-3, C-7 and C-23 ($\Delta\delta_C \cong$ + 2.4, + 2.5 + 3.6 ppm, α-carbons, respectively) corroborated the presence of benzoate groups at C-3, C-7, and C-23.

Table 2.11. ^{1}H NMR data of balsaminol F (**3**), triacetylbalsaminol F (**23**) and tribenzoylbalsaminol F (**24**) (400 MHz, MeOD[a], CD_3COCD_3[b], δ in ppm, J in Hz).

Position	3[a]	23[b,c]	24[b,d]
3	3.50 *br s*	4.72 *br s*	5.02 *br s*
6	5.74 *d* (5.1)	5.67 *d* (4.8)	5.92 [e]
7	3.93 *br d* (5.2)	5.12 [e]	5.50 *d* (5.6)
8	1.98 *br s*	1.97 *br s*	2.16 *br s*
10	2.32 *br d* (7.0)	2.47 *br d* (12.0)	2.69 *br d* (12.4)
18	0.96 *s*	0.88 *s*	0.88 *s*
19	1.04 *s*	1.01 *s*	1.25 *s*
21	0.97 *d* (6.4)	0.96 *d* (6.0)	1.06 *d* (5.2)
23	4.41 *td* (9.6, 3.2)	5.63 *td* (8.8, 3.2)	5.92 [e]
24	5.16 *d* (8.5)	5.12 [e]	5.29 *d* (8.8)
26	1.66 *s*	1.68 *s*	1.83 *s*
27	1.69 *s*	1.71 *s*	1.73 *s*
28	1.03 *s*	1.14 *s*	1.27 *s*
29	1.18 *s*	1.09 *s*	1.21 *s*
30	0.74 *s*	0.82 *s*	0.88 *s*

[c] Other signals for compound **23**: 1.98 (6H, *s*), 1.96 (3H, *s*), (Me-2'/Me-2''/Me-2''').

[d] Other signals for compound **24**: 8.10-7.99 (6H, *m*, H-3'/H-3''/H-3''/H-7'/H-7''/H-7'''), 7.70-7.37 (9H, *m*, H-4'/H-4''/H-4'''/H-5'/H-5''/H-5'''/H-6'/H-6''/H-6'''). [e] Overlapped signals.

Table 2.12. ^{13}C NMR data of balsaminol F (**3**), triacetylbalsaminol F (**23**) and tribenzoylbalsaminol F (**24**) (100.61 MHz, MeOD[a], CD_3COCD_3[b], δ in ppm).

Position	3[a]	23[b,c]	24[b,d]	DEPT
1	22.4	22.4	22.4	CH_2
2	30.1	27.0	26.4	CH_2
3	77.5	79.0	79.9	CH
4	42.3	40.8	41.3	C
5	148.3	150.0	150.5	C
6	122.5	118.5	118.6	CH
7	68.8	70.8	71.3	CH
8	54.1	51.4	51.2	CH
9	35.0	34.6	34.5	C
10	40.1	39.3	38.9	CH
11	33.9	33.0	32.9	CH_2
12	31.5	30.8	30.6	CH_2
13	47.2	46.8	46.7	C
14	49.5	49.0	48.9	C
15	35.7	35.3	35.2	CH_2
16	28.9	28.6	28.6	CH_2
17	52.1	51.1	50.9	CH
18	15.9	15.7	15.7	CH_3
19	29.8	29.0	29.7	CH_3
20	33.8	33.6	33.6	CH
21	19.3	19.3	19.2	CH_3
22	45.6	42.7	42.6	CH_2
23	66.6	69.4	70.2	CH
24	130.5	125.9	125.5	CH
25	133.4	135.7	136.2	C
26	18.1	18.5	18.5	CH_3
27	26.0	25.7	25.6	CH_3
28	28.8	28.4	27.2	CH_3
29	26.1	25.2	25.5	CH_3
30	18.7	18.4	18.4	CH_3

[c] Other signals for compound **23**: δ 170.5, 170.4, 170.3 (C-1'/C-1''/C-1'''); 21.4, 21.2, 21.1 (C-2'/C-2''/C-2'''); interchangeable signals within each set.

[d] Other signals for compound **24**: δ 166.0, 165.5, 165.8 (C-1'/C-1''/C-1'''); 133.6, 133.5 (C-5'/C-5''/C-5'''), 131.9, 131.6, 131.5 (C-2'/C-2''/C-2'''); 129.9, 129.8 (C-3'/C-3''/C-3'''/C-7'/C-7''/C-7'''), 129.3, 129.2 (C-4'/C-4''/C-4'''/C-6'/C-6''/C-6'''); interchangeable signals within each set.

1.11. Karavilagenin C [7β-methoxycucurbita-5,24-diene-3β,23(*R*)-diol]

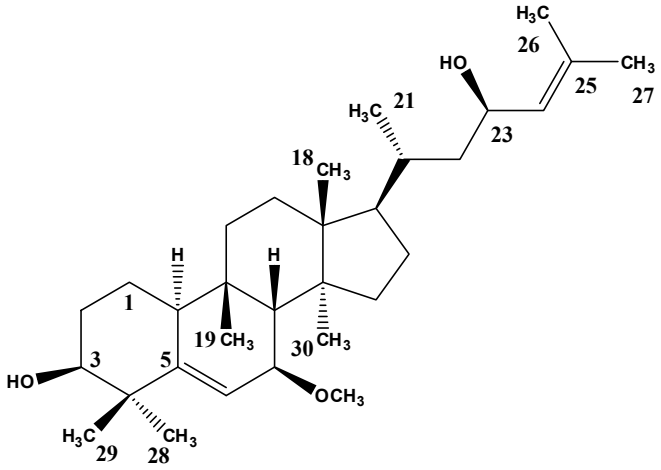

1

Compound **1** was isolated as colourless needles with $[\alpha]_D^{26}$ + 136 (*c* 0.17, MeOH). It gave a pseudomecular ion at *m/z* 495 $[M + Na]^+$, corresponding to the molecular formula $C_{31}H_{52}O_3$, from which six degrees of unsaturation were deduced. In the ESIMS, the ion at *m/z* 423 $[M + H – H_2O – HOCH_3]^+$ was also observed and suggested the presence of hydroxyl and methoxyl groups in compound **1**. The presence of hydroxyl groups was corroborated by the IR spectrum. The ^1H and ^{13}C spectra of compound **1** (Table 2.13) closely resembled those recorded for balsaminol F (**3**). In fact, the main differences were observed at ring B due to the presence of a methoxyl group instead a hydroxyl group at C-7. Analysis of its spectroscopic data indicated that compound **1** was a known cucurbitane-type triterpene identified as karavilagenin C, isolated for the first time from the fruits of *M. charantia* (Nakamura et al., 2006). The configuration at C-23, not previously described, was found to be identical, by comparison of its ^{13}C NMR data, with those of balsaminols A (**35**), B (**27**), E (**26**), and F (**3**). A strong NOE correlation between Me-21 and the oxymethine proton H-23 was also found in the NOESY spectrum of compound **1**, corroborating the *R* configuration at C-23. Thus compound **1**, was identified as 7β-methoxycucurbita-5,24-diene-3β,23(*R*)-diol.

Table 2.13. NMR data of karavilagenin C (**1**), ($CDCl_3$, ^1H 400 MHz, ^{13}C 100.61 MHz; δ in ppm, J in Hz).

Position	^1H	^{13}C	DEPT	Position	^1H	^{13}C	DEPT
1	1.49 *m*; 1.60 *m*	21.1	CH_2	**17**	1.45 *m*	50.8	CH
2	1.73 *m*; 1.89 *m*	28.6	CH_2	**18**	0.94 *s*	15.4	CH_3
3	3.50 *br s*	76.7	CH	**19**	0.97 *s*	28.8	CH_3
4	–	41.7	C	**20**	1.47 *m*	32.7	CH
5	–	146.7	C	**21**	0.96 *d* (6.7)	18.7	CH_3
6	5.82 *d* (5.1)	121.0	CH	**22**	1.02 *m*; 1.65 *m*	44.4	CH_2
7	3.41 *br d* (5.1)	77.2	CH	**23**	4.45 *td* (10.0, 2.8)	65.9	CH
8	2.04 *br s*	47.9	CH	**24**	5.18 *d* (8.4)	129.0	CH
9	–	34.0	C	**25**	–	133.8	C
10	2.27 *dd* (11.7, 4.0)	38.7	CH	**26**	1.67 *s*	18.1	CH_3
11	1.47 *m*; 1.65 *m*	32.7	CH_2	**27**	1.69 *s*	25.8	CH_3
12	1.51 *m*	30.2	CH_2	**28**	1.02 *s*	27.8	CH_3
13	–	46.2	C	**29**	1.19 *s*	25.4	CH_3
14	–	47.8	C	**30**	0.69 *s*	18.0	CH_3
15	1.34 *m*	34.6	CH_2	**7-OMe**	3.33 *s*	56.3	CH_3
16	1.33 *m*; 1.90 *m*	27.9	CH_2				

1.12. Acylated derivatives of karavilagenin C

1.12.1. Alkanoyl esters

Karavilagenin C (**1**), isolated in large amount, was derivatized with four different alkanoyl anhydrides, namely acetic, propionic, butyric, and succinic anhydrides (Scheme 2.1). From these reactions eight new ester analogues were obtained: four monoacylated, karavoate A (**5**), karavoate C (**7**), karavoate E (**9**), and karavoate Q (**21**), and four diacylated derivatives, karavoate B (**6**), karavoate D (**8**), karavoate F (**10**), and karavoate R (**22**). As expected, the main differences, between the NMR data of karavilagenin C (**1**) and those of the alkanoyl derivatives (**5 - 10**, **21**, **22**), (Tables 2.14 and 2.15), were observed for carbon and proton signals of ring A and side chain. In this way, in the ^1H NMR data of the monoacylated derivatives (**5**, **7**, **9**, **21**) a significant paramagnetic effect was observed for the chemical shift of H-23, which appeared, approximately, 1.2 ppm downfield. Similarly, deshielding effects at C-23 ($\Delta\delta_C \cong +$ 3.6 ppm, α-carbon), C-20, and C-25 ($\Delta\delta_C \cong +$ 0.1, and + 1.9 ppm, respectively,

γ-carbons), together with shielding effects at C-22 and C-24 ($\Delta\delta_C \cong -2.4, -4.3$ ppm, respectively, β-carbons) were observed. In the diacyl derivatives (**6**, **8**, **10**) (Tables 2.14 and 2.15), besides the difference in chemical shift of H-23, the signal of H-3 was also shifted downfield ($\Delta\delta_H \cong +1.24$ ppm). In the same way, in the ^{13}C NMR spectra (Table 2.16) a paramagnetic effect at C-3 ($\Delta\delta_C \cong +3.6$ ppm, α-carbon), and diamagnetic effects at C-2 and C-4 ($\Delta\delta_C \cong -2.1, -1.9$ ppm, β-carbons) were also observed.

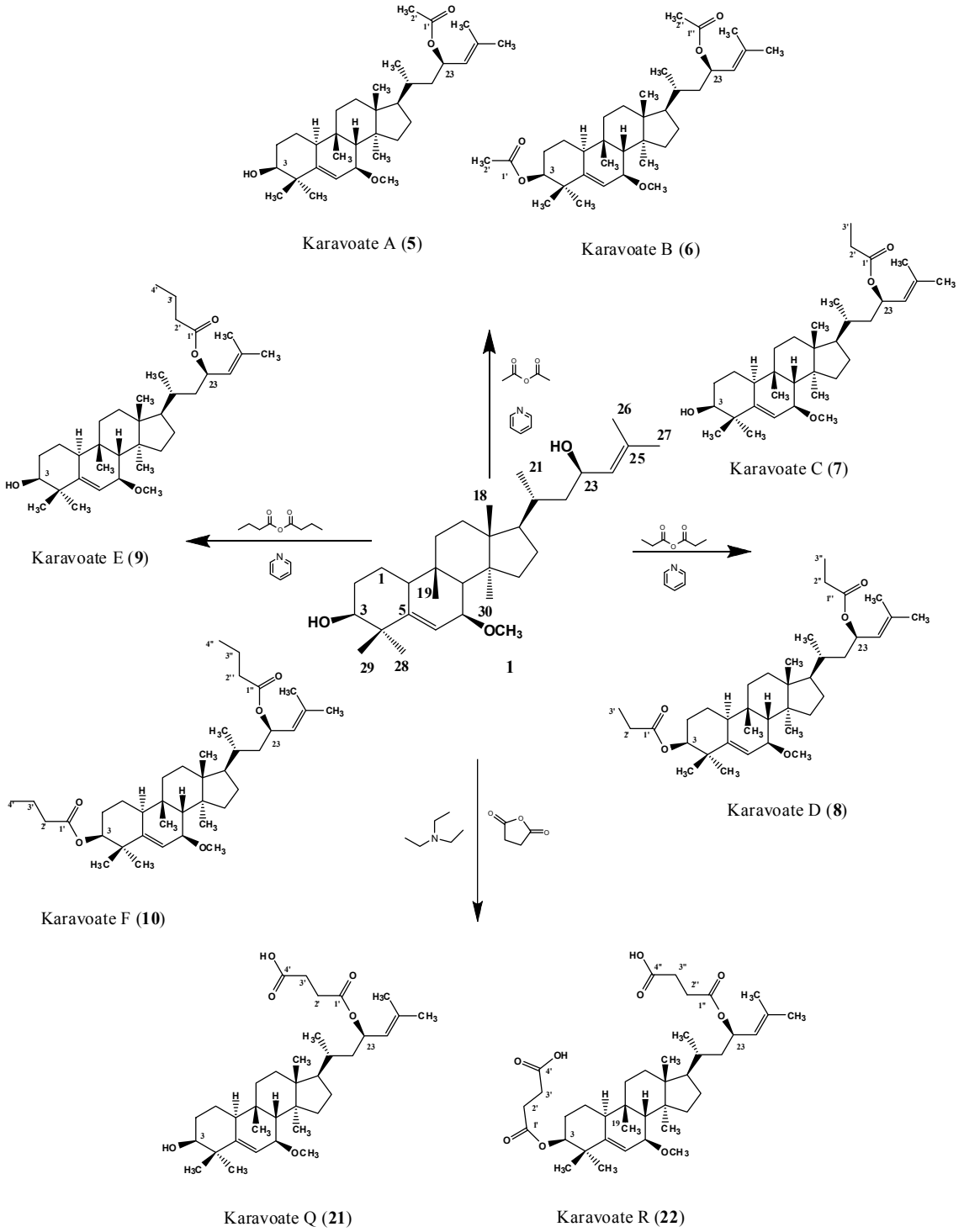

Scheme 2.1. Alkanoyl esters of karavilagenin C (**1**).

Table 2.14. ^{1}H NMR data of karavilagenin C (**1**) and karavoates A - F (**5** - **10**), ($CDCl_3$ [a], CD_3COCD_3 [b], 400 MHz; δ in ppm, J in Hz).

Position	1 [a]	5 [a]	6 [a]	7 [a]	8 [a]	9 [b]	10 [b]
3	3.50 *br s*	3.53 *br s*	4.74 *br s*	3.53 *br s*	4.77 *br s*	3.50 *br s*	4.72 *br s*
6	5.82 *d* (5.1)	5.85 *d* (4.9)	5.77 *d* (4.9)	5.85 *d* (5.1)	5.79 *d* (4.4)	5.77 *d* (4.5)	5.79 *d* (5.0)
7	3.41 *br d* (5.1)	3.44 *br d* (4.8)	3.42 *br d* (5.0)	3.44 *br d* (5.3)	3.45 *br d* (4.4)	3.40 *br d* (4.4)	3.43 *br d* (5.1)
8	2.04 *br s*	2.06 *br s*	2.04 *br s*	2.06 *br s*	2.06 *br s*	2.04 *br s*	2.04 *br s*
10	2.27 *dd* (11.7, 4.0)	2.29 *br d* (10.5)	2.27 *br d* (10.7)	2.25 - 2.36[c]	2.25 - 2.36[c]	2.35 *br d* (10.3)	2.42 *br d* (10.6)
18	0.94 *s*	0.93 *s*	0.91 *s*	0.92 *s*	0.93 *s*	0.94 *s*	0.95 *s*
19	0.97 *s*	1.00 *s*	0.97 *s*	1.00 *s*	0.99 *s*	0.96 *s*	0.98 *s*
21	0.96 *d* (6.7)	0.96 *d* (5.5)	0.94 *d* (5.5)	0.96 *d* (5.2)	0.96 *d* (5.6)	0.98 *d* (5.8)	0.98 *d* (5.3)
23	4.45 *td* (10.0, 2.8)	5.60 *td* (9.8, 2.7)	5.60 *td* (9.8, 2.7)	5.63 *td* (9.9, 2.9)	5.63 *td* (9.9, 2.9)	5.67 *td* (10.4, 2.9)	5.67 *td* (10.5, 3.0)
24	5.18 *d* (8.4)	5.11 *d* (8.7)	5.09 *d* (8.8)	5.10 *d* (8.2)	5.11 *d* (8.8)	5.13 *d* (8.9)	5.13 *d* (8.9)
26	1.67 *s*	1.71 *s*	1.69 *s*	1.71 *s*	1.71 *s*	1.72 *s*	1.72 *s*
27	1.69 *s*	1.74 *s*	1.72 *s*	1.75 *s*	1.76 *s*	1.69 *s*	1.69 *s*
28	1.02 *s*	1.05 *s*	1.06 *s*	1.05 *s*	1.08 *s*	1.03 *s*	1.12 *s*
29	1.19 *s*	1.22 *s*	1.10 *s*	1.22 *s*	1.10 *s*	1.19 *s*	1.11 s
30	0.69 *s*	0.71 *s*	0.70 *s*	0.71 *s*	0.73 *s*	0.77 *s*	0.78 *s*
7-OMe	3.33 *s*	3.36 *s*	3.35 *s*	3.36 *s*	3.37 *s*	3.31 *s*	3.30 *s*
2'	–	2.04 *s*	1.99 *s*	2.25 - 2.36[c]	2.25 - 2.36[c]	2.24 *td* (3.7, 7.3)	2.26 *t* (7.3)
3'	–	–	–	1.15 *t* (7.2)	1.12 *t* (7.2)	1.62 *m*	1.62 *m*[c]
4'	–	–	–	–	–	0.92 *t* (7.4)	0.94 *t* (7.4)
2''	–	–	2.01 *s*	–	2.25 - 2.36[c]	–	2.24 *t* (7.3)
3''	–	–	–		1.15 *t* (7.2)	–	1.62 *m*[c]
4''	–	–	–		–	–	0.92 *t* (7.3)

[c] overlapped signals

Table 2.15. ^{1}H NMR data of karavoates Q (**21**) and R (**22**), ($CDCl_3$[a], MeOD[b], 400 MHz, δ in ppm, J in Hz).

Position	1[a]	21[b]	22[b]
3	3.50 *br s*	3.48 *br s*	4.74 *br s*
6	5.82 *d* (5.1)	5.79 *d* (4.9)	5.78 *d* (4.9)
7	3.41 *br d* (5.1)	3.48 *br s*	3.48 *br d* (5.0)
8	2.04 *br s*	2.06 *br s*	2.07 *br s*
10	2.27 *dd* (11.7, 4.0)	2.34 *br d* (10.0)	2.38 *br d* (9.8)
18	0.94 *s*	0.96 *s*	0.96 *s*
19	0.97 *s*	1.04 *s*	0.96 *s*
21	0.96 *d* (6.7)	0.97 *d* (6.4)	0.96 *m*[c]
23	4.45 *td* (10.0, 2.8)	5.65 *td* (10.1, 3.0)	5.62 *td* (9.9, 2.8)
24	5.18 *d* (8.4)	5.11 *d* (8.9)	5.10 *d* (8.7)
26	1.67 *s*	1.72 *s*	1.70 *s*
27	1.69 *s*	1.70 *s*	1.68 *s*
28	1.02 *s*	1.05 *s*	1.09 *s*
29	1.19 *s*	1.19 *s*	1.10 *s*
30	0.69 *s*	0.76 *s*	0.75 *s*
7-OMe	3.33 *s*	3.33 *s*	3.33 *s*
2'	–	2.51 *m*[c]	2.51 *m*[c]
3'	–	2.51 *m*[c]	2.51 *m*[c]
4'	–	–	–
2''	–	–	2.51 *m*[c]
3''	–	–	2.51 *m*[c]
4''	–	–	–

[c] overlapped signals

Table 2.16. ^{13}C NMR data of karavilagenin C (**1**), and karavoates A - F (**5** - **10**), and Q (**21**) ($CDCl_3$[a], CD_3COCD_3[b], MeOD[c], 100.61 MHz, δ in ppm).

Position	1[a]	5[a]	6[a]	7[a]	8[a]	9[b]	10[b]	21[c]
1	21.1	21.1	21.7	21.1	21.6	21.9	22.4	22.4
2	28.6	28.6	26.4	28.6	26.4	30.0	27.0	30.1
3	76.7	76.8	78.6	76.8	78.4	76.4	78.9	77.5
4	41.7	41.8	39.9	41.7	40.0	42.1	40.7	42.5
5	146.7	146.8	146.8	146.8	146.9	148.1	147.0	149.4
6	121.0	120.9	119.2	120.9	119.2	120.2	120.4	120.3
7	77.2	77.2	77.3	77.2	77.3	77.9	77.7	78.9
8	47.9	47.9	47.7	47.9	48.0	49.3	49.3	48.4
9	34.0	34.0	34.0	34.0	34.0	34.8	34.8	35.1
10	38.7	38.7	38.7	38.7	38.6	39.7	39.3	40.3
11	32.65	32.6	32.4	32.6	32.4	33.6	33.6	33.8
12	30.2	30.1	30.1	30.1	30.1	31.0	30.9	31.8
13	46.2	46.2	46.1	46.2	46.2	46.9	46.9	47.4
14	47.8	47.9	47.9	47.9	48.0	48.8	48.8	49.5
15	34.6	34.6	34.6	34.6	34.6	35.4	35.3	35.8
16	27.9	27.8	27.8	27.8	27.8	28.6	28.6	28.9
17	50.8	50.5	50.5	50.5	50.5	51.3	51.3	51.8
18	15.4	15.3	15.3	15.3	15.3	15.7	15.7	15.8
19	28.8	28.8	28.5	28.8	28.5	29.3	29.3	29.4
20	32.67	32.8	32.8	32.8	32.8	33.4	33.2	34.1
21	18.7	19.0	18.9	19.0	19.0	19.3	19.2	19.4
22	44.4	42.0	41.9	42.0	42.0	42.8	42.8	43.1
23	65.9	69.5	69.4	69.3	69.3	69.1	69.1	71.0
24	129.0	124.7	124.7	124.7	124.7	126.0	126.0	125.8
25	133.8	135.7	135.7	135.6	135.6	135.7	135.7	136.7
26	18.1	18.4	18.3	18.3	18.3	18.5	18.4	18.5
27	25.8	25.7	25.7	25.7	25.7	26.1	25.7	25.8
28	27.8	27.9	28.0	27.8	28.0	28.5	28.3	28.8
29	25.4	25.4	24.8	25.4	24.9	25.7	25.4	26.0
30	18.0	18.0	17.9	18.0	17.9	18.4	18.4	18.7
7-OMe	56.3	56.3	56.3	56.3	56.3	56.2	56.3	56.4

To be continued

Table 2.16. Cont.

Position	5[a]	6[a,d]	7[a]	8[a,d]	9[b]	10[b,d]	21[c]
1'	170.7	170.6	174.0	174.2	173.0	172.9	173.8
2'	21.4	21.3	28.0	28.0	36.9	36.9	29.0
3'	–	–	9.3	9.4	19.3	19.3	30.6
4'	–	–	–	–	13.9	13.9	n.d.
1''	–	170.9	–	174.0	–	173.0	–
2''	–	21.4	–	28.0	–	36.9	–
3''	–	–	–	9.3	–	19.3	–
4''	–	–	–		–	13.9	–

[d] signals for the same carbon can be interchangeable; n.d. not determined

1.12.1. Aroyl and cinnamoyl esters

Karavilagenin C (**1**) was also acylated with four different aroyl chlorides, namely benzoyl, *p*-nitrobenzoyl, *p*-chlorobenzoyl, and *p*-methoxybenzoyl chlorides (Scheme 2.2), yielding eight new esters: four monoacylated, karavoate G (**11**), karavoate I (**13**), karavoate K (**15**), and karavoate M (**17**), and four diacylated, karavoate H (**12**), karavoate J (**14**), karavoate L (**16**), and karavoate N (**18**). Two cinnamoyl derivatives were also obtained, namely the monoester, karavoate O (**19**), and the diester, karavoate P (**20**). The IR spectra of these new compounds showed characteristics absorption bands for the aromatic ring, and the ester carbonyl groups. An absorption band for the hydroxyl group was also observed in the IR spectra of the monoesters. Moreover, the NMR data (Tables 2.17 - 2.21) of the triterpenic nucleus closely resemble those observed for the acyl derivatives.

The monobenzoyl derivative, karavoate G (**11**), was obtained as a colourless oil with $[\alpha]_D^{20}$ + 105. Its IR spectrum showed the absorption bands for the aromatic ring (1454 and 712 cm^{-1}), the hydroxyl group (3416 cm^{-1}), and the ester carbonyl group (1712 cm^{-1}). Comparison of the ^1H and ^{13}C spectra of compound **11** with those of compound **1** (Tables 2.17 and 2.19), provided evidence for the benzoylation at C-3. However, significant differences for carbon and proton signals of side chain were found. On the other hand, comparison of NMR data of compound **11** with those of balsaminagenin A (**34**), (Table 2.4) showed that both compounds had identical side chains, namely one *trans*-disubstituted double bond (δ_H 5.62, *m*, H-23/H-24; δ_C 139.5, 125.4), and a terminal hydroxyl at C-25. This

structural feature can be explained by an isomerization of the side chain during the derivatization process (Figure 2.7).

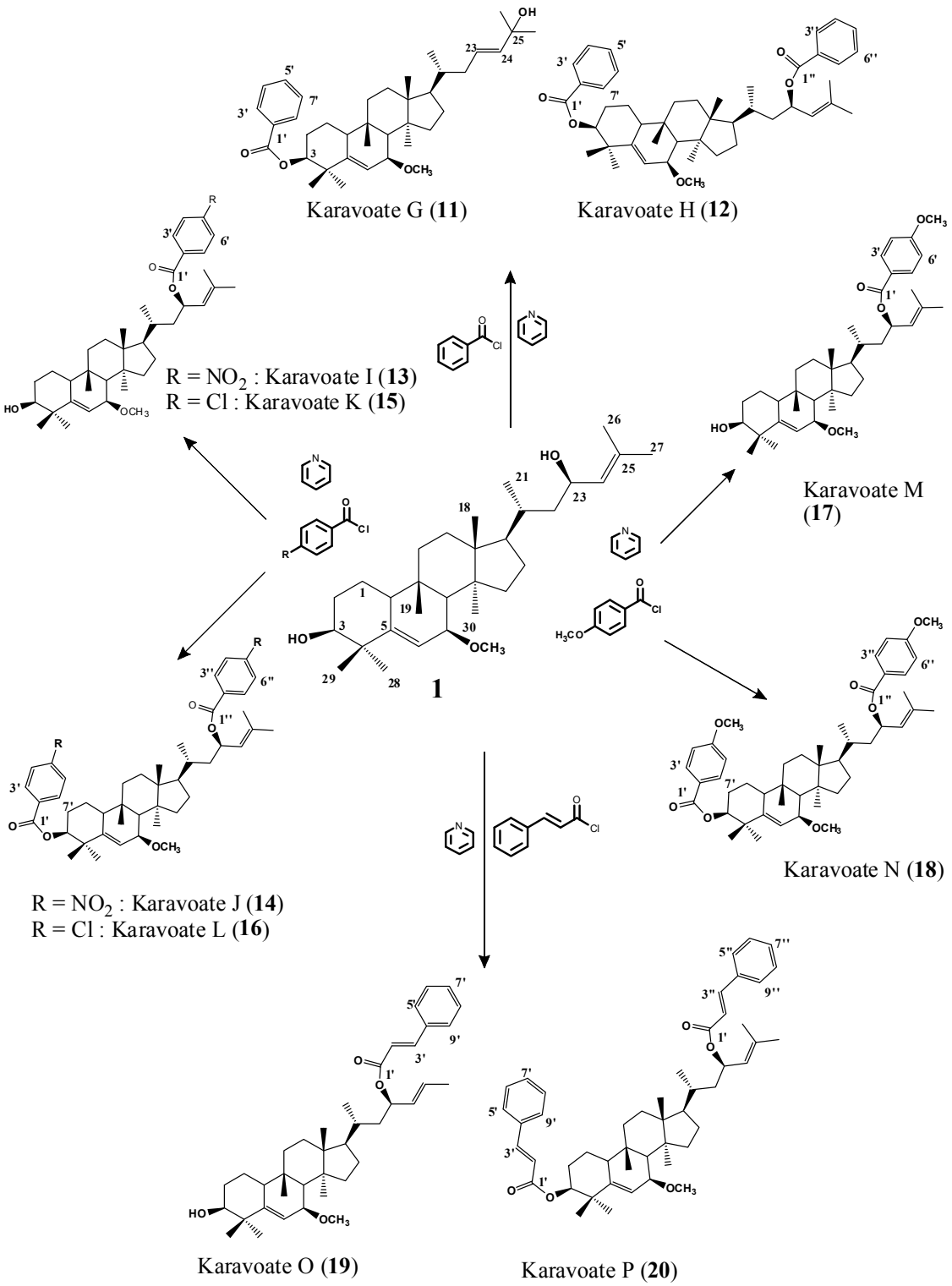

Scheme 2.2. Aroyl and cinnamoyl esters of karavilagenin C (**1**).

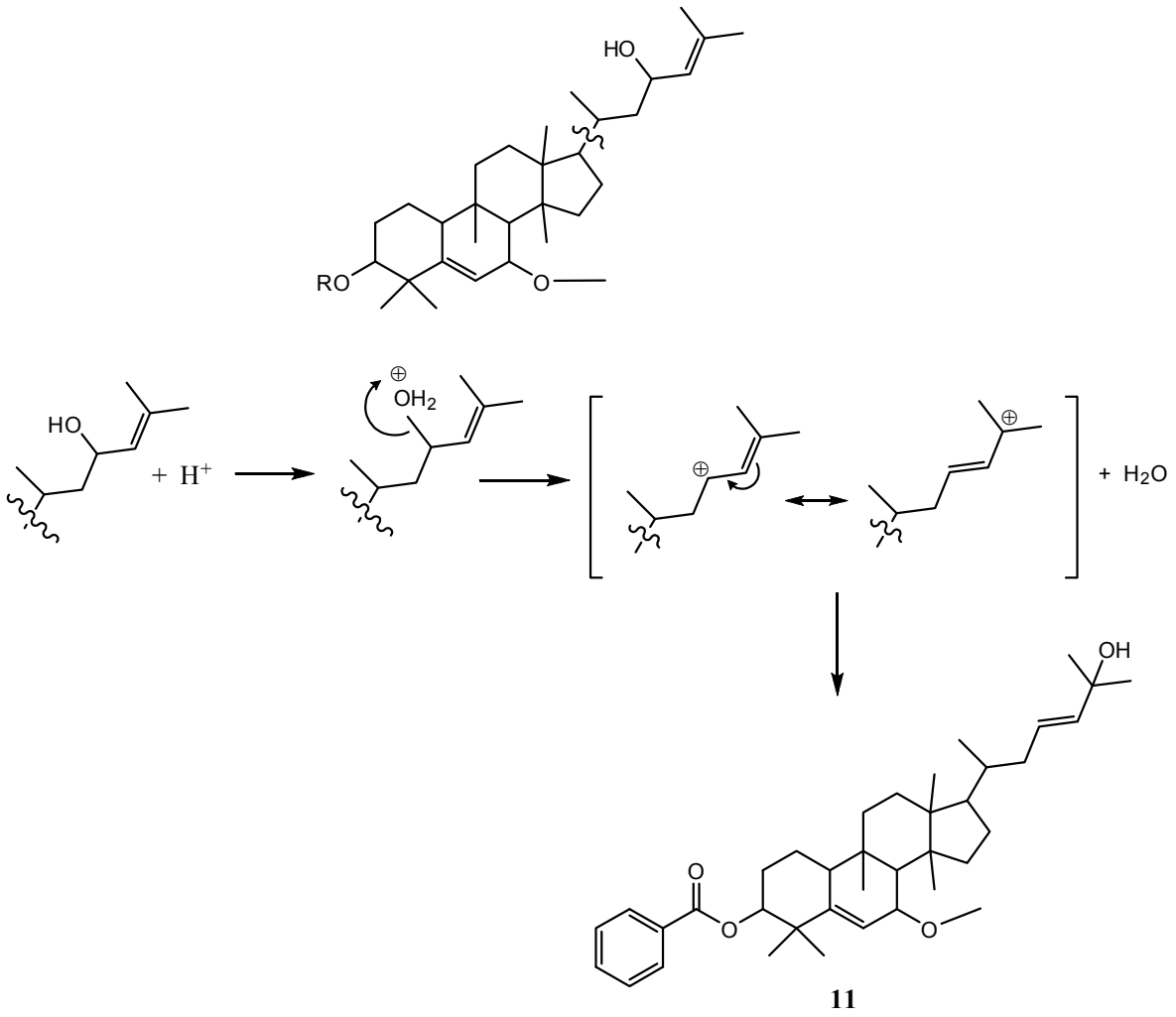

11

Figure 2.7. Isomerization of the side chain of karavoate G (**11**).

.

Table 2.17. ^{1}H NMR data of karavilagenin C (**1**), and karavoates G - L (**11 - 16**), ($CDCl_3$[a], CD_3COCD_3[b], 400 MHz, δ in ppm, *J* in Hz).

Position	1[a]	11[a]	12[a]	13[b]	14[b]	15[b]	16[b]
3	3.50 *br s*	5.03 *br s*	5.03 *br s*	3.46 *br s*	5.06 *br s*	3. 49 *br s*	4.99 *br s*
6	5.82 *d* (5.1)	5.89 *d* (4.7)	5.89 *d* (4.7)	5.73 *d* (5.0)	5.90 *d* (4.7)	5.75 *d* (5.0)	5.87 *d* (4.7)
7	3.41 *br d* (5.1)	3.50 *br d* (4.4)	3.49 *br d* (4.3)	3.36 *br d* (5.2)	3.49 *br d* (4.7)	3.39 *br d* (5.3)	3.47 *br d* (5.0)
8	2.04 *br s*	2.09 *br s*	2.08 *br s*	1.98 *br s*	2.10 *br s*	2.00 *br s*	2.12 *br s*
10	2.27 *dd* (11.7, 4.0)	2.40 *dd* (11.2, 4.4)	2.40 *dd* (11.2, 4.4)	2.30 *br d* (10.5)	2.55 *br d* (10.0)	2.33 *br d* (10.3)	2.52 *br d* (10.0)
18	0.94 *s*	0.97 *s*	0.92 *s*	0.86 *s*	0.93 *s*	0.88 *s*	0.93 *s*
19	0.97 *s*	1.06 *s*	1.04 *s*	0.91 *s*	1.03 *s*	0.93 *s*	1.03 *s*
21	0.96 *d* (6.7)	0.92 *d* (5.9)	1.03 *d* (6.3)	1.02 *d* (6.3)	1.06 *d* (6.4)	1.02 *d* (7.7)	1.04 *d* (6.0)
23	4.45 *td* (10.0, 2.8)	5.62 *m*	5.87 *td* (9.2, 2.8)	5.91 *dt* (8.8, 2.0)	5.96 *dt* (9.0, 3.0)	5.88 *dt* (9.0, 3.3)	5.88 *dt* (9.0, 3.3)
24	5.18 *d* (8.4)	5.62 *m*	5.24 *d* (8.9)	5.27 *d* (8.9)	5.32 *d* (9.0)	5.25 *d* (8.8)	5.27 *d* (8.8)
26	1.67 *s*	1.34 *s*	1.84 *s*	1.79 *s*	1.84 *s*	1.79 *s*	1.82 *s*
27	1.69 *s*	1.27 *s*	1.74 *s*	1.70 *s*	1.74 *s*	1.70 *s*	1.70 *s*
28	1.02 *s*	1.16 *s*	1.17 *s*	1.00 *s*	1.24 *s*	1.02 *s*	1.22 *s*
29	1.19 *s*	1.21 *s*	1.22 *s*	1.15 *s*	1.21 *s*	1.17 *s*	1.19 *s*
30	0.69 *s*	0.77 *s*	0.78 *s*	0.75 *s*	0.84 *s*	0.77 *s*	0.84 *s*
7-OMe	3.33 *s*	3.41 *s*	3.40 *s*	3.23 *s*	3.34 *s*	3.26 *s*	3.31 *s*
3', 7'	–	8.02 *d* (7.1)	8.02 *d* (7.1)	8.25 *d* (8.9)	8.30 *d* (8.9)	8.00 *d* (8.8)	7.98 *d* (8.8)
4', 6'	–	7.44 *t* (7.6)	7.45 *m*	8.34 *d* (7.8)	8.39 *dd* (8.9, 1.9)	7.54 *d* (8.8)	7.56 *m*
5'	–	7.55 *t* (7.4)	7.56 *m*	–	–	–	–
3'', 7''	–	–	8.04 *d* (7.1)	–	8.23 *d* (8.9)	–	8.04 *d* (8.8)
4'', 6''	–	–	7.45 *m*	–	8.39 *dd* (8.9, 1.9)	–	7.56 *m*
5''	–	–	7.56 *m*	–	–	–	–

Table 2.18. ^{1}H NMR data of karavoates M (**17**) and N (**18**), ($CDCl_3$[a], CD_3COCD_3[b], 400 MHz, δ in ppm, J in Hz).

Position	**1**[a]	**17**[b]	**18**[b]
3	3.50 *br s*	3. 49 *br s*	4.95 *br s*
6	5.82 *d* (5.1)	5.76 *d* (5.0)	5.88 *d* (5.0)
7	3.41 *br d* (5.1)	3.39 *br d* (5.3)	3.47 *br d* (4.7)
8	2.04 *br s*	2.01 *br s*	2.08 *br s*
10	2.27 *dd* (11.7, 4.0)	2.33 *br d* (10.3)	2.50 *dd* (11.0, 3.0)
18	0.94 *s*	0.88 *s*	0.91 *s*
19	0.97 *s*	0.94 *s*	1.03 *s*
21	0.96 *d* (6.7)	1.02 *d* (7.7)	1.02 *d* (5.8)
23	4.45 *td* (10.0, 2.8)	5.86 *td* (10.0, 3.2)	5.86 *td* (10.0, 3.2)
24	5.18 *d* (8.4)	5.24 *d* (8.8)	5.26 *d* (8.2)
26	1.67 *s*	1.79 *s*	1.80 *s*
27	1.69 *s*	1.69 *s*	1.71 *s*
28	1.02 *s*	1.03 *s*	1.17 *s*
29	1.19 *s*	1.18 *s*	1.19 *s*
30	0.69 *s*	0.77 *s*	0.82 *s*
7-OMe	3.33 *s*	3.26 *s*	3.33 *s*
3', 7'	–	7.97 *d* (8.8)	7.93 *d* (8.8)
4', 6'	–	7.02 *d* (8.8)	7.02 *m*
5'-OMe	–	3.87 *s*	3.88 *s*
3'', 7''	–	–	7.96 *d* (8.8)
4'', 6''	–	–	7.02 *m*
5''-OMe	–	–	3.88 *s*

Table 2.19. ^{13}C NMR data of karavilagenin C (**1**) and karavoates G - N (**11** - **18**), ($CDCl_3$[a], CD_3COCD_3[b], 100.61 MHz, δ in ppm).

Position	1[a]	11[a]	12[a]	13[b]	14[b]	15[b]	16[b]	17[b]	18[b]
1	21.1	21.7	21.7	21.9	22.6	21.9	22.6	22.0	22.5
2	28.6	26.5	26.5	30.0	26.9	30.1	27.0	30.1	27.0
3	76.7	79.3	79.3	76.5	81.3	76.5	80.5	76.5	79.5
4	41.7	40.3	40.3	42.1	41.0	42.1	41.0	42.0	41.0
5	146.7	146.8	146.8	148.0	146.6	148.1	146.8	148.0	147.0
6	121.0	119.5	119.5	120.1	121.0	120.1	120.8	120.1	120.6
7	77.2	77.3	77.4	77.8	77.6	77.8	77.7	77.8	77.7
8	47.9	48.3	48.2	49.1	49.1	49.2	49.1	49.1	49.1
9	34.0	34.2	34.1	34.7	34.8	34.7	34.9	34.7	34.8
10	38.7	38.6	38.6	39.6	39.1	39.6	39.1	39.6	39.1
11	32.65	32.2	32.2	33.3	33.1	33.3	33.2	33.3	33.1
12	30.2	30.1	30.1	31.0	30.9	30.9	30.9	30.9	30.9
13	46.2	46.1	46.2	46.9	47.0	46.9	46.9	46.9	46.9
14	47.8	48.0	48.0	48.8	48.8	48.8	48.8	48.7	48.8
15	34.6	34.7	34.7	35.4	35.4	35.3	35.4	35.3	35.3
16	27.9	27.6	28.0	28.7	28.7	28.7	28.8	28.7	28.7
17	50.8	50.0	50.5	51.2	51.3	51.2	51.3	51.2	51.2
18	15.4	15.5	15.4	15.7	15.7	15.6	15.6	15.6	15.7
19	28.8	28.5	28.5	29.2	29.2	29.2	29.1	29.2	29.1
20	32.67	36.3	33.0	33.8	33.8	33.8	33.8	33.7	33.7
21	18.7	18.7	19.1	19.4	19.4	19.4	19.4	19.4	19.4
22	44.4	39.1	42.1	42.7	42.7	42.7	42.7	42.8	42.8
23	65.9	125.4	70.3	71.7	71.8	70.9	70.9	69.9	69.9
24	129.0	139.5	124.6	125.1	125.1	125.4	125.4	125.9	125.9
25	133.8	70.8	135.9	137.0	137.0	136.6	136.6	135.9	136.0
26	18.1	30.0	18.4	18.6	18.5	18.4	18.4	18.4	18.4
27	25.8	29.9	25.8	25.8	25.8	25.7	25.8	25.8	25.8
28	27.8	28.1	28.1	28.5	28.1	28.5	28.1	28.5	28.1
29	25.4	25.2	25.2	26.0	25.6	26.0	25.6	26.0	25.6
30	18.0	18.0	18.0	18.5	18.5	18.5	18.5	18.5	18.5
7-OMe	56.3	56.3	56.3	56.2	56.3	56.2	56.3	56.2	56.3

To be continued

Table 2.19. Cont.

Position	11[a]	12[a]	13[b]	14[b]	15[b]	16[b]	17[b]	18[b]
1'	166.0	166.0	164.6	164.4	165.3	165.1	165.9	165.6
2'	130.6	130.6	137.1	137.1	130.5	130.5	124.0	123.9
3', 7'	129.6	129.7	131.4	131.4	131.8	131.8	132.1	132.0
4', 6'	128.4	128.4	124.5	124.6	129.6	129.7	114.5	114.6
5'	132.8	132.8	151.5	151.6	139.4	139.5	164.3	164.3
5'-OMe	–	–	–	–	–	–	55.9	55.9
1''	–	166.1	–	164.7	–	165.4	–	165.9
2''	–	130.9	–	137.1	–	130.5	–	124.0
3'', 7''	–	129.5	–	131.4	–	131.8	–	132.1
4'', 6''	–	128.3	–	124.6	–	129.7	–	114.6
5''	–	132.7	–	151.6	–	139.5	–	164.4
5''-OMe	–	–	–	–	–	–	–	55.9

Table 2.20. ^{1}H NMR data of karavoates O (**19**), and P (**20**) (CD_3COCD_3, 400 MHz, δ in ppm, J in Hz).

Position	19[a]	20[b]	Position	19[a]	20[b]
3	3. 50 *br s*	4.85 *br s*	**23**	5.80 *td* (9.2, 2.8)	5.80 *td* (10.0, 2.4)
6	5.77 *d* (5.2)	5.82 *d* (5.6)	**24**	5.22 *d* (8.9)	5.20 *d* (8.8)
7	3.41 *d* (5.3)	3.44 *d* (4.6)	**26**	1.80 *s*	1.76 *s*
8	2.00 *s*	2.12 *s*	**27**	1.72 *s*	1.70 *s*
10	2.36 *br d* (11.2)	2.46 *br d* (11.6)	**28**	1.05 *s*	1.16 *s*
18	0.94 *s*	0.93 *s*	**29**	1.20 *s*	1.14 *s*
19	0.97 *s*	1.00 *s*	**30**	0.79 *s*	0.80 *s*
21	1.03 *d* (6.2)	1.01 *d* (6.0)	**7-OMe**	3.28 *s*	3.31 *s*

[a]Other signals for compound **19**: 23-OCin: δ_H 7.68 - 7.63 (2H, *m*, H-5'/H-9'), 7.67 (1H, *d*, J = 16.0 Hz, H-3'), 7.45 (3H, *m*, H-6'/H-8'/H-7'), 6.56 (1H, *d*, J = 16.0 Hz, H-2').

[b] Other signals for compound **20**: 3-OCin and 23-OCin: δ_H 7.70 - 7.62 (4H, *m*, H-5'/H-5''/H-9'/H-9''), 7.68 (1H, *d*, J = 16.0 Hz, H-3''), 7.66 (1H, *d*, J = 16.0 Hz, H-3'), 7.47 - 7.40 (6H, *m*, H-6'/H-6''/H-7'/H-7''/H-8'/H-8''), 6.55 (1H, *d*, J = 16.0 Hz, H-2''), 6.54 (1H, *d*, J = 16.0 Hz, H-2').

Table 2.21. ^{13}C NMR data of karavoates O (**19**) and P (**20**) (CD_3COCD_3, 100.61 MHz, δ in ppm).

Position	19	20	Position	19	20
1	21.8	22.4	**25**	136.0	136.0
2	29.9	26.9	**26**	18.3	18.4
3	76.4	79.2	**27**	25.9	25.7
4	42.0	40.8	**28**	28.4	28.1
5	148.0	146.9	**29**	25.6	25.4
6	120.0	120.5	**30**	18.3	18.3
7	77.7	77.6	**7-OMe**	56.3	56.2
8	49.1	49.0			
9	34.6	34.7	**1'**	166.5	166.3
10	39.6	39.1	**2'**	119.4	119.4
11	33.2	33.1	**3'**	144.9	145.1
12	30.7	30.8	**4'**	135.4	135.4
13	46.8	46.8	**5', 9'**	128.9	128.9
14	48.7	48.7	**6', 8'**	131.0	131.0
15	35.2	35.2	**7'**	129.7	129.7
16	28.5	28.5			
17	51.2	51.2	**1''**	–	166.3
18	15.6	15.6	**2''**	–	119.4
19	29.1	29.1	**3''**	–	144.9
20	33.6	33.6	**4''**	–	135.4
21	19.3	19.3	**5'', 9''**	–	128.9
22	42.7	42.7	**6'', 8''**	–	131.0
23	69.5	69.6	**7''**	–	129.7
24	125.8	125.8			

1.13. Cucurbalsaminol A [cucurbita-5,23(*E*)-diene-3β,7β,12β,25-tetraol]

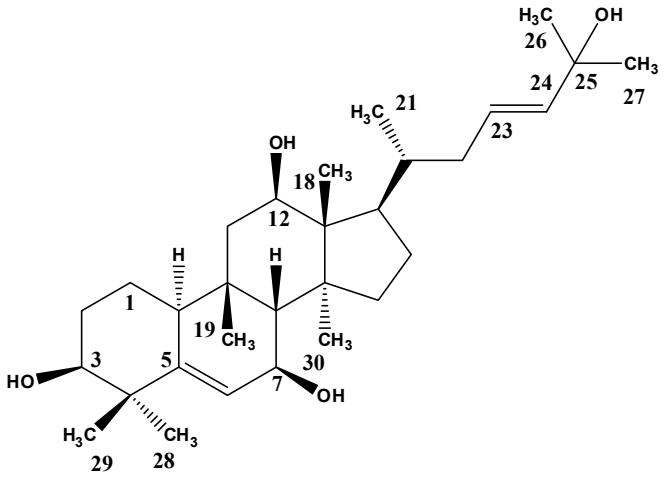

32

Compound **32**, a new structure named cucurbalsaminol A, revealed a molecular formula of $C_{30}H_{50}O_4$, indicated by the pseudomolecular ion $[M + Na]^+$ at *m/z* 497.3601 (calcd. for $C_{30}H_{50}O_4Na$: 497.3601), in the HR-ESITOFMS spectrum. The absorption band at 3447 cm^{-1}, in its IR spectrum, evidenced the presence of hydroxyl functions. When comparing the ^1H and ^{13}C NMR data (Table 2.22) of the tetracyclic skeleton of **32** with those of balsaminagenin A (**34**) (Table 2.4), significant differences were detected. In addition to the differences resulting from the absence of the hydroxyl group at C-29, the presence of an unusual hydroxyl group at C-12 was indicated by a signal at δ_H 3.86 (dd, J = 11.4, 5.0 Hz), in the ^1H NMR, and the marked downfield shift at C-12 ($\Delta\delta_C \cong +$ 40 ppm, α-carbon), C-11 and C-13 ($\Delta\delta_C \cong +$ 10.6, + 5.0 ppm, β-carbons), in the ^{13}C NMR. Other significant differences were observed, mainly at carbons of ring C and Me-18, which showed a clear diamagnetic effect ($\Delta\delta_C \cong -$ 5.8 ppm, γ-carbon). The HMBC spectrum corroborated the presence of a hydroxyl group at C-12 by coupling constants observed between C-18 and H-12, and between C-10 and H-11, and the $^2J_{C\text{-}H}$ correlations between C-11, C-13 and H-12.

The relative configuration at C-12 was deduced by significant NOE correlations observed in the NOESY spectrum, which also provided the relative stereochemistry of the remaining tetrahedral stereocenters of the compound. In this way, NOE effects between H-12/H-10 (δ_H 2.30), H-12/Me-30 (δ_H 0.74), and H-12/H-17, together with coupling constant values indicated an equatorial β-oriented hydroxyl group. Furthermore, taking into account that a significant NOE can usually be detected if the distance between the dipolar-coupled

protons is less than 3.5 Å, the calculated conformation[12] of compound **32** agreed well with the above-mentioned spectroscopic results (Figure 2.8). Therefore, compound **32** was concluded to be the new compound named cucurbita-5,23(*E*)-diene-3β,7β,12β,25-tetraol.

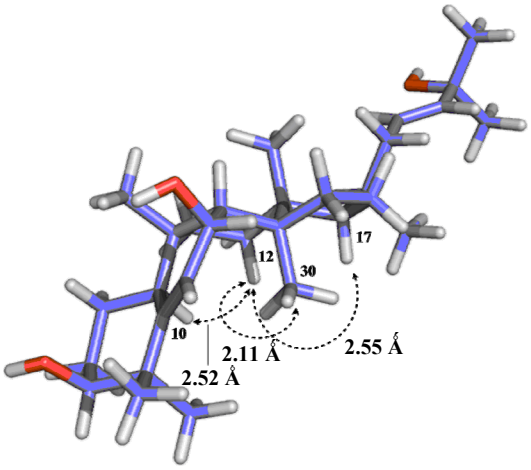

Figure 2.8. Energy-minimized 3D structure of compound **32**.

1.14. Cucurbalsaminol B [7β-methoxycucurbita-5,23(*E*)-diene-3β,12β,25-triol]

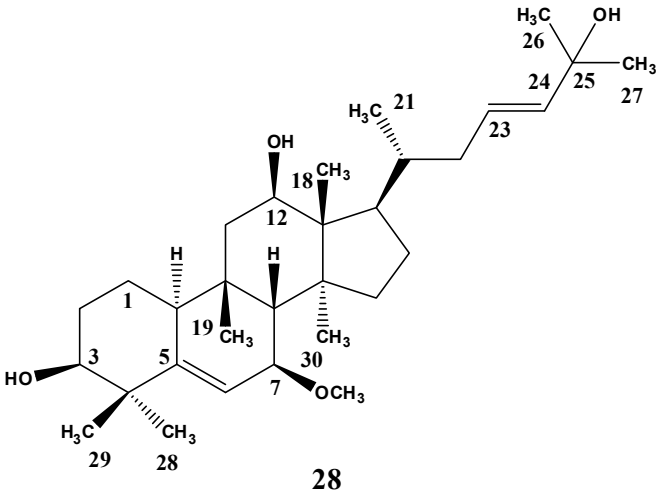

28

Compound **28**, a new structure named cucurbalsaminol B, was obtained as a white amorphous powder. Its molecular formula, $C_{31}H_{52}O_4$, was established from the molecular ion

[12] *Chemical Computing Group Inc. MOE v 2008. 1010 Montreal, Quebec, Canada, 2008* and. *Warren L. DeLano 'The PyMOL Molecular Graphics System.' DeLano Scientific LLC, San Carlos, CA, USA. http://www.pymol.org*

peak $[M]^+$ at *m/z* 488.3853 (calcd. for $C_{31}H_{52}O_4$: 488.3866), found in the HR-EIMS spectrum. Analysis of the spectroscopic data of **28** (Table 2.23) pointed to a structure similar to that of compound **32** (Table 2.22), excepting the signals corresponding to the proton *geminal* to the hydroxyl group at C-7, which was replaced by a methoxyl group in **28**, as in compounds **1** and **27**. This structural feature was supported by the shielding effect at H-7 (δ_H 3.49), displayed as a broad singlet, when compared with that of compound **32**, and by the HMBC correlation between the methoxyl group and H-7. Therefore, compound **28** was determined as the new compound 7β-methoxycucurbita-5,23(*E*)-diene-3β,12β,25-triol.

1.15. Cucurbalsaminol C [7β-methoxycucurbita-5,24-diene-3β,12β,23(*R*)-triol]

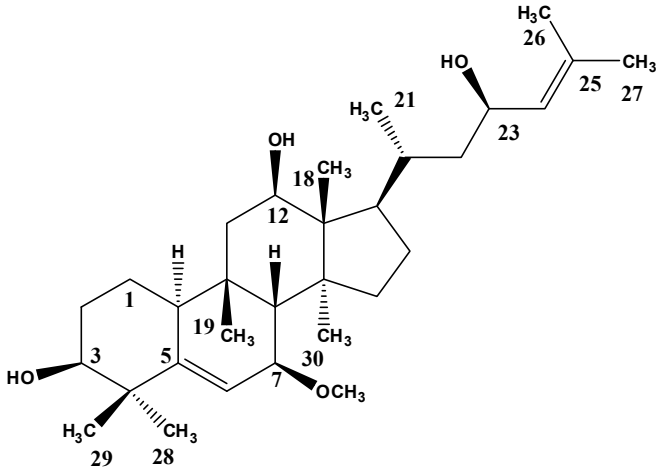

30

Compound **30**, a new structure named cucurbalsaminol C, was obtained as a white amorphous powder, with a molecular formula of $C_{31}H_{52}O_4$ deduced by HR-EIMS, which showed a molecular ion peak $[M]^+$ at *m/z* 588.3867 (calcd. for $C_{31}H_{52}O_4$: 488.3866). Its IR spectrum exhibited a characteristic absorption band at 3443 cm^{-1} due to hydroxyl groups. The low resolution EIMS supported the presence of three hydroxyls and a methoxyl group in compound **30**, by the fragment ions at *m/z* 434 $[M - 3 \times H_2O]^+$, 420 $[M - 2 \times H_2O - CH_3OH]^+$, 402 $[M - 3 \times H_2O - CH_3OH]^+$. The NMR spectra of **30** (Table 2.23) were similar to those of cucurbalsaminol B (**28**). The major differences were found in the side chain signals due to the presence of a hydroxyl group at C-23 and a double bond at C-24, also

observed in balsamiols A, B, E and F. Therefore, the structure of compound **30** was established as 7β-methoxycucurbita-5,24-diene-3β,12β 23(*R*)-triol.

Compounds **28**, **30**, and **32** were the first cucurbitane-type triterpenes, having an oxidation at C-12.

Table 2.22. NMR data of cucurbalsaminol A (**32**), (MeOD, ^{1}H 400 MHz, ^{13}C 100.61 MHz; δ in ppm, *J* in Hz).

Position	^{1}H	^{13}C	DEPT	Position	^{1}H	^{13}C	DEPT
1	1.61 *m*; 1.65 *m*	22.5	CH_2	**16**	1.64 *m*; 1.90 *m*	25.7	CH_2
2	1.70 *m*; 1.90 *m*	30.10	CH_2	**17**	1.88 *m*	51.9	CH
3	3.49 *br s*	77.4	CH	**18**	0.89 *s*	10.6	CH_3
4	–	42.3	C	**19**	1.08 *s*	29.7	CH_3
5	–	148.0	C	**20**	1.81 *m*	35.0	CH
6	5.74 *d* (4.5)	122.5	CH	**21**	1.02 *d* (6.8)	22.1	CH_3
7	3.94 *br d* (4.9)	68.2	CH	**22**	1.75 *m*; 2.29 *m*[a]	39.7	CH_2
8	1.90 *br s*	53.3	CH	**23**	5.58 *m*[a]	127.3	CH
9	–	37.3	C	**24**	5.58 *m*[a]	140.0	CH
10	2.32 *m*[a]	41.4	CH	**25**	–	71.2	C
11	1.34 *m*; 1.89 *m*	44.5	CH_2	**26**	1.25 *s*	30.09	CH_3
12	3.86 *dd* (11.4, 5.0)	71.9	CH	**27**	1.25 *s*	30.0	CH_3
13	–	52.1	C	**28**	1.01 *s*	28.7	CH_3
14	–	51.4	C	**29**	1.18 *s*	26.1	CH_3
15	1.33 *m*; 1.56 *m*	36.1	CH_2	**30**	0.74 *s*	18.5	CH_3

[a] Overlapped signals.

Table 2.23. NMR data of cucurbalsaminols B (**28**) and C (**30**), (MeOD, ^{1}H 400 MHz, ^{13}C 100.61 MHz; δ in ppm, J in Hz).

Position	28			30		
	^{1}H	^{13}C	DEPT	^{1}H	^{13}C	DEPT
1	1.63 *m*; 1.70 *m*	22.5	CH_2	1.63 *m*; 1.70 *m*	22.5	CH_2
2	1.71 *m*; 1.98 *m*	30.10	CH_2	1.71 *m*; 1.98 *m*	30.1	CH_2
3	3.49 *br s*[a]	77.4	CH	3.49 *br s*[a]	77.4	CH
4	–	42.4	C	–	42.4	C
5	–	149.1	C	–	149.1	C
6	5.78 *d* (4.9)	120.3	CH	5.78 *d* (4.8)	120.3	CH
7	3.49 *br s*[a]	78.4	CH	3.49 *br s*[a]	78.4	CH
8	1.98 *br s*	48.9	CH	1.98 *br s*	48.8	CH
9	–	37.4	C	–	37.4	C
10	2.33 *m*[a]	41.6	CH	2.33 *br d* (10.0)	41.6	CH
11	1.34 *m*; 1.88 *m*	44.4	CH_2	1.38 *m*; 1.88 *m*	44.4	CH_2
12	3.86 *dd* (11.4, 4.9)	71.8	CH	3.86 *dd* (11.2, 4.8)	72.0	CH
13	–	52.3	C	–	52.4	C
14	–	51.1	C	–	51.1	C
15	1.36 *m*; 1.53 *m*	36.2	CH_2	1.30 *m*; 1.51 *m*	36.2	CH_2
16	1.63 *m*; 1.92 *m*	25.6	CH_2	1.65 *m*; 1.92 *m*	25.7	CH_2
17	1.88 *m*	52.0	CH	1.88 *m*	52.6	CH
18	0.92 *s*	10.6	CH_3	0.93 *s*	10.7	CH_3
19	1.01 *s*	29.3	CH_3	1.01 *s*	29.3	CH_3
20	1.83 *m*	35.0	CH	1.86 *m*	31.0	CH
21	1.02 *d* (6.8)	22.1	CH_3	1.07 *d* (6.4)	22.4	CH_3
22	1.75 *m*; 2.31 *m*[a]	39.7	CH_2	0.98 *m*; 1.77 *m*	44.8	CH_2
23	5.58 *m*[a]	127.3	CH	4.41 *td* (8.9, 3.6)	67.8	CH
24	5.58 *m*[a]	140.1	CH	5.16 *d* (8.4)	130.6	CH
25	–	71.2	C	–	133.4	C
26	1.26 *s*	30.09	CH_3	1.67 *s*	18.2	CH_3
27	1.26 *s*	30.0	CH_3	1.70 *s*	25.9	CH_3
28	1.01 *s*	28.7	CH_3	1.02 *s*	28.7	CH_3
29	1.18 *s*	26.0	CH_3	1.18 *s*	26.0	CH_3
30	0.75 *s*	18.5	CH_3	0.76 *s*	18.6	CH_3
7-OMe	3.33 *s*	56.4	CH_3	3.33 *s*	56.4	CH_3

[a] overlapped signal

1.16. Balsaminoside A [25-methoxycucurbita-5,23(*E*)-dien-3β-ol-7-O-β-D-allopyranoside]

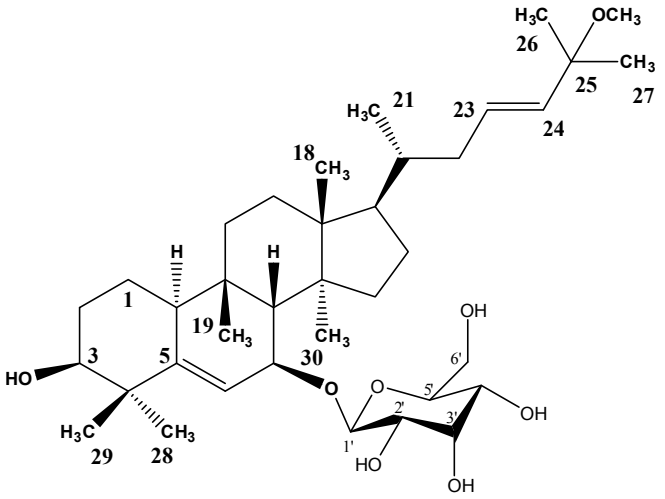

40

Compound **40**, a new structure named balsaminoside A, was obtained as white crystals, whose molecular formula was determined as $C_{37}H_{62}O_8$ from its HR-ESITOFMS, which showed a pseudomolecular ion at *m/z* 657.4335 $[M + Na]^+$ (calcd. for $C_{37}H_{62}O_8Na$: 657.4337). The low resolution ESIMS of **40** exhibited pseudomolecular ions at *m/z* 657 $[M + Na]^+$ and 673 $[M + K]^+$. The ions at *m/z* 478 $[M + Na + H - C_6H_{12}O_6]^+$ and 203 $[C_6H_{12}O_6 + Na]^+$ suggested the presence of a sugar unit. Analysis of the IR spectrum of **40** provided evidence for hydroxyl groups in the molecule (3409 cm^{-1}). Comparison of the ^1H and ^{13}C NMR spectra (Tables 2.24 and 2.25) of **40** with those of compound **33** (Table 2.5), revealed six additional signals in the former, due to the sugar moiety, and the absence of the hydroxymethyl group at C-4. In the ^{13}C NMR spectrum of **40**, the signal corresponding to C-7 was shifted downfield ($\Delta\delta_C$ = + 5.9), suggesting that the sugar moiety was located at this carbon. This was identified, unambiguously, as allose based on the equatorial configuration of H-3′, revealed by a broad singlet at δ_H 4.05. In glucose, H-3′ is axially oriented and generally appears as a triplet ($J_{3ax,\ 2ax} \cong J_{3ax,\ 2ax} \cong$ 8,8), (Fatope et al., 1990; Liu et al., 2005). The identification of the allopyranosyl moiety was corroborated by the values of the carbon signals, which were in good agreement with those reported for allose (Li et al., 2007b). To compare with other compounds described in literature, the ^1H and ^{13}C NMR spectra were also recorded in pyridine (Tables 2.24 and 2.25). The heteronuclear $^3J_{C\text{-}H}$ correlations observed in the HMBC spectrum between C-7 (δ_C 74.4) of the aglycone moiety and the anomeric proton (δ_H 4.75) confirmed that the allopyranosyl unit was bounded at C-7. The relative

configuration of **40** was deduced from a NOESY experiment. The configuration of the glycosidic linkage was determined as β based on the coupling constant value of the anomeric proton (J = 7.8 Hz). Therefore, based on the above data, the structure of **40** was assigned as 25-methoxycucurbita-5,23(*E*)-dien-3β-ol-7-O-β-D-allopyranoside.

1.17. Balsaminoside B [cucurbita-5,24-diene-3β,23(*R*)-diol-7-O-β-D-allopyranoside]

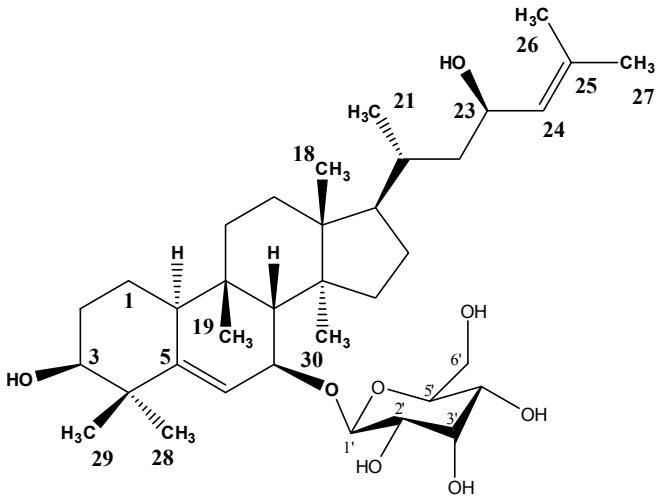

38

Compound **38**, named balsaminoside B, is a new compound isolated as white crystals (mp 230 - 232 ºC). The IR spectrum showed a strong absorption band for hydroxyl groups (3396 cm^{-1}). Its molecular formula, $C_{36}H_{60}O_8$, was established from the pseudomolecular ion peak at *m/z* 643.4180 $[M + Na]^+$ in its HR-ESITOFMS data. In the low resolution ESIMS spectrum of **38** was observed an ion at *m/z* 423 $[M + H - H_2O - C_6H_{12}O_6]^+$. The ^1H and ^{13}C NMR spectra of **38** (Tables 2.24 and 2.25) were very similar to those of **40** (Tables 2.24 and 2.25), except for the signals due to the side chain, which were consistent with those observed for compounds **1**, **3**, **26**, **27**, **30**, and **35**. The placement of the sugar unit at C-7 was unambiguously defined by a cross-peak between C-7 (δ_C 74.4) and the anomeric proton signal at δ_H 4.75 (d, J = 8.0 Hz) observed in the HMBC spectrum. From the above data, the structure of **38** was deduced as cucurbita-5,24-diene-3β,23(*R*)-diol-7-O-β-D-allopyranoside.

1.18. Balsaminoside C [cucurbita-5,24-diene-3β,23(*R*)-diol-7-O-β-D-glucopyranoside]

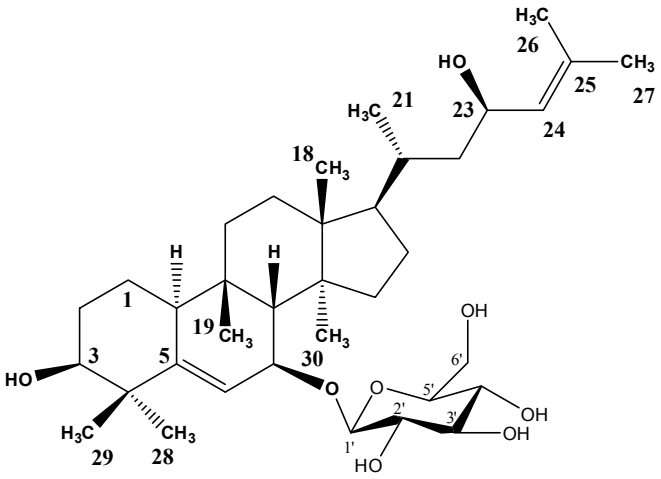

39

Compound **39** was isolated as a white powder with a positive rotation. Its MS, IR, ^{1}H and ^{13}C NMR data were very similar to those obtained for balsaminoside B (**38**), except for the signals due to the sugar unit. The downfield chemical shift values showed for the carbons of the sugar unit were consistent with the presence of a β-glucopyranosyl unit in compound **39** instead the β-allopyranosyl unit found in **38** (Tables 2.24 and 2.25), (Fatope et al., 1990). By comparison of all the spectroscopic data with those reported in the literature, compound **39** was identified as cucurbita-5,24-diene-3β,23(*R*)-diol-7-O-β-D-glucopyranoside, previously isolated from *M. charantia* (Fatope et al., 1990). This compound was here designated balsaminoside C, in order to facilitate its use in tables.

Table 2.24. ^{1}H NMR data of balsaminosides A (**40**), B (**38**), and C (**39**), (MeOD[a], C_5H_5N[b], 400 MHz, δ in ppm, *J* in Hz).

Position	38[a]	39[a]	40[a]	40[b]
1	1.57 *m*; 1.70 *m*	1.57 *m*; 1.70 *m*	1.57 *m*; 1.67 *m*	n d
2	1.67 *m*; 1.97 *m*	1.67 *m*; 1.97 *m*	1.68 *m*; 1.97 *m*	n d
3	3.49 *br s*	3.49 *br s*	3.49 *br s*	3.82 *br s*
6	5.76 *d* (4.8)	5.75 *d* (4.9)	5.75 *d* (4.9)	6.09 *d* (5.0)
7	4.11 *br d* (4.5)	4.11 *br d* (7.0)	4.11 *br d* (5.0)	4.60 [a]
8	2.13 *br s*	2.12 *br s*	2.13 *br s*	2.46 *br s*
10	2.34 *br d* (9.3)	2.34 *br d* (10.1)	2.33 *br d* (9.8)	2.40 *m*
11	1.48 *m*; 1.70 *m*	1.48 *m*; 1.70 *m*	1.48 *m*; 1.70 *m*	n.d.
12	1.58 *m*; 1.69 *m*	1.55 *m*	1.49 *m*; 1.71 *m*	n.d.
15	1.36 *m*	1.34 *m*	1.38 *m*	n.d.
16	1.40 *m*; 1.91 *m*	1.40 *m*; 1.91 *m*	1.59 *m*; 1.96 *m*	n.d.
17	1.48 *m*	1.48 *m*	1.57 *m*	n.d.
18	0.99 *s*	0.99 *s*	0.98 *s*	0.82 *s*
19	1.03 *s*	1.03 *s*	1.03 *s*	1.40 *s*
20	1.54 *m*	1.48 *m*	1.54 *m*	n.d.
21	0.98 *d* (7.2)	0.98 *d* (6.5)	0.94 *d* (5.8)	0.98 *d* (4.8)
22	1.82 *m*; 2.21 *m*	0.96 *m*; 1.62 *m*	1.82 *m*; 2.21 *m*	n.d.
23	4.41 *td* (9.4, 2.8)	4.40 *td* (9.4, 3.0)	5.58 *m*	5.64 *m*
24	5.16 *d* (8.4)	5.16 *d* (8.2)	5.38 *d* (15.7)	5.58 *d* (15.9)
26	1.67 *s*	1.66 *s*	1.24 *s*	1.34 *s*
27	1.70 *s*	1.74 *s*	1.24 *s*	1.34 *s*
28	1.03 *s*	1.03 *s*	1.03 *s*	1.46 *s*
29	1.18 *s*	1.18 *s*	1.18 *s*	1.14 *s*
30	0.75 *s*	0.75 *s*	0.74 *s*	0.73 *s*
25-OMe	–	–	3.14 *s*	3.23 *s*
7-Sugar				
1'	4.75 *d* (8.0)	4.34 *d* (7.7)	4.75 *d* (7.8)	5.59 *d* (7.6)
2'	3.32 *m*[a]	3.17 *m*[a]	3.32 *m*[a]	4.07 br s
3'	4.05 *br s*	3.36 *m*[a]	4.05 *br s*	4.79 *br s*
4'	3.51 *m*	3.30 *m*[a]	3.50 *m*	4.32 *br s*
5'	3.66 *m*[a]	3.22 *m*[a]	3.63 *m*	4.53 *m*
6'	3.66 *m*[a] 3.84 *br d* (9.4)	3.66 *dd* (11.8, 5.4) 3.86 *dd* (11.8, 2.4)	3.65 *m* 3.84 *br d* (9.8)	4.48 *m*; 4.60 *m*[a]

[a] Overlapped signals; n.d. not determined

Table 2.25. ^{13}C NMR data of balsaminosides A (**40**), B (**38**), and C (**39**), (MeOD[a], C_5H_5N[b], 100.61 MHz, δ in ppm).

Position	38[a]	39[a]	40[a]	40[b]	DEPT
1	22.3	22.4	22.3	21.7	CH_2
2	30.1	30.1	30.1	30.1	CH_2
3	77.4	77.5	77.5	76.0	CH
4	42.4	42.4	42.4	41.9	C
5	148.7	148.8	148.7	148.2	C
6	122.1	122.9	122.0	121.2	CH
7	74.4	74.6	74.4	72.0	CH
8	49.9	49.9	49.9	48.2	CH
9	35.1	35.1	35.1	34.4	C
10	40.1	40.1	40.1	39.2	CH
11	33.7	33.8	33.7	28.4	CH_2
12	31.5	31.5	31.3	32.9	CH_2
13	47.3	47.3	47.2	46.2	C
14	49.2	49.7	49.6	48.4	C
15	35.7	35.8	35.7	34.8	CH_2
16	28.8	28.8	28.8	30.4	CH_2
17	52.3	52.3	51.3	50.3	CH
18	16.1	16.0	16.1	15.6	CH_3
19	29.4	29.5	29.4	29.3	CH_3
20	33.8	33.7	37.6	36.4	CH
21	19.3	19.3	19.3	19.0	CH_3
22	45.7	45.6	40.5	39.7	CH_2
23	66.6	66.6	130.2	128.5	CH
24	130.5	130.5	137.6	137.6	CH
25	133.3	133.4	76.5	74.8	C
26	18.2	18.1	26.2	26.0	CH_3
27	26.0	26.0	26.5	26.4	CH_3
28	28.8	28.8	28.7	27.8	CH_3
29	26.1	26.1	26.1	26.0	CH_3
30	18.8	18.8	18.7	18.0	CH_3
25-OMe	–	–	50.4	50.1	CH_3

To be continued

Table 2.25. Cont.

Position	38	39	40[a]	40[b]	DEPT
1'	99.0	101.7	99.0	98.3	CH
2'	72.3	75.1	72.3	72.4	CH
3'	73.0	78.3	73.0	73.2	CH
4'	69.1	71.8	69.1	69.3	CH
5'	75.4	78.0	75.4	76.1	CH
6'	63.2	62.8	63.2	63.3	CH_2

1.19. Kuguaglycoside A [7β-methoxycucurbita-5,24-dien-3β-ol-23-O-β-D-glucopyranoside]

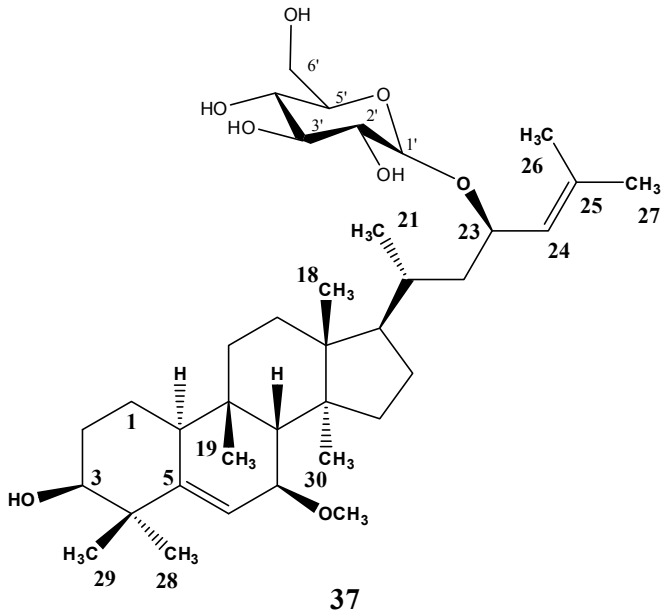

37

Compound **37**, identified as kuguaglycoside A, was isolated as a white amorphous powder with a positive optical rotation. Its molecular formula was deduced as $C_{37}H_{62}O_8$ by the HR-ESITOFMS, which showed a pseudomolecular ion peak at *m/z* 657.4334, as well as the analysis of NMR data. The ESIMS suggested the presence of a sugar unit due to the fragments at *m/z* 477 $[M + Na + C_6H_{12}O_6]^+$ and 203 $[C_6H_{12}O_6 + Na]^+$. In addition, careful comparison of the ^1H and ^{13}C data of **37** (Table 2.26) with those of karavilagenin C (**1**) revealed that the two compounds differed only in the signals of side chain. In fact, in the ^{13}C NMR spectrum of **37**, the signal corresponding to C-23 was shifted downfield ($\Delta\delta_C$ = + 10

ppm), indicating that the sugar moiety was attached to this carbon. The HMBC correlation observed between C-23 and the anomeric proton supported the above feature. By comparison of all the spectroscopic data to those reported in the literature, compound **37** was identified as 7β-methoxycucurbita-5,24-dien-3β-ol-23-O-β-D-glucopyranoside, only previously isolated from the roots of *M. charantia* (Chen et al., 2008a).

Table 2.26. NMR data of kuguaglycoside A (**37**), (MeOD, ^{1}H 400 MHz, ^{13}C 100.61 MHz; δ in ppm, J in Hz).

Position	^{1}H	^{13}C	DEPT	Position	^{1}H	^{13}C	DEPT
1	1.57 *m*; 1.70 *m*	22.4	CH_2	**20**	1.54 *m*	33.7	CH
2	1.67 *m*; 1.97 *m*	30.1	CH_2	**21**	0.99 *d* (6.5)	19.8	CH_3
3	3.48 *br s*[a]	77.9	CH	**22**	1.01 *m*; 1.81 *m*	44.2	CH_2
4	–	42.5	C	**23**	4.54 *td* (8.8, 4.2)	76.7	CH
5	–	149.4	C	**24**	5.25 *d* (9.1)	128.9	CH
6	5.78 *d* (5.0)	120.3	CH	**25**	–	134.1	C
7	3.48 *br s*[a]	78.9	CH	**26**	1.70 *s*	18.2	CH_3
8	2.05 *br s*	49.4	CH	**27**	1.71 *s*	25.9	CH_3
9	–	35.1	C	**28**	1.03 *s*	28.7	CH_3
10	2.34 *dd* (11.6, 4.1)	40.3	CH	**29**	1.18 *s*	26.0	CH_3
11	1.48 *m*; 1.70 *m*	33.8	CH_2	**30**	0.75 *s*	18.8	CH_3
12	1.58 *m*; 1.69 *m*	31.4	CH_2	**7-OMe**	3.32 *s*	56.4	CH_3
13	–	47.4	C	**23-glu**	–	–	–
14	–	49.5	C	**1'**	4.26 *d* (7.8)	103.8	CH
15	1.34 *m*	35.8	CH_2	**2'**	3.15 *m*[a]	75.5	CH
16	1.47 *m*; 1.94 *m*	28.8	CH_2	**3'**	3.30 *m*[a]	78.5	CH
17	1.45 *m*	52.2	CH	**4'**	3.31 *m*[a]	71.6	CH
18	0.97 *s*	15.9	CH_3	**5'**	3.17 *m*[a]	77.5	CH
19	0.97 *s*	29.4	CH_3	**6'**	3.65 *dd* (11.8, 5.4); 3.79 *dd* (11.8, 2.4)	62.8	CH_2

[a] Overlapped signals

1.20. Balsaminagenin C [cucurbita-5,23(*E*)-diene-3β,7β,25-triol]

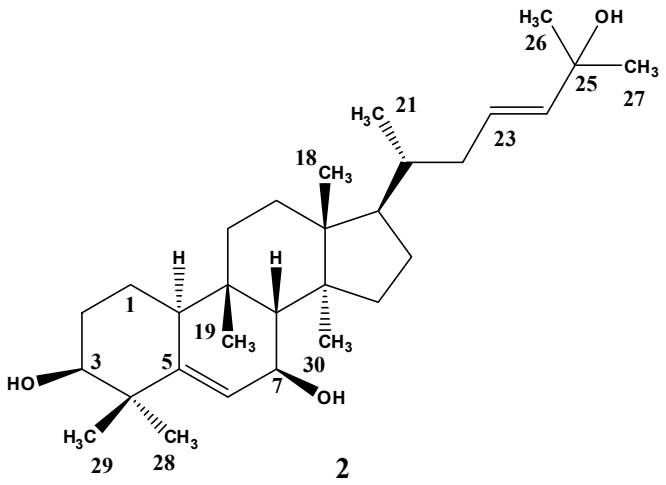

2

Compound **2** was isolated as a white amorphous powder with $[\alpha]_D^{26}$ + 74. Its ESIMS showed a pseudomolecular ion at *m/z* 481 $[M + Na]^+$, consistent with the molecular formula $C_{30}H_{52}O_3$ (six degrees of unsaturation). The low resolution ESIMS spectrum showed also an ion at *m/z* 441 $[M + H - H_2O]^+$, suggesting the existence of hydroxyl groups, which was confirmed by the IR spectrum. Comparison of NMR spectra of **2** (Table 2.27) with those of compound **34** (Table 2.4) showed that the most evident differences were the replacement of the hydroxymethyl group at C-4 in compound **34** by a methyl group in **2**. Therefore, the structure of compound **2** was established as the known compound cucurbita-5,23(*E*)-diene-3β,7β,25-triol. Compound **2** was only previously isolated, from the methanolic extract of *M. charantia* stems (Chang et al., 2008). This compound was here designated balsaminagenin C, in order to facilitate its use in tables.

Table 2.27. NMR data of cucurbita-5,23(*E*)-diene-3β,7β,25-triol (**2**), (MeOD, ^{1}H 400 MHz, ^{13}C 100.61 MHz; δ in ppm, *J* in Hz).

Position	^{1}H	^{13}C	DEPT	Position	^{1}H	^{13}C	DEPT
1	1.56 *m*; 1.66 *m*	22.4	CH_2	**16**	1.37 *m*; 1.90 *m*	28.8	CH_2
2	1.71 *m*; 1.95 *m*	30.0	CH_2	**17**	1.51 *m*	51.2	CH
3	3.50 *br s*	77.5	CH	**18**	0.94 *s*	16.0	CH_3
4	–	42.3	C	**19**	1.04 *s*	29.8	CH_3
5	–	148.3	C	**20**	1.51 *m*	37.7	CH
6	5.74 *d* (4.9)	122.5	CH	**21**	0.92 *d* (5.8)	19.2	CH_3
7	3.93 *br d* (5.1)	68.8	CH	**22**	1.75 *m*; 2.15 *dd* (9.6, 7.0)	40.3	CH_2
8	1.97 *br s*	54.1	CH	**23**	5.55 *m*	125.9	CH
9	–	35.0	C	**24**	5.55 *m*	140.8	CH
10	2.33 *dd* (11.2, 4.3)	40.1	CH	**25**	–	71.2	C
11	1.48 *m*; 1.68 *m*	33.9	CH_2	**26**	1.25 *s*	30.1	CH_3
12	1.46 *m*; 1.66 *m*	31.3	CH_2	**27**	1.25 *s*	30.1	CH_3
13	–	47.1	C	**28**	1.03 *s*	28.7	CH_3
14	–	49.2	C	**29**	1.18 *s*	26.1	CH_3
15	1.34 *m*	35.7	CH_2	**30**	0.73 *s*	18.6	CH_3

1.21. Karavilagenin E [5β,19β-epoxycucurbita-6,24-diene-3β,23(*R*)-diol]

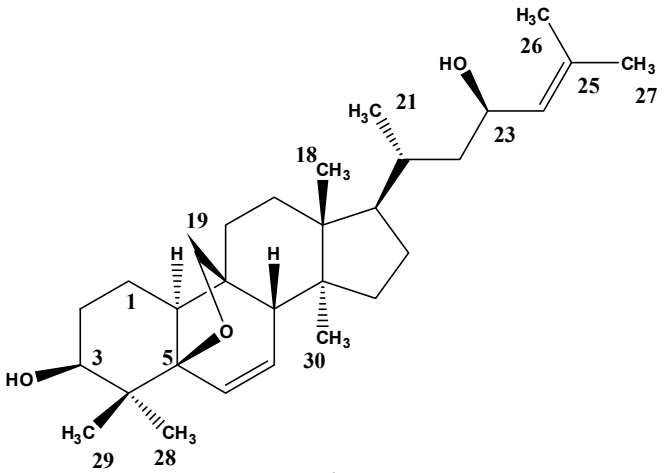

4

Compound **4** was obtained as a white amorphous powder with a negative optical rotation ($[\alpha]_D^{26}$ – 53). The ESIMS showed a pseudomolecular ion at *m/z* 479 $[M + Na]^+$, which was consistent with the molecular formula $C_{30}H_{48}O_3$, indicating the presence of seven degrees

of unsaturation. Its IR spectrum showed an ether absorption band (1081 cm^{-1}), as well as a band for a hydroxyl group. Comparing the ^{1}H and ^{13}C NMR data (Table 2.28) of compound **4**, with those of the compounds previously presented, significant differences were observed in the chemical shifts regarding the cucurbitane skeleton. In this way, in the ^{13}C NMR spectrum two olefinic carbon signals at δ_C 132.6 and 132.8 appeared, instead the characteristic signals ascribed to the vinylic carbons C-5, and C-6 at $\delta_C \cong$ 148.3 and 122.5, respectively. Their corresponding ^{1}H NMR resonances occurred at δ_H 6.05 (d, J = 9.8 Hz) for δ_C 132.8 and 5.64 (dd, J = 9.6, 3.4 Hz) and δ_C 132.6, and were assigned to H-6 and H-7, respectively. This assignment was supported by the long-range correlations, displayed by the HMBC spectrum (Figure 2.9), between C-6 (δ_C 132.8) and H-10 (δ_H 2.34) and C-7 (δ_C 132.6) and H-8 (δ_H 2.38). Moreover, the COSY correlations between H-6/H-7, H-6/H-8, and H-7/H-8 corroborated this assignment. Furthermore, the ^{1}H NMR spectrum also showed, instead of the characteristic signal of the methyl at C-19, the presence of a pair of coupled doublets at δ_H 3.66 and 3.50, which were both correlated with a carbon at δ_C 80.8, in the HMQC spectrum. Taking into account the degree of unsaturation, and the absence of a proton at C-5, an additional ring formed by a C-5, C-19 ether linkage was indicated. This structural feature was corroborated by the long range correlations displayed in the HMBC spectrum between C-19 (δ_C 80.8) and H-8 (δ_H 2.38), and C-9 (δ_C 46.6) and C-10 (δ_C 40.2) with the two diastereotopic methylene protons at C-19. By comparison of all the spectroscopic data with those reported in the literature, compound **4** was identified as karavilagenin E, 5β,19β-epoxycucurbita-6,24-diene-3β,23(*R*)-diol, only previously isolated from the fruits of *M. charantia*, (Matsuda et al., 2007).

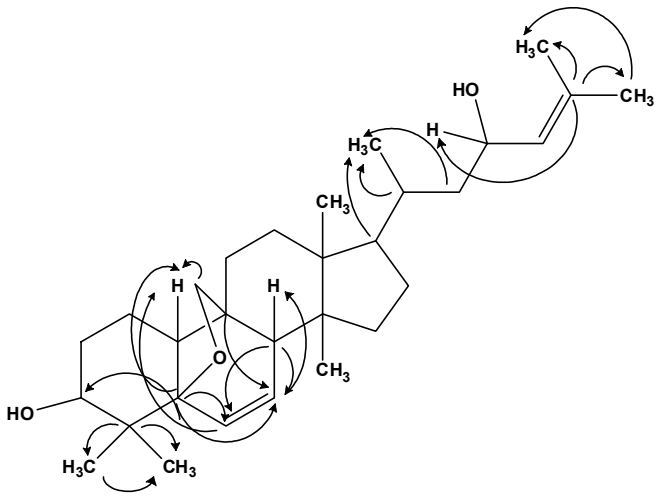

Figure 2.9. Main HMBC correlations of compound **4**.

Table 2.28. NMR data of karavilagenin E (**4**), (MeOD, ^{1}H 400 MHz, ^{13}C 100.61 MHz; δ in ppm, J in Hz).

Position	^{1}H	^{13}C	DEPT	Position	^{1}H	^{13}C	DEPT
1	1.35 *m*; 1.47 *m*	18.6	CH_2	**17**	1.46 *m*	52.2	CH
2	1.72 *m*; 1.88 *m*	29.2	CH_2	**18**	0.93 *s*	15.4	CH_3
3	3.36 *br s*	77.7	CH	**19**	3.66 *d* (8.4)	80.8	CH_2
4	–	38.3	C		3.50 *d* (8.4)		
5	–	88.8	C	**20**	1.74 *m*	33.7	CH
6	6.05 *d* (9.8)	132.8	CH	**21**	0.96 *d* (6.2)	19.2	CH_3
7	5.64 *dd* (9.8, 3.4)	132.6	CH	**22**	0.95 *m*; 1.63 *m*	45.6	CH_2
8	2.38 *br s*	53.4	CH	**23**	4.41 *td* (9.6, 3.2)	66.6	CH
9	–	46.6	C	**24**	5.15 *d* (8.5)	130.4	CH
10	2.34 *m*	40.2	CH	**25**	–	133.5	C
11	1.52 *m*; 1.81 *m*	24.7	CH_2	**26**	1.65 *s*	18.1	CH_3
12	1.64 *m*; 1.74 *m*	32.2	CH_2	**27**	1.69 *s*	26.0	CH_3
13	–	46.6	C	**28**	1.14 *s*	20.9	CH_3
14	–	49.5	C	**29**	0.91 *s*	24.9	CH_3
15	1.31 *m*; 1.40 *m*	34.2	CH_2	**30**	0.90 *s*	20.6	CH_3
16	1.73 *m*; 1.89 *m*	28.3	CH_2				

1.22. (+)-Dehydrovomifoliol

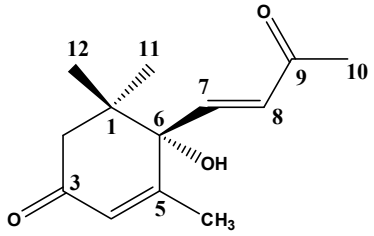

25

Compound **25** was isolated as a yellow oil with a positive optical rotation. Its IR spectrum displayed absorption bands for hydroxyl (3462 cm^{-1}), and α,β-unsaturated ketone (1655 cm^{-1}) groups. Its molecular formula, $C_{13}H_{18}O_3$, was deduced by its EIMS spectrum that exhibited a molecular ion at m/z 222. The ^{1}H NMR spectrum (Table 2.29) displayed signals due to four methyl groups: two *gem*-dimethyls at δ_H 0.94 and 1.05, one vinylic at δ_H 1.89 (d, J = 1.2 Hz), and one methyl adjacent to a carbonyl group at δ_H 2.30. In addition, a singlet of a vinylic proton at δ_H 5.93, two *trans*-olefinic protons at δ_H 6.42 (d, J = 15.6 Hz) and 6.99 (d, J = 15.6 Hz), and two methylenic protons *vicinal* to a carbonyl group, displayed as doublets at δ_H 2.26 and 2.60 (J = 17.2 Hz), were also observed. The ^{13}C NMR and DEPT spectra (Table

2.29) exhibited four methyls, one methylene, three sp^2 methines (δ_C 128.1, 131.8, and 148.4), and also five quaternary carbons (two carbonyls at δ_C 200.4, 200.5, one olefinic at δ_C 164.7 and an oxygenated carbon at δ_C 80.0). Analysis of the 2D NMR data (HMQC, ^{1}H-^{1}H COSY and HMBC), (Figure 2.10) led to the unambiguous assignment of all protons and carbons of compound **25**. By comparison of all the physical and spectroscopic data obtained with those reported in literature, compound **25** was identified as (+)-dehydrovomifoliol, a megastigmane-type *nor*-isoprenoid, isolated for the first time from *Beta vulgaris* var. *cicla* (Chenopodiaceae), (Kim et al., 2004). Its isolation from *Cucumis sativus* (Cucurbitaceae) was also reported (Kai et al., 2007).

Table 2.29. NMR data of dehydrovomifoliol (**25**), (MeOD, ^{1}H 400 MHz, ^{13}C 100.61 MHz; δ in ppm, J in Hz).

Position	^{1}H	^{13}C	DEPT	COSY	HMBC
1	–	42.7	C	–	2a, 2b, 11, 12
2a	2.26 *d* (17.2)	50.6	CH_2	2b	11, 12
2b	2.60 *d* (17.2)			2a	
3	–	200.4	C	–	2a, 2b
4	5.93 *br s*	128.1	CH	13	2b, 13
5	–	164.7	C	–	7, 13
6	–	80.0	C	–	2a, 2b, 4, 7, 8, 11, 12, 13
7	6.99 *d* (15.6)	148.4	CH	8	8
8	6.42 *d* (15.6)	131.8	CH	7	7, 10
9	–	200.5	C	–	7, 8, 10
10	2.30 *s*	27.7	CH_3	–	8
11	0.94 *s*	24.8	CH_3	–	2a, 2b, 12
12	1.05 *s*	23.6	CH_3	–	11
13	1.89 *d* (1.2)	19.2	CH_3	4	4

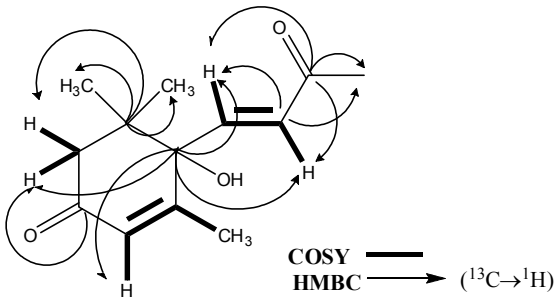

Figure 2.10. Key COSY and HMBC correlations of compound **25**.

CHAPTER 3

Results and Discussion

Biological Studies

1. ANTIMALARIAL ACTIVITY

The antimalarial activity results obtained with extracts and pure compounds will be presented and discussed.

1.1. Screening for antimalarial activity of selected plants

The main goal of this work was to investigate the potential antimalarial properties of some plants used in traditional medicine, mostly in Mozambique, against malaria and/or fever. Thus, the selection of plant species for the antimalarial screening assay was mainly based on an ethnobotanical basis (Bandeira et al., 2001; Clarkson et al., 2004; Jansen, 1982; 1983; 1990; 1991; Jurg et al., 1991; Menan et al., 2006). In a few cases, namely for *Aloe parvibracteata*, *Plumbago capensis*, *Pittosporum tobira*, and *Schefflera actinophylla*, a chemotaxonomic approach was also considered (Clarkson et al., 2004; Menan et al., 2006).

A total of fifty eight extracts from fifteen species, belonging to several families, were screened for their potential antimalarial properties against the chloroquine (CQ) - sensitive 3D7 *Plasmodium falciparum* strain. The extracts were prepared by sequentially extracting the plant material with *n*-hexane, dichloromethane, ethyl acetate, and methanol (see experimental chapter). The results are summarized in Table 3.1. The antimalarial activity of extracts was defined according to the IC_{50} values (drug concentration required to inhibit the growth of 50 % of parasites) obtained. It should be noted that IC_{50} endpoint criteria are not consensual. For all anti-infective bioassays, some authors consider that for extracts, a stringent endpoint criteria is an IC_{50} value bellow 100 μg/mL (Cos et al., 2006). In this work, a stricter criterion was used. Therefore, an extract showing an IC_{50} value ≤ 5 μg/mL was classified as highly active. Extracts with IC_{50} values ≥ 10 μg/mL and ≤ 50 μg/mL were considered moderately active, and those with IC_{50} values > 50 μg/mL inactive. As it can be observed in Table 3.1, the lowest IC_{50} values were found for the ethyl acetate extracts of *Momordica balsamina* (IC_{50} = 1.0 μg/mL) and *Pittosporum tobira* (IC_{50} = 4.8 μg/mL). Significant IC_{50} values were also found for the *n*-hexane extract of *Cassia occidentalis* (IC_{50} = 19.3 μg/mL), and *n*-hexane and CH_2Cl_2 extracts of *Parkinsonia aculeata* (IC_{50} = 24.5 μg/mL). According to the criterion adopted in this work, the remaining species either have showed a moderate/weak antiplasmodial activity or were inactive.

Therefore, based on the results obtained (Table 3.1), *M. balsamina* L. was selected for further studies.

Table 3.1. *In vitro* antimalarial activity (IC_{50} values, µg/mL) of selected plants against *Plasmodium falciparum* 3D7 strain.

Plant species	Plant part	Extract			
		***n*-Hexane**	**CH_2Cl_2**	**EtOAc**	**MeOH**
Acacia karroo	Aerial parts	99.0 ± 17.3	60.0 ± 12.3	70.2± 1.9	> 100
Aloe parvibracteata	Leaves	> 100	> 100	> 100	> 100
Bridelia cathartica	Roots	99.0 ± 20.2	>100	44.0 ± 1.4	> 100
Cassia abbreviata	Stem Barks	> 100	40.0 ± 1.8	> 100	> 100
Cassia occidentalis	Roots	19.3 ± 2.0	59.9 ± 15.3	31.9 ± 4.7	88.2 ± 2.3
Crossopteryx febrifuga	Aerial parts	–	44.4 ± 3.1	–	> 100
Leonotis leonurus	Aerial parts	> 100	45.4 ± 9.6	38.4 ± 4.7	> 100
Momordica balsamina	Aerial parts	> 100	35.5 ± 2.9	1.0 ± 0.1	46.9 ± 2.4
Parkinsonia aculeata	Aerial parts	24.5 ± 2.9	26.3 ± 2.9	36.4 ± 14.1	54.9 ± 1.8
Pittosporum tobira	Aerial parts	34.4 ± 2.9	44.6 ± 2.5	4.8 ± 1.9	> 100
Plumbago auriculata	Aerial parts	45.9 ± 3.4	40.2 ± 1.7	53.8 ± 3.2	80.0 ± 15.1
Senna didymobotrya	Twigs	57.6 ± 22.3	92.0 ± 21.4	> 100	56.0 ± 9.9
Schefflera actinophylla	Leaves	32.5 ± 0.6	36.3 ± 3.9	41.7 ± 4.8	> 100
Tabernaemontana elegans	Leaves	59.0 ± 8.4	26.9 ± 5.4	> 100	> 100
Trichilia emetica	Seeds	> 100	> 100	> 100	> 100

1.2. Antimalarial activity of *Momordica balsamina* constituents

Bioassay-guided fractionation of the soluble ethyl acetate fraction of the methanol extract of *M. balsamina* led to the isolation of a large number of cucurbitane-type triterpenoids (see experimental chapter). The isolated compounds (**1** - **4** and **26** - **40**), together with the acyl derivatives **5** - **20** of karavilagenin C (**1**), and also **23** and **24** of balsaminol F (**3**), were evaluated for their *in vitro* antimalarial activity against the CQ-sensitive (3D7) and CQ-

resistant (Dd2) *P. falciparum* strains. CQ was used as a positive control. The *in vitro* antiplasmodial effect was measured by a standardized SYBER Green I-based fluorescence assay (Johnson et al., 2007; Smilkstein et al., 2004). SYBER Green I is one of the most sensitive stains available for detection of double-stranded DNA, due to its remarkable fluorescence enhancement caused by its interaction with the nucleic acid (Krettli et al., 2009).

Moreover, the cytotoxicity of all the compounds was determined on the human breast cancer (MCF-7) cell line. The antimalarial activity was defined as IC_{50} values, and was expressed in μM and μg/mL. The cytotoxic effect was also expressed as IC_{50} values in μM.

Like for extracts, a great diversity of criteria has also been adopted for classifying *in vitro* antimalarial activity of pure compounds. In this way, for instance, Batista and co-workers adopted the following criteria: $IC_{50} \leq 1$ μM, excellent/potent activity; IC_{50} of 1 - 20 μM, good activity; IC_{50} of 20 - 100 μM, moderate activity, IC_{50} of 100 - 200 μM, low activity; and $IC_{50} > 200$ μM, inactive (Batista et al., 2009). Cos and collaborators defined that a stringent endpoint criterion for pure compounds is an IC_{50} value below 25 μM (Cos et al., 2006). Taking into account these criteria, in this work the antimalarial activity of compounds was defined as: $IC_{50} \leq 1$ μM, excellent/potent activity; $1 < IC_{50} \leq 10$ μM, good activity; and $10 < IC_{50} \leq 30$ μM, moderate activity. A compound with an $IC_{50} > 30$ μM, was considered without activity.

1.2.1. Cucurbitane-type triterpenoids activity

As it can be observed in Table 3.2, most of the compounds displayed antimalarial activity. The cucurbitane glycosides, kuguaglycoside A (**37**, IC_{50} = 3.9 and 4.7 μM, for 3D7 and Dd2, respectively), balsaminosides B (**38**, IC_{50} = 2.9 and 6.3 μM, for 3D7 and Dd2, respectively), C (**39**, IC_{50} = 3.4 and 7.2 μM, for 3D7 and Dd2, respectively), and A (**40**, IC_{50} = 4.6 and 4.0 μM, for 3D7 and Dd2, respectively) revealed the highest antimalarial activity against both strains of *P. falciparum* tested. Significant antiplasmodial activity was also found for karavilagenins E (**4**, IC_{50} = 7.4 and 8.2 μM, for 3D7 and Dd2, respectively), and C (**1**, IC_{50} = 10.4 and 11.2 μM, for 3D7 and Dd2, respectively), having both a similar activity against the CQ-sensitive and CQ-resistant strains. Balsaminols A (**35**), B (**27**), C (**29**), E (**26**), F (**3**), balsaminagenins A (**34**), B (**33**), cucurbalsaminols A (**32**), and B (**28**) showed a moderate antimalarial activity, with IC_{50} values ranging from 13.2 μM to 28.3 μM, against both strains. Balsaminapentaol (**36**) showed a moderate activity against 3D7 strain, inhibiting the parasite

with an IC_{50} value of 14.6 μM; however, a significant decrease against the resistant strain was observed (IC_{50} = 33.0 μM).

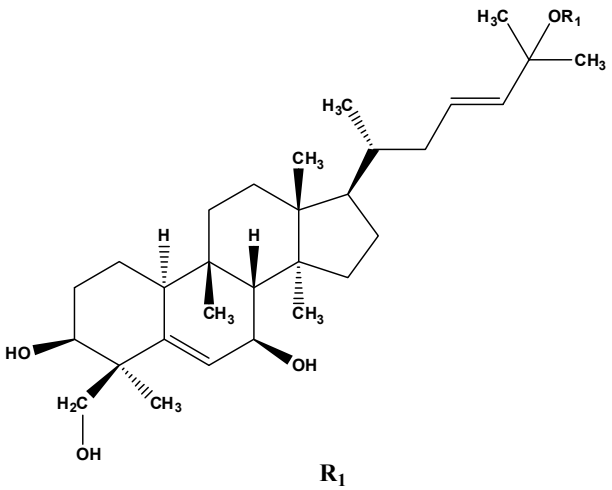

	R_1
Balsaminagenin A (**34**)	H
Balsaminagenin B (**33**)	CH_3

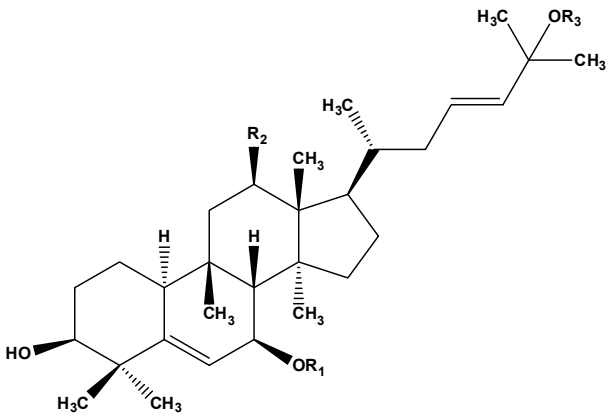

	R_1	R_2	R_3
Balsaminagenin C (**2**)	H	H	H
Cucurbalsaminol A (**32**)	H	OH	H
Cucurbalsaminol B (**28**)	CH_3	OH	H
Balsaminoside A (**40**)	all	H	CH_3

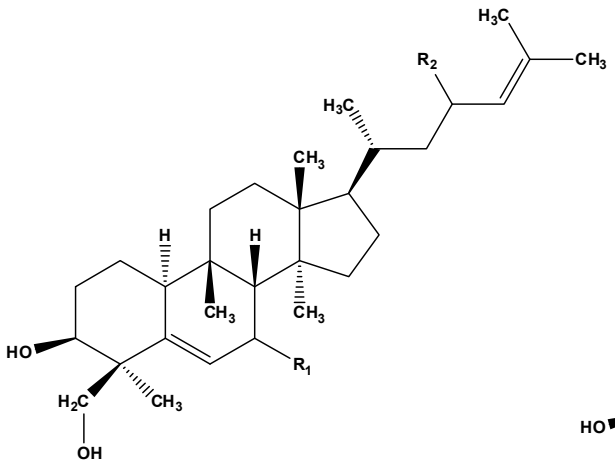

	R_1	R_2
Balsaminol A (**35**)	β–OH	β–OH
Balsaminol B (**27**)	β–OCH_3	β–OH
Balsaminol C (**29**)	=O	=O

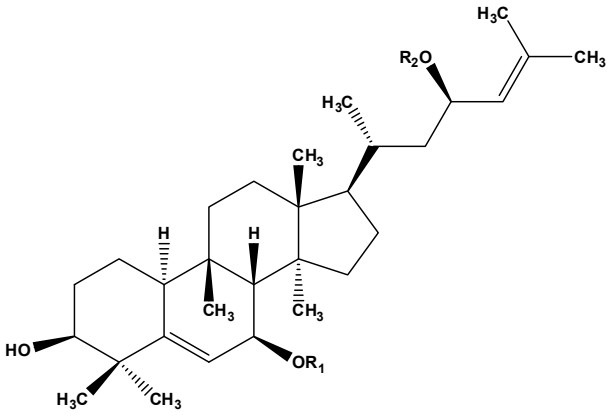

	R_1	R_2
Balsaminoside B (**38**)	all	H
Balsaminoside C (**39**)	glc	H
Kuguaglycoside A (**37**)	CH_3	glc

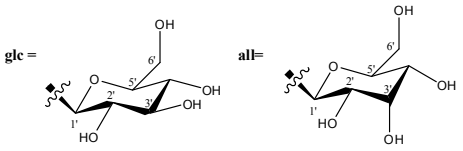

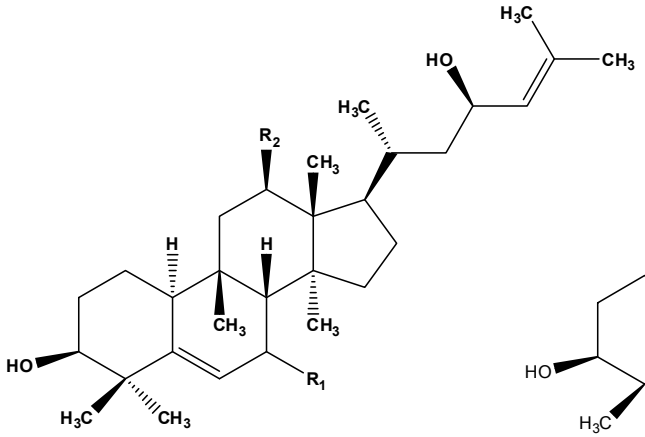

	R_1	R_2
Balsaminol E (**26**)	=O	H
Balsaminol F (**3**)	β–OH	H
Karavilagenin C (**1**)	β–OCH_3	H
Cucurbalsainol C (**30**)	β–OCH_3	OH

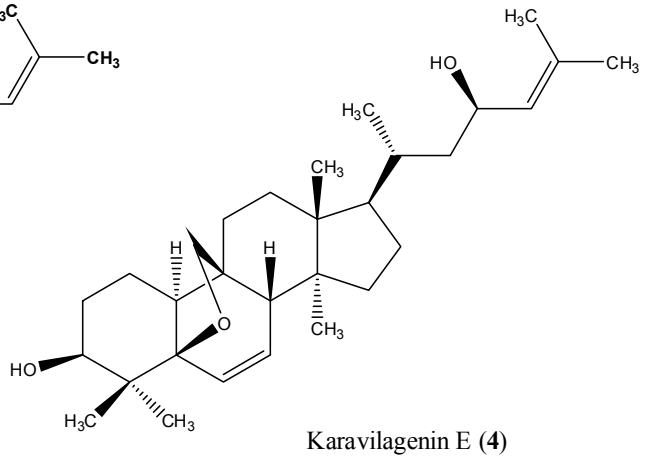

Karavilagenin E (**4**)

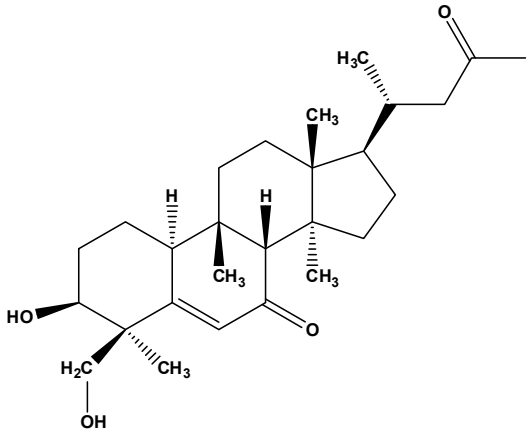

Balsaminol D (**31**)

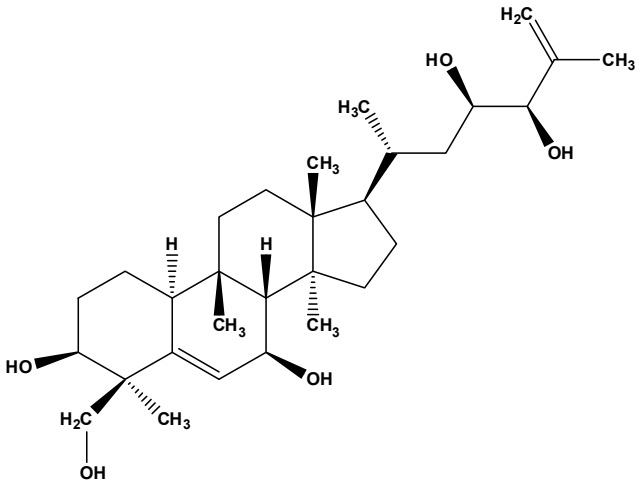

Balsaminapentaol (**36**)

1.2.2. Acyl derivatives activity

In order to find out some structure-activity relationships, balsaminol F (**3**) and karavilagenin C (**1**), isolated in large amount, were derivatized with different acylating reagents. From balsaminol F (**3**) two new esters, triacetylbalsaminol F (**23**) and tribenzoylbalsaminol F (**24**) were prepared. In the same way, from karavilagenin C (**1**) fourteen new mono or diacylated alkanoyl (**5** - **10**) or aroyl (**11** - **18**) derivatives were obtained. Moreover, the mono (**19**) and dicinnamoyl (**20**) esters of karavilagenin C were also prepared. The results are summarized in Tables 3.3 - 3.5.

As shown in Table 3.3, triacetylbalsaminol F (**23**) displayed a strong antimalarial activity, being 22.5 (IC_{50} = 0.8 μM for 3D7) and 50-fold (IC_{50} = 0.4 μM, for Dd2) more

active than balsaminol F (**3**, IC_{50} = 18.0 and 20.0 μM for 3D7 and Dd2, respectively) against the sensitive and resistant strains, respectively. These IC_{50} values are comparable with those obtained with CQ, especially against the resistant Dd2 strain (IC_{50} = 0.016 μM and 0.20 μM for 3D7 and Dd2, respectively). Conversely, tribenzoylbalsaminol F (**24**) showed to be inactive against both strains (IC_{50} = 57.3 and 68.4 μM for 3D7 and Dd2, respectively).

A remarkable activity was also observed for most of the alkanoyl esters (**5** - **10**) of karavilagenin C (**1**) (Tables 3.4 and 3.5). The best activity against both *P. falciparum* strains was displayed by the diacylated derivatives, karavoates B (**6**, IC_{50} = 0.5 and 0.5 μM, for 3D7 and Dd2, respectively) and D (**8**, IC_{50} = 1.5 and 0.4 μM, for 3D7 and Dd2, respectively). When compared with karavilagenin C, the former ester was approximately 20-fold more active against both strains. Importantly, it is interesting to point that compound **8** was much more active against the resistant strain (7 and 28-fold against 3D7 and Dd2, respectively). Similar results were also found for the monoacylated derivative, karavoate E (**9**) that showed a strong antiplasmodial activity, mainly against Dd2 strain (IC_{50} = 3.5 and 0.6 μM, for 3D7 and Dd2, respectively). Regarding the aroyl derivatives of karavilagenin C (Table 3.5), karavoates I (**13**, IC_{50} = 2.6 and 0.5 μM, for 3D7 and Dd2, respectively) and M (**17**, IC_{50} = 1.3 and 0.6 μM, for 3D7 and Dd2, respectively), bearing a *p*-nitrobenzoyl and a *p*-methoxybenzoyl moiety at C-23, respectively, displayed the strongest activity, mainly against the Dd2 resistant strain. However, karavoate K (**15**), with a *p*-chlorobenzoyl residue at C-23, exhibited an activity lower (IC_{50} = 13.3 and 23.3 μM, for 3D7 and Dd2, respectively) than karavilagenin C, against both strains. A decrease of activity was still more evident when both positions, C-3 and C-23, bear an aroyl moiety, as shown for karavoates H (**12**), J (**14**), and L (**16**) (Table 3.5). In the same way, a large increase in IC_{50} values was found for the dicinnamoyl derivative (**20**, IC_{50} = 65.2 and 56.6 μM, for 3D7 and Dd2, respectively), showing the monocinnamoyl ester a good antimalarial activity (**19**, IC_{50} = 6.6 and 26.7 μM, for 3D7 and Dd2, respectively).

Karavoate G (**11**) was also one of the most active compounds (IC_{50} = 0.9 and 0.9 μM, for 3D7 and Dd2, respectively). As already mentioned, in spite of being a karavilagenin C derivative, obtained by a similar acylation procedure as the remaining esters, karavoate G has a different side chain.

Table 3.2. Antimalarial activity, cytotoxicity and selectivity index of compounds **1** - **4** and **26** - **40**.

Compounds	IC_{50} ± SD					Selectivity Index [a]	
	P. falciparum 3D7		*P. falciparum* Dd2		MCF-7 cells	MCF-7/3D7	MCF-7/Dd2
	μM	μg/mL	μM	μg/mL	μM		
Balsaminol A (**35**)	17.1 ± 0.4	8.1 ± 0.2	23.5 ± 4.9	11.1 ± 2.4	40.0 ± 1.3	2.3	1.7
Balsaminol B (**27**)	15.2 ± 5.4	7.4 ± 2.6	17.9 ± 3.7	8.7 ± 1.8	31.0 ± 3.7	2.0	1.7
Balsaminol C (**29**)	19.6 ± 1.5	9.2 ± 0.7	22.4 ± 4.0	10.5 ± 1.9	70.5 ± 2.9	3.6	3.2
Balsaminol D (**31**)	25.9 ± 5.6	11.1 ± 2.4	45.6 ± 1.9	19.6 ± 0.8	> 133.3	> 5.1	> 2.9
Balsaminol E (**26**)	20.4 ± 2.1	9.3 ± 0.9	19.6 ± 4.6	9.0 ± 2.1	44.2 ± 3.9	2.2	2.3
Balsaminol F (**3**)	18.0 ± 1.7	8.2 ± 0.8	20.0 ± 4.3	9.2 ± 2.0	27.3 ± 1.2	1.5	1.4
Balsaminagenin A (**34**)	19.1 ± 3.4	9.0 ± 1.6	27.3 ± 6.1	12.9 ± 2.9	65.1 ± 1.6	3.4	2.4
Balsaminagenin B (**33**)	18.7 ± 1.6	9.1 ± 0.8	19.2 ± 2.7	9.4 ± 1.3	34.0 ± 0.1	1.8	1.8
Balsaminagenin C (**2**)	30.6 ± 6.4	14.0 ± 2.9	50.1 ± 0.1	23.0 ± 0.1	45.3 ± 0.7	1.5	0.9
Balsaminapentaol (**36**)	14.6 ± 1.3	7.2 ± 0.6	33.0 ± 6.3	16.2 ± 3.1	47.0 ± 0.4	3.2	1.4
Balsaminoside A (**40**)	4.6 ± 0.5	2.9 ± 0.3	4.0 ± 0.5	2.5 ± 0.3	19.0 ± 0.8	4.2	4.7
Balsaminoside B (**38**)	2.9 ± 0.1	1.8 ± 0.1	6.3 ± 0.7	3.9 ± 0.4	14.2 ± 0.8	4.8	2.3
Balsaminoside C (**39**)	3.4 ± 0.6	2.1 ± 0.3	7.2 ± 0.4	4.5 ± 0.3	23.9 ± 6.6	7.0	3.3
Cucurbalsaminol A (**32**)	13.2 ± 0.8	6.2 ± 0.4	17.6 ± 0.7	8.3 ± 0.3	> 133.3	> 10.1	> 7.6
Cucurbalsaminol B (**28**)	17.7 ± 1.3	8.6 ± 0.6	28.3 ± 4.6	13.8 ± 2.2	55.4 ± 2.9	3.1	2.0
Cucurbalsaminol C (**30**)	52.7 ± 2.4	25.7 ± 1.2	67.6 ± 7.4	33.0 ± 3.6	43.3 ± 3.7	0.8	0.6
Karavilagenin C (**1**)	10.4 ± 0.7	4.9 ± 0.3	11.2 ± 0.7	5.3 ± 0.3	16.7 ± 2.1	1.6	1.4
Karavilagenin E (**4**)	7.4 ± 0.8	3.3 ± 0.4	8.2 ± 0.7	3.8 ± 0.3	30.7 ± 2.3	4.2	3.7
Kuguaglycoside A (**37**)	3.9 ± 0.4	2.5 ± 0.2	4.7 ± 0.4	2.9 ± 0.2	13.5 ± 4.9	3.5	2.9
CQ	0.016	–	0.2	–	–	–	–

[a] Selectivity index (SI) = cytotoxic IC_{50}/antiplasmodial IC_{50}

Table 3.3. Antimalarial activity, cytotoxicity and selectivity index of balsaminol F (**3**) and its derivatives, triacetylbalsaminol F (**23**) and tribenzoylbalsaminol F (**24**).

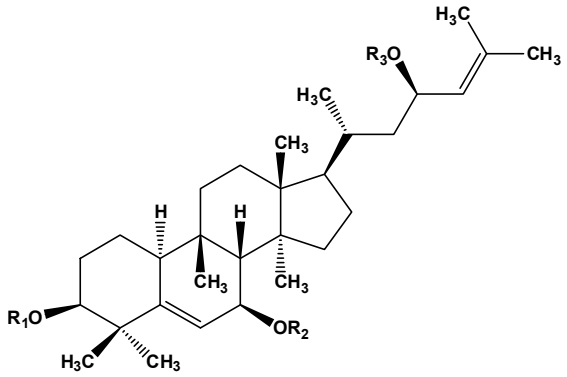

	R_1	R_2	R_3
Balsaminol F (**3**)	H	H	H
Triacetylbalsaminol F (**23**)	Ac	Ac	Ac
Tribenzoylbalsaminol F (**24**)	Bz	Bz	Bz

Compounds	**IC_{50} ± SD**					**Selectivity Index** [a]	
	P. falciparum 3D7		*P. falciparum* Dd2		MCF-7 cells	MCF-7/3D7	MCF-7/Dd2
	μM	μg/mL	μM	μg/mL	μM		
Balsaminol F (**3**)	18.0 ± 1.7	8.2 ± 0.8	20.0 ± 4.3	9.2 ± 2.0	27.3 ± 1.2	1.5	1.4
Triacetylbalsaminol F (**23**)	0.8 ± 0.1	0.5 ± 0.1	0.4 ± 0.04	0.2 ± 0.02	> 133.3	> 162.4	> 342.9
Tribenzoylbalsaminol F (**24**)	57.3 ± 3.1	44.2 ± 2.4	68.4 ± 8.6	52.7 ± 6.7	> 133.3	> 2.3	> 2.0
CQ	0.016	–	0.2	–	–	–	–

[a]Selectivity index (SI) = cytotoxic IC_{50}/antiplasmodial IC_{50}

Table 3.4. Antimalarial activity, cytotoxicity and selectivity index of the alkanoyl derivatives **5** - **10** of karavilagenin C (**1**).

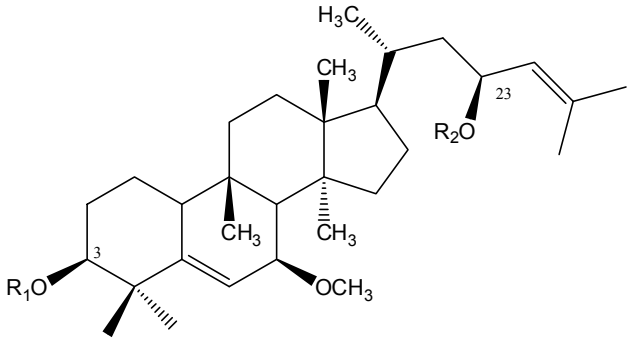

Compounds	R_1	R_2	**IC_{50}±SD**					**Selectivity Index** [a]	
			P. falciparum 3D7		*P. falciparum* Dd2		MCF-7 cells	MCF-7/3D7	MCF-7/Dd2
			µM	µg/mL	µM	µg/mL	µM		
Karavoate A (**5**)	H	Ac	6.7 ± 1.1	3.5 ± 0.6	9.2 ± 0.6	4.7 ± 0.3	22.9 ± 1.2	3.4	2.5
Karavoate B (**6**)	Ac	Ac	0.5 ± 0.01	0.3 ± 0.01	0.5 ± 0.03	0.3 ± 0.01	68.1 ± 1.6	151.2	126.0
Karavoate C (**7**)	H	Pr	5.1 ± 0.02	2.7 ± 0.01	22.0 ± 2.3	11.6 ± 1.2	19.1 ± 0.8	3.7	0.9
Karavoate D (**8**)	Pr	Pr	1.5 ± 0.04	0.9 ± 0.02	0.4 ± 0.04	0.2 ± 0.02	> 133.3	> 89.0	> 349.9
Karavoate E (**9**)	H	Bu	3.5 ± 0.02	1.9 ± 0.01	0.6 ± 0.2	0.3 ± 0.1	73.8 ± 2.1	20.8	116.3
Karavoate F (**10**)	Bu	Bu	6.9 ± 1.9	4.2 ± 1.2	8.4 ± 3.2	5.1 ± 1.9	> 133.3	> 19.4	> 15.8
CQ	–	–	0.016	_	0.2	_	–	–	–

[a] Selectivity index (SI) = cytotoxic IC_{50}/antiplasmodial IC_{50}

Table 3.5. Antimalarial activity, cytotoxicity and selectivity index of the aroyl (**11** - **18**) and cinnamoyl derivatives **19** and **20** of karavilagenin C (**1**).

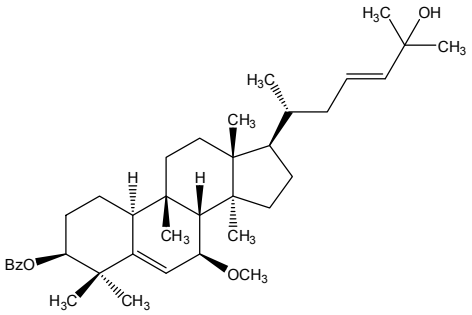

Karavoate G (**11**)

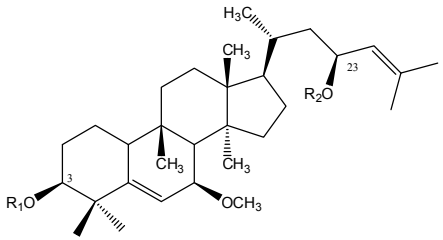

Compounds	R_1	R_2	IC_{50}±SD					Selectivity Index [a]	
			P. falciparum 3D7		*P. falciparum* Dd2		MCF-7 cells	MCF-7/3D7	MCF-7/Dd2
			μM	μg/mL	μM	μg/mL	μM		
Karavoate G (**11**)	-	-	0.9 ± 0.001	0.5 ± 0.001	0.9 ± 0.4	0.5 ± 0.3	> 133.3	> 152.8	> 145.0
Karavoate H (**12**)	Bz	Bz	36.4 ± 7.4	24.8 ± 5.1	30.5 ± 3.9	20.8 ± 2.7	> 133.3	> 3.7	> 4.4
Karavoate I (**13**)	H	*p*-nitroBz	2.6 ± 0.1	1.6 ± 0.05	0.5 ± 0.1	0.3 ± 0.08	> 133.3	> 51.4	> 296.2
Karavoate J (**14**)	*p*-nitroBz	*p*-nitroBz	18.6 ± 2.5	14.3 ± 1.9	20.7 ± 4.1	16.0 ± 3.2	> 133.3	> 7.2	> 6.43
Karavoate K (**15**)	H	*p*-chloroBz	13.3 ± 0.9	8.1 ± 0.5	23.3 ± 2.9	14.3 ± 1.8	> 133.3	> 10.0	> 5.7
Karavoate L (**16**)	*p*-chloroBz	*p*-chloroBz	22.5 ± 0.5	16.8 ± 0.4	66.0 ± 2.2	49.4 ± 1.7	> 133.3	> 5.9	> 2.0
Karavoate M (**17**)	H	*p*-methoxyBz	1.3 ± 0.01	0.8 ± 0.01	0.6 ± 0.2	0.4 ± 0.1	> 133.3	> 43.6	> 214.8
Karavoate N (**18**)	*p*-methoxyBz	*p*-methoxyBz	2.4 ± 0.1	1.8 ± 0.07	47.9 ± 12.7	35.5 ± 9.4	> 133.3	> 55.4	> 2.8
Karavoate O (**19**)	H	Cin	6.6 ± 3.5	3.9 ± 2.1	26.7 ± 9.9	16.0 ± 6.0	> 133.3	> 20.3	> 5.0
Karavoate P (**20**)	Cin	Cin	65.2 ± 5.3	47.8 ± 3.9	56.6 ± 1.2	41.5 ± 0.9	> 133.3	> 2.0	> 2.4
CQ	-	-	0.016	–	0.2	–	–	–	–

[a]Selectivity index (SI) = cytotoxic IC_{50}/antiplasmodial IC_{50}

1.2.3. Cytotoxic activity of isolated compounds and derivatives

The cytotoxic activity for all compounds was evaluated in order to calculate the selectivity index (SI), defined as the ratio between cytotoxic (IC_{50}) and parasitic (IC_{50}) activities. According to Vicente and collaborators, a promising drug discovery lead should have a SI > 10 (Vicente et al., 2008).

As it can be observed in Table 3.2, the isolated compounds (**1** - **4** and **26** - **40**) were inactive or showed a low toxicity (IC_{50} > 13.5 μM), against the human breast cancer cell line (MCF-7) studied. However, a low SI was found for most of the compounds (SI < 7.0).

On the other hand, no significant cytotoxic activity was found for most of balsaminol F (**3**) and karavilagenin C (**1**) esters. In fact, for the esters of balsaminol F (**23** and **24**), and the alkanoyl (**8** and **10**), aroyl (**11** - **18**) and cinnamoyl derivatives (**19** and **20**), (Tables 3.3 - 3.5) of karavilagenin C an IC_{50} > 133.3 μM was found. The remaining esters (**5** - **7** and **9**) were also inactive or showed a weak activity, displaying IC_{50} values ranging from 19.1 to 73.8 μM. More importantly, all derivatives (**5** - **20** and **23**, **24**) showed selectivity index values higher than those obtained for the original compounds balsaminol F (**3**, SI = 1.5 and 1.4, for 3D7 and Dd2, respectively) and karavilagenin C (**1**, SI = 1.6 and 1.4, for 3D7 and Dd2, respectively). The best selectivity index values were found for compounds **23** (SI > 162.4 and 342.9 for 3D7 and Dd2 *P. falciparum* strains, respectively), **6** (SI = 151.2 and 126.0, for 3D7 and Dd2, respectively), **8** (SI > 89.0 and 349.9, for 3D7 and Dd2, respectively) and **11** (SI > 152.8 and 145.0, for 3D7 and Dd2, respectively).

1.2.4. Structure-activity relationships

Isolated compounds

The isolated compounds **1** - **4**, and **26** - **40** share the same triterpenic scaffold, differing only in the substitution pattern of rings A, B, and C, or/and in side chain. The results obtained showed that ring B might play an important role in the antiplasmodial activity. In fact, a comparison of the activities of karavilagenin C (**1**, IC_{50} = 10.4 and 11.2 μM, 3D7 and Dd2, respectively), balsaminol F (**3**, IC_{50} = 18.0 and 20.0 μM, 3D7 and Dd2, respectively), and balsaminol E (**26**, IC_{50} = 20.4 and 19.6 μM, 3D7 and Dd2, respectively) suggests that the presence of a methoxyl group at C-7 in **1**, instead of a hydroxyl or a carbonyl group, found in

3 and **26**, respectively, increases the antimalarial activity. Conversely, the replacement of a methoxyl by a sugar unit led to a significant enhance of activity, as illustrated by balsaminosides B (**38**, IC_{50} = 2.9 and 6.3 μM, 3D7 and Dd2, respectively) and C (**39**, IC_{50} = 3.4 and 7.2 μM, 3D7 and Dd2, respectively). The same effect was observed, when a hydroxyl group was replaced by a sugar moiety at C-23 in kuguaglycoside A (**37**, IC_{50} = 3.9 and 4.7 μM, 3D7 and Dd2, respectively). On the other hand, according to these results, an additional hydroxyl group at C-12 (compounds **28**, **30**, and **32**) or at C-29 (compounds **35** and **27**) does not improve the antimalarial activity. These features are highlighted by the results obtained for balsaminol A (**35**), which differs from balsaminol F (**3**), having an extra hydroxyl group at C-29, but with a similar activity against *P. falciparum* parasites. Similarly, cucurbalsaminol C, with an extra hydroxyl group at C-12, showed a weaker activity than karavilagenin C (**1**). Moreover, other structural features of the side chain also seem to interfere with the antimalarial activity. In fact, balsaminols C (**29**, IC_{50} = 22.4 μM) and D (**31**, IC_{50} = 45.6 μM), despite sharing the same triterpenic nucleus showed a significant difference in the activity against the resistant strain, which may be assignable to the unusual C_6 side chain of compound **31**.

When analysing the physico-chemical properties of this set of compounds (Table 3.6), it can be observed that glycoside derivatives (**37 - 40**), the most active compounds, also have the highest TPSA values (TPSA = 128.8 or 139.8) and the largest number of H-bond acceptors (8) and donors (5 or 6), as well.

Ester derivatives

When analysing the results obtained for the esters, it was found that all the alkanoyl derivatives were more active than the parent compounds **1** and **3**. Furthermore, the lowest IC_{50} values were found when both positions C-3 and C-23 bear acetyl or propanoyl groups, as in karavoates B (**6**, IC_{50} = 0.5 and 0.5 μM, for 3D7 and Dd2, respectively) and D (**8,** IC_{50} = 1.5 and 0.4 μM, for 3D7 and Dd2, respectively), or in triacetylbalsaminol F (**23**, IC_{50} = 0.8 and 0.4 μM, for 3D7 and Dd2, respectively). Surprisingly, between butanoyl esters, the most active was the monoacylated derivative, karavoate E (**9**, IC_{50} = 3.5 and 0.6 μM, for 3D7 and Dd2, respectively). This compound displayed a very strong antimalarial activity against the

Dd2 resistant strain, which was comparable with that found for CQ (IC_{50} = 0.016 μM and 0.20 μM for 3D7 and Dd2, respectively).

Table 3.6. Physico-chemical properties of compounds **1** - **4** and **26** - **40** (topological polar surface area, number of hydrogen bond acceptors and donors, molecular weight, octanol/water partition coefficient, and volume)[a].

Compounds	TPSA	N° H[b]		MW	log *P*	Volume
		acc.	don.			
Balsaminol A (**35**)	80.9	4	4	474	5.5	490.3
Balsaminol B (**27**)	69.9	4	3	488	6.2	507.9
Balsaminol C (**29**)	74.6	4	2	470	5.2	478.6
Balsaminol D (**31**)	74.6	4	2	430	3.8	434.6
Balsaminol E (**26**)	57.5	3	2	456	6.5	476.2
Balsaminol F (**3**)	60.7	3	3	458	6.7	482.0
Balsaminagenin A (**34**)	80.9	4	4	474	5.2	490.0
Balsaminagenin B (**33**)	69.9	4	3	488	5.8	507.5
Balsaminagenin C (**2**)	60.7	3	3	458	6.4	481.7
Balsaminapentaol (**36**)	101.14	5	5	490	4.4	498.9
Balsaminoside A (**40**)	128.8	8	5	634	5.3	631.4
Balsaminoside B (**38**)	139.8	8	6	620	5.0	614.2
Balsaminoside C (**39**)	139.8	8	6	620	5.0	614.2
Cucurbalsaminol A (**32**)	80.9	4	4	474	5.5	489.8
Cucurbalsaminol B (**28**)	69.9	4	3	488	6.1	507.3
Cucurbalsaminol C (**30**)	69.9	4	3	488	6.4	507.6
Karavilagenin C (**1**)	49.7	3	2	472	7.3	499.6
Karavilagenin E (**4**)	49.7	3	2	456	6.3	472.1
Kuguaglycoside A (**37**)	128.8	8	5	634	5.6	631.7

[a] Physico-chemical parameters were determined by using the JME molecular editor (version January 2010, http://www.molinspiration.com/).

[b] Number of hydrogen acceptors (acc.) and hydrogen donors (don.).

In the same way, for the aroyl and cinnamoyl derivatives of karavilagenin C, the best antimalarial activity was found for the monoesters. This is highlighted by the IC_{50} values obtained for karavoates I (**13**, IC_{50} = 2.6 and 0.5 μM, for 3D7 and Dd2, respectively), M (**17**, IC_{50} = 1.3 and 0.6 μM, for 3D7 and Dd2, respectively), and O (**19**, IC_{50} = 6.6 and 26.7 μM, for 3D7 and Dd2, respectively), which showed much better antiplasmodial activity than the

corresponding diesters (**14**, **18**, and **20**, respectively). Moreover, these differences were more accentuated for the esters without any substituent at the aroyl/cinnamoyl moiety, karavoates H (**12**) and P (**20**).

Therefore, these results suggest that the antimalarial activity might be influenced by molecular steric effects. In fact, compounds with molecular volumes between 536.1 - 618.4 showed an excellent/good activity, and those with values between 682.3 - 739.9 exhibited a weak effect or were inactive (Table 3.7). Furthermore, the highest IC_{50} values were found for compounds **20** and **24** with the highest molecular volumes.

Table 3.7. Physico-chemical properties of esters **5** - **20** of karavilagenin C, and **23** and **24** of balsaminol F (**3**) (topological polar surface area, number of hydrogen bond acceptors and donors, molecular weight, octanol/water partition coefficient, and volume)[a].

Compounds	TPSA	N° H[b]		MW	log *P*	Volume
		acc.	don.			
Triacetylbalsaminol F (**23**)	78.9	3	0	584	8.6	575.4
Tribenzoylbalsaminol F (**24**)	78.9	3	0	770	9.9	739.9
Karavoate A (**5**)	55.8	4	1	514	8.0	536.1
Karavoate B (**6**)	61.8	5	0	556	8.6	572.6
Karavoate C (**7**)	55.8	4	1	528	8.3	552.9
Karavoate D (**8**)	61.8	5	0	584	8.9	606.2
Karavoate E (**9**)	55.8	4	1	542	8.7	569.7
Karavoate F (**10**)	61.8	5	0	612	9.3	639.8
Karavoate G (**11**)	55.8	4	1	576	9.0	591.0
Karavoate H (**12**)	61.8	5	0	680	9.6	682.3
Karavoate I (**13**)	101.6	7	1	621	9.0	614.3
Karavoate J (**14**)	153.5	11	0	770	9.6	729.0
Karavoate K (**15**)	55.8	4	1	610	9.2	604.5
Karavoate L (**16**)	61.8	5	0	748	9.9	709.4
Karavoate M (**17**)	65.0	5	1	606	9.0	616.5
Karavoate N (**18**)	80.3	7	0	740	9.7	733.4
Karavoate O (**19**)	55.8	4	1	602	9.2	618.4
Karavoate P (**20**)	61.8	5	0	732	9.8	737.1

[a] Physico-chemical parameters were determined by using the JME molecular editor (version January 2010, http://www.molinspiration.com/).

[b] Number of hydrogen acceptors (acc.) and hydrogen donors (don.).

Based on these results, and considering *in vivo* previous data (Benoit-Vical et al., 2006), it can be concluded that these compounds may be interesting as leads for the development of new antimalarials. This study also supports the use of *M. balsamina* against malaria symptoms in the traditional medicine.

2. REVERSAL OF MULTIDRUG RESISTANCE IN CANCER CELLS

The evaluation of MDR reversal activity in cancer cells, namely on L15178 mouse T-lymphoma cell line transfected with the human *mdr1* gene, by two different techniques will be presented and discussed.

2.1. Evaluation of the inhibition of P-gp transport activity by flow cytometry

The evaluation of the MDR-reversing activity was carried out on L15178 mouse T-lymphoma cell line transfected with the human *mdr1* gene by flow cytometry. A standard functional assay that measures rhodamine-123 (Figure 3.1), a fluorescent analogue of doxorubicin, accumulation on the referred cells was used.

In flow cytometry assays, three parameters are evaluated: the forward scatter (FSC), the side scatter (SSC) and the fluorescence intensity (FL-1). The cells traversing the focus of a laser beam in a flow cytometer scatter the laser light (Darzynkiewicz et al., 1992). Analysis of the scattered light provides information about the cell size and structure (Darzynkiewicz et al., 1992). The intensity of scattered light at a forward direction (FSC) is correlated with cell size. On the other hand, the intensity of scattered light measured at a right angle to the laser beam, correlates with granularity, refractiveness and the presence of intracellular structures that can reflect the light (Darzynkiewicz et al., 1992). In this manner, death cells have a lower value of FSC, while live cells present higher values of SSC (Darzynkiewicz et al., 1992).

In this work, fluorescence intensity (FL-1) mean in percentage was calculated for the treated MDR and parental cell lines as compared with untreated cells. An activity ratio FAR was obtained according to the following equation:

$$FAR = \frac{MDR\ treated\ /\ MDR\ control}{parental\ treated\ /\ parental\ control}$$

Compounds with FAR values higher than 1 were considered active as P-gp inhibitors and those with FAR values higher than 10 were regarded as strong modulators (Voigt et al., 2007).

The isolated compounds (**1** - **4** and **26** - **40**), as well as the acyl derivatives **5** - **20** of karavilagenin C (**1**), and **23** and **24** of balsaminol F (**3**) were investigated for their potential ability as MDR modulators. Verapamil (Figure 3.1), a calcium channel blocker and a well known chemosensitizer, was applied as a positive control. Two concentrations (2 and 20 μM) were used in the experiments. Karavilagenin C was also studied at 0.5 and 1 μM. The results for the MDR reversal activity are summarized in Tables 3.8 - 3.11.

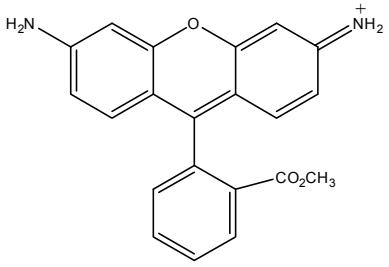

1

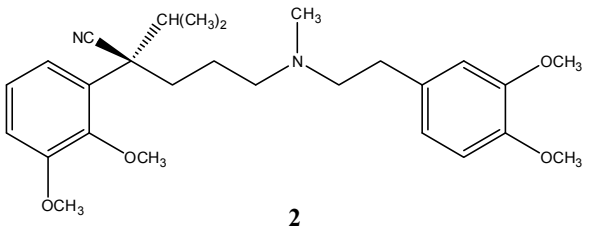

2

Figure 3.1. Chemical structure of rhodamine-123 (**1**) and verapamil (**2**).

The antiproliferative effects of the compounds were also assessed on MDR and PAR cell lines. The results are summarized in Tables 3.12 and 3.13. As it can be observed, in the MDR subline, the compounds showed no significant toxic effect or a weak activity at a concentration similar to or higher than the highest concentration used in the MDR reversal experiments. It is interesting to note that the esters showed a marked decrease of cytotoxicity, which corroborates the results found for MCF-7 cell line (Tables 3.2 - 3.5). Besides, it should be emphasised that cytotoxicity and MDR reversal activity can not be directly compared. In fact, MDR assay is a short term experiment (30 min), where a large number of cells (10.000) were treated with the compounds, while in the antiproliferative assay a few thousands of cells were treated with the compounds for 72 h.

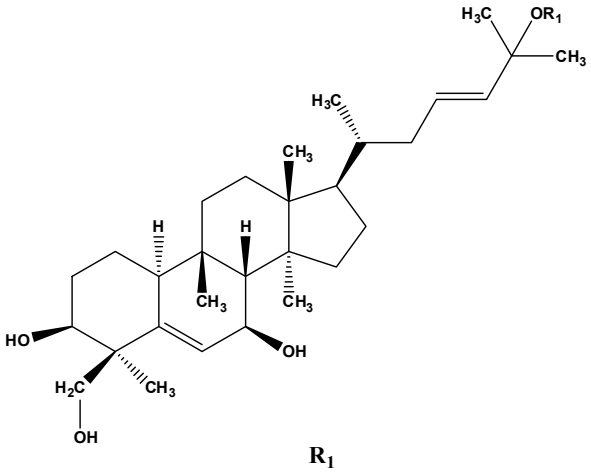

	R_1
Balsaminagenin A (**34**)	H
Balsaminagenin B (**33**)	CH_3

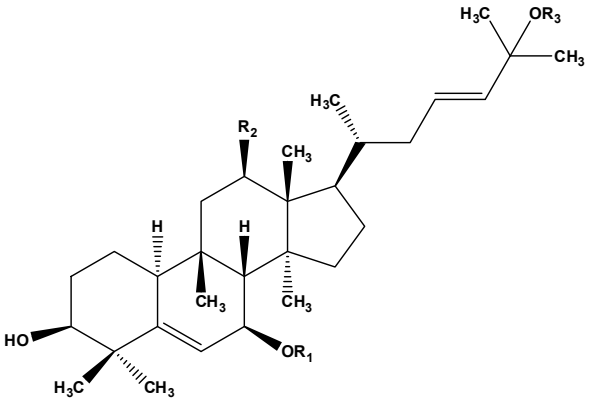

	R_1	R_2	R_3
Balsaminagenin C (**2**)	H	H	H
Cucurbalsaminol A (**32**)	H	OH	H
Cucurbalsaminol B (**28**)	CH_3	OH	H
Balsaminoside A (**40**)	all	H	CH_3

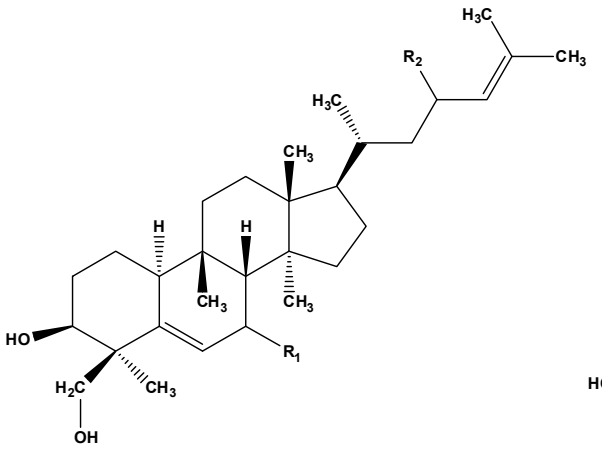

	R_1	R_2
Balsaminol A (**35**)	β–OH	β–OH
Balsaminol B (**27**)	β–OCH_3	β–OH
Balsaminol C (**29**)	=O	=O

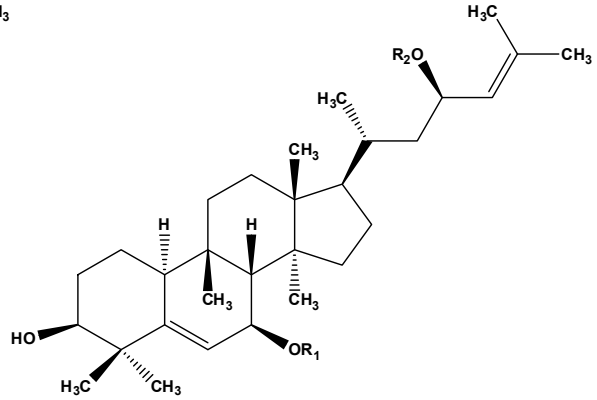

	R_1	R_2
Balsaminoside B (**38**)	all	H
Balsaminoside C (**39**)	glc	H
Kuguaglycoside A (**37**)	CH_3	glc

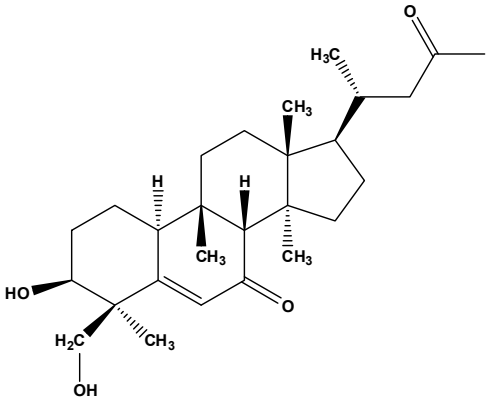

Balsaminol D (**31**)

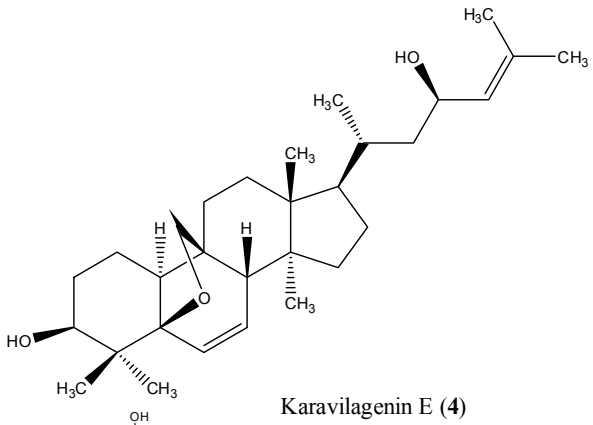

Karavilagenin E (**4**)

glc =

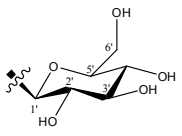

all=

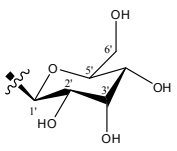

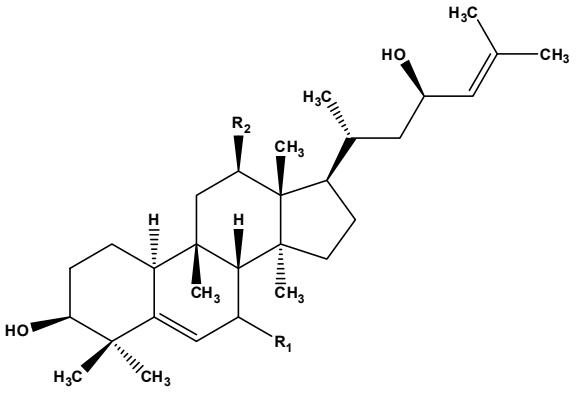

	R_1	R_2
Balsaminol E (**26**)	=O	H
Balsaminol F (**3**)	β–OH	H
Karavilagenin C (**1**)	β–OCH_3	H
Cucurbalsainol C (**30**)	β-OCH_3	OH

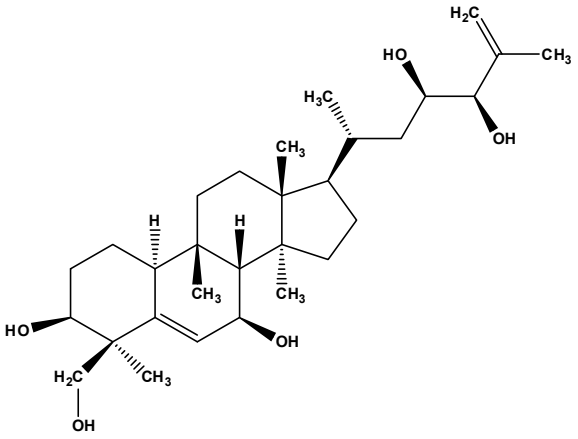

Balsaminapentaol (**36**)

Table 3.8. Effects of balsaminols A - F (**35**, **27**, **29**, **31**, **26**, **3**), balsaminagenins A - C (**34**, **33**, **2**) on the reversal of MDR in human *MDR1* gene-transfected mouse lymphoma cells.

Compounds	Concentration μM	FSC	SSC	FL-1	FAR
PAR + R123	–	436.8	194.0	959.5	–
MDR + R123	–	455.7	286.4	18.6	–
Verapamil	22.0	451.4	277.0	97.1	7.4
Balsaminol A (**35**)	2	432.9	259.0	20.1	1.5
	20	454.5	260.0	766.1	47.6
Balsaminol B (**27**)	2	439.5	258.8	95.7	7.3
	20	461.8	260.7	899.1	68.7
Balsaminol C (**29**)	2	502.3	205.4	22.3	2.9
	20	502.2	195.7	1537.8	198.9
Balsaminol D (**31**)	2	439.9	254.3	10.3	1.0
	20	434.2	256.5	25.9	1.9
Balsaminol E (**26**)	2	582.7	243.4	20.8	2.0
	20	593.0	234.5	663.1	64.8
Balsaminol F (**3**)[b]	2	490.7	202.1	20.1	2.6
Balsaminagenin A (**34**)	2	441.8	261.2	14.0	1.1
	20	447.4	257.6	579.8	44.3
Balsaminagenin B (**33**)	2	428.7	261.1	78.4	6.0
	20	454.4	238.6	1365.1	104.2
Balsaminagenin C (**2**)	2	570.5	249.0	73.1	7.1
	20	395.2	243.9	368.4	36.0
DMSO	10 μL	430.7	256.6	7.3	0.8

[a] Some results were obtained from different assays. For compounds **3** and **29**: (PAR + R123: FL-1 = 1062.8; MDR + R123: FL-1 = 8.7; Verapamil: FL-1 = 101.3, FAR = 13.1). For compounds **2** and **26**: (PAR + R123: FL-1 = 1018.2; MDR + R123: FL-1 = 10.5; Verapamil: FL-1 = 98.9, FAR = 9.7). [b] Compound **3** showed to be toxic at 20 μM.

Table 3.9. Effects of balsaminapentaol (**36**), balsaminosides A - C (**40**, **38**, **39**), cucurbalsaminols A - C (**32**, **28**, **30**), karavilagenins C (**1**), E (**4**) and kuguaglycoside A (**37**) on the reversal of MDR in human *MDR1* gene-transfected mouse lymphoma cells.

Compounds	Concentration µM	FSC	SSC	FL-1	FAR
PAR + R123	–	436.8	194.0	959.5	–
MDR + R123	–	455.7	286.4	18.6	–
Verapamil	22.0	451.4	277.0	97.1	7.4
Balsaminapentaol (**36**)	2	427.2	254.7	8.8	0.7
	20	429.0	252.0	38.2	2.9
Balsaminoside A (**40**)	2	429.6	253.8	19.0	1.5
	20	441.6	249.7	1171.1	89.4
Balsaminoside B (**38**)	2	443.8	267.4	11.5	0.9
	20	457.9	277.2	487.1	37.2
Balsaminoside C (**39**)	2	557.9	235.6	10.7	1.0
	20	573.0	236.9	23.6	2.3
Cucurbalsaminol A (**32**)	2	427.2	254.7	8.8	0.7
	20	429.0	252.0	38.2	2.9
Cucurbalsaminol B (**28**)	2	568.6	249.6	27.2	2.7
	20	585.0	235.8	391.6	38.2
Cucurbalsaminol C (**30**)	2	568.5	241.8	31.6	3.1
	20	564.3	237.6	202.8	19.8
Karavilagenin C (**1**)	0.5	456.4	215.3	12.7	1.5
	1	460.7	215.4	130.0	15.0
	2	468.8	215.4	365.7	42.1
	20	551.8	206.8	399.5	46.0
Karavilagenin E (**4**)	2	568.8	234.2	38.4	3.8
	20	474.0	242.0	743.8	72.6
Kuguaglycoside A (**37**)	2	446.8	266.8	12.4	1.0
	20	457.3	269.2	643.1	49.1
DMSO	10 µL	430.7	256.6	7.3	0.8

[a] Some results were obtained from different assays: for compounds **4**, **39**, **28**, **30** and **36**: (PAR + R123: FL-1 = 1018.2; MDR + R123: FL-1 = 10.5; Verapamil: FL-1 = 98.9, FAR = 9.7). For compound **1**: (PAR + R123: FL-1 = 1034.3; MDR + R123: FL-1 = 9.5; Verapamil: FL-1 = 73.7, FAR = 8.5).

Table 3.10. Effects of the esters **5** - **10** and **21** - **23** on the reversal of MDR in human *MDR1* gene-transfected mouse lymphoma cells.

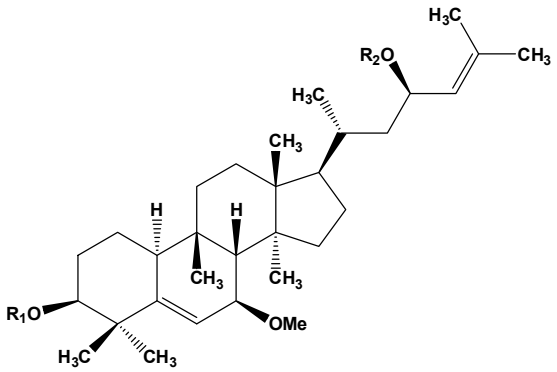

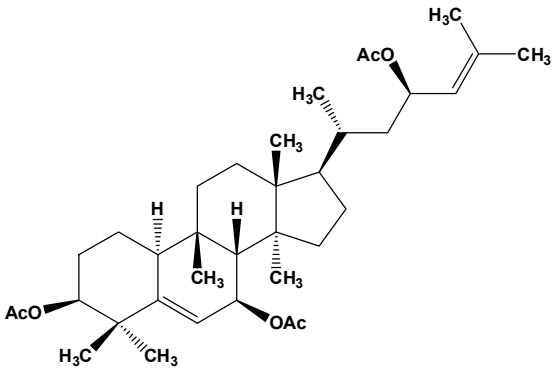

Triacetylbalsaminol F (**23**)

Compounds	R_1	R_2	Concentration µM	FSC	SSC	FL-1	FAR
PAR + R123				464.7	195.7	974.2	–
MDR + R123				468.8	247.0	25.6	–
Verapamil			22.0	439.2	251.1	154.5	8.6
Karavoate A (**5**)	H	Ac	2	470.2	254.9	671.2	35.2
			20	518.1	222.4	612.7	34.2
Karavoate B (**6**)	Ac	Ac	2	454.9	247.0	102.1	5.7
			20	462.9	249.3	671.2	37.5
Karavoate C (**7**)	H	Pr	2	466.3	249.9	30.3	1.7
			20	481.3	242.5	726.8	40.6
Karavoate D (**8**)	Pr	Pr	2	454.0	237.9	16.2	0.9
			20	463.1	230.8	42.3	2.4
Karavoate E (**9**)	H	Bu	2	448.7	235.9	18.0	1.0
			20	461.9	236.3	388.7	21.7
Karavoate F (**10**)	Bu	Bu	2	542.6	218.3	10.8	1.4
			20	541.0	218.7	12.3	1.6
Karavoate Q (**21**)	H	Suc[b]	2	545.2	184.1	7.5	1.1
			20	540.1	185.6	28.0	4.2
Karavoate R (**22**)	Suc[b]	Suc[b]	2	545.8	184.6	8.2	1.3
			20	546.7	187.0	39.5	5.9
Triacetylbalsaminol F (**23**)	-	-	2	541.9	182.1	20.0	3.0
			20	533.5	179.9	100.6	15.0
DMSO	-	-	10 µL	441.8	237.5	13.8	0.8

[a] Some results were obtained from different assays. For compound **10**: (PAR + R123: FL-1 = 1062.8; MDR + R123: FL-1 = 8.7; Verapamil: FL-1 = 101.3, FAR = 13.1). For compounds **21** - **24**: (PAR + R123: FL-1 = 974.5; MDR + R123: FL-1 = 7.1; Verapamil: FL-1 = 36.3, FAR = 7.1).

[b] Suc: Succinoyl

Table 3.11. Effects of esters **11** - **20** and **24** on the reversal of MDR in human *MDR*1 gene-transfected mouse lymphoma cells.

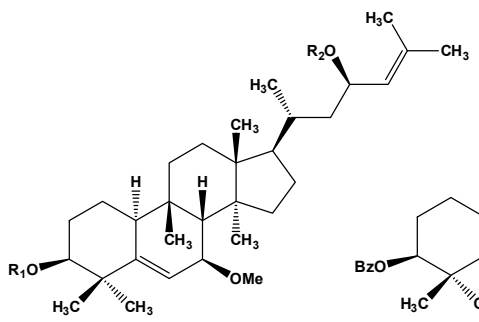

Karavoate G (**11**)

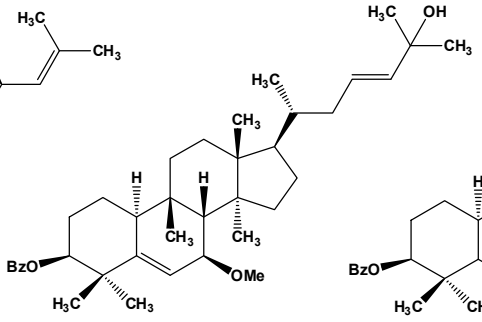

Tribenzoylbalsaminol F (**24**)

Compounds	R_1	R_2	Conc. μM	FSC	SSC	FL-1	FAR
PAR + R123				509.3	174.2	974.5	–
MDR + R123				509.9	194.6	7.1	–
Verapamil			22.0	515.0	198.8	36.3	7.1
Karavoate G (**11**)	-	-	2	454.2	233.1	17.9	1.0
			20	444.8	235.1	140.0	7.8
Karavoate H (**12**)	Bz	Bz	2	504.9	200.4	9.0	1.2
			20	519.8	215.4	10.4	1.3
Karavoate I (**13**)	H	*p*-nitroBz	2	537.3	184.1	14.3	2.1
			20	534.1	182.9	25.9	3.9
Karavoate J (**14**)	*p*-nitroBz	*p*-nitroBz	2	543.4	186.3	9.5	1.4
			20	537.3	184.1	14.3	2.1
Karavoate K (**15**)	H	*p*-chloroBz	2	517.9	207.0	10.7	1.4
			20	511.1	210.8	12.2	1.6
Karavoate L (**16**)	*p*-chloroBz	*p*-chloroBz	2	504.6	206.4	8.1	1.0
			20	512.2	202.4	9.0	1.2
Karavoate M (**17**)	H	*p*-methoxyBz	2	526.0	192.3	12.3	1.8
			20	531.9	181.8	11.4	1.7
Karavoate N (**18**)	*p*-methoxyBz	*p*-methoxyBz	2	528.1	184.1	6.3	0.9
			20	548.9	186.7	9.7	1.4
Karavoate O (**19**)	H	Cin	2	496.9	197.9	10.0	1.3
			20	505.9	206.9	11.0	1.4
Karavoate P (**20**)	Cin	Cin	2	528.0	191.2	6.9	1.0
			20	503.0	177.0	18.1	2.7
Tribenzoylbalsaminol F (**24**)	-	-	2	524.2	188.7	7.6	1.3
			20	538.1	181.7	7.1	1.1
DMSO			10 μL	547.4	185.7	7.4	1.1

[a] Some results were obtained from different assays. For compound **11**: (PAR + R123: FL-1 = 974.2; MDR + R123: FL-1 = 25.6; Verapamil: FL-1 = 154.5, FAR = 8.6). For compounds **12**, **15**, **16**, and **19**: (PAR + R123: FL-1 = 1062.8; MDR + R123: FL-1 = 8.7; Verapamil: FL-1 = 101.3, FAR = 13.1).

Table 3.12. Antiproliferative effects of compounds **1 - 4** and **26 - 40**.

Compounds	**PAR[a] ID_{50} (μM)**	**MDR[a] ID_{50} (μM)**
Balsaminol A (**35**)	7.2 ± 1.9	12.6 ± 2.6
Balsaminol B (**27**)	7.7 ± 3.0	31.0 ± 3.6
Balsaminol C (**29**)	19.0 ± 4.7	42.6 ± 1.9
Balsaminol D (**31**)	27.8 ± 1.8	67.1 ± 3.9
Balsaminol E (**26**)	41.3 ± 2.1	55.2 ± 0.02
Balsaminol F (**3**)	8.3 ± 1.9	20.8 ± 1.7
Balsaminagenin A (**34**)	19.5 ± 0.7	25.9 ± 2.4
Balsaminagenin B (**33**)	15.4 ± 2.4	16.8 ± 1.9
Balsaminagenin C (**2**)	18.7 ± 1.3	27.4 ± 0.7
Balsaminapentaol (**36**)	13.7 ± 0.4	29.3 ± 3.6
Balsaminoside A (**40**)	5.4 ± 1.7	35.5 ± 2.6
Balsaminoside B (**38**)	18.7 ± 2.0	42.6 ± 5.3
Balsaminoside C (**39**)	19.2 ± 1.2	54.2 ± 3.1
Cucurbalsaminol A (**32**)	48.2 ± 8.1	63.4 ± 3.1
Cucurbalsaminol B (**28**)	44.4 ± 2.3	46.3 ± 3.6
Cucurbalsaminol C (**30**)	19.5 ± 1.8	34.6 ± 3.9
Karavilagenin C (**1**)	6.3 ± 1.5	16.8 ± 2.2
Karavilagenin E (**4**)	21.3 ± 4.5	45.2 ± 3.6
Kuguaglycoside A (**37**)	3.5 ± 0.9	32.8 ± 3.6

[a] Values represent the mean ± SD of three independent experiments.

As it can be observed, at the highest concentration (20 μM) most of the isolated compounds (**1 - 4** and **26 - 40**) were found to be strong P-gp inhibitors. At this concentration, the highest effects were found for balsaminol C (**29**, FAR = 2.9 and 198.9 at 2 and 20 μM, respectively) and balsaminagenin B (**33**, FAR = 6.0 and 104.2 at 2 and 20 μM, respectively), which showed a manifold activity when compared to that of verapamil (FAR = 7.4 - 9.6 at 22 μM). At the lowest concentration tested (2 μM), karavilagenin C (**1**, FAR = 42.1 at 2 μM), exhibited the highest effect in reversing MDR (Table 3.9). Nevertheless, this concentration was at the saturation zone. In fact, when compound **1** was assayed at 0.5 and 1 μM a dose-dependent effect was observed, with a very significant activity at the highest concentration applied 1 μM (FAR = 1.5 and 15.0 at 0.5 and 1 μM, respectively), (Figure 3.2). A dose-

dependent effect was also found for the remaining compounds, excluding balsaminol F (**3**) that was found to be toxic at the highest concentration.

Table 3.13. Antiproliferative effects of esters **5** - **24**.

Compounds	**PAR[a] ID_{50} (μM)**	**MDR[a] ID_{50} (μM)**
Karavoate A (**5**)	26.0 ± 4.3	34.8 ± 3.6
Karavoate B (**6**)	48.8 ± 2.4	60.2 ± 5.6
Karavoate C (**7**)	41.4 ± 4.6	43.5 ± 2.0
Karavoate D (**8**)	> 133.3	> 133.3
Karavoate E (**9**)	51.0 ± 7.2	73.8 ± 2.1
Karavoate F (**10**)	93.2 ± 9.5	> 133.3
Karavoate G (**11**)	107.9 ± 14.3	129.9 ± 8.2
Karavoate H (**12**)	> 133.3	96.4 ± 3.1
Karavoate I (**13**)	29.0 ± 2.1	60.4 ± 4.0
Karavoate J (**14**)	59.4 ± 4.2	87.9 ± 3.9
Karavoate K (**15**)	63.4 ± 7.4	93.2 ± 2.6
Karavoate L (**16**)	> 133.3	> 133.3
Karavoate M (**17**)	59.4 ± 7.2	87.5 ± 6.1
Karavoate N (**18**)	74.6 ± 0.9	> 133.3
Karavoate O (**19**)	> 133.3	90.0 ± 3.3
Karavoate P (**20**)	> 133.3	> 133.3
Karavoate Q (**21**)	20.8 ± 2.3	40.6 ± 1.2
Karavoate R (**22**)	16.9 ± 7.1	46.9 ± 5.8
Triacetylbalsaminol F (**23**)	> 133.3	> 133.3
Tribenzoylbalsaminol F (**24**)	74.7 ± 3.5	87.9 ± 0.2

[a] Values represent the mean ± SD of three independent experiments.

When comparing with the parent compounds (balsaminol F and karavilagenin C), a decrease of activity was found for the ester derivatives. However, it should be emphasised that, in opposition to the parent compound balsaminol F, triacetylbalsaminol F (**23**) and tribenzoylbalsaminol F (**24**) did not show toxicity to the cells (Table 3.13), displaying the former ester a strong activity at 20 μM (FAR = 15.0). On the other hand, the benzoylated

derivative (**24**) was ineffective at both concentrations (Table 3.11). In the same way, when considering karavilagenin C esters, only the alkanoyl derivatives, karavoates A (**5**, FAR = 34.2 at 20 μM), B (**6**, FAR = 37.5 at 20 μM), C (**7**, FAR = 40.6 at 20 μM), and E (**9**, FAR = 21.7 at 20 μM) exhibited a significant activity at the highest concentration. Except for karavoate A (**5**, FAR = 35.2 and 34.5 at 2 and 20 μM), a dose-dependent effect was also found for the active esters.

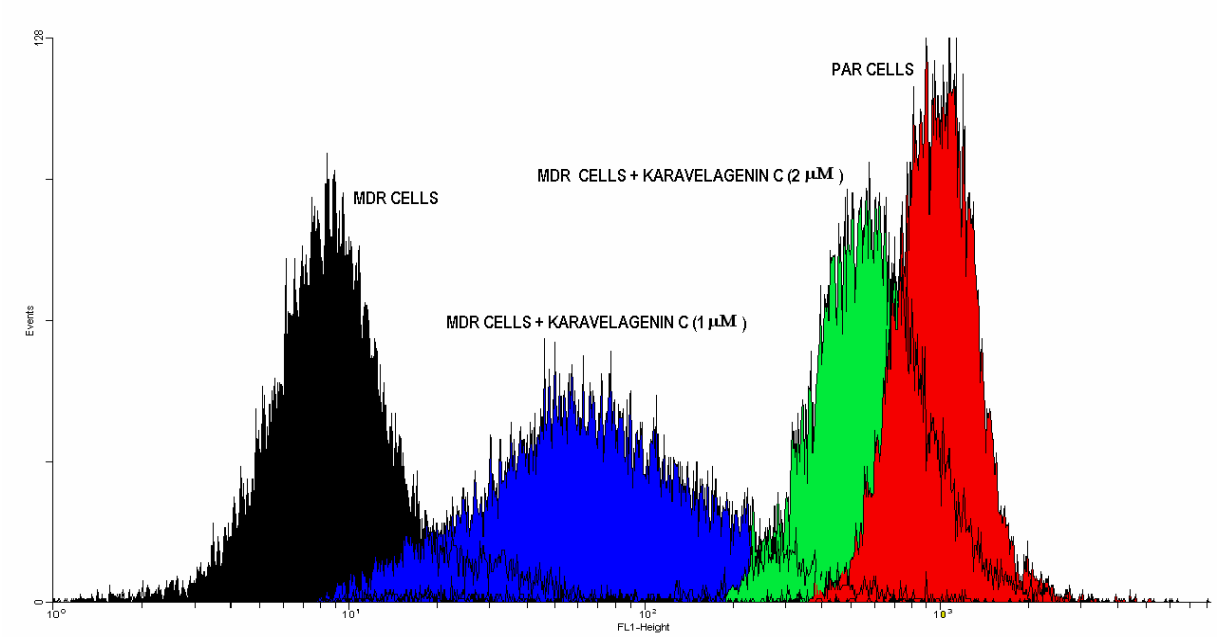

Figure 3.2. Histogram of the amount of rhodamine accumulated in MDR (black) and parental (red) cells and in MDR cell line treated with 1 μM (blue) and 2 μM (green) of karavilagenin C (**1**).

Structure-activity relationships

In order to find out structure-activity relationships, the calculated physico-chemical properties for compounds were analysed (Tables 3.14 and 3.15). As it can be observed, all compounds are lipophilic, exhibiting the natural products log *P* values in the range of 3.8 - 7.3, and the esters values between 6.7 - 9.9. They have a molecular weight comprised between 771 and 430 and are H-bond acceptors (between 3 and 11). Excluding the esters without free hydroxyl groups (**6**, **8**, **10**, **12**, **14**, **16**, **18**, **20**, **23**, and **24**), they are also H-bond donors (between 1 and 6). It is interesting to point that karavilagenin C (**1**), the most active

compound at the lowest concentration, has the lowest value of topological polar surface area (TPSA = 49.7).

The presence of methoxyl groups at C-7 and C-25 appears to play an important role in MDR reversing activity. In fact, balsaminol B (**27**, FAR = 7.3 and 68.7, at 2 and 20 μM, respectively) that differs from balsaminol A (**35**, FAR = 1.5 and 47.6, at 2 and 20 μM, respectively), having a methoxyl group at C-7, instead of a hydroxyl function, showed higher FAR values. A similar difference was observed for cucurbalsaminols A (**32**, FAR = 0.7 and 2.9, at 2 and 20 μM, respectively) and B (**28**, FAR = 2.7 and 38.2, at 2 and 20 μM, respectively), having the latter a methoxyl group at C-7. In the same way, the importance of a methoxyl group at C-25 is illustrated by the results obtained for balsaminagenins A (**34**, FAR = 1.1 and 44.3, at 2 and 20 μM, respectively), and B (**33**, FAR = 6.0 and 104.2, at 2 and 20 μM, respectively).

Similarly to the results obtained for the antimalarial activity, the side chain structure also seems to interfere with the reversing activity. In fact, balsaminol C (**29**, FAR = 2.9 and 198.9, at 2 and 20 μM, respectively), which showed the strongest MDR reversal activity at 20 μM, only differs from balsaminol D (**31**, FAR = 1.0 and 1.9, at 2 and 20 μM, respectively) in the structure of the side chain, having the latter a shorter side chain (C_6).

When comparing FAR values of compound **1** with its ester derivatives, it may be considered that free hydroxyl groups at both C-3 and C-23 are crucial for the activity. In fact, compound **1** showed a much higher activity than its corresponding monoacylated derivatives **5**, **7** and **9** (FAR = 35.2, 1.7 and 1.0, respectively at 2 μM). This decrease of rhodamine accumulation was still higher in the diacylated derivatives **6**, **8**, and **10** (FAR = 5.7, 0.9, and 1.4, respectively at 2 μM). Similarly, remarkable decrease in FAR values was also found for the mono and diacylated aroyl, cinnamoyl, and succinoyl esters (Tables 3.10 **-** 3.11).

Furthermore, MDR reversal activity was also affected by the number of carbons of the acylating agent. In fact, at 2 μM, a drastic decrease was observed in FAR values for propanoyl (**7**, log *P* = 8.3) and butanoyl (**9**, log *P* = 8.7) monoesters in comparison with the monoacetylated derivative (**5**, log *P* = 8.0), highlighting the involvement of other factors in the activity, besides lipophilicity.

In conclusion, this work corroborates the importance of lipophilicity for P-gp modulation. However, the most active compounds were not those with the highest log *P* values as exemplified by the decrease of activity found for the esters. Probably, some optimal lipophilicity needs to exist for effective MDR reversals. The importance of H-bonding

potential and topological polar surface area was also highlighted. However, the correlation between the MDR reversing effects and calculated physico-chemical properties must be multifactorial because none of the calculated parameters were directly correlated alone.

Table 3.14. Comparison of MDR modulator activities with physico-chemical properties of natural compounds **1** - **4** and **26** - **40** (topological polar surface area, number of hydrogen bond acceptors and donors, molecular weight, and octanol/water partition coefficient)[a].

Compounds	TPSA	N° H[b]		MW	log *P*	FAR (2 µM)	FAR (20 µM)
		acc.	don.				
Balsaminol A (**35**)	80.9	4	4	474	5.5	1.5	47.6
Balsaminol B (**27**)	69.9	4	3	488	6.2	7.3	68.7
Balsaminol C (**29**)	74.6	4	2	470	5.2	2.9	198.9
Balsaminol D (**31**)	74.6	4	2	430	3.8	1.0	1.9
Balsaminol E (**26**)	57.5	3	2	456	6.5	2.0	64.8
Balsaminol F (**3**)[b]	60.7	3	3	458	6.7	2.6	
Balsaminagenin A (**34**)	80.9	4	4	474	5.2	1.1	44.3
Balsaminagenin B (**33**)	69.9	4	3	488	5.8	6.0	104.2
Balsaminagenin C (**2**)	60.7	3	3	458	6.4	7.1	36.0
Balsaminapentaol (**36**)	101.1	5	5	490	4.4	0.7	2.9
Balsaminoside A (**40**)	128.8	8	5	634	5.3	1.5	89.4
Balsaminoside B (**38**)	139.8	8	6	620	5.0	0.9	37.2
Balsaminoside C (**39**)	139.8	8	6	620	5.0	1.0	2.3
Cucurbalsaminol A (**32**)	80.9	4	4	474	5.5	0.7	2.9
Cucurbalsaminol B (**28**)	69.9	4	3	488	6.1	2.7	38.2
Cucurbalsaminol C (**30**)	69.9	4	3	488	6.4	3.1	19.8
Karavilagenin C (**1**)	49.7	3	2	472	7.3	42.1	46.0
Karavilagenin E (**4**)	49.7	3	2	456	6.3	3.8	72.6
Kuguaglycoside A (**37**)	128.8	8	5	634	5.6	1.0	49.1

[a] Physico-chemical parameters were determined by using the JME molecular editor (version January 2010, http://www.molinspiration.com/). [b] Compound **3** showed to be toxic at 20 µM.

[b] Number of hydrogen acceptors (acc.) and hydrogen donors (don.).

Table 3.15. Comparison of MDR modulator activities with physico-chemical properties of esters **5** - **24** (topological polar surface area, number of hydrogen bond acceptors and donors, molecular weight, and octanol/water partition coefficient)[a].

Compounds	TPSA	N° H[b]		MW	log *P*	FAR (2 µM)	FAR (20 µM)
		acc.	don.				
Triacetylbalsaminol F (**23**)	78.9	3	0	584	8.6	3.0	15.0
Tribenzoylbalsaminol F (**24**)	78.9	3	0	770	9.9	1.3	1.1
Karavoate A (**5**)	55.8	4	1	514	8.0	35.2	34.2
Karavoate B (**6**)	61.8	5	0	556	8.6	5.7	37.5
Karavoate C (**7**)	55.8	4	1	528	8.3	1.7	40.6
Karavoate D (**8**)	61.8	5	0	584	8.9	0.9	2.4
Karavoate E (**9**)	55.8	4	1	542	8.7	1.0	21.7
Karavoate F (**10**)	61.8	5	0	612	9.3	1.4	1.6
Karavoate G (**11**)	55.8	4	1	576	9.0	1.0	7.8
Karavoate H (**12**)	61.8	5	0	680	9.6	1.2	1.3
Karavoate I (**13**)	101.6	7	1	621	9.0	2.1	3.9
Karavoate J (**14**)	153.5	11	0	770	9.6	1.4	2.1
Karavoate K (**15**)	55.8	4	1	610	9.2	1.4	1.6
Karavoate L (**16**)	61.8	5	0	748	9.9	1.0	1.2
Karavoate M (**17**)	65.0	5	1	606	9.0	1.8	1.7
Karavoate N (**18**)	80.3	7	0	740	9.7	0.9	1.4
Karavoate O (**19**)	55.8	4	1	602	9.2	1.3	1.4
Karavoate P (**20**)	61.8	5	0	732	9.8	1.0	2.7
Karavoate Q (**21**)	93.1	6	2	572	7.0	1.1	4.2
Karavoate R (**22**)	136.4	9	2	672	6.7	1.3	5.9

[a] Physico-chemical parameters were determined by using the JME molecular editor (version January 2010, http://www.molinspiration.com/).

[b] Number of hydrogen acceptors (acc.) and hydrogen donors (don.).

In further experiments, some of the compounds were studied in combination with doxorubicin, on mouse lymphoma cells transfected with the human *mdr1* gene, by using the checkerboard microplate method (Eliopoulos, 1991). Several concentrations of doxorubicin and resistance modifiers were tested. As it can be observed (Table 3.16, and Figures 3.3 - 3.9), all the tested compounds, excepting balsaminoside B (**38**, FIX = 0.82), showed a synergistic interaction with doxorubicin (FIX = 0.07 - 0.44). The most effective compound was balsaminol C (**29**), which expressed a FIX value of 0.07.

The above results highlighted the cucurbitane skeleton as lead in the development of new potent P-gp modulators.

Table 3.16. *In vitro* effects of some selected compounds (**1**, **2**, **4**, **5**, **26** - **30**, **32** - **35**, **38** and **40**) in combination with doxorubicin on human MDR1 gene-transfected mouse lymphoma cell line.

Compounds	FIX values[a]	Interaction
Balsaminol A (**35**)	0.28	Synergism
Balsaminol B (**27**)	0.10	Synergism
Balsaminol C (**29**)	0.07	Synergism
Balsaminol E (**26**)	0.16	Synergism
Balsaminol F (**3**)	0.40	Synergism
Karavoate A (**5**)	0.44	Synergism
Balsaminagenin A (**34**)	0.39	Synergism
Balsaminagenin B (**33**)	0.18	Synergism
Balsaminagenin C (**2**)	0.24	Synergism
Balsaminoside A (**40**)	0.37	Synergism
Balsaminoside B (**38**)	0.82	Additive
Cucurbalsaminol A (**32**)	0.44	Synergism
Cucurbalsaminol B (**28**)	0.14	Synergism
Cucurbalsaminol C (**30**)	0.22	Synergism
Karavilagenin C (**1**)	0.23	Synergism
Karavilagenin E (**4**)	0.18	Synergism
Kuguaglycoside A (**37**)	0.50	Synergism

[a] FIX = Fractional inhibitory index; FIX ≤ 0.5 synergism; FIX = 0.51 - 1 additive effect; FIX = 1 - 2 indifferent effect; FIX = > 2 antagonism.

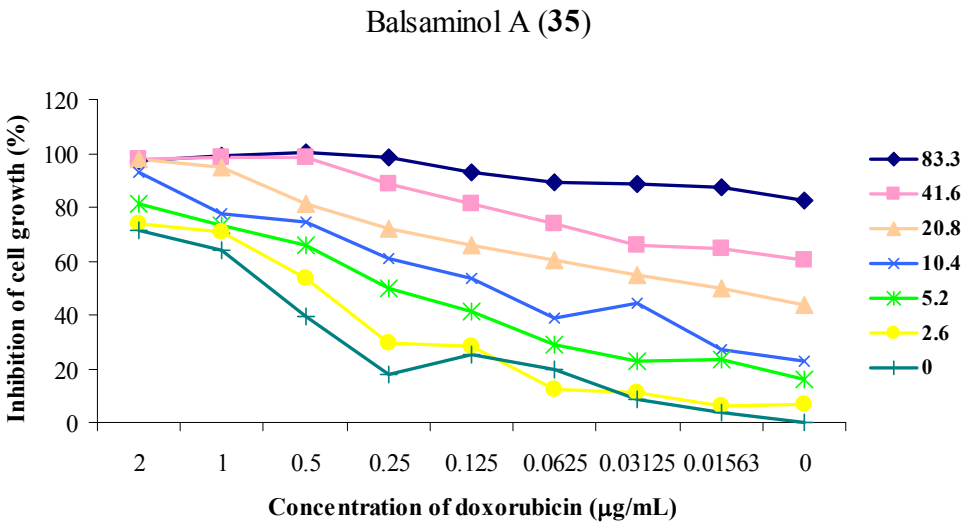

Figure 3.3. Effects of balsaminol A (**35**), (concentrations between 0 and 83.3 µM), in combination with doxorubicin on human *MDR1* gene-transfected mouse lymphoma cell line.

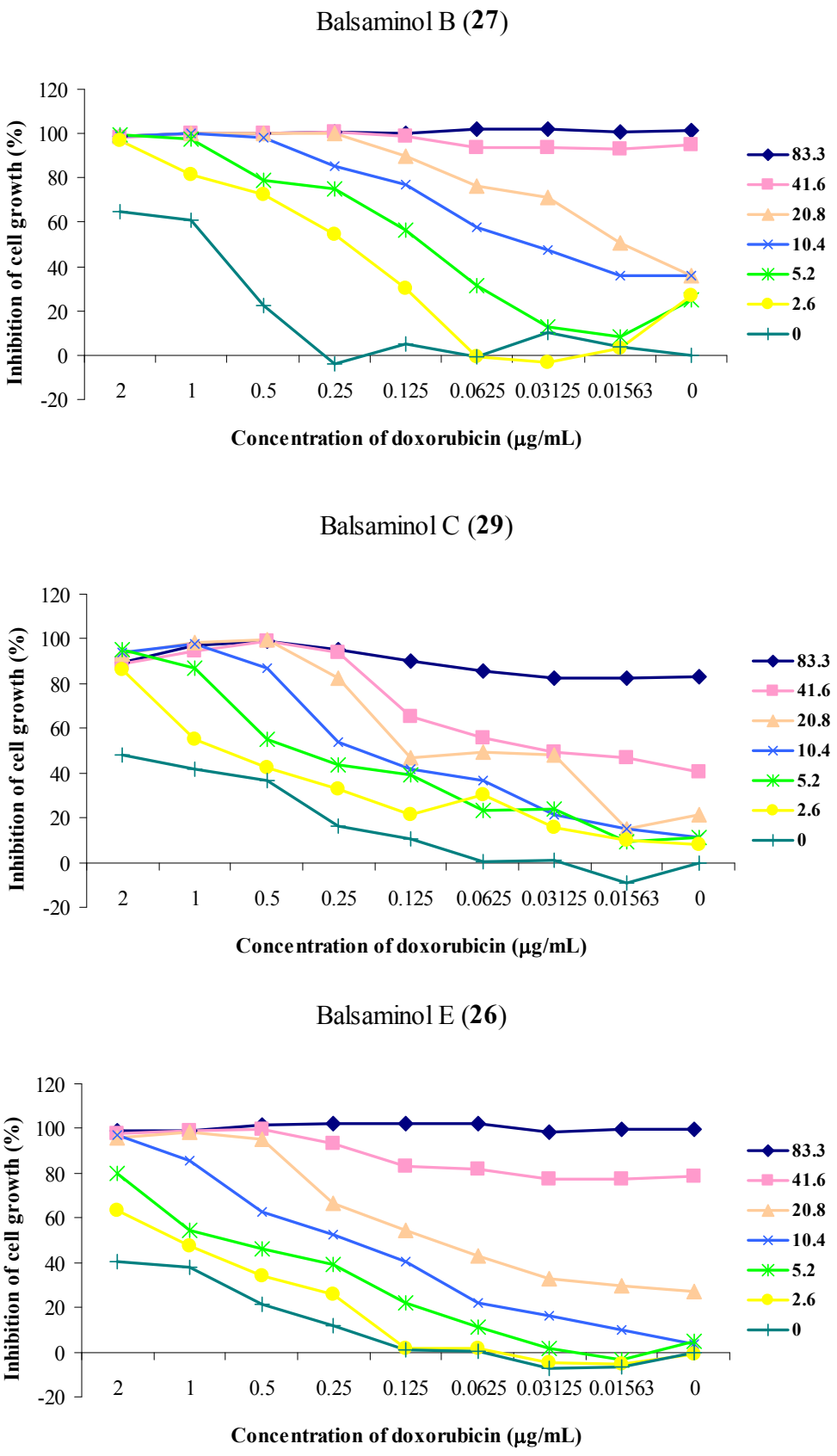

Figure 3.4. Effects of balsaminols B (**27**), C (**29**) and E (**26**), (concentrations between 0 and 83.3 µM), in combination with doxorubicin on human *MDR1* gene-transfected mouse lymphoma cell line.

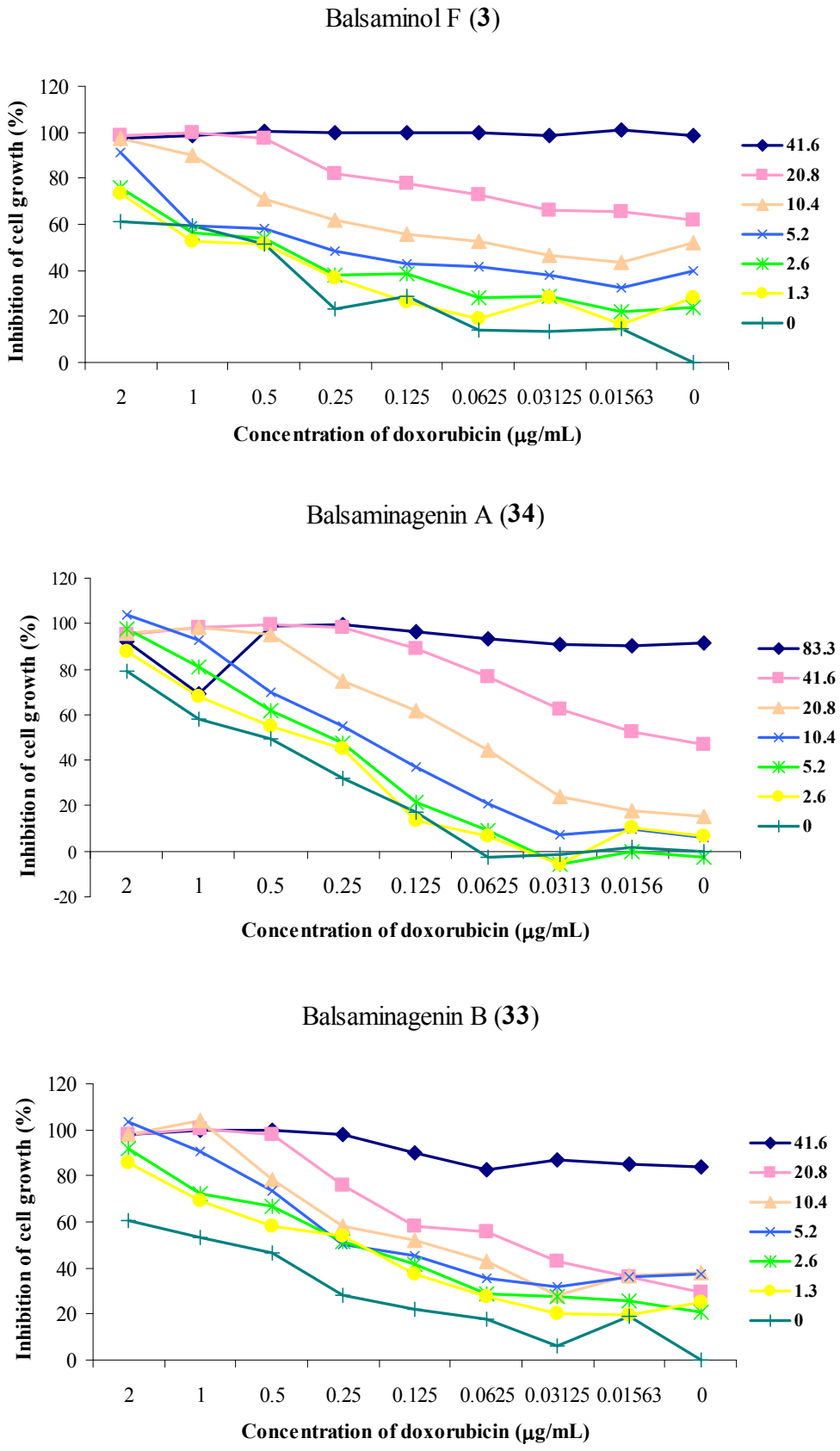

Figure 3.5. Effects of balsaminol F (**3**) and balsaminagenin B (**33**), (concentrations between 0 and 41.6 µM), and balsaminagenin A (**34**), (concentrations between 0 and 83.3 µM), in combination with doxorubicin on human *MDR1* gene-transfected mouse lymphoma cell line.

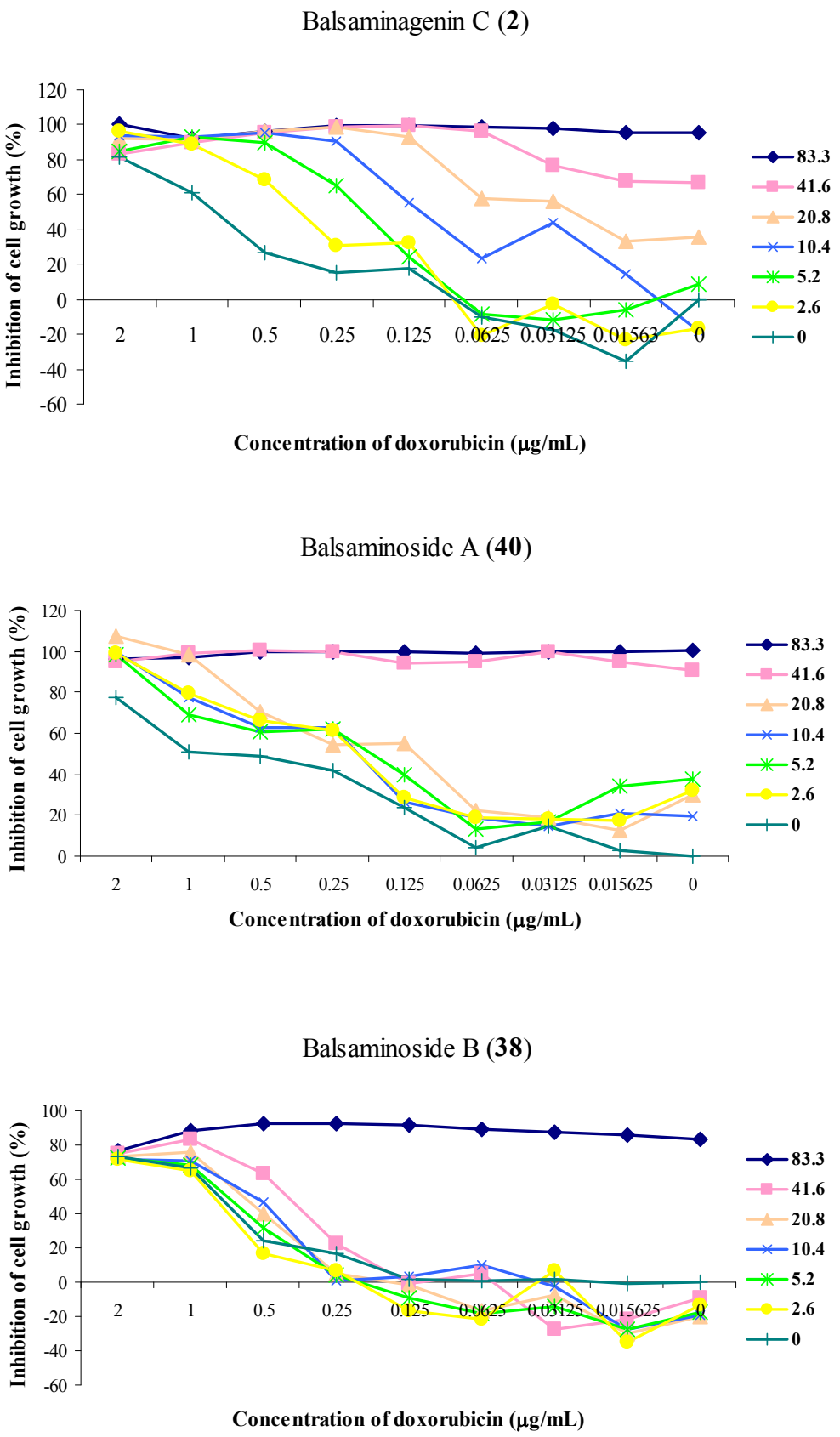

Figure 3.6. Effect of balsaminagenin C (**2**), and balsaminosides A (**40**), B (**38**), (concentrations between 0 and 83.3 µM), in combination with doxorubicin on human *MDR1* gene-transfected mouse lymphoma cell line.

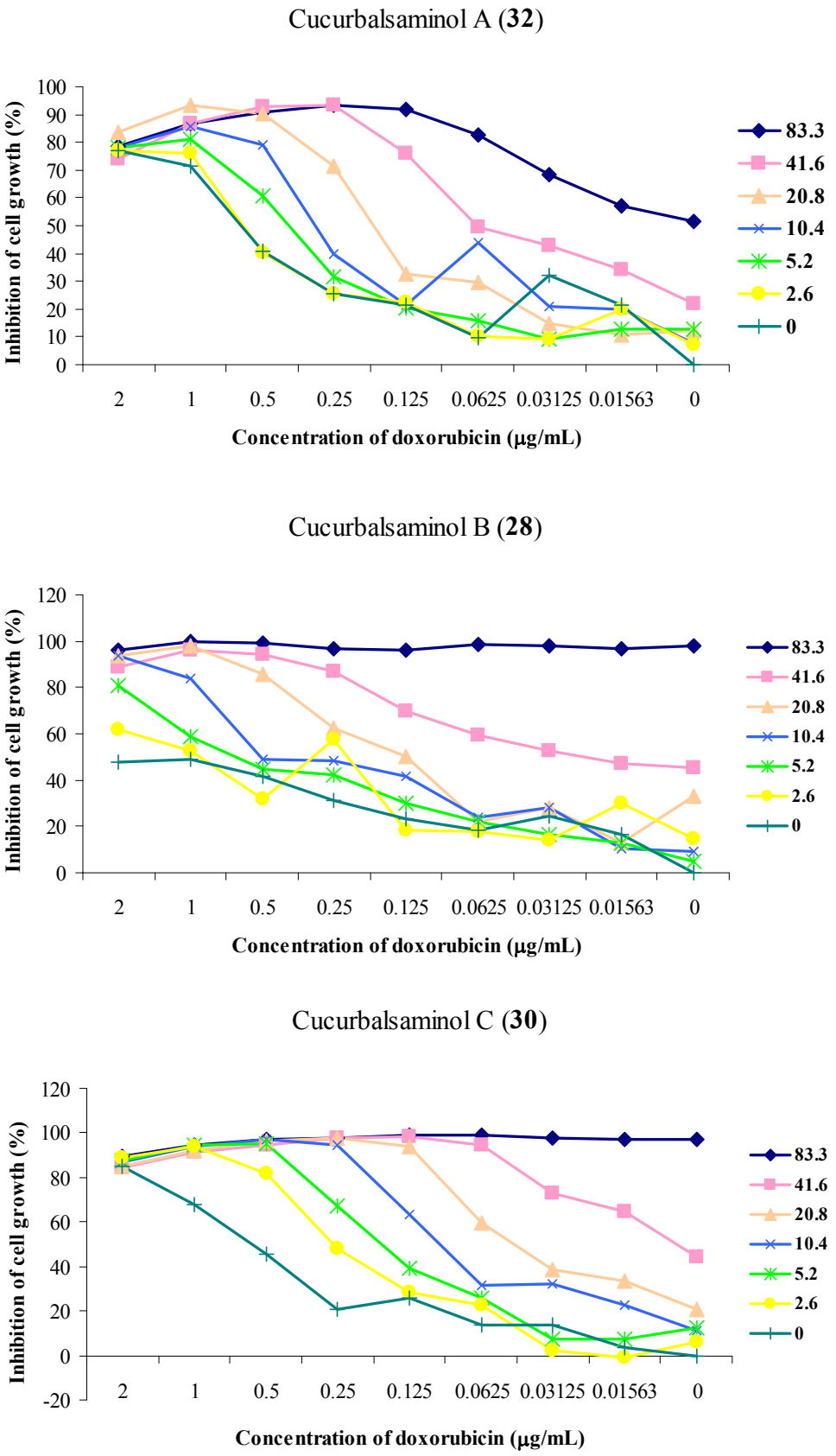

Figure 3.7. Effects of cucurbalsaminols A (**32**), B (**28**) and C (**30**), (concentrations between 0 and 83.3 µM), in combination with doxorubicin on human *MDR1* gene-transfected mouse lymphoma cell line.

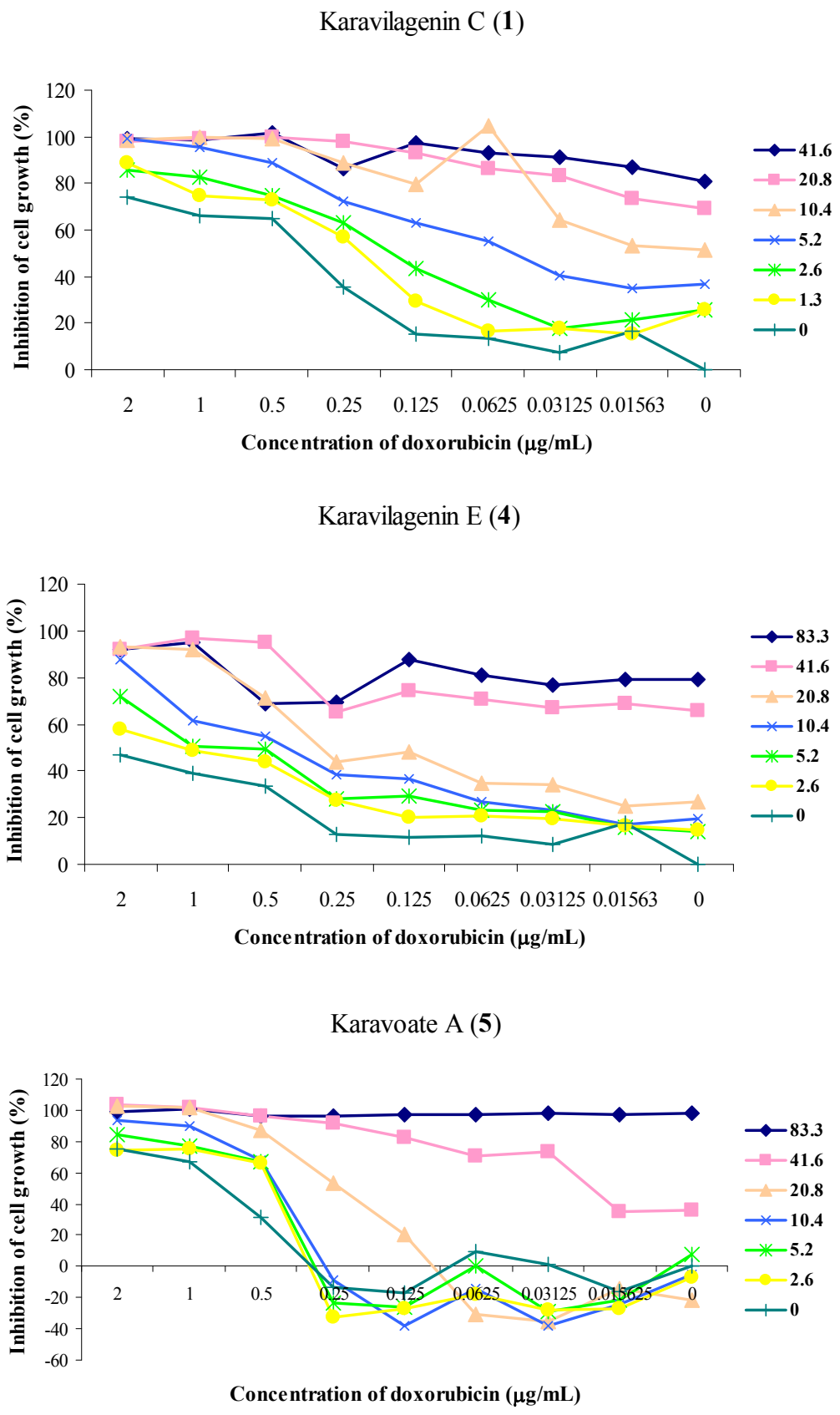

Figure 3.8. Effects of karavilagenin C (**1**) (concentrations between 0 and 41.6 µM), and karavilagenin E (**4**) and karavoate A (**5**), (concentrations between 0 and 83.3 µM), in combination with doxorubicin on human *MDR1* gene-transfected mouse lymphoma cell line.

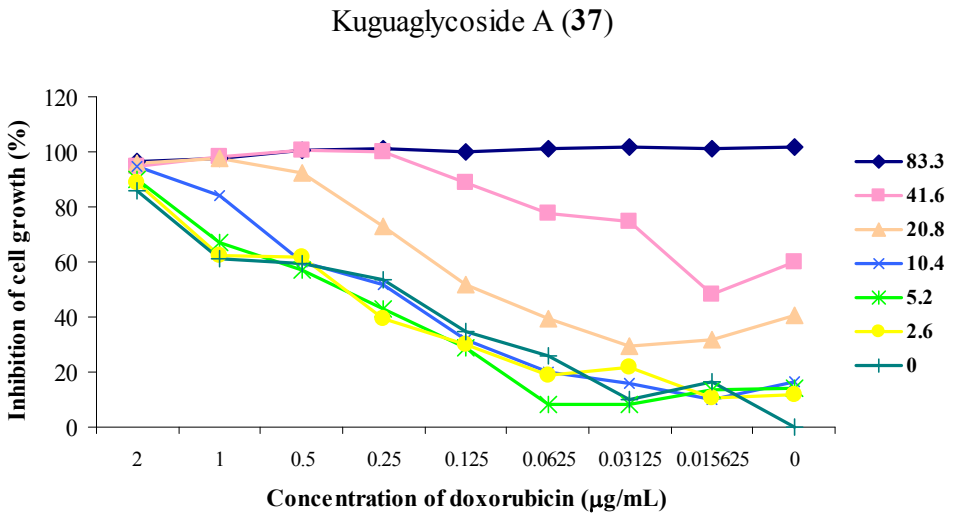

Figure 3.9. Effects of kuguaglycoside A (**37**), (concentrations between 0 and 83.3 µM), in combination with doxorubicin on human *MDR1* gene-transfected mouse lymphoma cell line.

2.2. Evaluation of the inhibition of P-gp transport activity by real-time fluorometry

Several methods have been used for assessing anti-MDR activity (Wiese and Pajeva, 2001). One of them is the flow cytometry, as previous described in section 2.1. As referred to, this technique involves the employment of a fluorochrome substrate such as rhodamine 123, which is extruded by the MDR1 transporter and is increasingly retained if the transporter is inhibited. In this dissertation, a new method, firstly described by Viveiros et al (2008), was also used for some compounds. It is a semiautomated method that utilizes the fluorochrome ethidium bromide (EB), a universal substrate of efflux pumps. Ethidium bromide has been shown to be particularly suitable to be used as a probe because it emits weak fluorescence in aqueous solution (outside cells) and becomes strongly fluorescent in non-polar and hydrophobic environments (inside cells). Moreover, it does not affect the cell viability or cellular functions at the concentrations tested. Moreover, the accumulation of the EB inside the cell can be detected by real time fluorescence spectroscopy.

Balsaminagenins A (**34**), B (**33**), karavilagenin C (**1**) and balsaminoside A (**40**), which showed a strong anti-MDR activity by the flow cytometry technique, were also investigated for their potential ability as MDR modulators, in the same cells, using the real-time fluorometry assay, described above. Verapamil was used as a positive control and the compounds were assayed at two concentrations (3 and 30 µM). The results for their anti-MDR

activity are summarized in Table 3.17. For the real-time data (as example, Figure 3.10), the relative final fluorescence (RFF) of the last time point (minute 60) of the assay was calculated (Table 3.17).

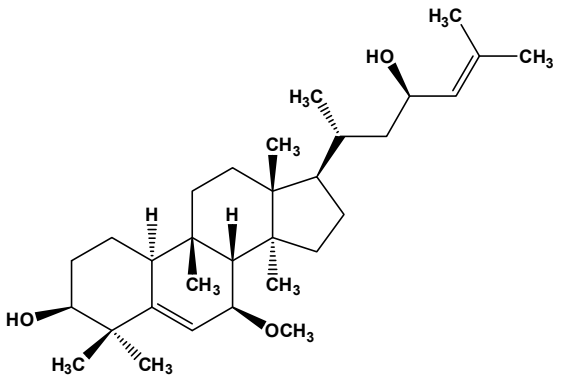

Karavilagenin C (**1**)

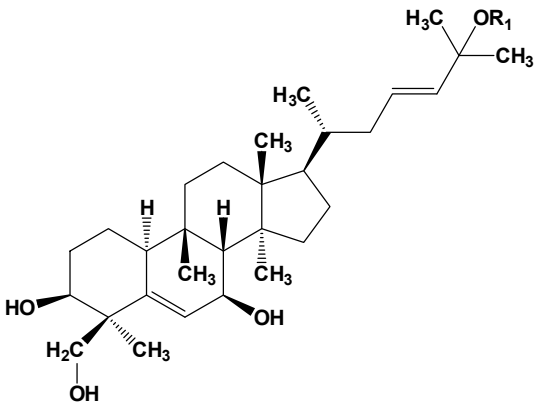

	R_1
Balsaminagenin A (**34**)	H
Balsaminagenin B (**33**)	CH_3

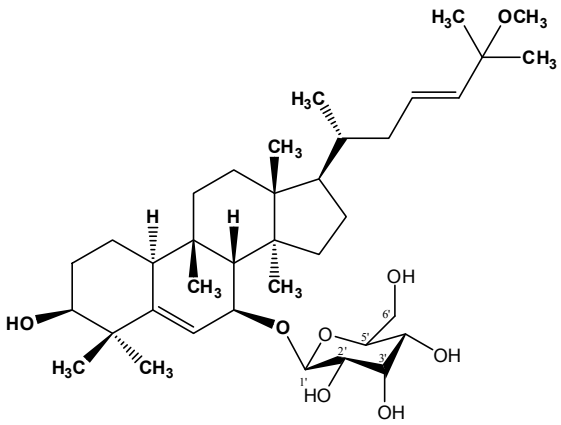

Balsaminoside A (**40**)

Table 3.17. Effects of balsaminagenins A (**34**), B (**33**), balsaminoside (**40**), and karavilagenin C (**1**) on the activity of MDR efflux pump of mouse lymphoma cells transfected with human ABCB1 gene by the real-time fluorometric method after 60 minutes.

Compounds	**Concentration µM**	**Relative final fluorescence (RFF)[a]**
Verapamil	81.5	100
Balsaminagenin A (**34**)	3	0
	30	64.0
Balsaminagenin B (**33**)	3	3.6
	30	65.0
Balsaminoside (**40**)	3	1.6
	30	86.7
Karavilagenin C (**1**)	3	64.0
	30	11.8
DMSO	10 µL	0.8

[a] Relative final fluorescence (RFF) = $RF_{treated} - RF_{untread}$

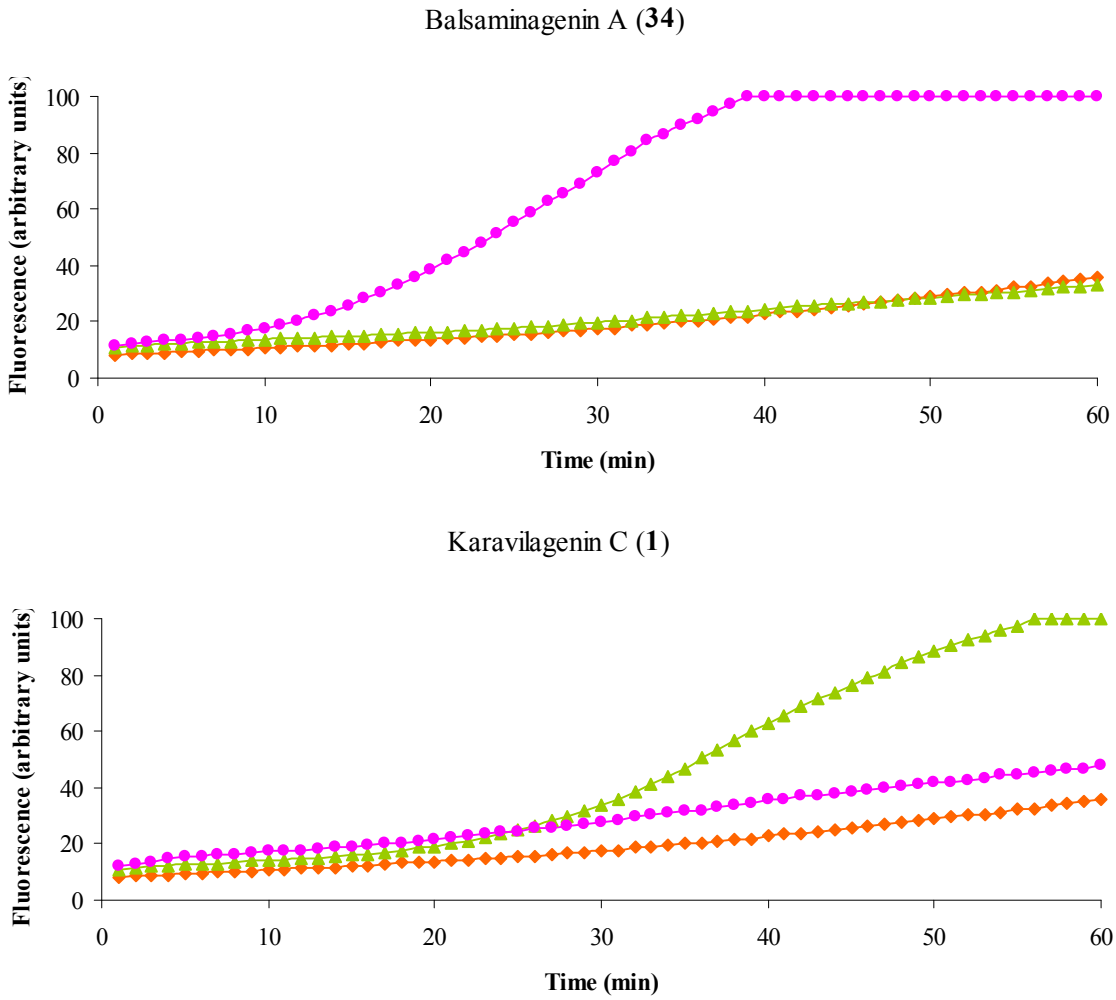

Figure 3.10. Accumulation of EB (1 µg/mL) by MDR mouse limphoma cells in the presence of balsaminagenin A (**34**) and karavilagenin C (**1**). ◆ DMSO control, ▲ 3 µM, ● 30 µM.

As it can be observed, all the compounds tested showed a high enhancement on the accumulation of EB inside the cells that could be explained by the inhibition of the P-gp efflux-pump activity. In this way, the results obtained with the EB semiautomated method are in accordance with those obtained in the flow cytometry assay. Similarly, karavilagenin C (**1**) showed the highest activity at the lower concentration tested.

3. EVALUATION OF THE INHIBITION OF BACTERIAL EFFLUX PUMPS

The searching for efflux pump inhibitors (EPIs) from plants has been considered a promising approach against resistant bacteria strains. In fact, according to some authors, plants use an anti-MDR strategy to potentiate their antimicrobial agents, which generally exhibit a weak activity (Gibbons, 2008; Lewis, 2001; Tegos et al., 2002).

Balsaminol A (**35**), balsaminol F (**3**), balsaminagenin A (**34**), balsaminagenin B (**33**), balsaminoside A (**40**), and karavilagenin C (**1**) were evaluated for their ability to reverse the activity of bacterial efflux pumps of some Gram-positive (MRSA COL_{oxa} and *E. faecalis* ATCC29212) and Gram-negative (*S. enteritidis* 5408, and *S. enteritidis* 5408_{CIP}) resistant strains. Furthermore, compounds **1**, **33**, and **40** were also tested on two resistant strains of *E. coli* (*E. coli* AG100 and *E. coli* $AG100_{TET8}$). The experiments were carried out by using the fluorometric method previously described in section 2.2. Two concentrations (3 and 30 μM) were applied in each experiment. The results are summarized in Tables 3.19 and 3.20 and Figures 3.11 and 3.12.

The minimum inhibitory concentration (MIC) values of compounds, against the bacteria strains used in the accumulation assay, were also determined (Table 3.18). Except for compounds **1** and **3**, which showed a weak activity against MRSA COL_{oxa} (MIC values of 25 μM for both compounds), no significant antibacterial activity (MIC range from 50 to ≥ 200 μM) was found at concentrations similar to or higher than the highest concentration used in the EB accumulation assay.

Table 3.18. Minimum inhibitory concentration (MIC) values of compounds **1**, **3**, **33** - **35**, and **40** on Gram-negative and Gram-positive bacteria strains**.**

Bacterial strains	**Compounds MIC (μM)**					
	1	**3**	**33**	**34**	**35**	**40**
E. coli AG100	> 200	> 200	> 200	> 200	> 200	> 200
***E. coli* AG100$_{TET8}$**	> 200	> 200	> 200	> 200	> 200	> 200
***S. enteritidis* 5408**	> 200	> 200	> 200	> 200	> 200	> 200
***S. enteritidis* 5408$_{CIP}$**	> 200	> 200	> 200	> 200	> 200	> 200
***E. faecalis* ATCC 29212**	> 200	200	200	> 200	100	> 200
MRSA COL_{oxa}	25	25	50	100	50	200

As shown in Table 3.19, and Figure 3.11, the most active efflux pump inhibitors of MRSA COL_{OXA} strain were karavilagenin C (**1**), and balsaminol F (**3**), (RFF = 21.8 and 21.1, respectively, at 3 μM). Contrary to remaining compounds, their modulating effect was not dose-dependent. In fact, for both compounds a decrease of activity was observed at the highest concentration (RFF = 9.7 and 14.2, respectively, at 30 μM), suggesting that these concentrations were at the saturation zone. Furthermore, it is interesting to note that balsaminoside A (**40**), which has shown the lowest EB accumulation at a low concentration, was the most active at the highest concentration (RFF = 8.1 and 34.1 at 3 and 30 μM, respectively). Compounds **33** - **35** showed a moderate activity (RFF range, 13.5 - 17.3 and 15.7 - 25.1 at 3 and 30 μM, respectively).

As regards *E. faecalis* (Table 3.19 and Figure 3.12), at the highest concentration, compounds **1**, **3** and **34** showed to increase, significantly, the accumulation of EB by the cells, exhibiting balsaminagenin B (**33**) the highest effect (RFF = 32.8 at 30 μM).

For the Gram-negative bacteria tested no significant activity was found (Table 3.20).

Table 3.19. Effects of compounds **1**, **33** - **35**, and **40** on the accumulation of EB by the Gram-positive MRSA COL_{OXA} (1μg/mL), and *E. faecalis* (0.5 μg/mL) strains.

Compounds	**Conc. (μM)**	**Relative final fluorescence (RFF)[a]**	
		MRSA COL_{OXA}	*E. faecalis*
Balsaminol A (**35**)	3	13.5	1.0
	30	15.7	18.3
Balsaminol F (**3**)	3	21.1	2.6
	30	14.2	23.4
Balsaminagenin A (**34**)	3	15.7	0.1
	30	21.7	3.1
Balsaminagenin B (**33**)	3	17.3	5.5
	30	25.1	32.8
Balsaminoside A (**40**)	3	8.1	5.3
	30	34.1	5.2
Karavilagenin C (**1**)	3	21.8	1.7
	30	9.7	10.4

[a] Relative final fluorescence (RFF) = $RF_{treated}$ - $RF_{untread}$

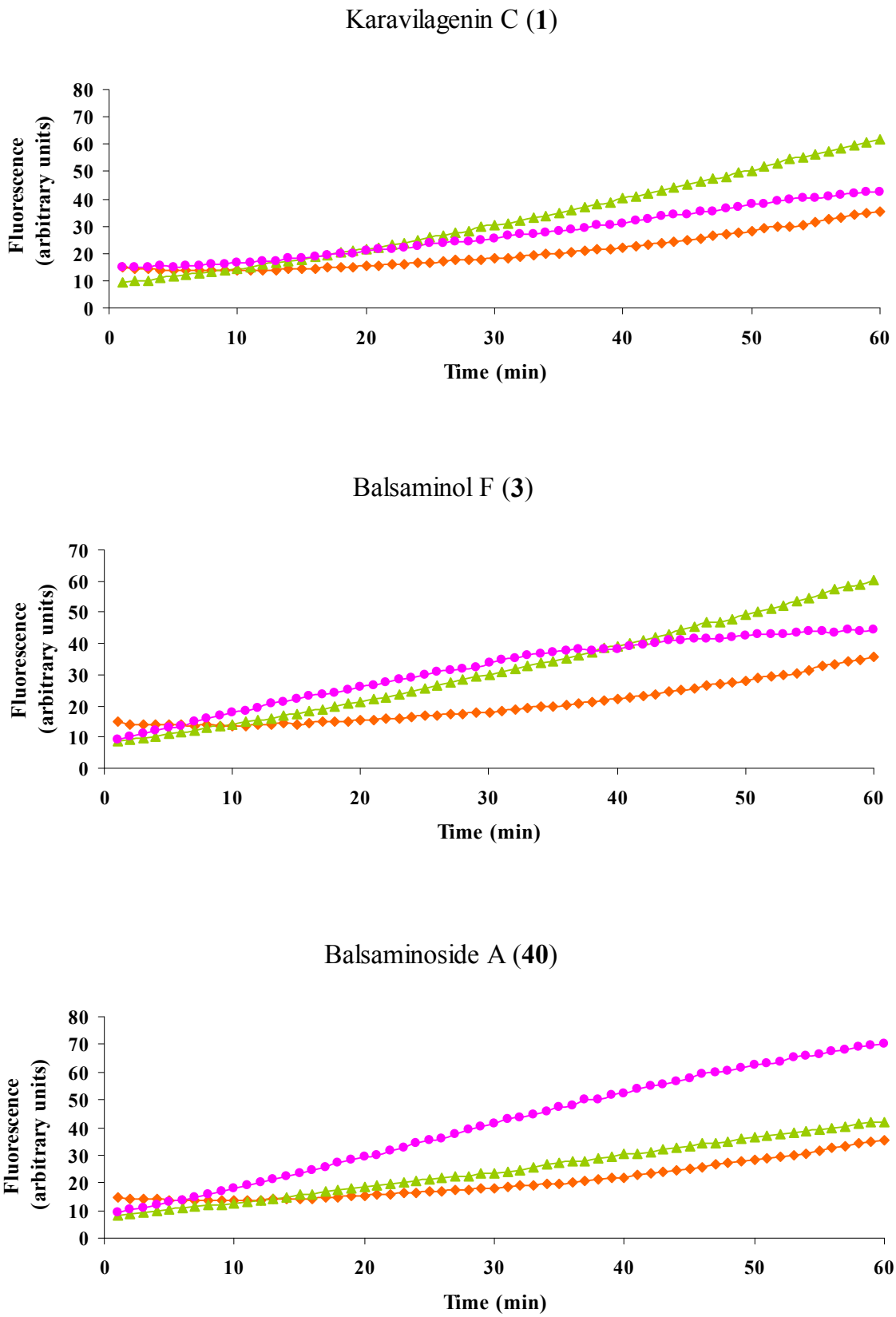

Figure 3.11. Effects of compounds **1**, **3**, and **40** on the accumulation of EB (1 µg/ mL) by MRSA COL_{OXA}. ◆ DMSO control, ▲ 3 µM, ● 30 µM.

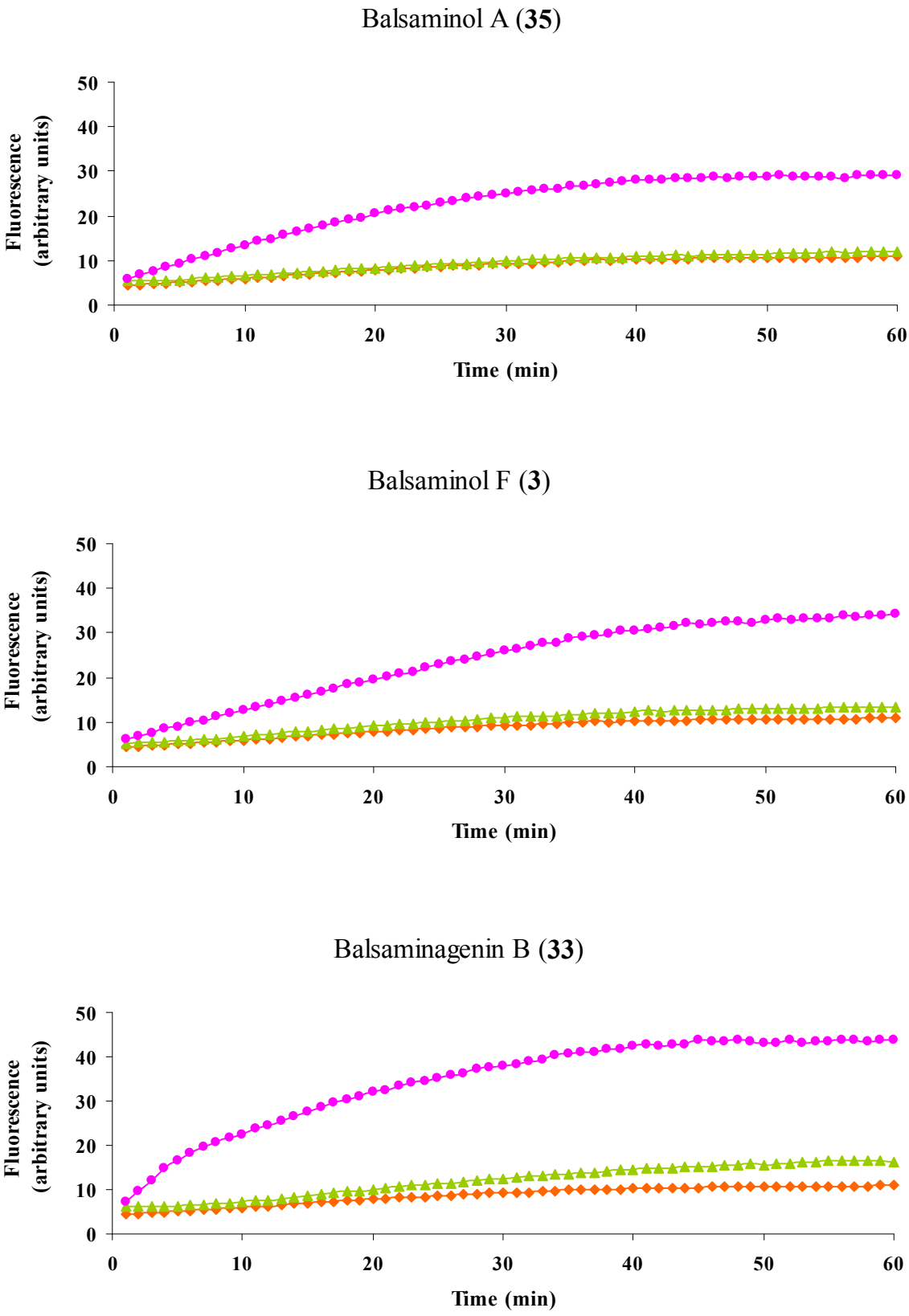

Figure 3.12. Effects of compounds **3**, **33**, and **35** on the accumulation of EB (0.5 µg/ mL) by *E. faecalis*. ◆ DMSO control, ▲ 3 µM, ● 30 µM.

Table 3.20. Effects of compounds **1**, **33 - 35**, and **40** on the accumulation of EB by the *E. coli* and *S. enteriditis* strains tested.

Compounds	Conc. (μM)	Relative final fluorescence (RFF) [a]			
		E. coli AG100	*E. coli* $AG100_{TET8}$	*S. enteridtidis*	*S. enteridtidis* 5408_{CIP}
Balsaminol A (**35**)	3	n.d. [b]	n.d. [b]	0	0
	30			0	0
Balsaminol F (**3**)	3	n.d. [b]	n.d. [b]	0	0
	30			0	1.3
Balsaminagenin A (**34**)	3	n.d. [b]	n.d. [b]	0	0.3
	30			0	2.8
Balsaminagenin B (**33**)	3	2.8	0	0	0
	30	4.6	1.8	0	3.4
Balsaminoside (**40**)	3	1.1	0	0	0
	30	7.8	0	0	0
Karavilagenin C (**1**)	3	2.8	0	0	0
	30	6.3	3.0	0	0

[a] Relative final fluorescence (RFF) = $RF_{treated} - RF_{untread}$; [b] not determined.

When comparing RFF values of compounds **1**, **3**, **33 - 35**, and **40**, against MRSA COL_{OXA}, at the lowest concentration, it is interesting to note that there is a correlation between RFF/TPSA (r^2 = 0.95), (Table 3.6 and Figure 3.13). In fact, the highest and lowest values of RFF were obtained for compounds **1** and **40** (RFF = 21. 8 and 8.1, respectively, at 3 μM), which exhibited the lowest (**1**, TPSA = 49.7) and highest (**40**, TPSA = 128.8) values of the topological polar surface area (Table 3.6). TPSA, defined as the sum of surfaces of polar atoms in a molecule, has been considered an important descriptor in drug discover, allowing of the prediction of molecular ability for crossing biological membranes (Fernandes and Gattass, 2009). Conversely, no significant correlation between RFF/log *P* values was found (r^2 = 0.58).

When analysing the results obtained for *E. faecalis* ATCC 29212, no apparent correlation was found between the reversing activity and the calculated physico-chemical properties (Table 3.6). Balsaminagenin B (**33**), the most active compound, differs from compound **34** in the substituent at C-25, bearing a methoxyl instead of a free hydroxyl group present in **34**. However, as it can be observed in Table 3.19, the latter compound was inactive,

suggesting that the methoxyl group at C-25 may play an important role in the activity. It should also be noted that karavilagenin C (**1**), the most effective compound at the lowest concentration on the assay with MRSA COL_{OXA}, increased weakly the accumulation of EB by *E. faecalis* (RFF = 1.7 and 10.4 at 3 and 30 μM, respectively), emphasizing the complexity of efflux systems in these bacteria. As referred to, compound **1** also showed the highest reversing activity in MDR cancer cells mediated by P-gp. Therefore, according to these results, this type of compounds might also interact with bacterial ABC-transporters, which are functionally related to the eukaryotic multi-drug resistance P-glycoprotein.

With regard to Gram-negative bacteria strains, the ineffectiveness of compounds may be explained by the presence of an outer membrane that acts as an effective barrier to compounds (Stavri et al., 2007).

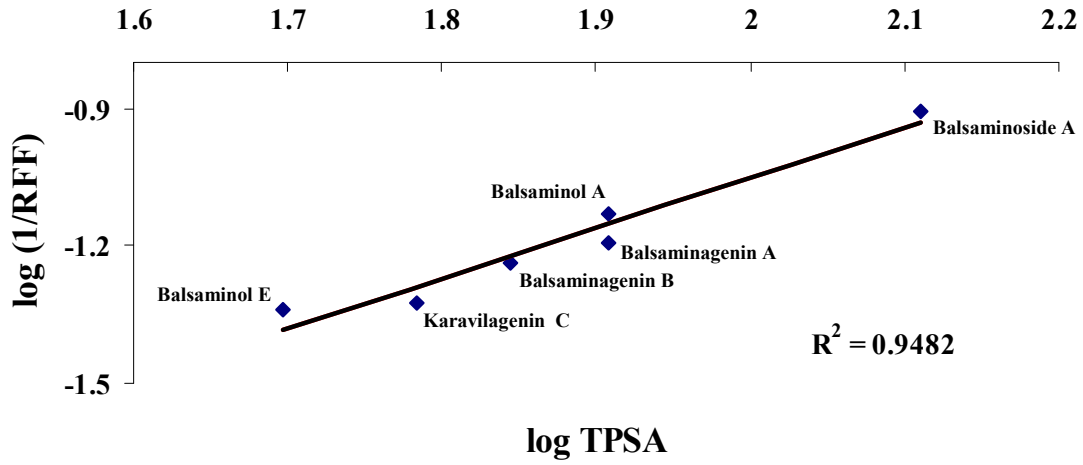

Figure 3.13. Relative final fluorescence (RFF), express as log (1/RFF), in MRSA COL_{OXA} strain versus the topological polar surface area, expressed as log (TPSA).

CHAPTER 4

Experimental Section

Phytochemical study

1. GENERAL EXPERIMENTAL PROCEDURES

Melting points were determined on a Köpffler apparatus and are uncorrected.

Optical rotations were obtained using a Perkin Elmer 241 polarimeter, with quartz cells of 1 dm path length; the samples were solubilised in $CHCl_3$ or MeOH.

IR spectra were determined on a FTIR Nicolet Impact 400 spectrophotometer.

UV spectra were recorded on a spectrophotometer Shimadzu UV-Visible 1240, using quartz cuvettes with an internal width of 1 cm.

NMR spectra were recorded on a Bruker ARX-400 NMR spectrometer (^1H 400 MHz; ^{13}C 100.61 MHz), or Bruker DRX-500 (^1H 500 MHz) using $CDCl_3$, MeOH, CD_3COCD_3, or C_5D_6N as solvents and TMS as internal standard.

Low resolution mass spectra were taken on a Micromass Quattro micro API (ESIMS), and on a Micromass Autospec spectrometer (EIMS); high resolution mass spectra were recorded on a Bruker-Microtof ESI-TOF (Biotof II Model, Bricker), and on a Micromass Autospec spectrometer (HR-EIMS and HR-CIMS).

Column chromatography was carried out on silica-gel (SiO_2, Merck 9385). Analytical and preparative Thin Layer Chromatography (TLC) were performed on precoated SiO_2 F_{254} plates (Merck 5554 and 5744, respectively) and visualized under visible and UV light (λ 254 and 366 nm) and by spraying with mixtures of H_2SO_4/MeOH (1:1) followed by heating.

HPLC was carried out on a Merck-Hitachi instrument, with UV detection and a Merck-Hitachi D-7500 integrator. Analytical HPLC was performed using a Merck LiChrospher 100 RP-18 (5 μm, 125 × 4 mm) column. Semipreparative HPLC was performed on a Merck LiChrospher 100 RP-18 (10 μm, 250 × 10 mm) column. Mixtures of MeOH/H_2O and MeCN/H_2O were used as eluents.

2. SELECTION OF PLANTS

The selection of plant species was based mainly on an ethnobotanical approach (Bandeira et al., 2001; Clarkson et al., 2004; Jansen, 1982; 1983; 1990; 1991; Jurg et al., 1991; Menan et al., 2006). In a few cases, chemotaxonomy was also considered. Plants were collected from Mozambique and Portugal. The information on the plant material is summarized in Table 4.1. The species collected in Mozambique were identified, locally, by Dr. Silva Mulhovo and voucher specimens (Table 4.1) have been deposited at the herbarium of the Instituto de Investigação Agronómica de Moçambique. The remaining species were collected in Portugal and identified by Dr. Teresa Vasconcelos from the Instituto Superior de Agronomia, Universidade de Lisboa, Portugal, where voucher specimens (Table 4.1) were deposited.

2.1. Preparation of extracts

Different plant parts (roots, leaves, seeds, and bark) or the entire plant, from selected species (Table 4.1), were dried at room temperature. Crude plant extracts were prepared by submitting 15 - 50 g of air-dried powdered plant material to a sequential extraction procedure with 150 - 500 mL of *n*-hexane, dichloromethane (CH_2Cl_2), ethyl acetate (EtOAc), and methanol (MeOH) for 48 h, at room temperature (Scheme 3.1). After filtration, the extracts were fully dried, under reduced pressure at 40 - 45 ºC, by using a *Büchi* rotatory evaporator, and then stored at low temperature (4ºC) until their use in antimalarial assays.

Table 4.1. Plant material data.

Plant species	Family	Plant part	Voucher number
[a]***Acacia karroo*** **Hayne**	Fabaceae	Aerial parts	111/2008
[b]***Aloe parvibracteata*** **Schonland**	Aloaceae	Leaves	113/2008
[c]***Bridelia cathartica*** **Bertol.f.**	Euphorbiaceae	Roots	24 SM
[d]***Cassia abbreviate*** **Oliv.**	Fabaceae	Stem Bark	26 SM
[c]***Cassia occidentalis*** **L.**	Fabaceae	Roots	29 SM
[e]***Crossopteryx febrifuga*** **(Afzel. ex G. Don) Benth**	Rubiaceae	Aerial parts	29 189
[f]***Leonotis leonurus*** **(L.) R.Br**	Lamiaceae	Aerial parts	562/2005
[d]***Momordica balsamina*** **L.**	Cucurbitaceae	Aerial parts	30 SM
[b]***Parkinsonia aculeata*** **L.**	Caesalpiniaceae	Aerial parts	574/2003
[a]***Pittosporum tobira*** **(Thunb.) W.T. Aiton**	Pittosporaceae	Aerial parts	116/2008
[b]***Plumbago auriculata*** **Lam.**	Plumbaginaceae	Aerial parts	269/2004
[f]***Senna didymobotrya*** **Fresen.**	Fabaceae	Twigs	115/2008
[a]***Schefflera actinophylla*** **(Endl.) Harms**	Araliaceae	Leaves	114/2008
[c]***Tabernaemontana elegans*** **Stapt.**	Apocynaceae	Leaves	23 SM
[c]***Trichilia emetica*** **Vahl**	Meliaceae	Seeds	25 SM

Plants collected in: [a]Garcia da Horta Garden (Lisbon, Portugal, January 2006), [b] Parque botânico da Tapada da Ajuda (Lisbon, Portugal. August, 2005), [c] Maputo (Mozambique, March 2006), [d] Gaza (Mozambique, January 2006), [e] Inhambane (Mozambique, April 2006), [f]Algarve (Portugal, July 2005).

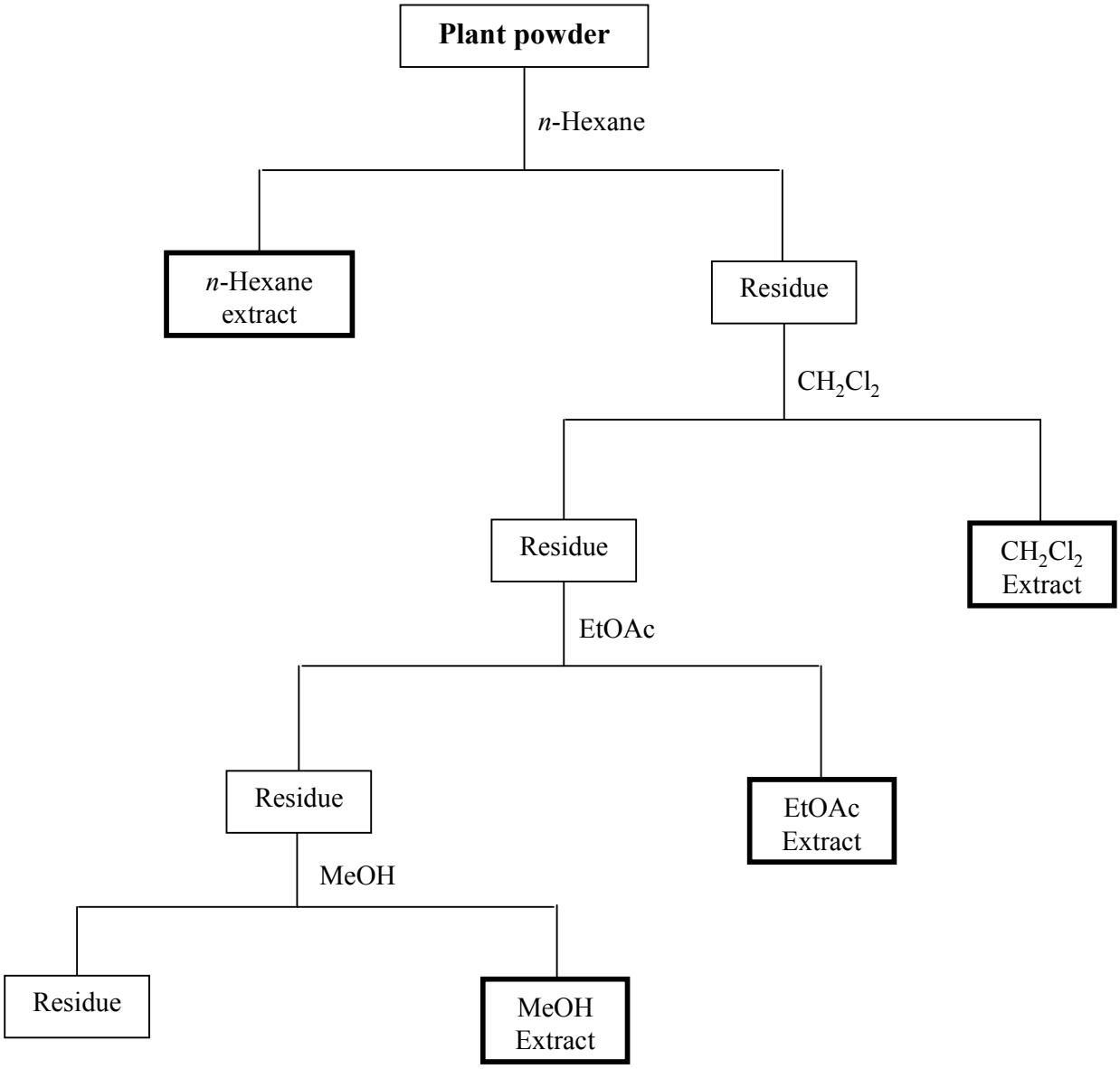

Scheme 3.1. Screening for antimalarial activity: extraction methodology.

3. STUDY OF *MOMORDICA BALSAMINA*

The aerial parts of *Momordica balsamina* were collected in Gaza, Mozambique, in August 2006. The plant material was identified by the botanist Dr. Silva Mulhovo, and a voucher specimen (30 SM) was deposited at the herbarium (LMS) of Instituto de Investigação Agronómica, Mozambique.

3.1. Extraction and isolation

The air-dried aerial parts of *M. balsamina* (1.2 kg) were mechanically powdered and exhaustively extracted with methanol (11 × 8 L) at room temperature. The MeOH extract was evaporated under vacuum (40 ºC) to afford a residue (280 g), which was suspended in H_2O (1 L) and extracted with EtOAc (9 × 0.5 L). The EtOAc residue (85 g) was suspended in MeOH/H_2O (9:1; 1 L), and extracted with *n*-hexane (5 × 0.5 L) for removal of waxy material that was not further studied. The remaining extract was evaporated under vacuum (40 ºC), yielding a residue (45 g) that was chromatographed over silica gel (1 Kg) using mixtures of *n*-hexane/EtOAc (1:0 to 0:1) and EtOAc/MeOH (19:1 to 0:1) as eluents to obtain eleven fractions (Fr M1 - M11), which were combined according to TLC analysis (Table 4.2 and Scheme 3.2). Fraction M1 and fractions M7 to M11 were not further studied.

3.2. Study of fraction M2

The fractions eluted with *n*-hexane/EtOAc (11:9 to 9:11) were pooled, after TLC monitoring (fraction M2, see Table 4.2), and recrystallized from *n*-hexane/EtOAc to give 1 g of compound **1** [karavilagenin C, 7β-methoxycucurbita-5,24-diene-3β,23(*R*)-diol]. The mother liquors of this fraction (2.1 g) were submitted to column chromatography (SiO_2, 100 g), using as eluents mixtures of *n*-hexane/EtOAc (1:0 to 0:1) and EtOAc/MeOH (1:0 to 0:1). After TLC monitoring, the chromatographic fractions were combined into four fractions (M2A to M2D, Table 4.3). Fractions M2A and M2D were not further studied.

Table 4.2. Column chromatography of the EtOAc extract.

Fraction	Mass (g)	Eluent (V/V)	
		***n*-hexane/EtOAc**	**EtOAc/MeOH**
M1	0.49	1:0 to 11:9	–
M2	3.11	11:9 to 9:11	–
M3	5.31	9:11 to 1:19	–
M4	3.25	1:19 to 0:1	1:0 to 19:1
M5	2.79	–	19:1 to 93:7
M6	11.91	–	93:7 to 9:1
M7	2.50	–	9:1
M8	3.00	–	17:3 to 4:1
M9	1.17	–	7:3 to 1:1
M10	3.27	–	1:1 to 1:3
M11	4.75	–	0:1

Table 4.3. Column chromatography of the fraction M2.

Fraction	Mass (g)	Eluent (V/V)
		***n*-hexane / EtOAc**
M2A	0.10	1:0 to 13:7
M2B	0.37	13:7 to 3:2
M2C	1.70	3:2 to 11:9
M2D	0.18	11:9 to 0:1

Fraction M2B (372 mg, Table 4.3) was successively fractionated by column chromatography, using mixtures of *n*-hexane/EtOAc (17:3 to 1:1), and CH_2Cl_2/Me_2CO (1:0 to 0:1). A final purification was carried out by HPLC, to afford 8 mg of compound **2** [balsaminagenin C, cucurbita-5,23(*E*)-diene-3β,7β,25-triol; 210 nm, MeOH/H_2O 41:9, 4 mL/min, R_t 26 min], 50 mg of compound **3** [balsaminol F, cucurbita-5,24-diene-3β,7β,23(*R*)-triol; 210 nm, MeOH/H_2O, 41:9, 4 mL/min, R_t 35 min], and 9 mg of compound **4** [karavilagenin E, 5β,19β-epoxycucurbita-6,24-diene-3β,23(*R*)-diol; 210 nm, ACN/H_2O, 22:3, 4 mL/min, R_t 26 min).

Fraction M2C (1.7 g) was recrystallized from *n*-hexane/EtOAc to afford 300 mg of compound **1**, previously isolated from fraction M2B. The mother liquors of the fraction M2C were repeatedly re-chromatographed with mixtures of CH_2Cl_2/Me_2CO (1:0 to 4:1), yielding an impure product that was recrystallized with the same mixture of solvents to afford more 707 mg of compound **1**.

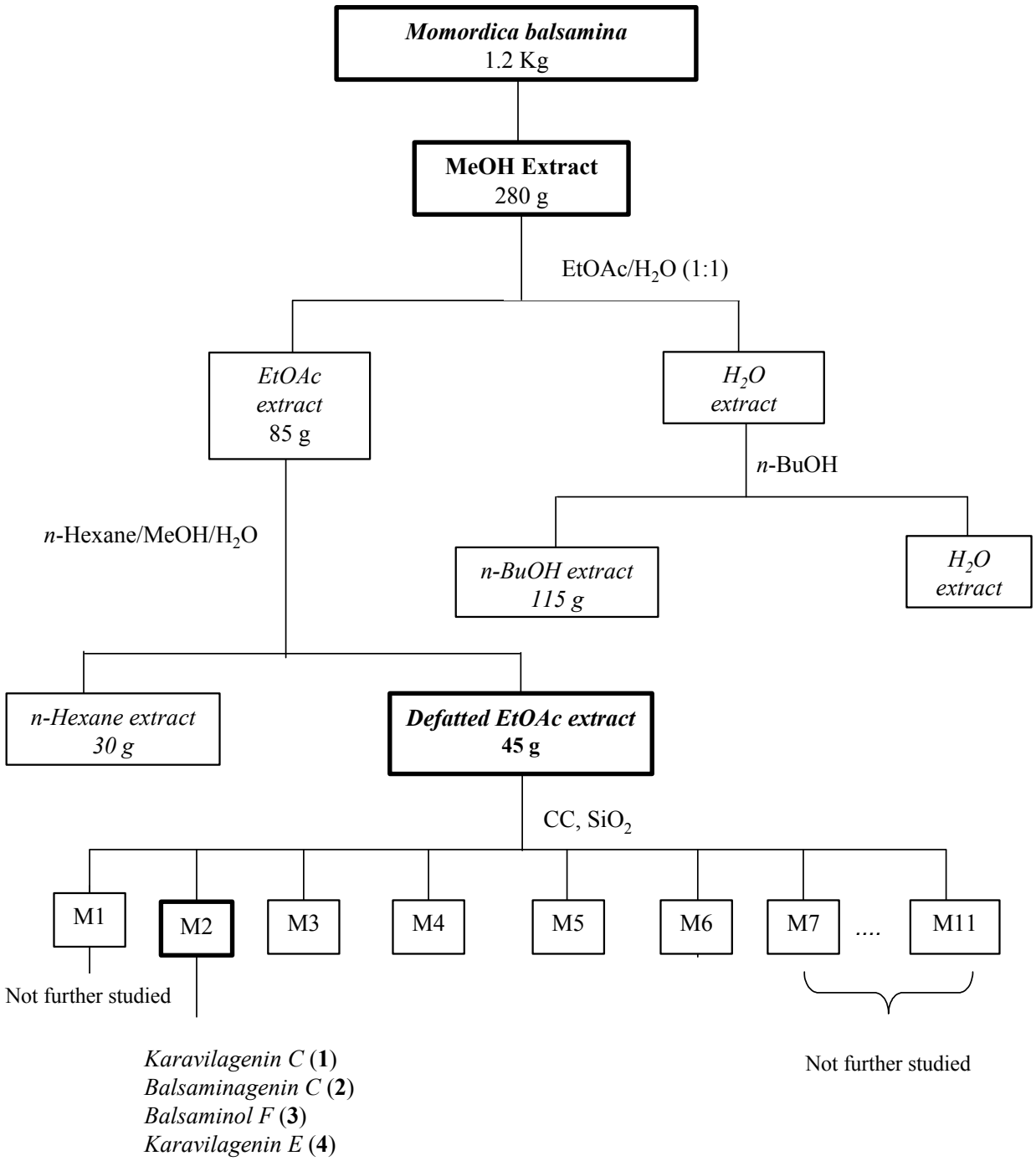

Scheme 3.2. Study of *Momordica balsamina*: extraction, fractionation procedures, and compounds isolated from fraction M2.

Karavilagenin C, 7β-methoxycucurbita-5,24-diene-3β,23(R)-diol (1)

Colourless needle crystals.

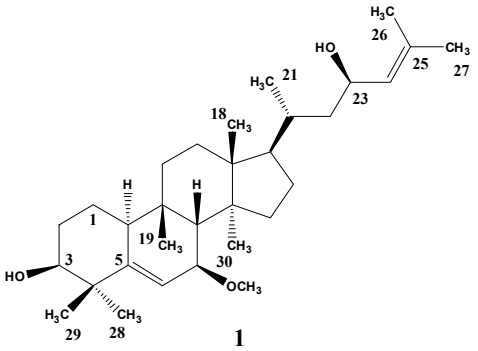

1

m.p. 190 - 191ºC (*n*-hexane/EtOAc).

R_f (SiO_2, *n*-hexane/EtOAc, 1:1): 0.50.

$[\alpha]_D^{26}$ + 128 (*c* 0.10, $CHCl_3$); $[\alpha]_D^{26}$ + 136 (*c* 0.17, MeOH); Lit. $[\alpha]_D^{26}$ + 98.1 (*c* 0.10, MeOH), (Nakamura et al., 2006).

IR, ν_{max} cm^{-1} (KBr): 3460, 2933, 1651, 1460, 1383, 1255, 1070, 981, 929, 829.

ESIMS, *m/z* (rel. int.): 511 $[M + K]^+$ (9), 495 $[M + Na]^+$ (19), 441 (10), 423 $[M + H - H_2O - HOCH_3]^+$ (73).

^{1}H NMR (400 MHz, $CDCl_3$): δ 5.82 (1H, *d*, *J* = 5.1 Hz, H-6), 5.18 (1H, *d*, *J* = 8.4 Hz, H-24), 4.45 (1H, *td*, *J* = 10.0, 2.8 Hz, H-23), 3.50 (1H, *br s*, H-3), 3.41 (1 H, *br d*, *J* = 5.1 Hz, H-7), 3.33 (3H, *s*, 7-OMe), 2.27 (1H, *dd*, *J* = 11.7, 4.0 Hz, H-10), 2.04 (1H, *br s*, H-8), 1.69 (3H, *s*, Me-27), 1.67 (3H, *s*, Me-26), 1.19 (3H, *s*, Me-29), 1.02 (3H, *s*, Me-28), 0.97 (3H, *s*, Me-19), 0.96 (3H, *d*, *J* = 6.7 Hz, Me-21), 0.94 (3H, *s*, Me-18), 0.69 (3H, *s*, Me-30).

^{1}H NMR (400 MHz, CD_3COCD_3): δ 5.76 (1H, *d*, *J* = 4.0 Hz, H-6), 5.15 (1H, *dd*, *J* = 8.0, 1.3 Hz, H-24), 4.41 (1H, *m*, H-23), 3.49 (1H, *br s*, H-3), 3.39 (1H, *br d*, *J* = 4.0 Hz, H-7), 3.27 (3H, *s*, 7-OMe), 2.34 (1H, *br d*, H-10), 2.04 (1H, *br s*, H-8), 1.62 (3H, *s*, Me-26), 1.65 (3H, *s*, Me-27), 1.17 (3H, *s*, Me-29), 1.02 (3H, *s*, Me-28), 0.97 (3H, *d*, *J* = 8.0 Hz, Me-21), 0.95 (6H, *s*, Me-18/Me-19), 0.76 (3H, *s*, Me-30).

^{13}C NMR (101 MHz, $CDCl_3$): δ 146.7 (C-5), 133.8 (C-25), 129.0 (C-24), 121.0 (C-6), 77.2 (C-7), 76.7 (C-3), 65.9 (C-23), 56.3 (7-OMe), 50.8 (C-17), 47.9 (C-8), 47.8 (C-14), 46.2 (C-13), 44.4 (C-22), 41.7 (C-4), 38.7 (C-10), 34.6 (C-15), 34.0 (C-9), 32.7 (C-20), 32.7 (C-11), 30.2 (C-12), 28.8 (C-19), 28.6 (C-2), 27.9 (C-16), 27.8 (C-28), 25.8 (C-27), 25.4 (C-29), 21.1 (C-1), 18.7 (C-21), 18.1 (C-26), 18.0 (C-30), 15.4 (C-18).

^{13}C NMR (101 MHz, CD_3COCD_3): δ 147.9 (C-5), 131.4 (C-25), 131.2 (C-24), 120.0 (C-6), 77.7 (C-7), 76.4 (C-3), 65.5 (C-23), 56.0 (7-OMe), 51.5 (C-17), 49.1 (C-8), 48.6 (C-14), 46.8 (C-13), 45.4 (C-22), 42.0 (C-4), 39.5 (C-10), 35.2 (C-15), 34.6 (C-9), 33.2 (C-11), 33.0 (C-

20), 30.9 (C-12), 29.9 (C-2), 29.1 (C-19), 28.31 (C-16), 28.30 (C-28), 25.7 (C-27), 25.9 (C-29), 21.8 (C-1), 19.0 (C-21), 17.9 (C-26), 18.3 (C-30), 15.6 (C-18).

Balsaminagenin C, cucurbita-5,23(E)-diene-3β,7β,25-triol (2)

White amorphous powder.

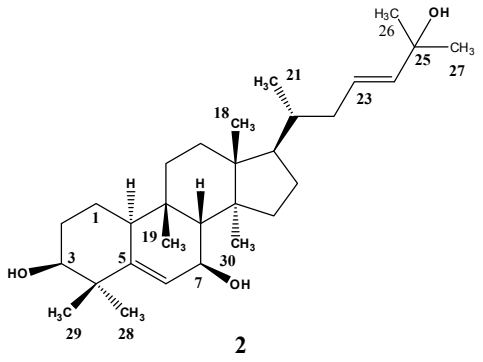

2

***R**f* (SiO_2, $CHCl_3$/Me_2CO, 1:1): 0.4; ***R**t* (HPLC, 210 nm, MeOH/H_2O, 41:9; 1 mL/min): 7 min. $[\alpha]_D^{26}$ + 74 (*c* 0.10, MeOH); Lit. $[\alpha]_D^{25}$ + 13.5 (*c* 0.40, $CHCl_3$), (Chang et al., 2008).

IR, ν_{max} cm^{-1} (KBr): 3416, 2952, 1656, 1459, 1380, 1151, 1081, 1020, 980.

ESIMS, *m/z* (rel. int.): 939 $[2M + Na]^+$ (39), 481 $[M + Na]^+$ (34), 441 $[M + H - H_2O]^+$ (8).

^{1}H NMR (400 MHz, MeOD): δ 5.74 (1H, *d*, *J* = 4.9 Hz, H-6), 5.55 (2H, *m*, H-23/H-24), 3.93 (1H, *br d*, *J* = 5.1 Hz, H-7), 3.50 (1H, *br s*, H-3), 2.33 (1H, *dd*, *J* = 11.2, 4.3 Hz, H-10), 2.15 (1H, *dd*, *J* = 9.6, 7.0 Hz, H-22), 1.97 (1H, *br s*, H-8), 1.25 (6H, *s*, Me-26/Me27), 1.18 (3H, *s*, Me-29), 1.04 (3H, *s*, Me-19), 1.03 (3H, *s*, Me-28), 0.94 (3H, *s*, Me-18), 0.92 (3H, *d*, *J* = 5.8 Hz, Me-21), 0.73 (3H, *s*, Me-30).

^{13}C NMR (101 MHz, MeOD): δ 148.3 (C-5), 140.8 (C-24), 125.9 (C-23), 122.5 (C-6), 77.5 (C-3), 71.2 (C-25), 68.8 (C-7), 54.1 (C-8), 51.2 (C-17), 49.2 (C-14), 47.1 (C-13), 42.3 (C-4), 40.3 (C-22), 40.1 (C-10), 37.7 (C-20), 35.7 (C-15), 35.0 (C-9), 33.9 (C-11), 31.3 (C-12), 30.1 (C-26/C-27), 30.0 (C-2), 29.8 (C-19), 28.8 (C-16), 28.7 (C-28), 26.1 (C-29), 22.4 (C-1), 19.2 (C-21), 18.6 (C-30), 16.0 (C-18).

Balsaminol F, cucurbita-5,24-diene-3β,7β,23(R)-triol (3)

White amorphous powder.

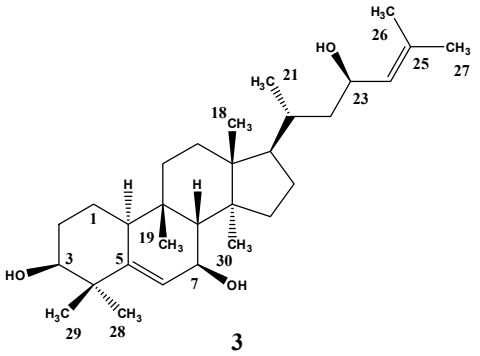

3

***R**f* (SiO_2, $CHCl_3$/Me_2CO, 1:1): 0.4; ***R**t* (HPLC, 210 nm, MeOH/H_2O, 41:9; 1 mL/min): 10 min.
$[\alpha]_D^{26}$ + 122 (*c* 0.12, MeOH).

IR, v_{max} cm^{-1} (KBr): 3396, 2936, 1645, 1459, 1389, 939.

ESIMS, *m/z* (rel. int.): 939 $[2M + Na]^+$ (20), 481 $[M + Na]^+$ (21).

HR-ESITOFMS: *m/z*: 481.3649 (calcd. $C_{30}H_{50}O_3Na$ for: 481.3652).

^{1}H NMR (400 MHz, MeOD): δ 5.74 (1H, *d*, *J* = 5.1 Hz, H-6), 5.16 (1H, *d*, *J* = 8.5 Hz, H-24), 4.41 (1H, *td*, *J* = 9.6, 3.2 Hz, H-23), 3.93 (1H, *br d*, *J* = 5.2 Hz, H-7), 3.50 (1H, *br s*, H-3), 2.32 (1H, *br d*, *J* = 7.0 Hz, H-10), 1.98 (1H, *br s*, H-8), 1.69 (3H, *s*, Me-27), 1.66 (3H, *s*, Me-26), 1.18 (3H, *s*, Me-29), 1.04 (3H, *s*, Me-19), 1.03 (3H, *s*, Me-28), 0.97 (3H, *d*, *J* = 6.4 Hz), 0.96 (3H, *s*, Me-18), 0.74 (3H, *s*, Me-30).

^{13}C NMR (101 MHz, MeOD): δ 148.3 (C-5), 133.4 (C-25), 130.5 (C-24), 122.5 (C-6), 77.5 (C-3), 68.8 (C-7), 66.6 (C-23), 54.1 (C-8), 52.1 (C-17), 49.5 (C-14), 47.2 (C-13), 45.6 (C-22), 42.3 (C-4), 40.1 (C-10), 35.7 (C-15), 35.0 (C-9), 33.9 (C-11), 33.8 (C-20), 31.5 (C-12), 30.1 (C-2), 29.8 (C-19), 28.9 (C-16), 28.8 (C-28), 26.1 (C-29), 26.0 (C-27), 22.4 (C-1), 19.3 (C-21), 18.7 (C-30), 18.1 (C-26), 15.9 (C-18).

Karavilagenin E, 5β,19β-epoxycucurbita-6,24-diene-3β,23(R)-diol (4)

White amorphous powder.

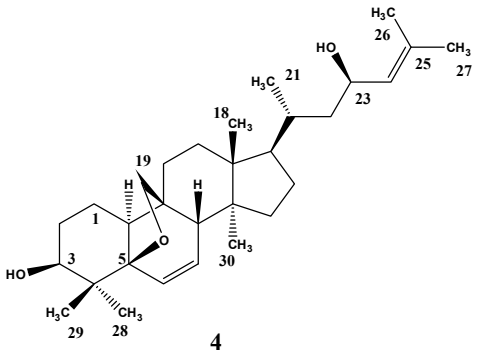

4

***R**f* (SiO_2, $CHCl_3$/MeOH, 1:19): 0.20; ***R**t* (HPLC, 210 nm, ACN/H_2O, 9:1; 1 mL/min): 7 min.

$[\alpha]_D^{26}$ – 53 (*c* 0.12, MeOH); $[\alpha]_D^{26}$ Lit. – 41 (*c* 0.10, MeOH), (Matsuda et al., 2007).

IR, ν_{max} cm^{-1} (KBr): 3447, 2952, 1656, 1459, 1380, 1151, 1081, 1020, 980.

ESIMS, *m/z* (rel. int.): 935 $[2M + Na]^+$ (45), 479 $[M + Na]^+$ (5), 394 (100).

^{1}H NMR (400 MHz, MeOD): δ 6.05 (1H, *d*, *J* = 9.8 Hz, H-6), 5.64 (1H, *dd*, *J* = 9.8, 3.4 Hz, H-7), 5.15 (1H, *d*, *J* = 8.5 Hz, H-24), 4.41 (1H, *td*, *J* = 9.6, 3.2 Hz, H-23), 3.66 (1H, *d*, *J* = 8.4 Hz, H-19a), 3.50 (1H, *d*, *J* = 8.4 Hz, H-19b), 3.36 (1H, *br s*, H-3), 2.38 (1H, *br s*, H-8), 2.34 (1H, *m*, H-10), 1.69 (3H, *s*, Me-27), 1.65 (3H, *s*, Me-26), 1.14 (3H, *s*, Me-28), 0.96 (3H, *d*, *J* = 6.2 Hz, Me-21), 0.93 (3H, *s*, Me-18), 0.91 (3H, *s*, Me-29), 0.90 (3H, s, Me-30).

^{13}C NMR (101 MHz, MeOD): δ 133.5 (C-25), 132.8 (C-6), 132.6 (C-7), 130.4 (C-24), 88.8 (C-5), 80.8 (C-19), 77.7 (C-3), 66.6 (C-23), 53.4 (C-8), 52.2 (C-17), 49.5 (C-14), 46.6 (C-9/C-13), 45.6 (C-22), 40.2 (C-10), 38.3 (C-4), 34.2 (C-15), 33.7 (C-20), 32.2 (C-12), 29.2 (C-2), 28.3 (C-16), 26.0 (C-27), 24.9 (C-29), 24.7 (C-11), 20.9 (C-28), 20.6 (C-30), 19.2 (C-21), 18.6 (C-1), 18.1 (C-26), 15.4 (C-18).

3.2.1. Derivatization of karavilagenin C

Karavilagenin C (**1**) was derivatized with several acylating reagents as described in the following pages, and presented in Schemes 3.3 and 3.4.

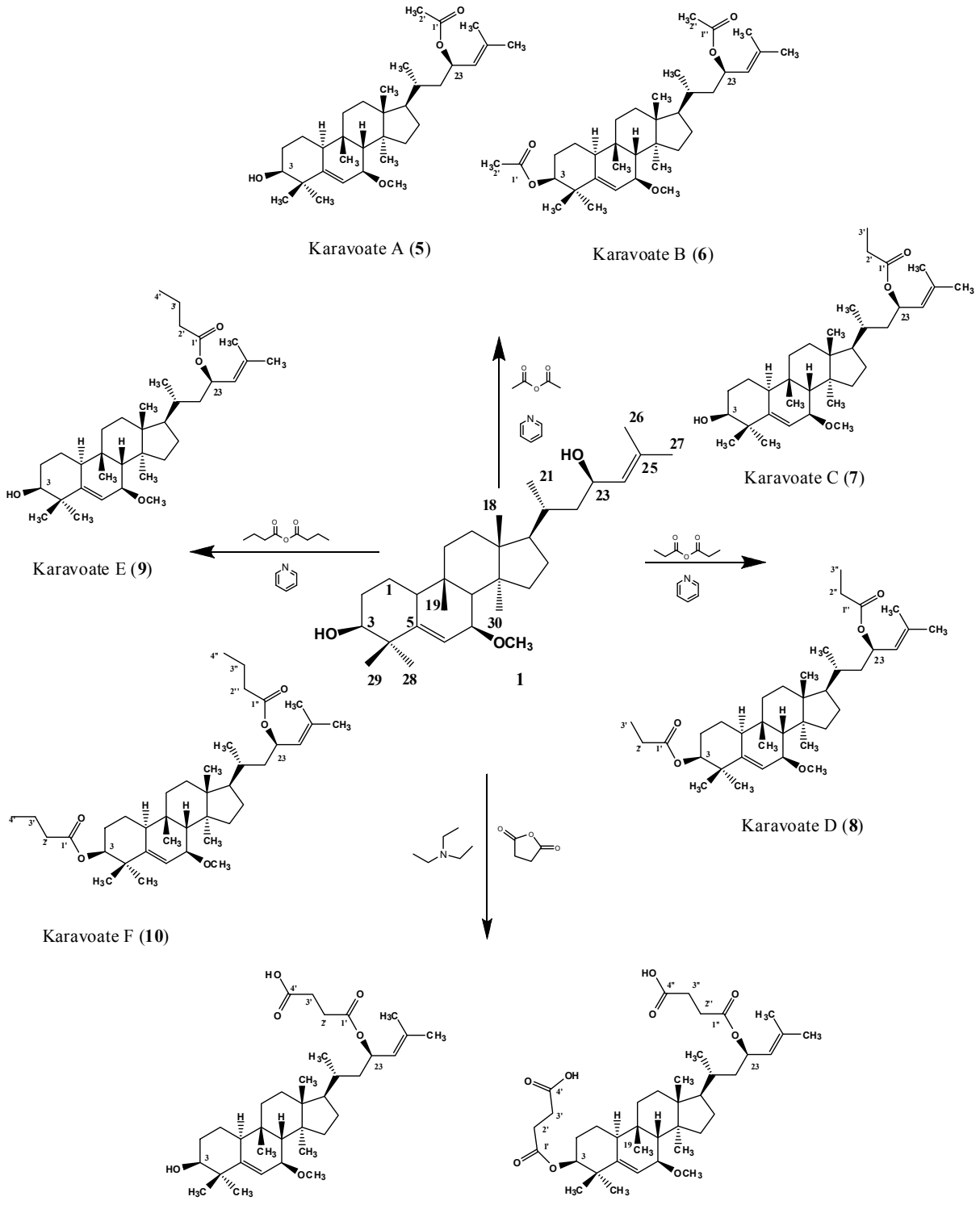

Scheme 3.3. Acylation of karavilagenin C (**1**) with alkanoyl anhydrides.

3.2.1.1. Acetylation with acetic anhydride.

Compound **1** (42.5 mg) was treated with acetic anhydride (1 mL) and pyridine (1 mL), and the mixture was stirred at room temperature for 1 hour. The excess of pyridine and acetic anhydride was removed with N_2. The residue was purified by column chromatography, using mixtures of *n*-hexane/EtOAc (1:0 to 4:1) as eluents, to give 11 mg of compound **5** [karavoate A, 23(*R*)-acetoxy-7β-methoxycucurbita-5,24-dien-3β-ol] and 32 mg of compound **6** [karavoate B, 3β,23(*R*)-diacetoxy-7β-methoxycucurbita-5,24-diene].

Karavoate A, 23(R)-acetoxy-7β-methoxycucurbita-5,24-dien-3β-ol (5)

Colourless oil.

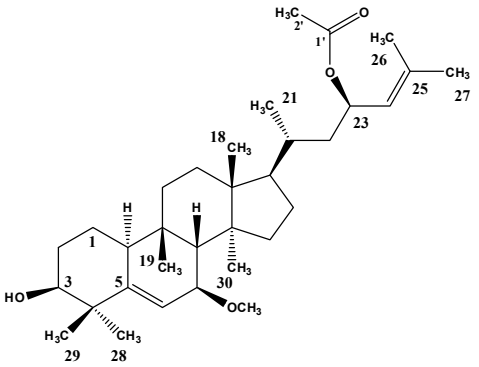

5

***R**f* (SiO_2, *n*-hexane/EtOAc, 3:2): 0.50.

IR, ν_{max} cm^{-1} (KBr): 3460, 2943, 1735, 1457, 1380, 1245, 1182, 1023, 937.

ESIMS, *m/z* (rel. int.): 537 $[M + Na]^+$ (18), 477 $[M + Na - CH_3COOH]^+$ (5).

^{1}H NMR (400 MHz, $CDCl_3$): δ 5.85 (1H, *d*, *J* = 4.9 Hz, H-6), 5.60 (1H, *td*, *J* = 9.8, 2.7 Hz, H-23), 5.11 (1H, *d*, *J* = 8.7 Hz, H-24), 3.53 (1H, *br s*, H-3), 3.44 (1H, *br d*, *J* = 4.8 Hz, H-7), 3.36 (3H, *s*, 7-OMe), 2.29 (1H, *br d*, *J* = 10.5 Hz, H-10), 2.06 (1H, *br s*, H-8), 2.04 (3H, *s*, Me-2'), 1.74 (3H, *s*, Me-27), 1.71 (3H, *s*, Me-26), 1.22 (3H, *s*, Me-29), 1.05 (3H, *s*, Me-28), 1.00 (3H, *s*, Me-19), 0.96 (3H, *d*, *J* = 5.5 Hz, Me-21), 0.93 (3H, *s*, Me-18), 0.71 (3H, *s*, Me-30).

^{13}C NMR (101 MHz, $CDCl_3$): δ 170.7 (C-1'), 146.8 (C-5), 135.7 (C-25), 124.7 (C-24), 120.9 (C-6), 77.2 (C-7), 76.8 (C-3), 69.5 (C-23), 56.3 (7-OMe), 50.5 (C-17), 47.9 (C-8/C-14), 46.2 (C-13), 42.0 (C-22), 41.8 (C-4), 38.7 (C-10), 34.6 (C-15), 34.0 (C-9), 32.8 (C-20), 32.6 (C-11), 30.1 (C-12), 28.8 (C-19), 28.6 (C-2), 27.9 (C-28), 27.8 (C-16), 25.7 (C-27), 25.4 (C-29), 21.4 (C-2'), 21.1 (C-1), 19.0 (C-21), 18.4 (C-26), 18.0 (C-30), 15.3 (C-18).

Karavoate B, 3β,23(R)-diacetoxy-7β-methoxycucurbita-5,24-diene (6)

Colourless oil.

R_f (SiO_2, *n*-hexane/EtOAc, 3:2): 0.90.

IR, v_{max} cm^{-1} (KBr): 1733, 1455, 1377, 1244, 1085, 1024, 938.

ESIMS, *m/z* (rel. int.): 579 $[M + Na]^+$ (31), 519 $[M + Na - CH_3COOH]^+$ (4).

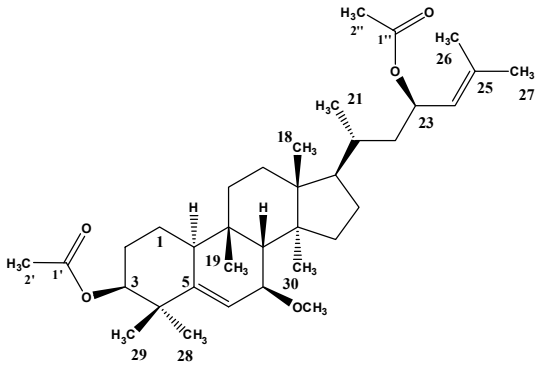

6

^{1}H NMR (400 MHz, $CDCl_3$): δ 5.77 (1H, *d*, *J* = 4.9 Hz, H-6), 5.60 (1H, *td*, *J* = 9.8, 2.7 Hz, H-23), 5.09 (1H, *d*, *J* = 8.8 Hz, H-24), 4.74 (1H, *br s*, H-3), 3.42 (1H, *br d*, *J* = 5.0 Hz, H-7), 3.35 (3H, *s*, 7-OMe), 2.27 (1H, *br d*, *J* = 10.7 Hz, H-10), 2.04 (1H, *br s*, H-8), 2.01 (3H, *s*, Me-2''), 1.99 (3H, *s*, Me-2'), 1.72 (3H, *s*, Me-27), 1.69 (3H, *s*, Me-26), 1.10 (3H, *s*, Me-29), 1.06 (3H, *s*, Me-28), 0.97 (3H, *s*, Me-19), 0.94 (3H, *d*, *J* = 5.5 Hz, Me-21), 0.91 (3H, *s*, Me-18), 0.70 (3H, *s*, Me-30).

^{13}C NMR (101 MHz, $CDCl_3$): δ 170.9 (C-1''), 170.6 (C-1'), 146.8 (C-5), 135.7 (C-25), 124.7 (C-24), 119.2 (C-6), 78.6 (C-3), 77.3 (C-7), 69.4 (C-23), 56.3 (7-OMe), 50.5 (C-17), 47.9 (C-14), 47.7 (C-8), 46.1 (C-13), 41.9 (C-22), 39.9 (C-4), 38.7 (C-10), 34.6 (C-15), 34.0 (C-9), 32.8 (C-20), 32.4 (C-11), 30.1 (C-12), 28.5 (C-19), 28.0 (C-28), 27.8 (C-16), 26.4 (C-2), 25.7 (C-27), 24.8 (C-29), 21.7 (C-1), 21.4 (C-2''), 21.3 (C-2'), 18.9 (C-21), 18.3 (C-26), 17.9 (C-30), 15.3 (C-18).

3.2.1.2. Acylation with propionic anhydride

To compound **1** (56 mg) pyridine (1 mL) and propionic anhydride (1 mL) were added, and the mixture was stirred at room temperature for 8 hours. The reaction mixture was poured into ice-water and extracted with CH_2Cl_2. The combined organic layers were washed sequentially with a solution of HCl (1%), and a solution of Na_2CO_3 (4%). The product obtained was purified by preparative TLC ($CHCl_3$/MeOH; 19:1) to afford 28 mg of

compound **7** [karavoate C, 23(*R*)-propanoyloxy-7β-methoxycucurbita-5,24-dien-3β-ol] and 11 mg of compound **8** [karavoate D, 3β,23(*R*)-dipropanoyloxy-7β-methoxycucurbita-5,24-diene].

Karavoate C, 23(R)-propanoyloxy-7β-methoxycucurbita-5,24-dien-3β-ol (7)

Colourless oil.

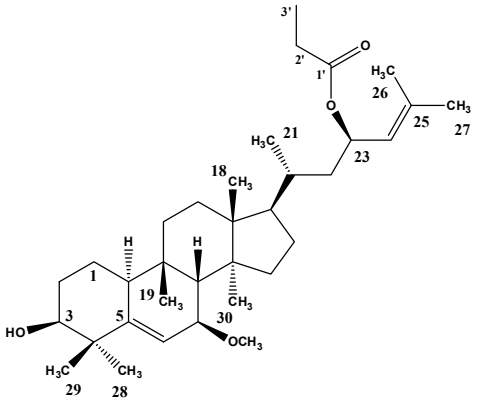

7

***R**f* (SiO_2, $CHCl_3$/MeOH, 19:1): 0.34.

IR, v_{max} cm^{-1} (KBr): 3462, 1728, 1656, 1458, 1380, 1081, 980, 929.

ESIMS, *m/z* (rel. int.): 552 $[M + H + Na]^+$ (79), 478 $[M + H + Na - CH_3CH_2COOH]^+$ (100).

^{1}H NMR (400 MHz, $CDCl_3$): δ 5.85 (1H, *d*, *J* = 5.1 Hz, H-6), 5.63 (1H, *td*, *J* = 9.9, 2.9 Hz, H-23), 5.10 (1H, *d*, *J* = 8.2 Hz, H-24), 3.53 (1H, *br s*, H-3), 3.44 (1H, *br d*, *J* = 5.3 Hz, H-7), 3.36 (3H, *s*, 7-OMe), 2.25 - 2.36 (3H, *m*, H-10/H-2'), 2.06 (1H, *br s*, H-8), 1.75 (3H, *s*, Me-27), 1.71 (3H, *s*, Me-26), 1.22 (3H, *s*, Me-29), 1.15 (3H, *t*, *J* = 7.5 Hz, Me-3'), 1.05 (3H, *s*, Me-28), 1.00 (3H, *s*, Me-19), 0.96 (3H, *d*, *J* = 5.2 Hz, Me-21), 0.92 (3H, *s*, Me-18), 0.71 (3H, *s*, Me-30).

^{13}C NMR (101 MHz, $CDCl_3$): δ 174.0 (C-1'), 146.8 (C-5), 135.6 (C-25), 124.7 (C-24), 120.9 (C-6), 77.2 (C-7), 76.8 (C-3), 69.3 (C-23), 56.3 (7-OMe), 50.5 (C-17), 47.9 (C-8/C-14), 46.2 (C-13), 42.0 (C-22), 41.7 (C-4), 38.7 (C-10), 34.6 (C-15), 34.0 (C-9), 32.8 (C-20), 32.6 (C-11), 30.1 (C-12), 28.8 (C-19), 28.6 (C-2), 28.0 (C-2'), 27.8 (C-28/C-16), 25.7 (C-27), 25.4 (C-24), 21.1 (C-1), 19.0 (C-21), 18.3 (C-26), 18.0 (C-30), 15.3 (C-18), 9.3 (C-3').

Karavoate D, 3β,23(R)-dipropanoyloxy-7β-methoxycucurbita-5,24-diene (8)

Colourless oil.

R_f (SiO_2, $CHCl_3$/MeOH, 19:1): 0.66.

IR, v_{max} cm^{-1} (KBr): 1730, 1450, 1378, 1084, 982, 930.

ESIMS, *m/z* (rel. int.): 608 $[M + H + Na]^+$ (11), 534 $[M+ H + Na – CH_2CH_3COOH]^+$ (15).

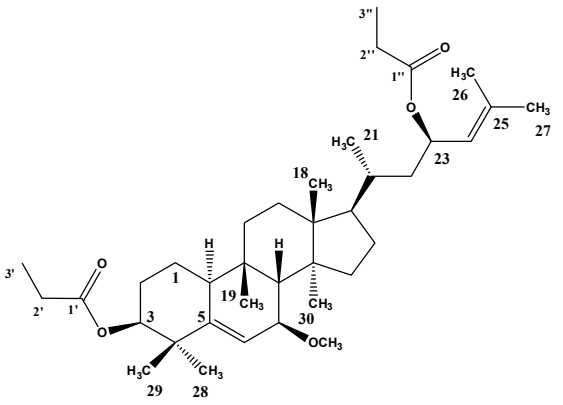

8

^{1}H NMR (400 MHz, $CDCl_3$): δ 5.79 (1H, *d*, *J* = 4.4 Hz, H-6), 5.63 (1H, *td*, *J* = 9.9, 2.9 Hz, H-23), 5.11 (1H, *d*, *J* = 8.8 Hz, H-24), 4.77 (1H, *br s*, H-3), 3.45 (1H, *br d*, *J* = 4.4 Hz, H-7), 3.37 (3H, *s*, 7-OMe), 2.25 - 2.36 (5H, *m*, H-10, H-2'/H-2''), 2.06 (1H, *br s*, H-8), 1.76 (3H, *s*, Me-27), 1.71 (3H, *s*, Me-26), 1.10 (3H, *s*, Me-29), 1.15 (3H, *t*, *J* = 7.2 Hz, Me-3''), 1.12 (3H, *t*, *J* = 7.2 Hz, Me-3'), 1.08 (3H, *s*, Me-28), 0.99 (3H, *s*, Me-19), 0.96 (3H, *d*, *J* = 5.6 Hz, Me-21), 0.93 (3H, *s*, Me-18), 0.73 (3H, *s*, Me-30).

^{13}C NMR (101 MHz, $CDCl_3$): δ 174.2 (C-1'), 174.0 (C-1''), 146.9 (C-5), 135.6 (C-25), 124.7 (C-24), 119.2 (C-6), 78.4 (C-3), 77.3 (C-7), 69.3 (C-23), 56.3 (7-OMe), 50.5 (C-17), 48.0 (C-8/C-14), 46.2 (C-13), 42.0 (C-22), 40.0 (C-4), 38.6 (C-10), 34.6 (C-15), 34.0 (C-9), 32.8 (C-20), 32.4 (C-11), 30.1 (C-12), 28.5 (C-19), 28.0 (C-2'/C-2''/Me-28), 27.8 (C-16), 26.4 (C-2), 25.7 (C-27), 24.9 (C-29), 21.6 (C-1), 19.0 (C-21), 18.3 (C-26), 17.9 (C-30), 15.3 (C-18), 9.4 (C-3'), 9.3 (C-3'').

3.2.1.3. Acylation with butyric anhydride

Compound **1** (30 mg) was suspended in butyric anhydride (0.5 mL) and pyridine (0.5 mL). After stirring at room temperature for 72 hours, the excess of pyridine was eliminated with N_2 and the residue was purified by column chromatography, using mixtures of *n*-hexane/EtOAc (13:7 to 1:1) as eluents, followed by preparative TLC (*n*-hexane/EtOAc, 3:2), to afford 15 mg of compound **9** [karavoate E, 23(*R*)-butanoyloxy-7β-methoxycucurbita-5,24-dien-3β-ol]. To obtain the diacylated derivative, 31 mg of compound **1** were suspended in

butyric anhydride (0.5 mL) and pyridine (0.5 mL), and the reaction mixture was stirred for 72 hours at 80ºC. The mixture was diluted with ethyl acetate, washed successively with Na_2CO_3 (5%) and HCl (1%) solutions, dried over Na_2SO_3, and filtered. The crude product was purified twice by preparative TLC, using *n*-hexane/EtOAc (13:7) and *n*-hexane/EtOAc (9:1), as eluents, to afford 26 mg of compound **10** [karavoate F, 3β,23(*R*)-dibutanoyloxy-7β-methoxycucurbita-5,24-diene].

Karavoate E, 23(R)-butanoyloxy-7β-methoxycucurbita-5,24-dien-3β-ol (9)

Colourless oil.

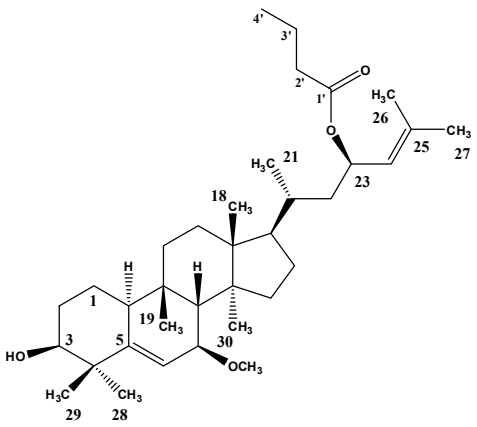

9

***R**f* (SiO_2, *n*-hexane/EtOAc, 7:3): 0.25.

IR, ν_{max} cm^{-1} (KBr): 3488, 1730, 1454, 1378, 1243, 1080, 980, 929.

ESIMS, *m/z* (rel. int.): 581 $[M + K]^+$ (11), 565 $[M + Na]^+$ (19), 477 $[M + Na - CH_3CH_2CH_2COOH]^+$ (9).

^{1}H NMR (400 MHz, CD_3COCD_3): δ 5.77 (1H, *d*, *J* = 4.5 Hz, H-6), 5.67 (1H, *td*, *J* = 10.4, 2.9 Hz, H-23), 5.13 (1H, *d*, *J* = 8.9 Hz, H-24), 3.50 (1H, *br s*, H-3), 3.40 (1H, *br d*, *J* = 4.4 Hz, H-7), 3.31 (3H, *s*, 7-OMe), 2.35 (1H, *br d*, *J* = 10.3 Hz, H-10), 2.24 (2H, *td*, *J* = 7.3, 3.7 Hz, H-2'), 2.04 (1H, *br s*, H-8), 1.72 (3H, *s*, Me-26), 1.69 (3H, *s*, Me-27), 1.62 (2H, *m*, H-3'), 1.19 (3H, *s*, Me-29), 1.03 (3H, *s*, Me-28), 0.98 (3H, *d*, *J* = 5.8 Hz, Me-21), 0.96 (3H, *s*, Me-19), 0.94 (3H, *s*, Me-18), 0.92 (3H, *t*, *J* = 7.4 Hz, Me-4'), 0.77 (3H, *s*, H-30).

^{13}C NMR (101 MHz, CD_3COCD_3): δ 173.0 (C-1'), 148.1 (C-5), 135.7 (C-25), 126.0 (C-24), 120.2 (C-6), 77.9 (C-7), 76.4 (C-3), 69.1 (C-23), 56.2 (7-OMe), 51.3 (C-17), 49.3 (C-8), 48.8 (C-14), 46.9 (C-13), 42.8 (C-22), 42.1 (C-4), 36.9 (C-2'), 39.7 (C-10), 35.4 (C-15), 34.8 (C-9), 33.6 (C-11), 33.4 (C-20), 31.0 (C-12), 30.0 (C-2), 29.3 (C-19), 28.6 (C-16), 28.5 (C-28), 26.1 (C-27), 25.7 (C-29), 21.9 (C-1), 19.3 (C-21/C-3'), 18.5 (C-26), 18.4 (C-30), 15.7 (C-18), 13.9 (C-4').

Karavoate F, 3β,23(R)-dibutanoyloxy-7β-methoxycucurbita-5,24-diene (10)

Colourless oil.

R_f (SiO_2, *n*-hexane/EtOAc, 7:3): 0.58.

IR, v_{max} cm^{-1} (KBr): 1730, 1450, 1380, 1243, 1087, 982, 930.

ESIMS, *m/z* (rel. int.): 635 $[M + Na]^+$ (62), 547 $[M + Na - CH_3CH_2CH_2COOH]^+$ (50), 517 (33), 454 (100).

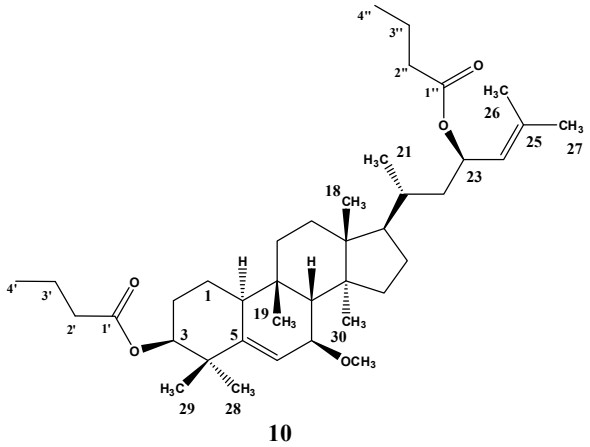

10

^{1}H NMR (400 MHz, CD_3COCD_3): δ 5.79 (1H, *d*, *J* = 5.0 Hz, H-6), 5.67 (1H, *td*, *J* = 10.5, 3.0 Hz, H-23), 5.13 (1H, *d*, *J* = 8.9 Hz, H-24), 4.72 (1H, *br s*, H-3), 3.43 (1H, *br d*, *J* = 5.1 Hz, H-7), 3.30 (3H, *s*, 7-OMe), 2.42 (1H, *br d*, *J* = 10.6 Hz, H-10), 2.26 (2H, *t*, *J* = 7.3 Hz, H-2'), 2.24 (2H, *t*, *J* = 7.3 Hz, H-2''), 2.04 (1H, *br s*, H-8), 1.72 (3H, *s*, Me-26), 1.69 (3H, *s*, Me-27), 1.62 (4H, *m*, H-3'/H-3''), 1.12 (3H, *s*, Me-28), 1.11 (3H, *s*, Me-29), 0.98 (3H, *d*, *J* = 5.3 Hz, Me-21), 0.98 (3H, *s*, Me-19), 0.95 (3H, *s*, Me-18), 0.94 (3H, *t*, *J* = 7.3 Hz, Me-4'), 0.92 (3H, *t*, *J* = 7.4 Hz, Me-4''), 0.78 (3H, *s*, Me-30).

^{13}C NMR (101 MHz, CD_3COCD_3): δ 173.0 (C-1''), 172.9 (C-1'), 147.0 (C-5), 135.7 (C-25), 126.0 (C-24), 120.4 (C-6), 78.9 (C-3), 77.7 (C-7), 69.1 (C-23), 56.3 (7-OMe), 51.3 (C-17), 49.3 (C-8), 48.8 (C-14), 46.9 (C-13), 42.8 (C-22), 40.7 (C-4), 39.3 (C-10), 36.9 (C-2'/C-2''), 35.3 (C-15), 34.8 (C-9), 33.6 (C-11), 33.2 (C-20), 30.9 (C-12), 29.3 (C-19), 28.6 (C-16), 28.3 (C-28), 27.0 (C-2), 25.7 (C-27), 25.4 (C-29), 22.4 (C-1), 19.3 (C-3'/C-3''), 19.2 (C-21), 18.4 (C-26/C-30), 15.7 (C-18), 13.9 (C-4'/C-4'').

3.2.1.4. Acylation with benzoyl chloride

To compound **1** (51.3 mg), pyridine (1 mL) and benzoyl chloride (0.5 mL) were added, and the mixture was stirred at room temperature for 1 hour. The reaction mixture was treated as above. The residue obtained was purified, sequentially by column chromatography (*n*-hexane/CH_2Cl_2, 2:3 to *n*-hexane/CH_2Cl_2, 0:1), and preparative TLC (*n*-hexane/CH_2Cl_2,

1:9), to afford 27 mg of compound **11** [karavoate G, 3β-benzoyloxy-7β-methoxycucurbita-5,23(*E*)-dien-25-ol] and 15 mg of compound **12** [karavoate H, 3β,23(*R*)-dibenzoyloxy-7β-methoxycucurbita-5,24-diene].

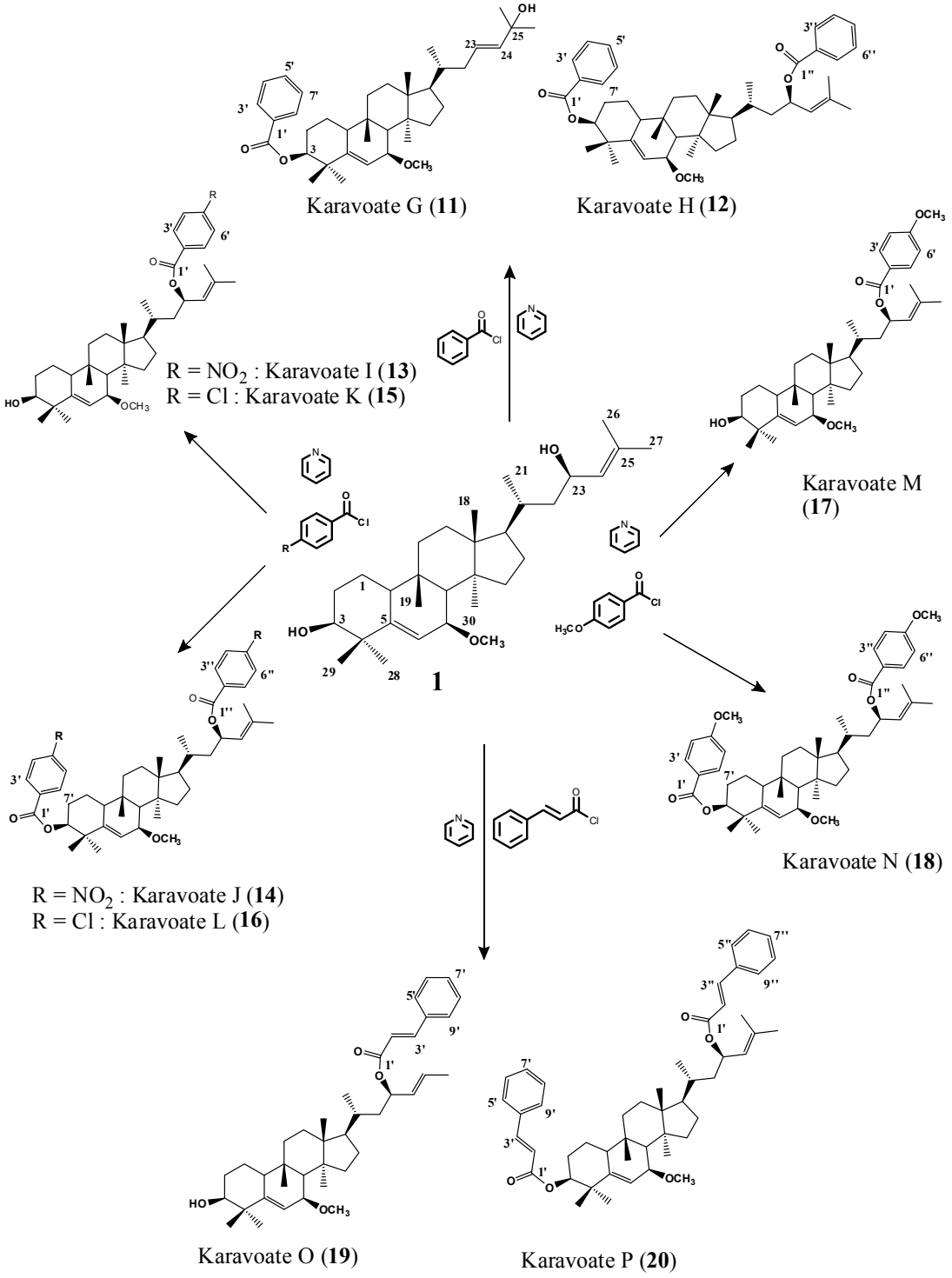

Scheme 3.4. Acylation of karavilagenin C (**1**) with different benzoyl chlorides.

Karavoate G, 3β-benzoyloxy-7β-methoxycucurbita-5,23(E)-dien-25-ol (11)

Colourless oil.

R_f (SiO_2, *n*-hexane/EtOAc, 3:1): 0.56.

$[\alpha]_D^{20}$ + 105 (*c* 0.11, MeOH).

IR, ν_{max} cm^{-1} (KBr): 3416, 1712, 1454, 1380, 1274, 1112, 1083, 1026, 973, 935, 712.

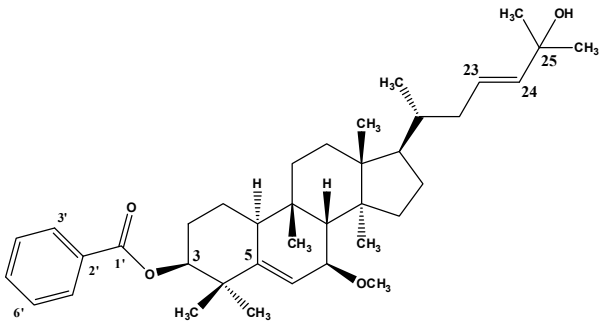

11

ESIMS, *m/z* (rel. int.): 599 $[M + Na]^+$ (96), 545 (53), 405 $[M + H - H_2O - CH_3OH - C_6H_5COOH]^+$ (7.4), 209 (41), 181 (52).

^{1}H NMR (400 MHz, $CDCl_3$): δ 8.02 (2H, *d*, *J* = 7.1 Hz, H-3'/H-7'), 7.55 (1H, *t*, *J* = 7.4 Hz, H-5'), 7.44 (2H, *t*, *J* = 7.6 Hz, H-4'/H-6'), 5.89 (1H, *d*, *J* = 4.7 Hz, H-6), 5.62 (2H, *m*, H-23/H-24), 5.03 (1H, *br s*, H-3), 3.50 (1H, *br d*, *J* = 4.4 Hz, H-7), 3.41 (3H, *s*, 7-OMe), 2.40 (1H, *dd*, *J* = 11.2, 4.4 Hz, H-10), 2.09 (1H, *br s*, H-8), 1.34 (3H, *s*, Me-26), 1.27 (3H, *s*, Me-27), 1.21 (3H, *s*, Me-29), 1.16 (3H, *s*, Me-28), 1.06 (3H, *s*, Me-19), 0.97 (3H, *s*, Me-18), 0.92 (3H, *d*, *J* = 5.9 Hz, Me-21), 0.77 (3H, *s*, Me-30).

^{13}C NMR (101 MHz, $CDCl_3$): δ 166.0 (C-1'), 146.8 (C-5), 139.5 (C-24), 132.8 (C-5'), 130.6 (C-2'), 129.6 (C-3'/C-7'), 128.4 (C-4'/C-6'), 125.4 (C-23), 119.5 (C-6), 79.3 (C-3), 77.3 (C-7), 70.8 (C-25), 56.3 (7-OMe), 50.0 (C-17), 48.3 (C-8), 48.0 (C-14), 46.1 (C-13), 40.3 (C-4), 39.1 (C-22), 38.6 (C-10), 36.3 (C-20), 34.7 (C-15), 34.2 (C-9), 32.2 (C-11), 30.1 (C-12), 30.0 (C-26), 29.9 (C-27), 28.5 (C-19), 28.1 (C-28), 27.6 (C-16), 26.5 (C-2), 25.2 (C-29), 21.7 (C-1), 18.7 (C-21), 18.0 (C-30), 15.5 (C-18).

Karavoate H, 3β,23(R)-dibenzoyloxy-7β-methoxycucurbita-5,24-diene (12)

Colourless oil.

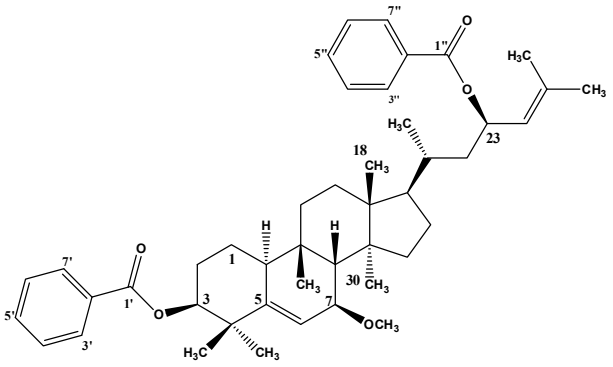

12

***R**f* (SiO_2, *n*-hexane/EtOAc, 3:1): 0.72.

IR, v_{max} cm^{-1} (KBr): 1716, 1520, 1455, 1270, 934, 712, 736.

ESIMS, *m/z* (rel. int.): 681 $[M + H]^+$ (18), 703 $[M + Na]^+$ (19), 581 $[M + Na - C_6H_5COOH]^+$ (28).

^{1}H NMR (400 MHz, $CDCl_3$): δ 8.04 (2H, *d*, *J* = 7.1 Hz, H-3''/H-7''), 8.02 (2H, *d*, *J* = 7.1 Hz, H-3'/H-7'), 7.56 (2H, *m*, H-5'/H-5''), 7.45 (4H, *m*, H-4'/H-4''/H-6'/H-6''), 5.89 (1H, *d*, *J* = 4.7 Hz, H-6), 5.87 (1H, *td*, *J* = 9.2, 2.8 Hz, H-23), 5.24 (1H, *d*, *J* = 8.9 Hz, H-24), 5.03 (1H, *br s*, H-3), 3.49 (1H, *br d*, *J* = 4.3 Hz, H-7), 3.40 (3H, *s*, 7-OMe), 2.40 (1H, *dd*, *J* = 11.2, 4.4 Hz, H-10), 2.08 (1H, *br s*, H-8), 1.84 (3H, *s*, Me-26), 1.74 (3H, *s*, Me-27), 1.22 (3H, *s*, Me-29), 1.17 (3H, *s*, Me-28), 1.04 (3H, *s*, Me-19), 1.03 (3H, *d*, *J* = 6.3 Hz, Me-21), 0.92 (3H, *s*, Me-18), 0.78 (3H, *s*, Me-30).

^{13}C NMR (101 MHz, $CDCl_3$): δ 166.1 (C-1''), 166.0 (C-1'), 146.8 (C-5), 135.9 (C-25), 132.8 (C-5'), 132.7 (C-5''), 130.9 (C-2''), 130.6 (C-2'), 129.7 (C-3'/C-7'), 129.5 (C-3''/C-7''), 128.4 (C-4'/C-6'), 128.3 (C-4''/C-6''), 124.6 (C-24), 119.5 (C-6), 79.3 (C-3), 77.4 (C-7), 70.3 (C-23), 56.3 (7-OMe), 50.5 (C-17), 48.2 (C-8), 48.0 (C-14), 46.2 (C-13), 42.1 (C-22), 40.3 (C-4), 38.6 (C-10), 34.7 (C-15), 34.1 (C-9), 33.0 (C-20), 32.2 (C-11), 30.1 (C-12), 28.5 (C-19), 28.1 (C-28), 28.0 (C-16), 26.5 (C-2), 25.8 (C-27), 25.2 (C-29), 21.7 (C-1), 19.1 (C-21), 18.4 (C-26), 18.0 (C-30), 15.4 (C-18).

3.3.1.5. Acylation with p-nitrobenzoyl chloride

To compound **1** (43.5 mg), pyridine (1 mL) and *p*-nitrobenzoyl chloride (150 mg) in excess were added, and the mixture was stirred at room temperature for 24 hours. The excess of pyridine was removed with N_2 and the residue was purified by column chromatography (*n*-

hexane/EtOAc, 0:1 to 1:1) and preparative TLC (*n*-hexane/EtOAc, 3:2) to afford 45 mg of compound **13** [karavoate I, 23(*R*)-(*p*-nitrobenzoyloxy)-7β-methoxycucurbita-5,24-dien-3β-ol] and 10 mg of compound **14** [karavoate J, 3β,23(*R*)-di-(*p*-nitrobenzoyloxy)-7β-methoxycucurbita-5,24-diene].

Karavoate I, 23(R)-(p-nitrobenzoyloxy)-7β-methoxycucurbita-5,24-dien-3β-ol (13)

Colourless oil.

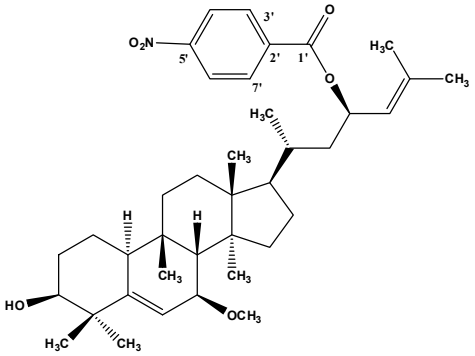

13

***R**f* (SiO_2, *n*-hexane/EtOAc, 1:1): 0.47.

IR, ν_{max} cm^{-1} (KBr): 3447, 1716, 1606, 1529, 1457, 1273, 1085, 850, 758.

ESIMS, *m/z* (rel. int.): 644 $[M + Na]^+$ (68), 509 (100), 495 (25), 477 $[M + Na - C_7H_5O_4N]^+$ (21), 423 (45), 316 (29), 288 (83), 249 (22), 241 (13).

^{1}H NMR (400 MHz, CD_3COCD_3): δ 8.34 (2H, *d*, *J* = 7.8 Hz, H-4'/H-6'), 8.25 (2H, *d*, *J* = 7.9 Hz, H-3'/H-7'), 5.91 (1H, *td*, *J* = 8.8, 2.0 Hz, H-23), 5.73 (1H, *d*, *J* = 5.0 Hz, H-6), 5.27 (1H, *d*, *J* = 8.9 Hz, H-24), 3.46 (1H, *br s*, H-3), 3.36 (1H, *br d*, *J* = 5.2 Hz, H-7), 3.23 (3H, *s*, 7-OMe), 2.30 (1H, *br d*, *J* = 10.5 Hz, H-10), 1.98 (1H, *br s*, H-8), 1.79 (3H, *s*, Me-26), 1.70 (3H, *s*, Me-27), 1.15 (3H, *s*, Me-29), 1.02 (3H, *d*, *J* = 6.3 Hz, Me-21), 1.00 (3H, *s*, Me-28), 0.91 (3H, *s*, Me-19), 0.86 (3H, *s*, Me-18), 0.75 (3H, *s*, Me-30).

^{13}C NMR (101 MHz, CD_3COCD_3): δ 164.6 (C-1'), 151.5 (C-5'), 148.0 (C-5), 137.1 (C-2'), 137.0 (C-25), 131.4 (C-3'/C-7'), 125.1 (C-24), 124.5 (C-4'/C-6'), 120.1 (C-6), 77.8 (C-7), 76.5 (C-3), 71.7 (C-23), 56.2 (7-OMe), 51.2 (C-17), 49.1 (C-8), 48.8 (C-14), 46.9 (C-13), 42.7 (C-22), 42.1 (C-4), 39.6 (C-10), 35.4 (C-15), 34.7 (C-9), 33.8 (C-20), 33.3 (C-11), 31.0 (C-12), 30.0 (C-2), 29.2 (C-19), 28.7 (C-16), 28.5 (C-28), 26.0 (C-29), 25.8 (C-27), 21.9 (C-1), 19.4 (C-21), 18.6 (C-26), 18.5 (C-30), 15.7 (C-18).

Karavoate J, 3β,23(R)-di-(p-nitrobenzoyloxy)-7β-methoxycucurbita-5,24-diene (14)

Colourless oil.

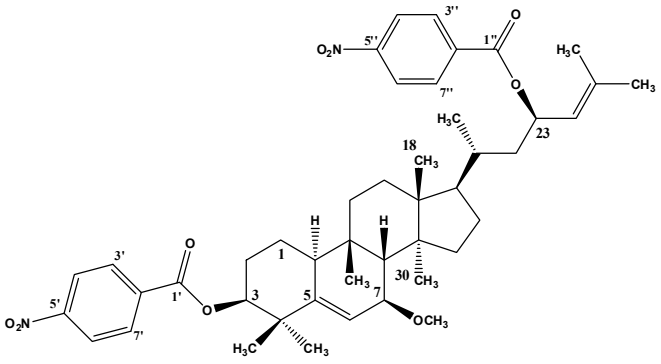

14

***R**f* (SiO_2, *n*-hexane/EtOAc, 1:1): 0.72.

IR, ν_{max} cm^{-1} (KBr): 1716, 1605, 1530, 1455, 1383, 1276, 1102, 850.

^{1}H NMR (400 MHz, CD_3COCD_3): δ 8.39 (4H, *dd*, *J* = 8.9, 1.9 Hz, H4'/H4''/H-6'/H-6''), 8.30 (2H, *d*, *J* = 8.9 Hz, H-4'/H-6'), 8.23 (2H, *d*, *J* = 8.9 Hz, H-4''/H-6''), 5.96 (1H, *td*, *J* = 9.0, 3.0 Hz, H-23), 5.90 (1H, *d*, *J* = 4.7 Hz, H-6), 5.32 (1H, *d*, *J* = 9.0 Hz, H-24), 5.06 (1H, *br s*, H-3), 3.49 (1H, *br d*, *J* = 4.7 Hz, H-7), 3.34 (3H, *s*, 7-OMe), 2.55 (1H, *br d*, *J* = 10.0 Hz, H-10), 2.10 (1H, *br s*, H-8), 1.84 (3H, *s*, Me-26), 1.74 (3H, *s*, Me-27), 1.24 (3H, *s*, Me-28), 1.21 (3H, *s*, Me-29), 1.06 (3H, *d*, *J* = 6.4 Hz, Me-21), 1.03 (3H, *s*, Me-19), 0.93 (3H, *s*, Me-18), 0.84 (3H, *s*, Me-30).

^{13}C NMR (101 MHz, CD_3COCD_3): δ 164.7 (C-1''), 164.4 (C-1'), 151.6 (C-5'/C-5''), 146.6 (C-5), 137.1 (C-2'/C-2''), 137.0 (C-25), 131.4 (C-3'/C-3''/C-7'/C-7''), 125.1 (C-24), 124.6 (C-4'/C-4''/C-6'/C-6''), 121.0 (C-6), 81.3 (C-3), 77.6 (C-7), 71.8 (C-23), 56.3 (7-OMe), 51.3 (C-17), 49.1 (C-8), 48.8 (C-14), 47.0 (C-13), 42.7 (C-22), 41.0 (C-4), 39.1 (C-10), 35.4 (C-15), 34.8 (C-9), 33.8 (C-20), 33.1 (C-11), 30.9 (C-12), 29.2 (C-19), 28.7 (C-16), 28.1 (C-28), 26.9 (C-2), 25.8 (C-27), 25.6 (C-29), 22.6 (C-1), 19.4 (C-21), 18.5 (C-26/C-30), 15.7 (C-18).

3.2.1.6. Acylation with p-chlorobenzoyl chloride

To a solution of compound **1** (25 mg) in pyridine, 60 μL of *p*-chlorobenzoyl chloride were added. The mixture was stirred at room temperature, and after 15 min the excess of pyridine was removed with N_2. The crude product was purified by column chromatography (*n*-hexane/EtOAc, 1:0 to 7:3) and preparative TLC (*n*-hexane/EtOAc, 3:2), giving rise 8 mg of compound **15** [karavoate K, 23(*R*)-(*p*-chlorobenzoyloxy)-7β-methoxycucurbita-5,24-dien-3β-ol] and 24 mg of compound **16** [karavoate L, 3β,23(*R*)-di-(*p*-chlorobenzoyloxy)-7β-methoxycucurbita-5,24-diene].

Karavoate K, 23(R)-(p-chlorobenzoyloxy)-7β-methoxycucurbita-5,24-dien-3β-ol (15)

Colourless oil.

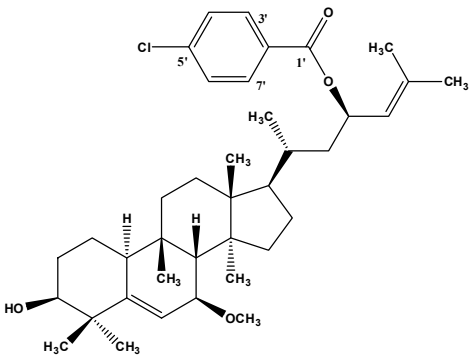

15

R_f (SiO$_2$, *n*-hexane/EtOAc, 1:1): 0.27.

IR, ν_{max} cm^{-1} (KBr): 3431, 1716, 1594, 1455, 1381, 1272, 1088, 935, 851, 759.

ESIMS, *m/z* (rel. int.): 649 $[M + K]^+$ (29), 633 $[M + Na]^+$ (56), 477 $[M + Na - C_7H_5O_2Cl]^+$ (100).

^{1}H NMR (400 MHz, CD_3COCD_3): δ 8.00 (2H, *d*, *J* = 8.8 Hz, H-3'/H-7'), 7.54 (2H, *d*, *J* = 8.8 Hz, H-4'/H-6'), 5.88 (1H, *td*, *J* = 9.0, 3.3 Hz, H-23), 5.75 (1H, *d*, *J* = 5.0 Hz, H-6), 5.25 (1H, *d*, *J* = 8.8 Hz, H-24), 3.49 (1H, *br s*, H-3), 3.39 (1H, *br d*, *J* = 5.3 Hz, H-7), 3.26 (3H, *s*, 7-OMe), 2.33 (1H, *br d*, *J* = 10.3 Hz, H-10), 2.00 (1H, *br s*, H-8), 1.79 (3H, *s*, Me-26), 1.70 (3H, *s*, Me-27), 1.17 (3H, *s*, Me-29), 1.02 (3H, *s*, Me-28), 1.02 (3H, *d*, *J* = 7.7 Hz, Me-21), 0.93 (3H, *s*, Me-19), 0.88 (3H, *s*, Me-18), 0.77 (3H, *s*, Me-30).

^{13}C NMR (101 MHz, CD_3COCD_3): δ 165.3 (C-1'), 148.1 (C-5), 139.4 (C-5'), 136.6 (C-25), 131.8 (C-3'/C-7'), 130.5 (C-2'), 129.6 (C-4'/C6'), 125.4 (C-24), 120.1 (C-6), 77.8 (C-7), 76.5 (C-3), 70.9 (C-23), 56.2 (7-OMe), 51.2 (C-17), 49.2 (C-8), 48.8 (C-14), 46.9 (C-13), 42.7 (C-22), 42.1 (C-4), 39.6 (C-10), 35.3 (C-15), 34.7 (C-9), 33.8 (C-20), 33.3 (C-11), 30.9 (C-12), 30.1 (C-2), 29.2 (C-19), 28.7 (C-16), 28.5 (C-28), 26.0 (C-29), 25.7 (C-27), 21.9 (C-1), 19.4 (C-21), 18.5 (C-30), 18.4 (C-26), 15.6 (C-18).

Karavoate L, 3β,23(R)-di-(p-chlorobenzoyloxy)-7β-methoxycucurbita-5,24-diene (16)

Colourless oil.

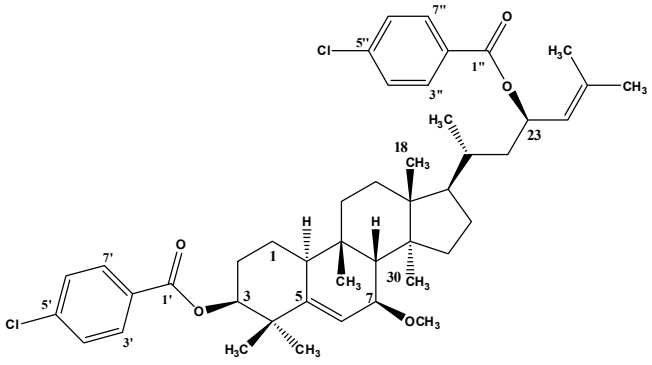

16

R_f (SiO$_2$, *n*-hexane/EtOAc, 1:1): 0.58.

IR, ν_{max} cm^{-1} (KBr): 1717, 1559, 1455, 1381, 1272, 1088, 935, 850, 758.

ESIMS, m/z (rel. int.): 771 $[M + Na]^+$ (2).

^{1}H NMR (400 MHz, CD_3COCD_3): δ 8.04 (2H, *d*, *J* = 8.8 Hz, H-3''/H-7''), 7.98 (2H, *d*, *J* = 8.8 Hz, H-3'/H-7'), 7.56 (4H, *m*, H-4'/H-4''/H-6'/H-6''), 5.88 (1H, *dt*, *J* = 9.0, 3.3 Hz, H-23), 5.87 (1H, *d*, *J*= 4.7 Hz, H-6), 5.27 (1H, *d*, *J* = 8.8 Hz, H-24), 4.99 (1H, *br s*, H-3), 3.47 (1H, *br d*, *J* = 5.0 Hz, H-7), 3.31 (3H, *s*, 7-OMe), 2.52 (1H, *br d*, *J* = 10.0 Hz, H-10), 2.12 (1H, *br s*, H-8), 1.82 (3H, *s*, Me-26), 1.73 (3H, *s*, Me-27), 1.19 (3H, *s*, Me-29), 1.22 (3H, *s*, Me-28), 1.04 (3H, *d*, *J* = 6.0 Hz, Me-21), 1.03 (3H, *s*, Me-19), 0.93 (3H, *s*, Me-18), 0.84 (3H, *s*, Me-30).

^{13}C NMR (101 MHz, CD_3COCD_3): δ 165.4 (C-1''), 165.1 (C-1'), 146.8 (C-5), 139.5 (C-5'/C-5''), 136.6 (C-25), 131.8 (C-3'/C-3''/C-7'/C-7''), 130.5 (C-2'/C-2''), 129.7 (C-4'/C-4''/C6'/C-6''), 125.4 (C-24), 120.8 (C-6), 80.5 (C-3), 77.7 (C-7), 70.9 (C-23), 56.3 (7-OMe), 51.3 (C-17), 49.1 (C-8), 48.8 (C-14), 46.9 (C-13), 42.7 (C-22), 41.0 (C-4), 39.1 (C-10), 35.4 (C-15), 34.9 (C-9), 33.8 (C-20), 33.2 (C-11), 30.9 (C-12), 29.1 (C-19), 28.8 (C-16), 28.1 (C-28), 27.0 (C-2), 25.8 (C-27), 25.6 (C-29), 22.6 (C-1), 19.4 (C-21), 18.5 (C-30), 18.4 (C-26), 15.6 (C-18).

3.2.1.7. Acylation with p-methoxybenzoyl chloride

To a solution of compound **1** (32.7 mg) in pyridine (1 mL), 50 μL of *p*-methoxybenzoyl chloride were added. The mixture was stirred at room temperature. After 24 hours, the excess of pyridine was removed with N_2. The crude product was purified by column chromatography (*n*-hexane/EtOAc, 1:0 to 4:1), and preparative TLC (*n*-hexane/EtOAc, 4:1), to afford 20 mg of compound **17** [karavoate M, 23(*R*)-(*p*-methoxybenzoyloxy)-7β-methoxycucurbita-5,24-dien-3β-ol] and 23 mg of compound **18** [karavoate N, 3β,23(*R*)-di-(*p*-methoxybenzoyloxy)-7β-methoxycucurbita-5,24-diene].

Karavoate M, 23(R)-(p-methoxybenzoyloxy)-7β-methoxycucurbita-5,24-dien-3β-ol (17)

Colourless oil.

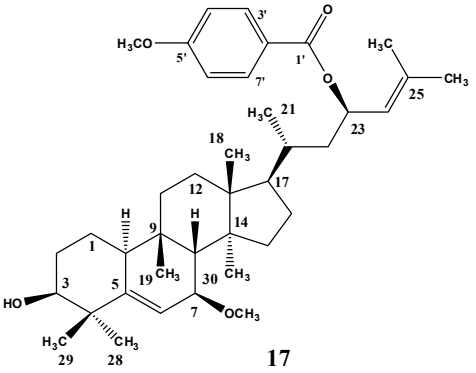

17

***R**f* (SiO_2, *n*-hexane/EtOAc, 1:1): 0.41.

IR, ν_{max} cm^{-1} (KBr): 3446, 1716, 1593, 1455, 1271, 1171, 1093, 934, 851. 759.

ESIMS, *m/z* (rel. int.): 629 $[M + Na]^+$ (2), 454 $[M - C_8H_8O_3]^+$ (100).

^{1}H NMR (400 MHz, CD_3COCD_3): δ 7.97 (2H, *d*, *J* = 8.8 Hz, H-3'/H-7'), 7.02 (2H, *d*, *J* = 8.8 Hz, H-4'/H-6'), 5.86 (1H, *td*, *J* = 10.0, 3.2 Hz, H-23), 5.76 (1H, *d*, *J* = 5.0 Hz, H-6), 5.24 (1H, *d*, *J* = 8.8 Hz, H-24), 3.87 (3H, *s*, 5'-OMe), 3.49 (1H, *br* s, H-3), 3.39 (1H, *d*, *J* = 5.3 Hz, H-7), 3.26 (3H, *s*, 7-OMe), 2.33 (1H, *br d*, *J* = 10.3 Hz, H-10), 2.01 (1H, *s*, H-8), 1.79 (3H, *s*, Me-26), 1.69 (3H, *s*, Me-27), 1.18 (3H, *s*, Me-29), 1.03 (3H, *s*, Me-28), 1.02 (3H, *d*, *J* = 7.7 Hz, Me-21), 0.94 (3H, *s*, Me-19), 0.88 (3H, *s*, Me-18), 0.77 (3H, *s*, Me-30).

^{13}C NMR (101 MHz, CD_3COCD_3): δ 165.9 (C-1'), 164.3 (C-5'), 148.0 (C-5), 135.9 (C-25), 132.1 (C-3'/C-7'), 125.9 (C-24), 124.0 (C-2'), 120.1 (C-6), 114.5 (C-4'/C-6'), 77.8 (C-7), 76.5 (C-3), 69.9 (C-23), 56.2 (7-OMe), 55.8 (5'-OMe), 51.2 (C-17), 49.1 (C-8), 48.7 (C-14), 46.9 (C-13), 42.8 (C-22), 42.0 (C-4), 39.6 (C-10), 35.3 (C-15), 34.7 (C-9), 33.7 (C-20), 33.3 (C-11), 30.9 (C-12), 30.1 (C-2), 29.2 (C-19), 28.7 (C-16), 28.5 (C-28), 26.0 (C-29), 25.8 (C-27), 22.0 (C-1), 19.4 (C-21), 18.5 (C-30), 18.4 (C-26), 15.6 (C-18).

Karavoate N, 3β,23(R)-di-(p-methoxybenzoyloxy)-7β-methoxycucurbita-5,24-diene (18)

Colourless oil.

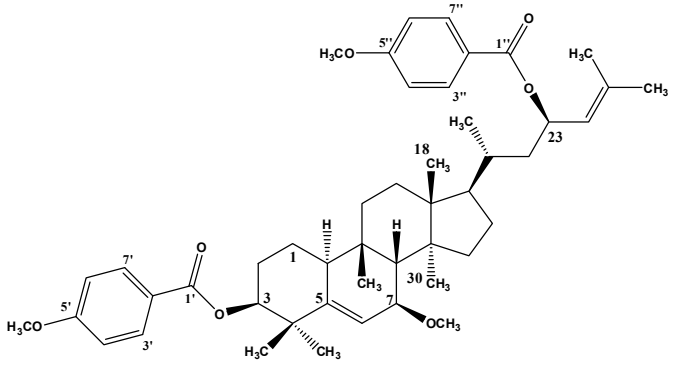

18

***R**f* (SiO_2, *n*-hexane/EtOAc, 1:1): 0.64.

IR, ν_{max} cm^{-1} (KBr): 1716, 1593, 1455, 1271, 1171, 1093, 934, 850, 759.

ESIMS, *m/z* (rel. int.): 763 $[M + Na]^+$ (67), 611 $[M + Na - C_8H_8O_3]^+$ (100), 589 (28), 561 (38), 517 (57), 501 (42), 473 (43), 457 (18).

^{1}H NMR (400 MHz, CD_3COCD_3): δ 7.96 (2H, *d* , *J* = 8.8 Hz, H-3''/H-7''), 7.93 (2H, *d* , *J* = 8.8 Hz, H-3'/H-7'), 7.02 (4H, *m*, H-4'/H-4''/H-6'/H-6''), 5.88 (1H, *d*, *J* = 5.0 Hz, H-6), 5.86 (1H, *td*, *J* = 10.0, 3.2 Hz, H-23), 5.26 (1H, *d*, *J* = 8.2 Hz, H-24), 4.95 (1H, *br s*, H-3), 3.88 (6H, *s*, 5'-OMe/5''-OMe), 3.47 (1H, *br d*, *J* = 4.7 Hz, H-7), 3.33 (3H, *s*, 7-OMe), 2.50 (1H, *dd*, *J* = 11.0, 3.0 Hz, H-10), 2.08 (1H, *br s*, H-8), 1.80 (3H, *s*, Me-26), 1.71 (3H, *s*, Me-27), 1.19 (3H, *s*, Me-29), 1.17 (3H, *s*, Me-28), 1.03 (3H, *s*, Me-19), 1.02 (3H, *d*, *J* = 5.8 Hz, Me-21), 0.91 (3H, *s*, Me-18), 0.82 (3H, *s*, Me-30).

^{13}C NMR (101 MHz, CD_3COCD_3): δ 165.9 (C-1''), 165.6 (C-1'), 164.4 (C-5''), 164.3 (C-5'), 147.0 (C-5), 136.0 (C-25), 132.1 (C-3''/C-7''), 132.0 (C-3'/C-7'), 125.9 (C-24), 124.0 (C-2''), 123.9 (C-2'), 120.6 (C-6), 114.6 (C-4'/C-4''/C-6'/C-6''), 79.5 (C-3), 77.7 (C-7), 69.9 (C-23), 56.3 (7-OMe), 55.9 (5'-OMe/5''-OMe), 51.2 (C-17), 49.1 (C-8), 48.8 (C-14), 46.9 (C-13), 42.8 (C-22), 41.0 (C-4), 39.1 (C-10), 35.3 (C-15), 34.8 (C-9), 33.7 (C-20), 33.1 (C-11), 30.9 (C-12), 29.1 (C-19), 28.7 (C-16), 28.1 (C-28), 27.0 (C-2), 25.8 (C-27), 25.6 (C-29), 22.5 (C-1), 19.4 (C-21), 18.5 (C-30), 18.4 (C-26), 15.7 (C-18).

3.2.1.8. Acylation with cinnamoyl chloride

Compound **1** (30.6 mg), dissolved in pyridine (1 mL), was added to cinnamoyl chloride (10 mg), and the mixture was left at room temperature for 48 hours. After removal of the excess of pyridine, the mixture was purified by column chromatography (*n*-hexane/CH_2Cl_2, 1:4 to 0:1, and CH_2Cl_2/Me_2CO, 0:1 to 9:1), and preparative TLC (*n*-hexane/EtOAc, 7:3) to give 12 mg of compound **19** [karavoate O, 23(*R*)-cinnamoyloxy-7β-methoxycucurbita-5,24-dien-3β-ol] and 8 mg of compound **20** [karavoate P, 3β,23(*R*)-dicinnamoyloxy-7β-methoxycucurbita-5,24-diene].

Karavoate O, 23(R)-cinnamoyloxy-7β-methoxycucurbita-5,24-dien-3β-ol (19)

Colourless oil.

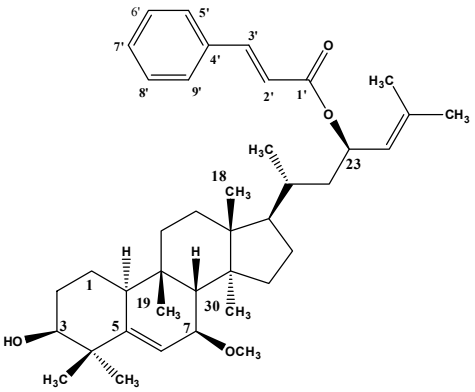

19

R_f (SiO_2, *n*-hexane/EtOAc, 7:3): 0.18.

IR, v_{max} cm^{-1} (KBr): 3446, 1718, 1450, 1271, 1171, 759, 735.

ESIMS, *m/z* (rel. int.): 625 $[M + Na]^+$ (100), 477 $[M + Na - C_9H_8O_2]^+$ (49).

^{1}H NMR (400 MHz, CD_3COCD_3): δ 7.68 - 7.63 (2H, *m*, H-5'/H-9'), 7.67 (1H, *d*, *J* = 16.0 Hz, H-3'), 7.45 (3H, *m*, H-6'/H-8'/H-7'), 6.56 (1H, *d*, *J* = 16.0 Hz, H-2'), 5.80 (1H, *td*, *J* = 9.2, 2.8 Hz, H-23), 5.77 (1H, *d*, *J* = 5.2 Hz, H-6), 5.22 (1H, *d*, *J* = 8.9 Hz, H-24), 3.50 (1H, *br s*, H-3), 3.41 (1H, *br d*, *J* = 5.3 Hz, H-7), 3.28 (3H, *s*, 7-OMe), 2.36 (1H, *br d*, *J* = 11.2 Hz, H-10), 2.00 (1H, *br s*, H-8), 1.80 (3H, *s*, Me-26), 1.72 (3H, *s*, Me-27), 1.20 (3H, *s*, Me-29), 1.05 (3H, *s*, Me-28), 1.03 (3H, *d*, *J* = 6.2 Hz, Me-21), 0.97 (3H, *s*, Me-19), 0.94 (3H, *s*, Me-18), 0.79 (3H, *s*, Me-30).

^{13}C NMR (101 MHz, CD_3COCD_3): δ 166.5 (C-1'), 148.0 (C-5), 144.9 (C-3'), 136.0 (C-25), 135.4 (C-4'), 131.0 (C-6'/C-8'), 129.7 (C-7'), 128.9 (C-5'/C9'), 125.8 (C-24), 120.0 (C-6), 119.4 (C-2'), 77.7 (C-7), 76.4 (C-3), 69.5 (C-23), 56.3 (7-OMe), 51.2 (C-17), 49.1 (C-8), 48.7 (C-14), 46.8 (C-13), 42.7 (C-22), 42.0 (C-4), 39.6 (C-10), 35.2 (C-15), 34.6 (C-9), 33.6 (C-20), 33.2 (C-11), 30.7 (C-12), 29.9 (C-2), 29.1 (C-19), 28.5 (C-16), 28.4 (C-28), 25.9 (C-27), 25.6 (C-29), 21.8 (C-1), 19.3 (C-21), 18.3 (C-26/C-30), 15.6 (C-18).

Karavoate P, 3β,23(R)-dicinnamoyloxy-7β-methoxycucurbita-5,24-diene (20)

Colourless oil.

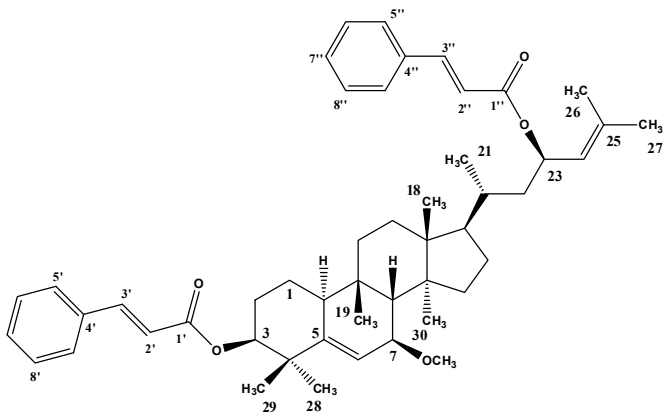

20

***R**f* (SiO_2, *n*-hexane/EtOAc, 7:3): 0.56.

IR, ν_{max} cm^{-1} (KBr): 1718, 1455, 1271, 1171, 759, 735.

ESIMS, *m/z* (rel. int.): 755 $[M + Na]^+$ (54), 607 $[M + Na - C_9H_8O_2]^+$ (100).

^{1}H NMR (400 MHz, CD_3COCD_3): δ 7.70 - 7.62 (4H, *m*, H-5'/H-5''/H-9'/H-9''), 7.68 (1H, *d*, *J* = 16.0 Hz, H-3''), 7.66 (1H, *d*, *J* = 16.0 Hz, H-3'), 7.47 - 7.40 (6H, *m*, H-6'/H-6''/H-7'/H-7''/H-8'/H-8''), 6.55 (1H, *d*, *J* = 16.0 Hz, H-2''), 6.54 (1H, *d*, *J* = 16.0 Hz, H-2'), 5.82 (1H, *d*, *J* = 5.6 Hz, H-6), 5.80 (1H, *td*, *J* = 9.6, 3.2 Hz, H-23), 5.20 (1H, *d*, *J* = 9.0 Hz, H-24), 4.85 (1H, *br s*, H-3), 3.44 (1H, *d*, *J* = 4.6 Hz, H-7), 3.31 (3H, *s*, 7-OMe), 2.46 (1H, *br d*, *J* = 11.2 Hz, H-10), 2.12 (1H, *br s*, H-8), 1.76 (3H, *s*, Me-26), 1.70 (3H, *s*, Me-27), 1.16 (3H, *s*, Me-28), 1.14 (3H, *s*, Me-29), 1.01 (3H, *d*, *J* = 6.0 Hz, Me-21), 1.00 (3H, *s*, Me-19), 0.93 (3H, *s*, Me-18), 0.80 (3H, *s*, Me-30).

^{13}C NMR (101 MHz, CD_3COCD_3): δ 166.3 (C-1'/C-1''), 146.9 (C-5), 145.1 (C-3'), 144.9 (C-3''), 136.0 (C-25), 135.4 (C-4'/C-4''), 131.0 (C-6'/C-6''/C-8'/C-8''), 129.7 (C-7'/C-7''), 128.9 (C-5'/C-5''/C9'/C-9''), 125.8 (C-24), 120.5 (C-6), 119.4 (C-2'/C-2''), 79.2 (C-3), 77.6 (C-7), 69.6 (C-23), 56.2 (7-OMe), 51.2 (C-17), 49.0 (C-8), 48.7 (C-14), 46.8 (C-13), 42.7 (C-22), 40.8 (C-4), 39.1 (C-10), 35.2 (C-15), 34.7 (C-9), 33.6 (C-20), 33.1 (C-11), 30.8 (C-12), 29.1 (C-19), 28.5 (C-16), 28.1 (C-28), 26.9 (C-2), 25.7 (C-27), 25.4 (C-29), 22.4 (C-1), 19.3 (C-21), 18.4 (C-26), 18.3 (C-30), 15.6 (C-18).

3.2.1.9. Acylation with succinic anhydride

To compound **1** (50.4 mg), dissolved in CH_2Cl_2 (2 mL) and triethylamine (1 mL), were added succinic anhydride (50 mg) and 4-dimethylaminopyridine (DMAP, 5 mg), and the mixture was left at room temperature for 24 hours. The solvent was removed by a stream of N_2, and the residue was re-dissolved in ethyl acetate, and was washed with a solution of HCl

(5%), water and dried with $MgSO_4$. After solvent removal the mixture was purified twice by column chromatography with mixtures of CH_2Cl_2/MeOH to afford 31.5 mg of compound **21** [karavoate Q, 23(*R*)-succinoyloxy-7β-methoxycucurbita-5,24-dien-3β-ol] and 7 mg of compound **22** [karavoate R, 3β,23(*R*)-disuccinoyloxy-7β-methoxycucurbita-5,24-diene].

Karavoate Q, 23(R)-succinoyloxy-7β-methoxycucurbita-5,24-dien-3β-ol (21)

White amorphous powder.

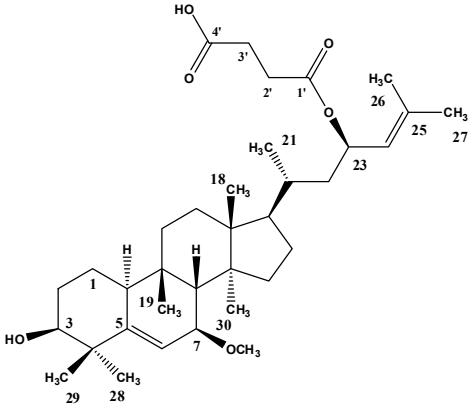

21

***R**f* (SiO_2, $CHCl_3$/MeOH, 17:3): 0.46.

IR, v_{max} cm^{-1} (KBr): 3382, 1734, 1702, 1440, 1382, 1274, 1172, 932, 627.

ESIMS, *m/z* (rel. int.): 595 $[M + Na]^+$ (31), 477 $[M + Na - C_4H_6O_4]^+$ (100).

^{1}H NMR (400 MHz, MeOD): δ 5.79 (1H, *d*, *J* = 4.9 Hz, H-6), 5.65 (1H, *td*, *J* = 10.1, 3.0 Hz, H-23), 5.11 (1H, *d*, *J* = 8.9 Hz, H-24), 3.48 (2H, *br s*, H-3/H7), 3.33 (3H, *s*, 7-OMe), 2.34 (1H, *br d*, *J* = 10.0 Hz, H-10), 2.06 (1H, *br s*, H-8), 1.72 (3H, *s*, Me-26), 1.70 (3H, *s*, Me-27), 1.19 (3H, *s*, Me-29), 1.04 (3H, *s*, Me-19), 0.97 (3H, *d*, *J* = 6.4 Hz, Me-21), 0.96 (3H, s, Me-18), 0.76 (3H, *s*, Me-30).

^{13}C NMR (101 MHz, CD_3COCD_3): δ 173.8 (C-1'), 149.4 (C-5), 136.7 (C-25), 125.8 (C-24), 120.3 (C-6), 78.9 (C-7), 77.5 (C-3), 71.0 (C-23), 56.4 (7-OMe), 51.8 (C-17), 49.5 (C-14), 48.4 (C-8), 47.4 (C-13), 43.1 (C-22), 42.5 (C-4), 40.3 (C-10), 35.8 (C-15), 35.1 (C-9), 34.1 (C-20), 33.8 (C-11), 31.3 (C-12), 30.6 (C-3'), 30.1 (C-2), 29.4 (C-19), 29.0 (C-2'), 28.8 (C-28), 26.0 (C-29), 25.8 (C-27), 22.4 (C-1), 19.4 (C-21), 18.7 (C-30), 18.5 (C-26), 15.8 (C-18).

Karavoate R, 3β,23(R)-disuccinoyloxy-7β-methoxycucurbita-5,24-diene (22)

White amorphous powder.

R_f (SiO$_2$, CHCl$_3$/MeOH, 17:3): 0.26.

IR, ν_{max} cm^{-1} (KBr): 3382, 1734, 1702, 1440, 1382, 1274, 1172, 932, 627.

ESIMS, *m/z* (rel. int.): 695 $[M + Na]^+$ (37), 577 $[M + Na - C_4H_6O_4]^+$ (100).

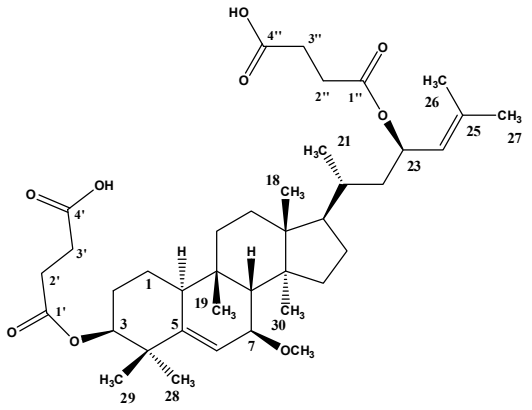

22

^{1}H NMR (400 MHz, MeOH): δ 5.78 (1H, *d*, *J* = 4.9 Hz, H-6), 5.62 (1H, *td*, *J* = 9.9, 2.8 Hz, H-23), 5.10 (1H, d, *J* = 8.7 Hz, H-24), 4.71 (1H, *br s*, H-3), 3.48 (1H, *d*, *J* = 5.0 Hz, H-7), 3.33 (3H, *s*, 7-OMe), 2.51 (8H, m, H-2'/H-2''/H-3'/H-3''), 2.38 (1H, *br d*, *J* = 9.8 Hz, H-10), 2.07 (1H, *br s*, H-8), 1.70 (3H, *s*, Me-26), 1.68 (3H, *s*, Me-27), 1.10 (3H, *s*, Me-29), 1.09 (3H, *s*, Me-28), 0.96 (9H, *s*, Me-18/Me-19/Me-21), 0.75 (3H, *s*, Me-30).

3.2.2. Derivatization of balsaminol F

3.2.2.1. Acylation with acetic anhydride

Compound **3** (10 mg) was suspended in acetic anhydride (1 mL) and pyridine (1 mL). After stirring at room temperature overnight, the excess of reagents was eliminated with N_2 and the product obtained was purified by column chromatography (*n*-hexane/EtOAc, 4:1) to afford 10 mg of compound **23** [triacetylbalsaminol F, 3β,7β,23(*R*)-triacetoxycucurbita-5,24-diene].

Triacetylbalsaminol F, 3β,7β,23(R)-triacetoxycucurbita-5,24-diene (23)

Colourless oil.

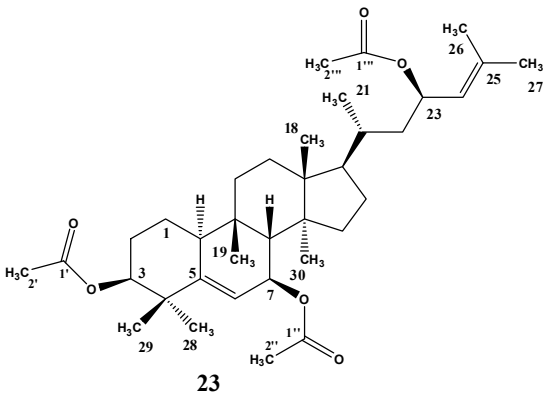

23

***R**f* (SiO_2, *n*-hexane/EtOAc, 1:1): 0.71.

IR, ν_{max} cm^{-1} (KBr): 1729, 1528, 1462, 1370, 1240, 1015, 987, 827, 611.

EIMS, *m/z* (rel. int.): 584 $[M]^+$ (< 1), 524 $[M - CH_3COOH]^+$ (27), 482 (100), 464 $[M - 2 \times CH_3COOH]^+$ (10), 421 (11), 404 $[M - 3 \times CH_3COOH]^+$ (4).

^{1}H NMR (400 MHz, CD_3COCD_3): δ 5.67 (1H, *d*, *J* = 4.8 Hz, H-6), 5.63 (1H, *td*, *J* = 8.8, 3.2 Hz, H-23), 5.12 (2H, *m*, H-7/H-24), 4.72 (1H, *br s*, H-3), 2.47 (1H, *br d*, *J* = 12.0 Hz, H-10), 1.98 and 1.96 (6H and 3H, *s*, Me-2'/Me-2''/Me-2'''), 1.97 (3H, *br s*, H-8), 1.71 (3H, *s*, Me-27), 1.68 (3H, *s*, Me-26), 1.14 (3H, *s*, Me-28), 1.09 (3H, *s*, Me-29), 1.01 (3H, *s*, Me-19), 0.96 (3H, *d*, *J* = 6.0 Hz, Me-21), 0.88 (3H, *s*, Me-18), 0.82 (3H, *s*, Me-30).

^{13}C NMR (101 MHz, CD_3COCD_3): δ 170.5, 170.4, 170.3 (C-1'/C-1''/C-1'''), 150.0 (C-5), 135.7 (C-25), 125.9 (C-24), 118.5 (C-6), 79.0 (C-3), 70.8 (C-7), 69.4 (C-23), 51.4 (C-8), 51.1 (C-17), 49.0 (C-14), 46.8 (C-13), 42.7 (C-22), 40.8 (C-4), 39.3 (C-10), 35.3 (C-15), 34.6 (C-9), 33.6 (C-20), 33.0 (C-11), 30.8 (C-12), 29.0 (C-19), 28.6 (C-16), 28.4 (C -28), 27.0 (C-2), 25.7 (C-27), 25.2 (C-29), 22.4 (C-1), 21.4, 21.2, 21.1 (C-1'/C-1''/C-1'''), 19.3 (C-21), 18.5 (C-26), 18.4 (C-30), 15.7 (C-18).

3.2.2.2. Benzoylation with benzoyl chloride

Compound **3** (17.6 mg) was suspended in benzoyl chloride (1 mL) and pyridine (1 mL). After stirring at room temperature overnight, the excess of pyridine was eliminated with N_2 and the product obtained was purified by column chromatography (*n*-hexane/EtOAc, 1:0 to 4:1). Further purification by preparative TLC (*n*-hexane/EtOAc, 9:1) afforded 17 mg of compound **24** [tribenzoylbalsaminol F, 3β,7β,23(*R*)-tribenzoyloxycucurbita-5,24-diene].

Tribenzoylbalsaminol F, 3β,7β,23(R)-tribenzoyloxycucurbita-5,24-diene (24)

Colourless oil.

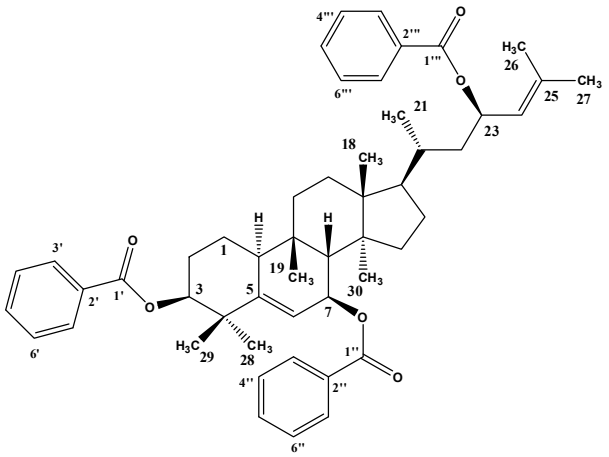

24

***R**f* (SiO_2, *n*-hexane/EtOAc, 9:1, 2 ×): 0.48.

IR, v_{max} cm^{-1} (KBr): 1718, 1528, 1462, 1370, 1240, 1015, 836, 870, 719.

EIMS, *m/z* (rel. int.): 770 $[M]^+$ (< 1), 526 $[M - 2 \times C_6H_5COOH]^+$ (26.7).

^{1}H NMR (400 MHz, CD_3COCD_3): *δ* 8.10 - 7.99 (6H, *m*, H-3'/H-3''/H-3'''/H-7'/H-7''/H-7'''), 7.70 - 7.37 (9H, *m*, H-4'/H-4''/H-4'''/H-5'/H-5''/H-5'''/H-6'/H-6''/H-6'''), 5.92 (2H, *m*, H-6/H-23), 5.50 (1H, *br d*, *J* = 5.6 Hz, H-7), 5.29 (1H, *d*, *J* = 8.8 Hz, H-24), 5.02 (1H, *br s*, H-3), 2.69 (1H, *br d*, *J* = 12.4 Hz, H-10), 2.16 (1H, *br s*, H-8), 1.83 (3H, *s*, Me-26), 1.73 (3H, *s*, Me-27), 1.27 (3H, *s*, Me-28), 1.25 (3H, *s*, Me-19), 1.21 (3H, *s*, Me-29), 1.06 (3H, *d*, *J* = 5.2 Hz, Me-21), 0.97 (3H, *s*, Me-18), 0.88 (3H, *s*, Me-30).

^{13}C NMR (101 MHz, CD_3COCD_3): *δ* 166.0, 165.8, 165.5 (C-1'/C-1''/C-1'''), 150.5 (C-5), 136.2 (C-25), 133.6, 133.5 (C-5'/C-5''/C-5'''), 131.9, 131.6, 131.5 (C-2'/C-2''/C-2'''), 129.9, 129.8 (C-3'/C-3''/C-3'''/C-7'/C-7''/C-7'''), 129.3, 129.2 (C-4'/C-4''/C-4'''/C-6'/C-6''/C-6'''), 125.5 (C-24), 118.6 (C-6), 79.9 (C-3), 71.3 (C-7), 70.2 (C-23), 51.2 (C-8), 50:9 (C-17), 48.9 (C-14), 46.7 (C-13), 42.6 (C-22), 41.3 (C-4), 38.9 (C-10), 35.2 (C-15), 34. 5 (C-9), 33.6 (C-20), 32.9 (C-11), 30.6 (C-12), 29.7 (C-19), 28.6 (C-16), 27.2 (C-28), 26.4 (C-2), 25.6 (C-27), 25.5 (C-28), 22.4 (C-1), 19.2 (C-21), 18.4 (C-30), 18.5 (C-26), 15.7 (C-18).

3.3. Study of fraction M3

The residue (5.3 g) of the crude fraction eluted with *n*-hexane/EtOAc (9:11 to 1:19, fraction M3) was subjected to column chromatography, over SiO_2 (200 g), using *n*-hexane/EtOAc (9:1 to 0:1) and mixtures of EtOAc/MeOH (1:0 to 1:1). The resulting

chromatographic fractions were pooled into nine fractions (M3A to M3I, Table 4.4 and Scheme 3.5).

3.3.1. Study of fraction M3C

The residue of the fraction M3C (150 mg, *n*-hexane/EtOAc, 3:2) was chromatographed by column chromatography, using gradients of CH_2Cl_2/Me_2CO (1:0 to 1:1). The residue of the fractions eluted with CH_2Cl_2/Me_2CO (19:1, 13 mg), showed the presence of a spot with strong absorption at 254 nm, which was purified by preparative TLC (CH_2Cl_2/Me_2CO, 2 ×) to afford 6 mg of compound **25** (dehydrovomifoliol).

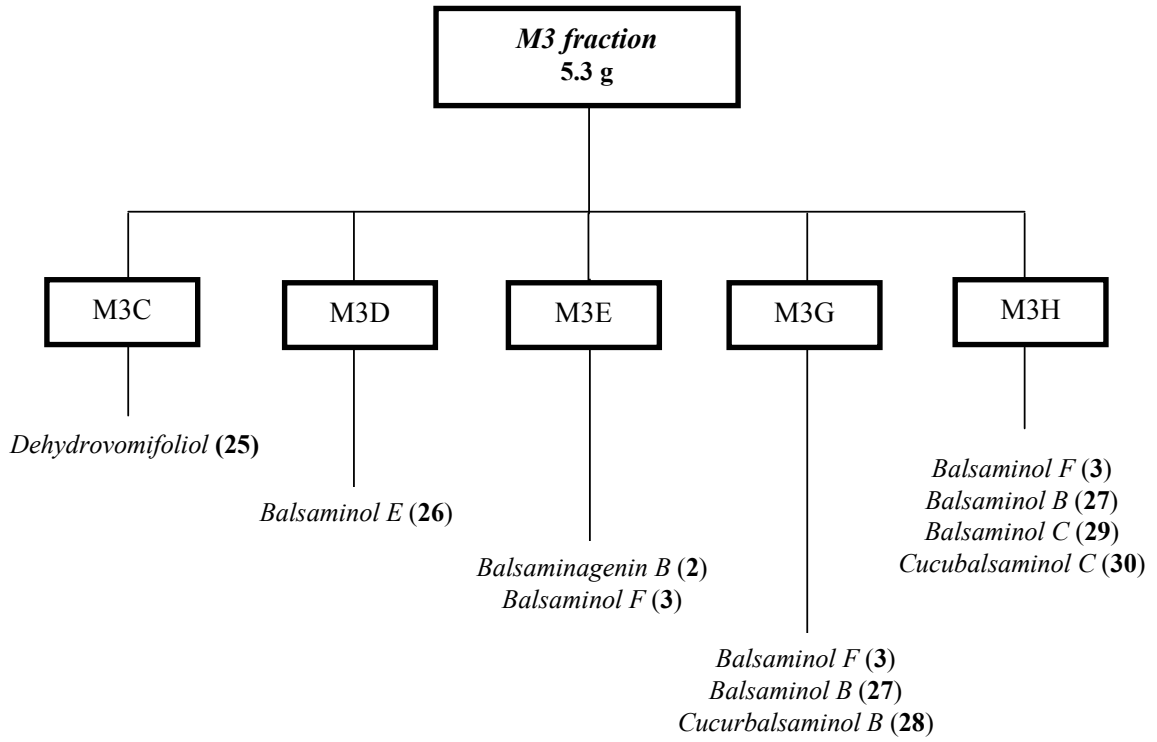

Scheme 3.5. Study of fraction M3.

Table 4.4. Column chromatography of the fraction M3.

Fraction	Mass (g)	Eluent (V/V)	
		***n*-hexane/EtOAc**	**EtOAc/MeOH**
M3A	0.10	9:1 to 13:7	–
M3B	0.30	13:7 to 3:2	–
M3C	0.15	3:2	–
M3D	1.13	3:2 to 1:1	–
M3E	0.80	1:1 to 2:3	–
M3F	0.77	2:3 to 7:13	–
M3G	0.41	1:3 to 3:17	–
M3H	0.84	3:17 to 0:1	0:1 to 4:1
M3I	0.23	-	4:1 to 1:1

Dehydrovomifoliol (25)

Yellow oil.

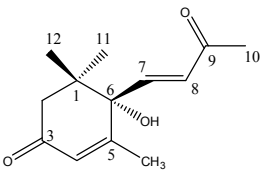

25

R_f (SiO_2, CH_2Cl_2/Me_2CO): 0.32.

$[\alpha]_D^{26}$ + 82 (*c* 0.12, $CDCl_3$); Lit. $[\alpha]_D^{26}$ + 139 (*c* 0.42, MeOH), (Kai et al., 2007).

IR, ν_{max} cm^{-1} (KBr): 3462, 2964, 1655, 1425, 1366, 1318, 1257, 1127, 980.

EIMS, *m/z* (rel. int.): 222 $[M]^+$ (1), 166 (19), 149 (10), 124 (100), 95 (10), 55 (11).

^{1}H NMR (400 MHz, MeOD): δ 6.99 (1H, *d*, *J* = 15.6 Hz, H-7), 6.42 (1H, *d*, *J* = 15.6 Hz, H-8), 5.93 (1H, *s*, H-4), 2.60 (1H, *d*, *J* = 17.2 Hz, H-2a), 2.30 (3H, *s*, Me-10), 2.26 (1H, *d*, *J* = 17.2 Hz, H-2b), 1.89 (3H, *d, J* = 1.2 Hz, Me-5), 1.05 (3H, *s*, Me-12), 0.94 (3H, *s*, Me-11).

^{13}C NMR (101 MHz, MeOD): δ 200.5 (C-9), 200.4 (C-3), 164.7 (C-5), 148.4 (C-7), 131.8 (C-8), 128.1 (C-4), 80.0 (C-6), 50.6 (C-2), 42.7 (C-1), 27.7 (C-10), 24.8 (C-11), 23.6 (C-12), 19.2 (C-5).

3.3.2. Study of fraction M3D

Fraction M3D (1.13 g, *n*-hexane/EtOAc, 3:2 to 1:1) was chromatographed by column chromatography, using eluents of increasing polarity CH_2Cl_2/Me_2CO (1:0 to 1:1). The residue of the fractions eluted with CH_2Cl_2/Me_2CO (4:1, 370 mg) was further chromatographed by column chromatography (SiO_2, 124 g), using gradients of CH_2Cl_2/Me_2CO (9:1 to 1:4) to afford seven fractions ($M3D_1$ to $M3D_7$). Fraction $M3D_4$ (104 mg) showed the presence of two spots with a strong absorption at 254 nm, which were separated by preparative TLC (*n*-hexane/EtOAc, 2:3, 3 ×) to afford 10 mg of compound **26** [balsaminol E, cucurbita-5,24-dien-7-one-3β,23(*R*)-diol].

Balsaminol E, cucurbita-5,24-dien-7-one-3β,23(R)-diol (26)

White amorphous powder.

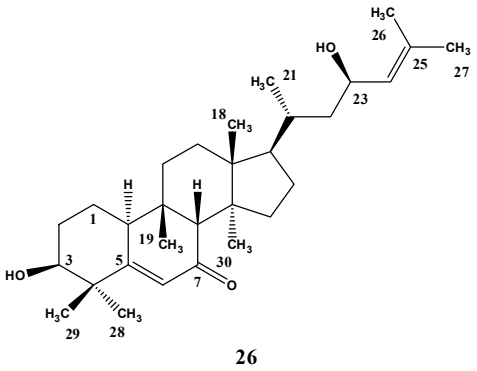

26

***R**f* (SiO_2, $CHCl_3$/MeOH, 9:1): 0.60.

$[\alpha]_D^{26}$ + 98 (*c* 0.11, MeOH).

UV (MeOH) λ_{max} (log ε): 204 (3.91), 241 (3.91).

IR, ν_{max} cm^{-1} (KBr): 3404, 1717, 1642, 1459, 1381, 1298, 972.

HR-EIMS *m/z*: 456.3606 $[M]^+$ (calcd. for $C_{30}H_{48}O_3$: 456.3603).

EIMS, *m/z* (rel. int.): 456 $[M]^+$ (12), 438 $[M - H_2O]^+$ (22), 423 (7), 357 $[M - CH_2CHOHCHC(CH_3)_2]^+$ (100), 329 [M – side chain]$^+$ (40), 287 (6), 252 (6), 219 (12), 207 (26), 189 (40), 166 (22), 149 (16), 133 (26), 109 (31), 81 (23).

^{1}H NMR (400 MHz, MeOD): δ 6.06 (1H, *s*, H-6), 5.17 (1H, *d*, *J* = 8.2 Hz, H-24), 4.42 (1H, *td*, *J* = 9.6, 3.2 Hz, H-23), 3.62 (1H, *br s*, H-3), 2.84 (1H, *br d*, *J* = 9.8 Hz, H-10), 2.39 (1H, *s*, H-8), 1.71 (3H, *s*, Me-27), 1.68 (3H, *s*, Me-26), 1.24 (3H, *s*, Me-28), 1.17 (3H, *s*, Me-29), 1.01 (3H, *d*, *J* = 7.0 Hz, Me-21), 0.98 (3H, *s*, Me-19), 0.95 (3H, *s*, Me-18), 0.91 (3H, *s*, Me-30).

^{13}C NMR (101 MHz, MeOD): δ 205.8 (C-7), 174.1 (C-5), 133.5 (C-25), 130.5 (C-24), 126.1 (C-6), 77.5 (C-3), 66.6 (C-23), 61.4 (C-8), 51.7 (C-17), 49.8 (C-14), 47.0 (C-13), 45.6 (C-22), 44.1 (C-4), 41.9 (C-10), 36.9 (C-9), 35.8 (C-15), 33.9 (C-20), 32.3 (C-11), 31.1 (C-12), 29.8 (C-2), 29.0 (C-16), 28.6 (C-28), 28.3 (C-19), 26.0 (C-29), 25.6 (C-27), 22.3 (C-1), 19.4 (C-21), 18.8 (C-30), 18.2 (C-26), 15.9 (C-18).

3.3.3. Study of fraction M3E

The residue of the crude fraction M3E (800 mg), eluted with mixtures of *n*-hexane/EtOAc (1:1 to 1:3), was submitted to a column chromatography, over SiO_2 (50 g), with mixtures of CH_2Cl_2/MeOH (1:0 to 3:1). Fractions eluted with CH_2Cl_2/MeOH (19:1) were successively re-chromatographed over silica gel, with mixtures of CH_2Cl_2/MeOH and CH_2Cl_2/Me_2CO to afford 240 mg of compound **3** [balsaminol F, cucurbita-5,24-diene-3β,7β,23(*R*)-triol] and 60 mg of compound **2** [balsaminagenin C, cucurbita-5,23(*E*)-diene-3β, 25-diol], both already isolated from fraction M2B (Scheme 3.2 and Table 4.3).

3.3.4. Study of fraction M3G

The residue (408 mg) of the crude fraction M3G, eluted with mixtures of *n*-hexane/EtOAc (1:3 to 3:17), was chromatographed, over SiO_2 (50 g), with mixtures of CH_2Cl_2/Me_2CO (9:1 to 1:1). After TLC monitoring, similar chromatographic fractions were combined into six fractions (Fr $M3G_1$ to $M3G_6$). Fraction $M3G_4$ (277 mg, CH_2Cl_2/Me_2CO, 3:1) was chromatographed with mixtures of CH_2Cl_2/MeOH (49:1 to 3:1). The resulting chromatographic fractions were pooled into five fractions (Fr $M3G_{4A}$ to $M3G_{4E}$). Fraction $M3G_{4A}$ was further purified by HPLC (210 nm, MeOH/H_2O, 17:3, 5 mL/min) to afford 24 mg of compound **27** [balsaminol B, 7β-methoxycucurbita-5,24-diene-3β,23(*R*),29-triol, R_t 13 min]. Fraction $M3G_{4C}$ was also purified by HPLC (220 nm, MeOH/H_2O, 17:3, 5 mL/min), affording 11 mg of compound **28** [cucurbalsaminol B, 7β-methoxycucurbita-5,23(*E*)-diene-3β,12β,25-triol, R_t 12 min] and 40 mg of compound **3** [balsaminol F, cucurbita-5,24-diene-3β,7β,23(*R*)-triol, R_t 16 min], which was previously isolated from fractions M2B and M3E (Schemes 3.2 and 3.5).

Balsaminol B, 7β-methoxycucurbita-5,24-diene-3β,23(R),29-triol (27)

White amorphous powder.

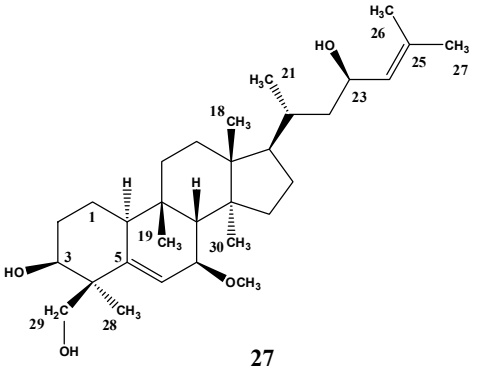

27

***R**f* (SiO_2, $CHCl_3$/MeOH, 9:1): 0.47; ***R**t* (HPLC, 210 nm, MeOH/H_2O, 17:3, 1 mL/min): 4.8 min.
$[\alpha]_D^{26}$ + 90 (*c* 0.10, MeOH).

IR, v_{max} cm^{-1} (KBr): 3398, 1455, 1382, 1182, 1078, 1030, 936.

HR-ESITOFMS *m/z*: 511.3757 $[M + Na]^+$ (calcd. for $C_{31}H_{52}O_4Na$: 511.3758).

ESIMS, *m/z* (rel. int.): 511 $[M + Na]^+$ (75).

^{1}H NMR (400 MHz, MeOD): δ 5.80 (1H, *d*, *J* = 4.8 Hz, H-6), 5.16 (1H, *d*, *J* = 8.8 Hz, H-24), 4.41 (1H, *td*, *J* = 9.6, 2.8 Hz, H-23), 3.95 (1H, *d*, *J* = 10.9 Hz, H-29b), 3.82 (1H, *br s*, H-3), 3.65 (1H, *d*, *J* = 10.8 Hz, H-29a), 3.49 (1H, *br d*, *J* = 3.7 Hz, H-7), 3.33 (3H, *s*, 7-OMe), 2.33 (1H, *br d*, *J* = 10.4 Hz, H-10), 2.06 (1H, *br s*, H-8), 1.69 (3H, *s*, Me-28), 1.66 (3H, *s*, Me-27), 0.98 (3H, *s*, Me-19), 0.97 (6H, *s*, Me-18/Me-21), 0.96 (3H, *s*, Me-28), 0.77 (3H, *s*, Me-30).

^{13}C NMR (101 MHz, MeOD): δ 146.2 (C-5), 133.4 (C-25), 130.5 (C-24), 121.1 (C-6), 78.7 (C-7), 75.4 (C-3), 69.6 (C-29), 66.6 (C-23), 56.5 (7-OMe), 52.2 (C-17), 49.2 (C-14), 47.4 (C-13), 45.6 (C-22), 45.5 (C-4), 40.1 (C-10), 35.8 (C-15), 35.1 (C-9), 33.8 (C-20), 33.7 (C-11), 31.4 (C-12), 30.1 (C-2), 28.8 (C-16), 29.3 (C-19), 26.0 (C-27), 23.6 (C-28), 22.0 (C-1), 19.3 (C-21), 18.8 (C-30), 18.1 (C-26), 15.9 (C-18).

Cucurbalsaminol B, 7β-methoxycucurbita-5,23(E)-diene-3β,12β,25-triol (28)

White amorphous powder.

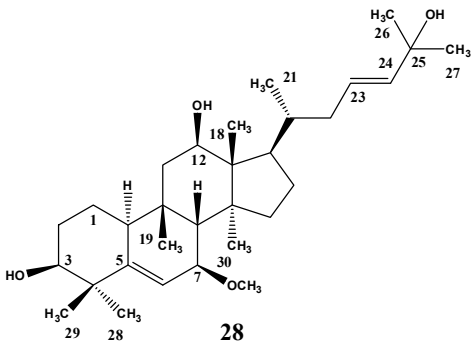

28

***R**f* (SiO_2, $CHCl_3$/MeOH, 9:1): 0.46; ***R**t* (HPLC, 210 nm, MeOH/H_2O, 41:9; 1 mL/min): 3.4 min.

$[\alpha]_D^{26}$ + 96 (*c* 0.11, MeOH).

IR, ν_{max} cm^{-1} (KBr): 3388, 1457, 1381, 1081, 1024, 975, 940.

HR-EIMS *m/z*: 488.3853 $[M]^+$ (calcd. for $C_{31}H_{52}O_4$ $[M]^+$: 488.3866).

EIMS *m/z* (rel. int.): 488 $[M]^+$ (28), 470 $[M - H_2O]^+$ (100), 456 (16), 452 $[M - 2 \times H_2O]^+$ (7), 420 $[M - 2 \times H_2O - CH_3HO]^+$ (2), 402 $[M - 3 \times H_2O - CH_3OH]^+$ (1), 388 (1), 344 (10), 312 (4), 270 (2); 223 (24), 203 (18), 182 (23), 173 (11), 164 (26), 149 (37), 123 (20), 109 (50), 81 (17).

^{1}H NMR (400 MHz, MeOD): δ 5.78 (1H, *d*, *J* = 4.9 Hz, H-6), 5.58 (2H, *m*, H-23/H-24), 3.86 (1H, *dd*, *J* = 11.4, 4.9, H-12), 3.49 (2H, *br s*, H-3/H-7), 3.33 (3H, *s*, 7-OMe), 2.33 (1H, *m*, H-10), 1.98 (1H, *br s*, H-8), 1.26 (6H, *s*, Me-26/Me-27), 1.18 (3H, *s*, Me-29), 1.02 (3H, *d*, *J* = 6.8 Hz, Me-21), 1.01 (6H, *s*, Me-19/Me-28), 0.92 (3H, *s*, Me-18), 0.75 (3H, *s*, Me-30).

^{13}C NMR (101 MHz, MeOD): δ 149.1 (C-5), 140.1 (C-24), 127.3 (C-23), 120.3 (C-6), 78.4 (C-7), 77.4 (C-3), 71.8 (C-12), 71.2 (C-25), 56.4 (7-OMe), 52.3 (C-13), 52.0 (C-17), 51.1 (C-14), 48.9 (C-8), 44.4 (C-11), 42.4 (C-4), 41.6 (C-10), 39.7 (C-22), 37.4 (C-9), 36.2 (C-15), 35.0 (C-20), 30.1 (C-2/C-26), 30.0 (C-27), 29.3 (C-19), 28.7 (C-28), 26.0 (C-29), 25.6 (C-16), 22.5 (C-1), 22.1 (C-21), 18.5 (C-30), 10.6 (C-18).

3.3.5. Study of fraction M3H

The crude fraction M3H (843 mg), eluted with mixtures of *n*-hexane/EtOAc (1:19 to 0:1) and EtOAc/MeOH (1:0 to 19:1), was chromatographed, over SiO_2 (100 g), with CH_2Cl_2/Me_2CO (17:3 to 1:4). After TLC monitoring, similar chromatographic fractions were pooled into five fractions ($M3H_1$ to $M3H_5$).

3.3.5.1. Study of fraction $M3H_1$

Fraction $M3H_1$ (217 mg) was submitted to column chromatography, over SiO_2, with mixtures of CH_2Cl_2/Me_2CO (17:3 to 1:1). After TLC monitoring, two main fractions ($M3H_{1A}$

and $M3H_{1B}$) were obtained. Fraction $M3H_{1A}$ (77 mg) was re-chromatographed twice, using mixtures of CH_2Cl_2/MeOH. The main fraction obtained (46 mg) was further purified by HPLC (220 nm, MeOH/H_2O, 4:1, 5 mL/min) to give 10 mg of compound **29** [balsaminol C, cucurbita-5,24-diene-7,23-dione-3β,29-diol, t_R 9 min]. From fraction $M3H_{1B}$ [87 mg, CH_2Cl_2/Me_2CO (4:1 to 3:1)], after analytical HPLC, the presence of compound **27** was shown.

Balsaminol C, cucurbita-5,24-diene-7,23-dione-3β,29-diol (29)

White amorphous powder.

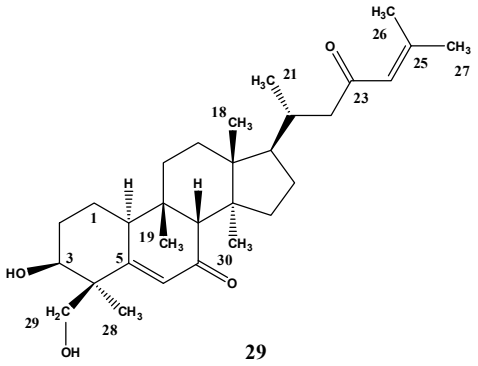

29

R_f (SiO_2, $CHCl_3$/MeOH, 9:1): 0.56; ***R_t*** (HPLC, 254 nm, MeOH/H_2O, 4:1, 1 mL/min): 4.5 min.
$[\alpha]_D^{26}$ + 84 (*c* 0.10, MeOH).

IR, v_{max} cm^{-1} (KBr): 3384, 2948, 1679, 1641, 1449, 1379, 1300, 1020, 944, 833, 733.

UV (MeOH) λ_{max} (log ε): 203 (3.88), 219 (3.84), 239 (3.83), 255 (3.8).

HR-CIMS *m/z*: 471.3466 $[M + 1]^+$ (calcd. for $C_{30}H_{47}O_4$: 471.3474).

EIMS, *m/z* (rel. int.): 470 $[M]^+$ (4), 373 $[M - CH_2COCHC(CH_3)_2]^+$ (63), 345 [M – side chain]$^+$ (9), 325 (100), 298 (18), 175 (41), 125 (18), 83 (57).

^{1}H NMR (400 MHz, MeOD): δ 6.18 (1H, *s*, H-24), 6.10 (1H, *s*, H-6), 3.92 (1H, *br s*, H-3), 3.90 (1H, *d*, *J* = 10.9 Hz, H-29b), 3.72 (1H, *d*, *J* = 10.9 Hz, H-29a), 2.84 (1H, *br d*, *J* = 11.3 Hz, H-10), 2.39 (1H, *s*, H-8), 2.12 (3H, *s*, Me-27), 1.91 (3H, *s*, Me-26), 1.11 (3H, *s*, Me-28), 0.98 (3H, *s*, Me-19), 0.96 (3H, *s*, Me-18), 0.92 (3H, *d*, *J* = 7.0 Hz, Me-21), 0.91 (3H, *s*, Me-30).

^{13}C NMR (101 MHz, MeOD): δ 205.5 (C-7), 203.9 (C-23), 170.6 (C-5), 157.1 (C-25), 126.9 (C-6), 125.3 (C-24), 75.5 (C-3), 68.7 (C-29), 61.1 (C-8), 52.7 (C-22), 51.3 (C-17), 49.7 (C-14), 47.2 (C-4), 47.0 (C-13), 41.7 (C-10), 37.0 (C-9), 35.8 (C-15), 34.9 (C-20), 32.2 (C-11),

30.9 (C-12), 29.8 (C-2), 29.0 (C-16), 28.2 (C-19), 27.7 (C-27), 23.3 (C-28), 22.0 (C-1), 20.9 (C-26), 20.2 (C-21), 18.8 (C-30), 15.9 (C-18).

3.3.5.2. Study of fraction $M3H_3$

The residue (338 mg) of fraction $M3H_3$ was submitted to column chromatography (SiO_2, 25 g), using as eluents mixtures of CH_2Cl_2/MeOH (19:1 to 1:1) to give, after TLC monitoring, two main fractions ($M3H_{3A}$ and $M3H_{3B}$). Fraction $M3H_{3A}$ (145.4 g) was successively re-chromatographed with mixtures of CH_2Cl_2/MeOH to give more 80 mg of compound **27** [balsaminol B, 7β-methoxycucurbita-5,24-diene-3β,23(*R*),29-triol]. Fraction $M3H_{3B}$ (157 mg) was re-chromatographed twice, using mixtures of CH_2Cl_2/MeOH. The residue (29 mg) was further purified by HPLC (210 nm, MeOH/H_2O, 17:3, 5mL/min), affording 18 mg more of compound **3** [balsaminol F, cucurbita-5,24-diene-3β,7β,23(*R*)-triol, R_t 16 min].

3.3.5.3. Study of fraction $M3H_4$

Fraction $M3H_4$ (297 mg), eluted with CH_2Cl_2/Me_2CO (13:7 to 2:3), was submitted to column chromatography (SiO_2, 23 g), using CH_2Cl_2/Me_2CO (7:3 to 1:1). Fractions were associated, after TLC monitoring, into two main fractions ($M3H_{4A}$ and $M3H_{4B}$). Fraction $M3H_{4A}$ was further chromatographed with CH_2Cl_2/Me_2CO (7:3). After TLC monitoring, one main fraction was obtained, which was further purified by HPLC (210 nm, MeOH/H_2O, 17:3, 5mL/min) to afford 50 mg of compound **30** [Cucurbalsaminol C, 7β-methoxycucurbita-5,24-diene-3β,12β 23(*R*)-triol, R_t 9 min].

Cucurbalsaminol C, 7β-methoxycucurbita-5,24-diene-3β,12β,23(R)-triol (30)

White amorphous powder.

R_f (SiO_2, $CHCl_3$/MeOH, 9:1): 0.46; ***R_t*** (HPLC, 210 nm, MeOH/H_2O, 17:3, 1 mL/min): 4.0 min.
$[\alpha]_D^{26}$ + 117 (*c* 0.11, MeOH).

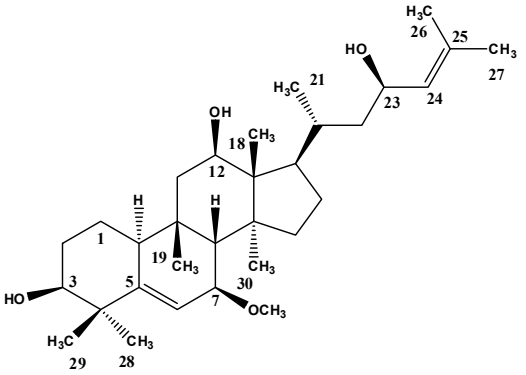

30

IR, *v_{max}* cm^{-1} (KBr): 3443, 1455, 1382, 1182, 1138, 1024, 978, 939.

HR-EIMS *m/z*: 488.3867 $[M]^+$ (calcd. for $C_{31}H_{52}O_4$: 488.3866).

EIMS *m/z* (rel. int.): 488 $[M]^+$ (29.6), 470 $[M - H_2O]^+$ (43), 452 $[M - 2 \times H_2O]^+$ (16), 438 (8), 434 $[M - 3 \times H_2O]^+$ (12), 420 $[M - 2 \times H_2O - CH_3OH]^+$ (12), 402 $[M - 3 \times H_2O - CH_3OH]^+$ (3.3), 388 (2), 344 (15), 312(13), 270 (7), 223 (23), 189 (19), 182 (18), 172 (17), 164 (25), 109 (100).

^{1}H NMR (400 MHz, MeOD): δ 5.78 (1H, *d*, *J* = 4.8 Hz, H-6), 5.16 (1H, *d*, *J* = 8.4 Hz, H-24), 4.41 (1H, *td*, *J* = 8.9, 3.6 Hz, H-23), 3.86 (1H, *dd*, *J* = 11.2, 4.8 Hz, H-12), 3.49 (2H, *br s*, H-3/H-7), 3.33 (3H, *s*, 7-OMe), 2.33 (1H, *br d*, *J* = 10 Hz, H-10), 1.98 (1H, *br s*, H-8), 1.70 (3H, *s*, Me-27), 1.67 (3H, *s*, Me-26), 1.18 (3H, *s*, Me-29), 1.07 (3H, *d*, *J* = 6.4 Hz, Me-21), 1.02 (3H, *s*, Me-28), 1.01 (3H, *s*, Me-19), 0.93 (3H, *s*, Me-18), 0.76 (3H, *s*, Me-30).

^{13}C NMR (101 MHz, MeOD): δ 149.1 (C-5), 133.4 (C-25), 130.6 (C-24), 120.3 (C-6), 78.4 (C-7), 77.4 (C-3), 72.0 (C-12), 67.8 (C-23), 56.4 (7-OMe), 52.6 (C-17), 52.4 (C-13), 51.1 (C-14), 48.8 (C-8), 44.8 (C-22), 44.4 (C-11), 42.4 (C-4), 41.6 (C-10), 37.4 (C-9), 36.2 (C-15), 31.0 (C-20), 30.1 (C-2), 29.3 (C-19), 28.7 (C-28), 26.0 (C-29), 25.9 (C-27), 25.7 (C-16), 22.5 (C-1), 22.4 (C-21), 18.6 (C-30), 18.2 (C-26), 10.7 (C-18).

3.4. Study of fraction M4

The crude fraction M4 (3.3 g), eluted with EtOAc/MeOH (1:0 to 24:1), was submitted to column chromatography (SiO_2, 200g), using as eluents, mixtures of *n*-hexane/EtOAc (1:3

to 0:1) and EtOAc/MeOH (1:0 to 1:3). After TLC monitoring, five main fractions were obtained (M4A to M4E, Table 4.5).

Table 4.5. Column chromatography of the fraction M4.

Fraction	Mass (g)	Eluent (V/V)	
		***n*-hexane/EtOAc**	**EtOAc/MeOH**
M4A	0,05	1:3	–
M4B	0.30	1:3	–
M4C	1.06	1:3 to 1:0	–
M4D	1.27	0:1	1:0 to 9:1
M4E	0.37	–	9:1 to 1:3

3.4.1. Study of fraction M4C

The residue of the crude fraction M4C (1.06 g), eluted with *n*-hexane/EtOAc (1:3 to1:0) was chromatographed, over SiO_2 (100 g), with mixtures of CH_2Cl_2/MeOH (99:1 to 1:1). After TLC monitoring, six fractions were obtained ($M4C_1$ to $M4C_6$, Table 4.6 and **Scheme 3.6**).

Table 4.6. Column chromatography of the fraction M4C.

Fraction	Mass (g)	Eluent (V/V)
		CH_2Cl_2/MeOH
$M4C_1$	0.05	99:1 to 97:3
$M4C_2$	0.20	97:3 to 96.5:3.5
$M4C_3$	0.04	96.5:3.5
$M4C_4$	0.20	24:1
$M4C_5$	0.25	24:1 to 23:2
$M4C_6$	0.20	23:2 to 1:3

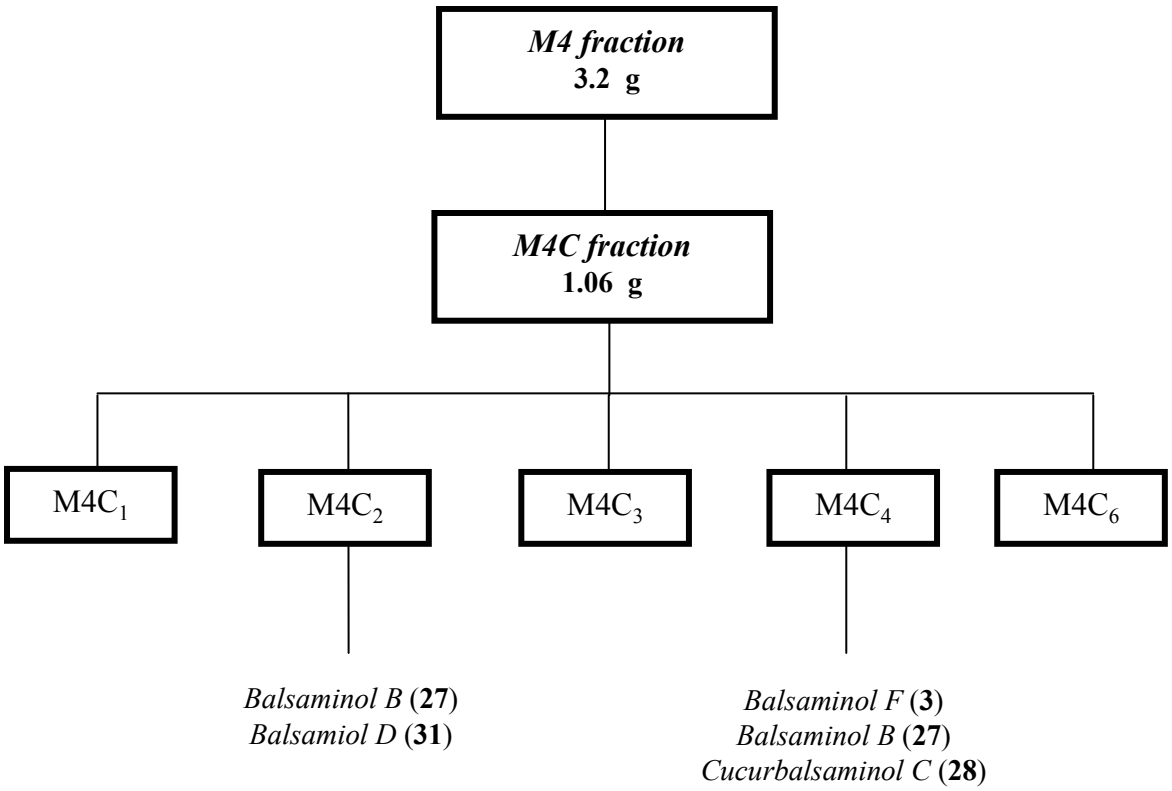

Scheme 3.6. Study of fraction M4C.

3.4.1.1. Study of fraction M4C$_2$

Fraction M4C$_2$ was successively re-chromatographed with mixtures of CH_2Cl_2/MeOH, and CH_2Cl_2/Me_2CO to get two main fractions (M4C$_{2A}$ and M4C$_{2B}$). Fraction M4C$_{2A}$ (39 mg) was purified by HPLC (210 nm, MeOH/H_2O, 73:27, 5 mL/min), affording 16 mg of compound **31** [balsaminol D, 25,26,27-*trinor*-cucurbit-5-ene-7,23-dione-3β,29-diol, R_t 9min]. Fraction M4C$_{2B}$ was also purified by HPLC (210 nm, MeOH/H_2O, 4:1, 5 mL/min), affording 11 mg of the already isolated compound **27** [balsaminol B, 7β-methoxycucurbita-5,24-diene-3β,23(*R*),29-triol, R_t 23 min]. Fraction M4C$_4$ (200 mg) was re-chromatographed twice with mixtures of CH_2Cl_2/Me_2CO by column chromatography, to give a main fraction (59 mg) with a visible dark brown spot, after spraying and heating. This fraction was purified by HPLC (210 nm, MeOH/H_2O, 41:9, 5 mL/min) to afford more 19 mg of compound **3** [balsaminol F, cucurbita-5,24-diene-3β,7β,23(*R*)-triol, R_t 23 min].

Balsaminol D, 25,26,27-trinor-cucurbit-5-ene-7,23-dione-3β,29-diol (31)

White amorphous powder.

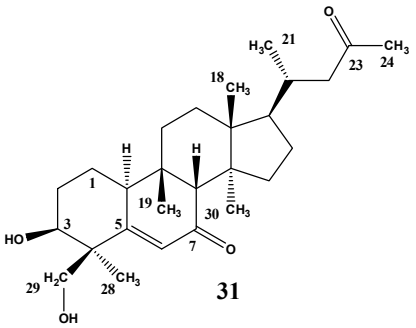

31

***R**f* (SiO_2, $CHCl_3$/MeOH, 9:1): 0.37; ***R**t* (HPLC, 210 nm, MeOH/H_2O, 73:27, 1 mL/min): 3.5 min.
$[\alpha]_D^{26}$ + 103 (*c* 0.11, MeOH).

IR, ν_{max} cm^{-1} (KBr): 3375, 2958, 1707, 1645, 1459, 1382, 1182, 1030, 936.

UV (MeOH) λ_{max} (log ε): 204 (3.87), 226 (3.81), 238 (3.81), 252 (3.79).

HR-ESITOFMS *m/z*: 431.3153 $[M + H]^+$ (calcd. for $C_{27}H_{43}O_4$: 431.3156).

ESIMS, *m/z* (rel. int.): 453 $[M + Na]^+$ (12).

^{1}H NMR (400 MHz, MeOD): δ 6.09 (1H, *s*, H-6), 3.91 (1H, *br s*, H-3), 3.90 (1H, *d*, *J* = 10.9 Hz, H-29b), 3.72 (1H, *d*, *J* = 10.9 Hz, H-29a), 2.84 (1H, *dd*, *J* = 11.3, 2.7 Hz, H-10), 2.38 (1H, *s*, H-8), 2.11 (3H, *s*, Me-24), 1.11 (3H, *s*, Me-28), 0.98 (3H, *s*, Me-19), 0.95 (3H, *s*, Me-18), 0.91 (3H, *d*, *J* = 7.0 Hz, Me-21), 0.90 (3H, *s*, Me-30).

^{13}C NMR (101 MHz, MeOD): δ 205.5 (C-7), 212.2 (C-23), 170.6 (C-5), 126.9 (C-6), 75.5 (C-3), 68.7 (C-29), 61.1 (C-8), 51.8 (C-22), 51.1 (C-17), 49.7 (C-14), 47.2 (C-4), 47.0 (C-13), 41.7 (C-10), 36.9 (C-9), 35.8 (C-15), 34.1 (C-20), 32.2 (C-11), 30.9 (C-12), 30.6 (C-24), 29.8 (C-2), 28.9 (C-16), 28.2 (C-19), 23.3 (C-28), 22.0 (C-1), 20.2 (C-21), 18.8 (C-30), 15.8 (C-18).

3.4.2. Study of fraction M4D

The residue of crude fraction M4D (1.3 g), eluted with EtOAc/MeOH (1:0 to 9:1), was submitted to column chromatography, over SiO_2 (120 g), with mixtures of CH_2Cl_2/Me_2CO (4:1 to 0:1). After TLC monitoring, five fractions ($M4D_1$ to $M4D_5$) were obtained (Scheme 3.7).

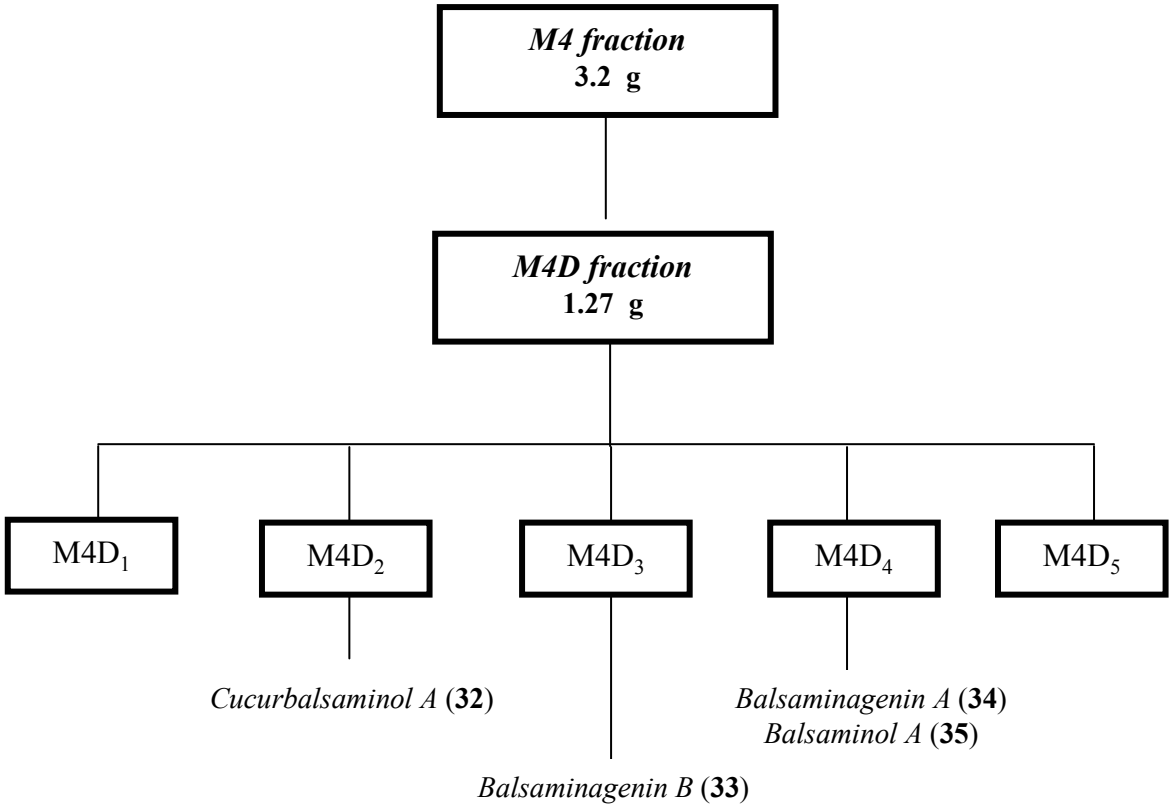

Scheme 3.7. Study of fraction M4D.

3.4.2.1. Study of fraction M4D$_2$

Fraction M4D$_2$ (603 mg), eluted with CH_2Cl_2/Me_2CO (1:1), was chromatographed, over SiO_2 (65 g), with mixtures of CH_2Cl_2/MeOH (97:3 to 1:1). After TLC monitoring, fractions with similar chromatographic profile were pooled into five fractions (M4D$_{2A}$ to M4D$_{2E}$). Fraction M4D$_{2E}$ (93 mg), eluted with CH_2Cl_2/MeOH (41:4), was chromatographed, over SiO_2 (14 g), with mixtures of CH_2Cl_2/MeOH (19:1 to 9:1). Fractions eluted with CH_2Cl_2/MeOH (97:3) were pooled to give 65 mg of a residue that was further purified by HPLC (210 nm, MeOH/H_2O, 75:25, 4 mL/min) to afford 25 mg of compound **32** [cucurbalsaminol A, cucurbita-5,23(*E*)-diene-3β,7β,12β,25-tetraol, R_t 16 min].

Cucurbalsaminol A, cucurbita-5,23(E)-diene-3β,7β,12β,25-tetraol (32)

White amorphous powder.

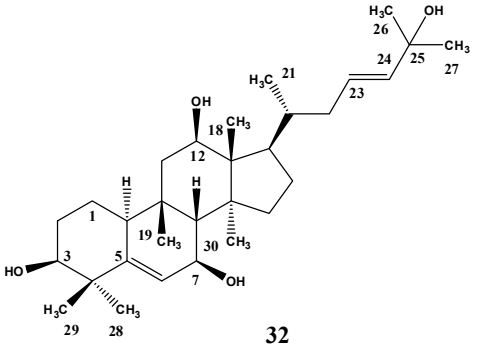

32

***R**f* (SiO_2, $CHCl_3$/MeOH, 9:1): 0.36; ***R**t* (HPLC, 210 nm, MeOH/H_2O, 77:23; 1 mL/min): 4.6 min.
$[\alpha]_D^{26}$ + 89 (*c* 0.11, MeOH).

IR, ν_{max} cm^{-1} (KBr): 3447, 1459, 1380, 1151, 1081, 1020, 980.

HR-ESITOFMS *m/z*: 497.3601 $[M + Na]^+$ (calcd. for $C_{30}H_{50}O_4Na$: 497.3601).

ESIMS *m/z*: 497 $[M + Na]^+$ (70), 369 [M + Na – side chain]$^+$ (71).

^{1}H NMR (400 MHz, MeOD): δ 5.74 (1H, *d*, *J* = 4.5 Hz, H-6), 5.58 (2H, *m*, H-23/H-24), 3.94 (1H, *br d*, *J* = 4.9 Hz, H-7), 3.86 (1H, *dd*, *J* = 11.4, 5.0 Hz, H-12), 3.49 (1H, *br s*, H-3), 2.32 (1H, *m*, H-10), 1.90 (1H, *br s*, H-8), 1.25 (6H, *s*, Me-26/Me-27), 1.18 (3H, *s*, Me-29), 1.08 (3H, *s*, Me-19), 1.02 (3H, *d*, *J* = 6.8 Hz, Me-21), 1.01 (3H, *s*, Me-28), 0.89 (3H, *s*, Me-18), 0.74 (3H, *s*, Me-30).

^{13}C NMR (101 MHz, MeOD): δ 148.0 (C-5), 140.0 (C-24), 127.3 (C-23), 122.5 (C-6), 77.4 (C-3), 71.9 (C-12), 71.2 (C-25), 68.2 (C-7), 53.3 (C-8), 52.1 (C-13), 51.9 (C-17), 51.4 (C-14), 44.5 (C-11), 42.3 (C-4), 41.4 (C-10), 39.7 (C-22), 37.3 (C-9), 36.1 (C-15), 35.0 (C-20), 30.1 (C-2/C-26), 30.0 (C-27), 29.7 (C-19), 28.7 (C-28), 26.1 (C-29), 25.7 (C-16), 22.5 (C-1), 22.1 (C-21), 18.5 (C-30), 10.6 (C-18).

3.4.2.2. Study of fraction M4D$_3$

The residue of the crude fraction M4D$_3$ (127 mg) was re-chromatographed twice with mixtures of *n*-hexane/EtOAc (3:17 to 0:1) and EtOAc/MeOH (1:0 to 1:1). Fractions eluted with *n*-hexane/EtOAc (1:9) were pooled to give 28 mg of a residue that was purified by preparative TLC ($CHCl_3$/MeOH 9:1, 2×) to yield 16 mg of compound **33** [balsaminagenin B, 25-methoxycucurbita-5,23(*E*)-diene-3β,7β,29-triol].

Balsaminagenin B, 25-methoxycucurbita-5,23(E)-diene-3β,7β,29-triol (33)

White needles.

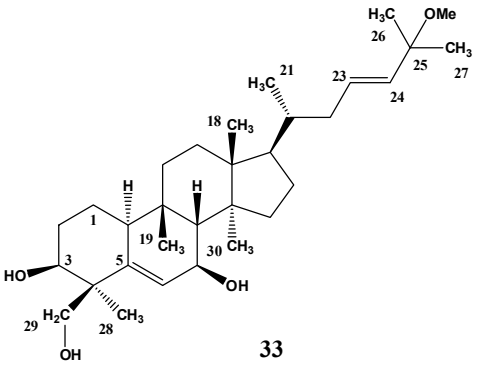

33

mp (MeOH): 110 - 112 ºC

***R**f* (SiO_2, $CHCl_3$/MeOH, 9:1): 0.39.

$[\alpha]_D^{20}$ + 101 (*c* 0.10, MeOH).

IR, v_{max} cm^{-1} (KBr): 3409, 2941, 1402, 1075.

HR-ESITOFMS, *m/z*: 511.3758 $[M + Na]^+$ (calcd. for $C_{31}H_{52}O_4Na$: 511.3758).

ESIMS, *m/z* (rel. int.): 511 $[M + Na]^+$ (100).

^{1}H NMR (400 MHz, MeOD): δ 5.74 (1H, *d*, *J* = 4.7 Hz, H-6), 5.58 (1H, *ddd*, *J* = 15.6, 8.8, 6.0 Hz, H-23), 5.38 (1H, *d*, *J* = 15.6 Hz, H-24), 3.95 (1H, *d*, *J* = 10.8 Hz, H-29b), 3.94 (1H, *br s*, H-7), 3.83 (1H, *br s*, H-3), 3.65 (1H, *d*, *J* = 10.8 Hz, H-29a), 3.13 (3H, *s*, 25-OMe), 2.32 (1H, *br d*, *J* = 9.2 Hz, H-10), 1.98 (1H, *br s*, H-8), 1.24 (6H, *s*, Me-26/Me-27), 1.05 (3H, *s*, Me-19), 0.97 (3H, *s*, Me-28), 0.95 (3H, *s*, Me-18), 0.94 (3H, *d*, *J* = 6.4 Hz, Me-21), 0.75 (3H, *s*, Me-30).

^{13}C NMR (101 MHz, MeOD): δ 145.1 (C-5), 137.6 (C-24), 130.1 (C-23), 123.1 (C-6), 76.5 (C-25), 75.3 (C-3), 69.5 (C-29), 68.5 (C-7), 53.9 (C-8), 51.2 (C-17), 50.6 (25-OMe), 49.2 (C-14), 47.1 (C-13), 45.3 (C-4), 40.5 (C-22), 39.9 (C-10), 37.6 (C-20), 35.7 (C-15), 35.0 (C-9), 33.7 (C-11), 31.3 (C-12), 30.1 (C-2), 29.7 (C-19), 28.8 (C-16), 26.5 (C-27), 26.0 (C-26), 23.6 (C-28), 22.0 (C-1), 19.3 (C-21), 18.6 (C-30), 16.0 (C-18).

3.4.2.3. Study of fraction M4D$_4$

Fraction M4D$_4$ (165 mg) was chromatographed over a column of silica gel (16 g), using mixtures of CH_2Cl_2/MeOH (19:1 to 1:1). After TLC monitoring, fractions eluted with CH_2Cl_2/MeOH (19:1) that showed the presence of a dark brown spot, after spraying and heating, were purified by HPLC (210 nm, MeOH/H_2O 4:1, 5 mL/min) to afford 13 mg of compound **34** [balsaminagenin A, cucurbita-5,23(*E*)-diene-3β,7β,25,29-tetraol, R_t 30 min] and

26 mg of compound **35** [balsaminol A, cucurbita-5,24-diene-3β,7β,23(*R*),29-tetraol, R_t 35 min].

Balsaminagenin A, cucurbita-5,23(E)-diene-3β,7β,25,29-tetraol (34)

White amorphous powder.

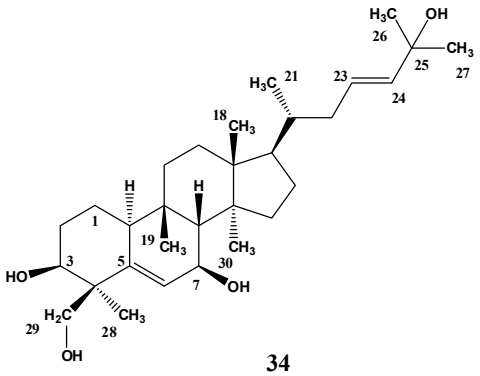

34

***R**f* (SiO_2, $CHCl_3$/MeOH, 9:1): 0.36; ***R**t* (HPLC, 210 nm, MeOH/H_2O, 4:1, 1 mL/min): 6.7 min.
$[\alpha]_D^{20}$ + 86 (*c* 0.11, MeOH).

IR, ν_{max} cm^{-1} (KBr): 3399, 2934, 1651, 1457, 1404, 1154, 1054.

HR-ESITOFMS, *m/z*: 497.3612 $[M + Na]^+$ (calcd. for $C_{30}H_{50}O_4Na$: 497.3601).

ESIMS, *m/z* (rel. int.): 513 $[M + K]^+$ (11), 498 $[M + Na + H]^+$ (24), 497 $[M + Na]^+$ (66).

^{1}H NMR (400 MHz, MeOD): δ 5.74 (1H, *d*, *J* = 4.5 Hz, H-6), 5.57 (2H, *m*, H-23/H-24), 3.95 (1H, *d*, *J* = 10.8 Hz, H-29b), 3.94 (1H, *br s*, H-7), 3.83 (1H, *br s*, H-3), 3.65 (1H, *d*, *J* = 10.8 Hz, H-29a), 2.32 (1H, *br d*, *J* = 10.2 Hz, H-10), 1.97 (1H, *br s*, H-8), 1.25 (6H, *s*, Me-26/Me-27), 1.05 (3H, *s*, Me-19), 0.97 (3H, *s*, Me-28), 0.94 (3H, *s*, Me-18), 0.92 (3H, *s*, *J* = 5.8 Hz, Me-21), 0.76 (3H, *s*, Me-30).

^{13}C NMR (101 MHz, MeOD): δ 145.2 (C-5), 140.8 (C-24), 126.0 (C-23), 123.1 (C-6), 75.3 (C-3), 71.4 (C-25), 69.5 (C-29), 68.6 (C-7), 53.9 (C-8), 51.2 (C-17), 49.0 (C-14), 47.1 (C-13), 45.3 (C-4), 40.3 (C-22), 39.9 (C-10), 37.7 (C-20), 35.7 (C-15), 35.0 (C-9), 33.7 (C-11), 31.3 (C-12), 30.1 (C-2/C-26), 30.0 (C-27), 29.7 (C-19), 28.8 (C-16), 23.6 (C-28), 22.0 (C-1), 19.2 (C-21), 18.6 (C-30), 16.0 (C-18).

Balsaminol A, cucurbita-5,24-diene-3β,7β,23(R),29-tetraol (35)

White amorphous powder.

R_f (SiO_2, $CHCl_3$/MeOH, 9:1): 0.34; ***R_t*** (HPLC, 210 nm, MeOH/H_2O, 4:1, 1 mL/min): 8.3 min.
$[\alpha]_D^{26}$ + 93 (*c* 0.12, MeOH).

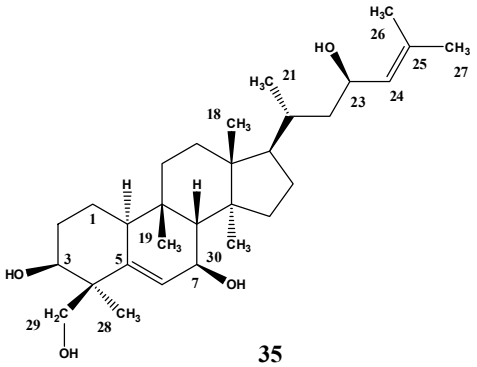

35

IR, v_{max} cm^{-1} (KBr): 3357, 1450, 1360, 1315, 1020, 944, 833, 733.

HR-ESITOFMS *m/z*: 497.3601 $[M + Na]^+$ (calcd. for $C_{30}H_{50}O_4Na$: 497.3601).

ESIMS, *m/z* (rel. int.): 497 $[M + Na]^+$ (<1).

^{1}H NMR (400 MHz, MeOD): δ 5.74 (1H, *d*, *J* = 4.4 Hz, H-6), 5.16 (1H, *d*, *J* = 8.5 Hz, H-24), 4.41 (1H, *td*, *J* = 9.5, 3.1 Hz, H-23), 3.95 (1H, *d*, *J* = 11.0 Hz, H-29b), 3.95 (1H, *br s*, H-7), 3.83 (1H, *br s*, H-3), 3.65 (1H, *d*, *J* = 11.0 Hz, H-29a), 2.33 (1H, *br d*, *J* = 10.4 Hz, H-10), 1.98 (1H, *br s*, H-8), 1.70 (3H, *s*, Me-27), 1.66 (3H, *s*, Me-26), 1.05 (3H, *s*, Me-19), 0.97 (6H, *s*, Me-18/Me-28), 0.96 (3H, *d*, *J* = 6.3 Hz, H-21), 0.76 (3H, *s*, Me-30).

^{13}C NMR (101 MHz, MeOD): δ 145.2 (C-5), 133.4 (C-25), 130.5 (C-24), 123.2 (C-6), 75.3 (C-3), 69.5 (C-29), 68.5 (C-7), 66.6 (C-23), 53.9 (C-8), 52.1 (C-17), 49.1 (C-14), 47.2 (C-13), 45.6 (C-22), 45.3 (C-4), 39.9 (C-10), 35.7 (C-15), 35.0 (C-9), 33.8 (C-20), 33.7 (C-11), 31.5 (C-12), 30.1 (C-2), 29.7 (C-19), 28.9 (C-16), 26.0 (C-27), 23.6 (C-28), 22.0 (C-1), 19.3 (C-21), 18.6 (C-30), 18.1 (C-26), 16.0 (C-18).

3.5. Study of fraction M5

The crude fraction M5 (2.79 g) was fractionated by column chromatography (SiO_2, 100g) with mixtures of *n*-hexane/EtOAc (1:1 to 0:1) and EtOAc/MeOH (1:0 to 1:1). After TLC monitoring, chromatographic fractions were pooled into four fractions (M5A to M5D, Table 4.7).

Table 4.7. Column chromatography of the fraction M5.

Fraction	Mass (g)	Eluent (V/V)	
		***n*-hexane/EtOAc**	**EtOAc/MeOH**
M5A	0.09	1:1 to 1:4	–
M5B	1.12	1:4 to 9:1	–
M5C	0.82	1:19 to 0:1	1:0 to 19:1
M5D	0.69	–	19:1 to 1:1

3.5.1. Study of fraction M5B

The residue of fraction M5B was subjected to column chromatography, over SiO_2 (90 g), using as eluents mixtures of *n*-hexane/CH_2Cl_2 (1:1 to 0:1) and CH_2Cl_2/MeOH (1:0 to 1:3). After TLC monitoring, fractions were pooled into six fractions ($M5B_1$ to $M5B_6$, Table 4.8).

Table 4.8. Column chromatography of the fraction M5B.

Fraction	Mass (g)	Eluent (V/V)	
		***n*-hexane/CH_2Cl_2**	**CH_2Cl_2/MeOH**
$M5B_1$	0.09	1:1 to 0:1	1:0 to 24:1
$M5B_2$	0.08	–	24:1to 19:1
$M5B_3$	0.34	–	19:1
$M5B_4$	0.18	–	47:3
$M5B_5$	0.07	–	47:3 to 9:1
$M5B_6$	0.15	–	9:1 to 1:3

3.5.1.1. Study of fraction $M5B_3$

Fraction $M5B_3$ was submitted to three sequenced column chromatographies, which were eluted with mixtures of CH_2Cl_2/MeOH of increasing polarity, to afford, after purification by HPLC (210 nm, MeOH/H_2O, 3:1, 5 ml/min), 15 mg of compound **34** and 40 mg of compound **35**, already isolated from fraction M4.

3.5.1.2. Study of fraction M5B$_5$

The residue of the fraction M5B$_5$ was fractionated by repeated column chromatography, using as eluents mixtures of CH_2Cl_2/MeOH of increasing polarity to yield, after purification by HPLC (210 nm, MeOH/H_2O, 7:3, 5 mL/min), 10 mg of compound **36** [balsaminapentaol, cucurbita-5,25-diene-3β,7β,23(*R*),24(*R*),29-pentaol, R_t 28 min].

Balsaminapentaol, cucurbita-5,25-diene-3β,7β,23(R),24(R),29-pentaol (36)

White amorphous powder.

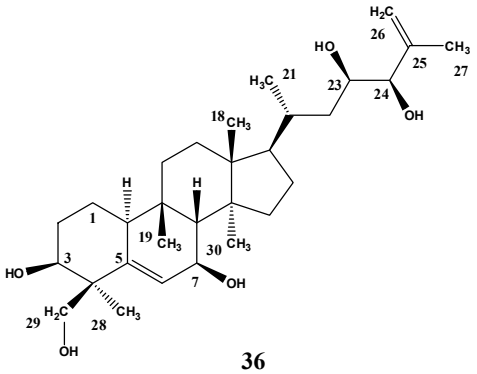

36

R$_f$ (SiO_2, $CHCl_3$/MeOH, 9:1): 0.28; ***R$_t$*** (HPLC, 210 nm, MeOH/H_2O, 7:3, 1 mL/min): 9.4 min.
$[\alpha]_D^{26}$ + 85 (*c* 0.11, MeOH).

IR, v_{max} cm^{-1} (KBr): 3408, 1651, 1457, 1408, 1380, 1078, 1030.

HR-ESITOFMS *m/z*: 513.3553 $[M + Na]^+$ (calcd. for $C_{30}H_{50}O_5Na$: 513.3550).

ESIMS, *m/z* (rel. int.): 513 $[M + Na]^+$ (89).

^{1}H NMR (500 MHz, MeOD): δ 5.74 (1H, *d*, *J* = 4.6 Hz, H-6), 4.84 (1H, *br s*, H-26b), 4.78 (1H, *br s*, H-26a), 3.95 (1H, *d*, *J* = 11.0 Hz, H-29b), 3.94 (1H, *br s*, H-7), 3.82 (1H, *br s*, H-3), 3.74 (1H, *d*, *J* = 7.0 Hz, H-24), 3.65 (1H, *d*, *J* = 11.0 Hz, H-29a), 3.63 (1H, *ddd*, *J* = 10.8, 7.0, 1.86 Hz, H-23), 2.33 (1H, *dd*, *J* = 12.0, 1.9 Hz, H-10), 1.98 (1H, *br s*, H-8), 1.70 (3H, *s*, Me-27), 1.05 (3H, *s*, Me-19), 0.96 (6H, *s*, Me-18/Me-28), 0.92 (3H, *d*, *J* = 6.5 Hz, Me-21), 0.76 (3H, *s*, Me-30).

^{13}C NMR (101 MHz, MeOD): δ 146.7 (C-25), 145.2 (C-5), 123.2 (C-6), 114.1 (C-26), 81.6 (C-24), 70.9 (C-23), 75.3 (C-3), 69.5 (C-29), 68.5 (C-7), 53.9 (C-8), 52.4 (C-17), 49.2 (C-14), 47.3 (C-13), 45.3 (C-4), 41.0 (C-22), 39.9 (C-10), 35.6 (C-15), 35.0 (C-9), 33.7 (C-11), 33.5 (C-20), 31.5 (C-12), 30.1 (C-2), 29.7 (C-19), 28.9 (C-16), 23.7 (C-28), 22.0 (C-1), 19.0 (C-21), 18.6 (C-30), 18.0 (C-27), 16.0 (C-18).

3.5.2. Study of fraction M5C

Fraction M5C (820 mg) was successively re-chromatographed by column chromatography with mixtures of CH_2Cl_2/MeOH to afford, after purification by HPLC (210 nm, MeOH/H_2O, 77:23, 5 mL/min), 7 mg of compound **37** [kuguaglycoside A, 7β-methoxycucurbita-5,24-dien-3β-ol-23-O-β-D-glucopyranoside, R_t 32 min].

Kuguaglycoside A, 7β-methoxycucurbita-5,24-dien-3β-ol-23-O-β-D-glucopyranoside (37)

White amorphous powder.

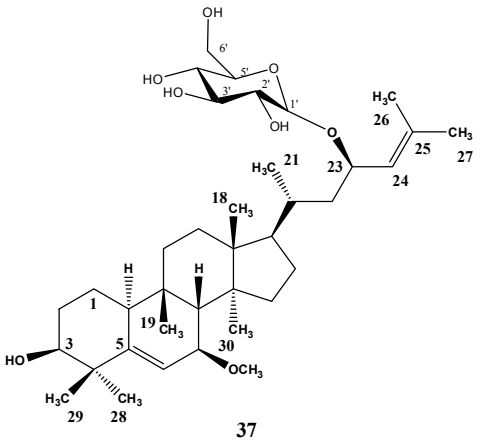

37

R_f (SiO_2, $CHCl_3$/MeOH, 17:3): 0.50; ***R_t*** (HPLC, 210 nm, MeOH/H_2O, 77:23, 1 mL/min): 12 min.
$[\alpha]_D^{26}$ + 62.0 (*c* 0.10, MeOH); Lit. $[\alpha]_D^{24}$ + 12.7 (*c* 0.6, MeOH), (Chen et al., 2008a).

IR, ν_{max} cm^{-1} (KBr): 3379, 2930, 1652, 1453, 1383, 1078, 1031, 937.

HR-ESITOFMS *m/z*: 657.4334 $[M + Na]^+$ (calcd. for $C_{37}H_{62}O_8Na$: 657.4337).

ESIMS, *m/z* (rel. int.): 657 $[M + Na]^+$ (70), 477 $[M + Na - C_6H_{12}O_6]^+$ (81), 203 $[C_6H_{12}O_6 + Na]^+$ (100).

^{1}H NMR (400 MHz, MeOD): δ 5.78 (1H, *d*, *J* = 5.0 Hz, H-6), 5.25 (1H, *d*, *J* = 9.1 Hz, H-24), 4.54 (1H, *td*, *J* = 8.8, 4.2 Hz, H-23), 4.26 (1H, *d*, *J* = 7.8 Hz, H-1'), 3.79 (1H, *dd*, *J* = 11.8, 2.4 Hz, H-6b'), 3.65 (1H, *dd*, *J* = 11.8, 5.4 Hz, H-6a'), 3.48 (2H, *br s*, H-3/H-7), 3.32 (3H, *s*, 7-OMe), 2.34 (1H, *dd*, *J* = 11.6, 4.1 Hz, H-10), 2.05 (1H, *br s*, H-8), 1.71 (3H, *s*, Me-27), 1.70 (3H, *s*, Me-26), 1.18 (3H, *s*, Me-29), 1.03 (3H, *s*, Me-28), 0.99 (3H, *d*, *J* = 6.5 Hz, Me-21), 0.97 (6H, *s*, Me-18/Me-19), 0.75 (3H, *s*, Me-30).

^{13}C NMR (101 MHz, MeOD): δ 149.4 (C-5), 134.1 (C-25), 128.9 (C-24), 120.3 (C-6), 103.8 (C-1'), 78.9 (C-7), 78.5 (C-3'), 77.9 (C-3), 77.5 (C-5'), 76.7 (C-23), 75.5 (C-2'), 71.6 (C-4'), 62.8 (C-6'), 56.4 (7-OMe), 52.2 (C-17), 49.4 (C-8), 49.5 (C-14), 47.4 (C-13), 44.2 (C-22), 42.5 (C-4), 40.3 (C-10), 35.8 (C-15), 35.1 (C-9), 33.7 (C-20), 33.8 (C-11), 31.4 (C-12), 30.1

(C-2), 29.4 (C-19), 28.8 (C-16), 28.7 (C-28), 26.0 (C-29), 22.4 (C-1), 19.8 (C-21), 18.8 (C-30), 18.4 (C-26), 15.9 (C-18).

3.6. Study of fraction M6

The crude fraction M6 was recrystallized from EtOAc/MeOH to give 500 mg of a mixture, which was fractionated by column chromatography (SiO_2, 50g) eluted with mixtures of *n*-hexane/EtOAc (3:1 to 1:0) and EtOAc/MeOH (1:0 to 1:1). The fractions eluted with EtOAc/MeOH (97:3) were evaporated and recrystallized, from *n*-hexane/EtOAc, to afford 160 mg of compound **38** [balsaminoside B, cucurbita-5,24-diene-3β,23(*R*)-diol-7-O-β-D-allopyranoside]. The mother liquors were associated to the remaining fractions and after evaporation, the residue (245 mg) was submitted to repeated column chromatography, using as eluents mixtures of EtOAc/MeOH, and CH_2Cl_2/MeOH of increasing polarity, to afford 110 mg more of compound **38** and 11 mg of compound **39** [balsaminoside C, cucurbita-5,24-diene-3β,23(*R*)-diol-7-O-β-D-glucopyranoside]. The mother liquors of the fraction M6 were submitted to column chromatography (SiO_2, 250 g) eluted with *n*-hexane/EtOAc (1:1 to 0:1) and EtOAc/MeOH (1:0 to 1:1). After TLC monitoring, fractions were pooled into five fractions (M6A to M6E). Apart from fraction M6B, the chromatographic profile of all all the fractions showed the presence of compounds **38** and **39**, which had similar R_f. Therefore, they were not further studied.

Balsaminoside B, cucurbita-5,24-diene-3β,23(R)-diol-7-O-β-D-allopyranoside (38)

White prismatic crystals.

mp: 230 - 231ºC (*n*-hexane/EtOAc).

***R*$_f$** (SiO_2, $CHCl_3$/MeOH, 17:3): 0.26.

$[\alpha]_D^{26}$ + 173 (*c* 0.11, MeOH).

IR, ν_{max} cm^{-1} (KBr): 3396, 2945, 1645, 1453, 1383,

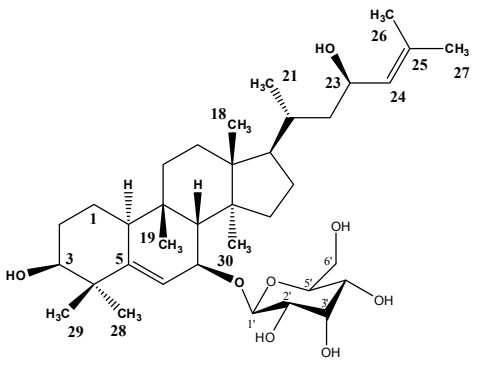

38

1057, 978, 939.

HR-ESITOFMS *m/z*: 643.4180 $[M + Na]^+$ (calcd. $C_{36}H_{60}O_8Na$ for: 643.4180).

ESIMS, *m/z* (rel. int.): 659 $[M + K]^+$ (4), 643 $[M + Na]^+$ (100), 423 $[M + H - H_2O - C_6H_{12}O_6]^+$ (10).

^{1}H NMR (400 MHz, MeOD): δ 5.76 (1H, *d*, *J* = 4.8 Hz, H-6), 5.16 (1H, *d*, *J* = 8.4 Hz, H-24), 4.41 (1H, *td*, *J* = 9.4, 2.8 Hz, H-23), 4.75 (1H, *d*, *J* = 8.0 Hz, H-1'), 4.11 (1H, *br d*, *J* = 4.5 Hz, H-7), 4.05 (1H, *br s*, H-3'), 3.84 (1H, *d*, *J* = 9.4 Hz, H-6b'), 3.66 (2H, *m*, H-5'/H-6a'), 3.51 (1H, *m*, H-4'), 3.49 (1H, *br s*, H-3), 3.32 (1H, *m*, H-2'), 2.34 (1H, *br d*, *J* = 9.3 Hz, H-10), 2.13 (1H, *br s*, H-8), 1.70 (3H, *s*, Me-27), 1.67 (3H, *s*, Me-26), 1.18 (3H, *s*, Me-29), 1.03 (6H, *s*, Me-19/Me-28), 0.99 (3H, s, Me-18), 0.98 (3H, *d*, *J* = 7.2 Hz, Me-21), 0.75 (3H, *s*, Me-30).

^{13}C NMR (100.61 MHz, MeOD): 148.7 (C-5), 133.3 (C-25), 130.5 (C-24), 122.1 (C-6), 99.0 (C-1'), 77.4 (C-3), 75.4 (C-5'), 74.4 (C-7), 73.0 (C-3'), 72.3 (C-2'), 69.1 (C-4'), 66.6 (C-23), 63.2 (C-6'), 52.3 (C-17), 49.9 (C-8), 49.2 (C-14), 47.3 (C-13), 45.7 (C-22), 42.4 (C-4), 40.1 (C-10), 35.7 (C-15), 35.1 (C-9), 33.8 (C-20), 33.7 (C-11), 31.5 (C-12), 30.1 (C-2), 29.4 (C-19), 28.8 (C-16/C-28), 26.1 (C-29), 26.0 (C-27), 22.3 (C-1), 19.3 (C-21), 18.8 (C-30), 18.2 (C-26), 16.1 (C-18).

Balsaminoside C, cucurbita-5,24-diene-3β,23(R)-diol-7-O-β-D-glucopyranoside (39)

White amorphous powder.

R_f (SiO_2, $CHCl_3$/MeOH, 17:3): 0.23.

$[\alpha]_D^{26}$ + 80 (*c* 0.09, MeOH); $[\alpha]_D^{26}$ Lit. + 89 (*c* 0.43, MeOH), (Fatope et al., 1990).

IR, ν_{max} cm^{-1} (KBr): 3347, 2938, 1636, 1455, 1382, 1076, 1032, 941.

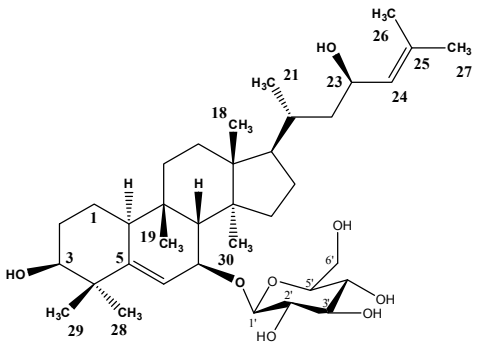

39

ESIMS, *m/z* (rel. int.): 643 $[M + Na]^+$ (16), 659 $[M + K]^+$ (32), 463 $[M + Na - C_6H_{12}O_6]^+$ (2), 203 $[Na + C_6H_{12}O_6]^+$ (100).

^{1}H NMR (400 MHz, MeOD): δ 5.75 (1H, *d*, *J* = 4.9 Hz, H-6), 5.16 (1H, *J* = 8.2 Hz, H-24), 4.40 (1H, *td*, *J* = 9.4, 3.0 Hz, H-23), 4.34 (1H, *d*, *J* = 7.7 Hz, H-1'), 4.11 (1H, *br d*, *J* = 7.0 Hz, H-7), 3.86 (1H, *dd*, *J* = 11.8, 2.4 Hz, H-6b'), 3.66 (1H, *dd*, *J* = 11.8, 5.4 Hz, H-6a'), 3.49 (1H, *br s*, H-3), 3.36 (1H, *m*, H-3'), 3.30 (1H, *m*, H-4'), 3.17 (1H, *m*, H-2'), 2.34 (1H, *br d*, *J* = 10.1 Hz, H-10), 2.12 (1H, *br s*, H-8), 1.74 (3H, *s*, Me-27), 1.66 (3H, *s*, Me-26), 1.18 (3H, *s*, Me-29), 1.03 (6H, *s*, Me-19/Me-28), 0.99 (3H, *s*, Me-18), 0.98 (3H, *d*, *J* = 6.5 Hz, Me-21), 0.75 (3H, *s*, Me-30).

^{13}C NMR (100.61 MHz, MeOD): 148.8 (C-5), 133.4 (C-25), 130.5 (C-24), 121.9 (C-6), 101.7 (C-1'), 78.3 (C-3'), 78.0 (C-5'), 77.5 (C-3), 75.1 (C-2'), 74.6 (C-7), 71.8 (C-4'), 66.6 (C-23), 62.8 (C-6'), 52.3 (C-17), 49.9 (C-8), 49.7 (C-14), 47.3 (C-13), 45.6 (C-22), 42.4 (C-4), 40.1 (C-10), 35.8 (C-15), 35.1 (C-9), 33.8 (C-20), 33.7 (C-11), 31.5 (C-12), 30.1 (C-2), 29.5 (C-19), 28.8 (C-16/C-28), 26.1 (C-29), 26.0 (C-27), 22.4 (C-1), 19.3 (C-21), 18.8 (C-30), 18.1 (C-26), 16.0 (C-18).

3.6.1. Study of fraction M6B

Fraction M6B (2 g) was recrystallized (*n*-hexane/EtOAc) to give 276 mg of an impure product, which was purified by column chromatography, using as eluents mixtures of CH_2Cl_2/MeOH (41:4 to 4:1), and by recrystallization (*n*-hexane/EtOAc) to afford 200 mg more of compound **38**. The mother liquors were subjected to column chromatography (SiO_2, 150 g), using as eluents mixtures of CH_2Cl_2/MeOH (41:4 to 4:1). After TLC monitoring, chromatographic fractions were combined into seven fractions ($M6B_1$ to $M6B_7$). Fraction $M6B_2$ (170 mg) was chromatographed, over SiO_2 (17 g), with mixtures of CH_2Cl_2/MeOH (93:7 to 1:1). Fractions eluted with CH_2Cl_2/MeOH (41:4) were purified by HPLC (210 nm, MeOH/H_2O, 4:1, 5 mL/min), to give 49 mg of compound **40** [balsaminoside A, 25-methoxycucurbita-5,23(*E*)-dien-3β-ol-O-β-D-allopyranoside, R_t 33 min].

***Balsaminoside A, 25-methoxycucurbita-5,23(E)-dien-3β-ol-7-O-β-D-allopyranoside (*40**)

White crystals.

Mp: 220 - 220 ºC (MeOH).

***R**f* (SiO_2, $CHCl_3$/MeOH, 17:3): 0.40; ***R**t* (HPLC, 210 nm, MeOH/H_2O, 4:1; 1 mL/min): 9.5 min.

$[\alpha]_D^{26}$ + 69.0 (*c* 0.10, MeOH).

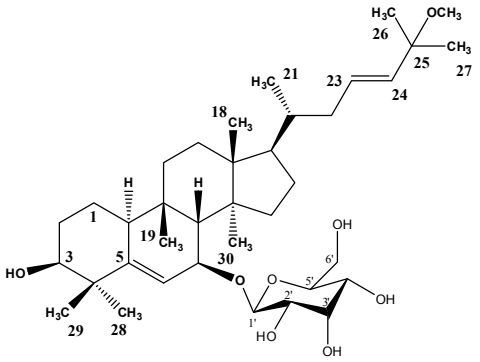

40

IR, ν_{max} cm^{-1} (KBr): 3409, 2928, 1456, 1375, 1068.

HR-ESITOFMS *m/z*: 657.4335 $[M + Na]^+$ (calcd. $C_{37}H_{62}O_8Na$ for: 657.4337).

ESIMS, *m/z* (rel. int.): 657 $[M + Na]^+$ (100), 673 $[M + K]^+$ (2), 478 $[M + H + Na - C_6H_{12}O_6]^+$ (1), 203 $[Na + C_6H_{12}O_6]^+$ (13).

^{1}H NMR (400 MHz, MeOD): δ 5.75 (1H, *d*, *J* = 4.9 Hz, H-6), 5.58 (1H, *m*, H-23), 5.38 (1H, *d*, *J* = 15.7 Hz, H-24), 4.75 (1H, *d*, *J* = 7.8 Hz, H-1'), 4.11 (1H, *br d*, *J* = 5.0 Hz, H-7), 4.05 (1H, *br s*, H-3'), 3.84 (1H, *d*, *J* = 9.8 Hz, H-6b'), 3.65 (1H, *m*, H-6a'), 3.50 (1H, *m*, H-4'), 3.49 (1H, *br s*, H-3), 3.32 (1H, *m*, H-2'), 3.14 (3H, *s*, 25-OMe), 2.33 (1H, *br d*, *J* = 9.8 Hz, H-10), 2.13 (1H, *br s*, H-8), 1.24 (6H, *s*, Me-26/Me-27), 1.18 (3H, *s*, Me-29), 1.03 (3H, *s*, Me-19/Me-28), 0.98 (3H, *s*, Me-18), 0.94 (3H, *d*, *J* = 5.8 Hz, Me-21), 0.74 (3H, *s*, Me-30).

^{1}H NMR (400 MHz, C_5D_5N): 6.09 (1H, *d*, *J* = 5.0 Hz, H-6), 5.64 (1H, *m*, H-23), 5.59 (1H, *d*, *J* = 7.6 Hz, H-1'), 5.58 (1H, *d*, *J* = 15.9 Hz, H-24), 4.79 (1H, *br s*, H-3'), 4.60 (2H, *m*, H-7/H-6b'), 4.53 (1H, *m*, H-5'), 4.48 (1H, *m*, H-6'), 4.32 (1H, *br s*, H-4'), 4.07 (1H, *br s*, H-2'), 3.82 (1H, *br s*, H-3), 3.23 (3H, *s*, 25-OMe), 2.46 (1H, *s*, H-8), 2.40 (1H, *m*, H-10), 1.46 (3H, *s*, Me-28), 1.40 (3H, *s*, Me-19), 1.34 (6H, *s*, Me-26/Me-27), 1.14 (3H, *s*, Me-29), 0.98 (3H, *d*, *J* = 4.8 Hz, Me-21), 0.82 (3H, *s*, Me-18), 0.73 (3H, *s*, Me-30).

^{13}C NMR (100.61 MHz, MeOD): 148.7 (C-5), 137.6 (C-24), 130.2 (C-23), 122.0 (C-6), 99.0 (C-1'), 77.5 (C-3), 76.5 (C-25), 75.4 (C-5'), 74.4 (C-7), 73.0 (C-3'), 72.3 (C-2'), 69.1 (C-4'), 63.2 (C-6'), 51.3 (C-17), 50.4 (25-OMe), 49.9 (C-8), 49.6 (C-14), 47.2 (C-13), 42.4 (C-4), 40.5 (C-22), 40.1 (C-10), 37.6 (C-20), 35.7 (C-15), 35.1 (C-9), 33.7 (C-11), 31.3 (C-12), 30.1 (C-2), 29.4 (C-19), 28.8 (C-16), 28.7 (C-28), 26.5 (C-27), 26.2 (C-26), 26.1 (C-29), 22.3 (C-1), 19.3 (C-21), 18.7 (C-30), 16.1 (C-18).

^{13}C NMR (100.61 MHz, C_5D_5N): 148.2 (C-5), 137.6 (C-24), 128.5 (C-23), 121.2 (C-6), 98.3 (C-1'), 76.1 (C-5'), 76.0 (C-3), 74.8 (C-25), 73.2 (C-3'), 72.4 (C-2'), 72.0 (C-7), 69.3 (C-4'), 63.3 (C-6'), 50.3 (C-17), 50.1 (7-OMe), 48.4 (C-14), 48.2 (C-8), 46.2 (C-13), 41.9 (C-4), 39.7 (C-22), 39.2 (C-10), 36.4 (C-20), 34.8 (C-15), 34.4 (C-9), 32.9 (C-12), 30.4 (C-16), 30.1 (C-2), 29.3 (C-19), 28.4 (C-11), 27.8 (C-28), 26.4 (C-27), 26.0 (C-26/C-29), 21.7 (C-1), 19.0 (C-21), 18.0 (C-30), 15.6 (C-18).

Biological assays

1. ANTIMALARIAL ACTIVITY

1.1. *In vitro* culture of *Plasmodium falciparum*

Human malaria parasites were cultured as previously described by Trager and Jensen (1976), with minor modifications (Trager and Jensen, 1976). Briefly, 3D7 and Dd2 *Plasmodium falciparum* strains were cultivated in recently collected erythrocytes as host cells in RPMI 1640 medium (Gibco), containing 25 mM HEPES (Sigma) and 6.8 mM hypoxanthine (Sigma) supplemented with 10% AlbuMAX II (Invitrogen). Cultures were maintained at 37ºC under an atmosphere of 5% O_2, 3 - 5% CO_2, and N_2. Drug-sensitivity assays were carried out on 96-well micro-plates, using a synchronized culture at ring-stage.

1.2. Antimalarial activity assay

The antimalarial activity was studied against *P. falciparum* intraerythrocytic stages. The screening of extracts and main fractions was carried out against the CQ sensitive *P. falciparum* 3D7, using the classical microscopic method. Pure compounds were tested against the CQ-sensitive (3D7) and CQ-resistant (Dd2) *P. falciparum* strains by means of a fluorometric method.

For the classical microscopic method, stock solutions of the extracts/fractions were prepared in ethanol or dimethyl sulfoxide (DMSO) and were diluted in RPMI to the required concentration until the final concentrations of samples in culture plate wells were 250, 100, 50, 25, 10, 5 and 1 μg/mL. Each well of a 96-well culture plate received 10 μL of parasite culture, with a parasitaemia between 0.6 - 0.8 % (5% haematocrit), and 90 μL of the different samples. The plates were incubated at 37ºC for 20 - 24 h, after confirmation of the presence of mature schizonts in negative control wells, without drug. At the end of this period, the erythrocytes from each well were harvested, and a thick film was prepared. The films were fixed with acetone, and stained for 1 hour in Giemsa stain at a dilution of 20 vol-% in buffered H_2O (pH 6.8). Three independent optical-microscopy readings of the number of schizonts with three or more nucleus were carried out in 200 parasitized red blood cells for

each dilution and duplicate. Growth inhibition was expressed as a percentage of the number of schizonts for each concentration, divided by the number of schizonts in untreated controls. Mean IC_{50} values were calculated from dose-response curves (percentage of schizonts vs. logarithm of drug concentration) by linear interpolation.

The antimalarial activity of the compounds was determined by a fluorometric method using SYBR Green I (Johnson et al., 2007; Smilkstein et al., 2004). In brief, stock solutions of the samples were prepared in DMSO (10 mg/mL), and were diluted to give a series of concentrations ranging from 0.156 to 100 μg/mL. 50 μL of each testing concentration, together with 50 μL of a 1% red blood parasitized cell suspension with ring stages and 2% haematocrit were distributed in duplicate, into each of the 96-well plates. Plates were incubated for 48 h at 37ºC. After, 100 μL of lysis buffer with SYBR Green I (Tris 20 mM; pH 7.5, EDTA - 5 mM, saponin - 0.008%; wt/vol, Triton X-100 - 0.08%; vol/vol, and 0.2 μL of SYBR Green I/mL of lysis buffer) were added to each well. Plates were covered, mixed and incubated in the dark at room temperature for 1 h. Fluorescence intensity was measured on a fluorescence multiwell plate reader, Anthos venyth 3100 (Alfagene) excitation and emission wavelengths of 485 nm and 535 nm, respectively. Values were expressed in relative fluorescence units. Evaluations of the results obtained and IC_{50} determination were performed with HN-NonLineV1.1 (H. Noedl, 2001) software.

2. CYTOTOXIC ACTIVITY

2.1. Cell culture, medium, and growth conditions

Human breast cancer MCF-7 cell line was cultured in RPMI 1640 medium supplemented with 10% heat inactivated horse serum, L-glutamine (2 mM), and antibiotics, in a humidified atmosphere of 5% CO_2 at 37 °C.

2.2. Cytotoxicity assay

The effects of increasing concentrations of the compounds on cell growth were tested in 96-well flat-bottomed microtiter plates. The compounds were diluted in a volume of 50 μL

cell culture medium. Then, 2×10^4 cells in 0.1 mL of culture medium were added to each well, with the exception of the medium control wells. The culture plates were further incubated at 37 °C for 24 h. At the end of the incubation period, 15 μL of MTT (thiazolyl blue, Sigma, St Louis, MO, USA) solution (from a 5 mg/mL stock) were added to each well. After incubation at 37 °C for 4 h, 100 μL of sodium dodecyl sulfate (SDS) (Sigma, St Louis, MO, USA) solution (10%) were added into each well and the plates were further incubated at 37 °C overnight. The cell growth was determined by measuring the optical density (OD) at 550 nm (ref. 630 nm) with a Dynatech MRX vertical beam ELISA reader. Inhibition of cell growth was determined according to the formula:

$$100-\left[\frac{\text{OD sample}-\text{OD medium control}}{\text{OD cell control}-\text{OD medium control}}\right]\times100$$

3. REVERSAL OF MULTIDRUG RESISTANCE ON L5178 MOUSE T-LYMPHOMA CELLS

Most of the MDR-reversing assays were carried out in collaboration with Prof. Joseph Molnár, at the University of Szeged (Department of Medical Microbiology and Immunobiology), Szeged, Hungary. The ethidium bromide accumulation assay (section 3.4) was performed in collaboration with Prof. Leonard Amaral, at Instituto de Higiene e Medicina Tropical, Lisbon, Portugal.

3.1. Cell culture, medium and growth conditions

L5178 mouse T-cell lymphoma cells were transfected with pHa *MDR1*/A retrovirus, as previously described (Cornwell et al., 1987; Pastan et al., 1988). *MDR1*-expressing cell lines were selected by culturing the MKJ infected cells with 60 ng/mL colchicine to maintain the expression of the MDR phenotype in all cells of the population (Choi et al., 1991). L5178 (parent, PAR) mouse T-cell lymphoma cells and the human *MDR1*-transfected subline were cultured in Mccoy's 5A medium supplemented with 10% heat-inactivated horse serum, L-glutamine and antibiotics (penicillin, streptomycin). These cell lines were cultured at 37°C, and 5% CO_2 atmosphere.

3.2. Antiproliferative assay

The effect of increasing concentrations of the drugs alone on cell growth was tested in 96-well flat-bottomed microtiter plates. The compounds were diluted in a volume of 50 μL cell culture medium. Then, 1×10^4 cells in 0.1 mL of culture medium were added to each well, with the exception of the medium control wells. The culture plates were further incubated at 37°C for 72 h; at the end of the incubation period, 15 μL of MTT (thiazoil blue, Sigma, St. Louis, MO, USA) solution (from a 5 mg/mL stock) was added to each well. After 4 h of incubation at 37°C, 100 μL of sodium dodecyl sulfate (SDS) (Sigma) solution (10%) was added to each well and the plates were further incubated at 37°C overnight. The cell growth was determined by measuring the optical density (OD) at 550 nm (ref. 630 nm) of each well with a Dynatec MRX vertical beam ELISA reader. Inhibition of the cell growth was determined according to the formula:

$$100-\left[\frac{\text{OD sample}-\text{OD medium control}}{\text{OD cell control}-\text{OD medium control}}\right]\times100$$

Where ID_{50} is defined as the inhibitory dose that reduces the growth of the compound-exposed cells by 50%. The ID_{50} values are expressed as means ± SD from three experiments.

3.3. Rhodamine-123 accumulation assay

The cells were adjusted to a density of 2×10^6 cells/mL, resuspended in serum-free McCoy's 5A medium and distributed in 0.5 mL aliquots into Eppendorf centrifuge tubes. 10 μL of the compounds to be tested were added to 0.5 mL of cells, yielding final concentrations between 0.5 - 20 μM. The samples were incubated for 10 min at room temperature, and 10 μL (5.2 mM final concentration) of the indicator rhodamine 123 were added. After 20 min of incubation at 37°C, the samples were washed twice and resuspended in 0.5 mL phosphate-buffered saline (PBS) for analysis. The fluorescence uptake of the cell population was measured with a Beckton Dickinson FACScan flow cytometry. Verapamil was used as a positive control in the rhodamine 123 exclusion experiments. The percentage mean fluorescence intensity was calculated for the treated MDR and parental cell lines as compared to untreated cells. An activity ratio FAR was calculated via the following equation, on the basis of the measured fluorescence values:

$$FAR = \frac{MDR\ treated\ /\ MDR\ control}{parental\ treated\ /\ parental\ control}$$

The results are from a representative flow cytometry experiment in which 10000 individual cells of the population were investigated; the histograms were evaluated based on the mean fluorescence intensity, standard deviation, peak channel in the total - and in the gated- populations.

3.4. Ethidium bromide accumulation assay

The cells were adjusted to a density of 2×10^6 cells/mL, centrifuged at 2000×*g* for 2 minutes and re-suspended in phosphate-buffered saline (PBS) pH 7.4. The cell suspension was distributed in 90 μL aliquots into 0.2 mL tubes. The tested compounds were individually added at different concentrations (3 and 30 μM) in 5 μL volumes of their stock solutions and the samples incubated for 10 minutes at 25ºC. Verapamil was used as a positive control (Spengler et al., 2009). After this incubation, 5 μL (1 μg/mL final concentration) of EB (20 μg/mL stock solution) were added to the samples and the tubes were placed into a Rotor-Gene 3000™ thermocycler with real-time analysis software (Corbett Research, Sidney, Australia) and the fluorescence monitored on a real-time basis. Prior to the assay, the instrument was programmed for temperature (37ºC), the appropriate excitation and emission wavelengths of EB (530 nm bandpass and 585 nm highpass, respectively), and the time and number of cycles for the recording of the fluorescence (Viveiros et al., 2008). The results were evaluated by Rotor-Gene Analysis Software 6.1 (Build 93) provided by Corbett Research. From the real-time data, the relative final fluorescence (RFF) of the last time point (minute 60) of the EB accumulation assay was calculated according to the formula:

Relative final fluorescence (RFF) = $RF_{treated} - RF_{untread}$

$RF_{treated}$ = relative fluorescence (RF) at the last time point of EB retention curve in the presence of an inhibitor.

$RF_{untread}$ = relative fluorescence at the last time point of EB retention curve of the untreated control having the solvent control (DMSO).

3.5. Checkerboard microplate method

The microplate method was applied to study the effects of drug interactions between resistance modifiers and doxorubicin on cancer cells (Eliopoulos, 1991). The effects of the anticancer drug doxorubicin and the resistance modifiers in combination were studied on *MDR1* gene-transfected mouse lymphoma cells. The dilution of doxorubicin (A) was made in a horizontal direction, and the dilutions of resistance modifiers (B) vertically in the microtiter plate, in a volume of 100 μL. The cell suspension in the tissue culture medium was distributed into each well in 100 mL containing 5×10^4 cells. The plates were incubated for 48 h at 37 °C under 5% of CO_2. The cell growth rate was determined after MTT staining and the intensity of the blue colour was measured on a micro ELISA reader. Drug interactions were evaluated according to the following system:

$FIC_A = ID_{50\ A\ in\ combination} / ID_{50\ A\ alone}$

$FIC_B = ID_{50\ B\ in\ combination} / ID_{50\ B\ alone}$

ID= inhibitory dose

FIC =fractional inhibitory concentration

FIX ≤ 0.5 Synergism

FIX = 0.51 - 1 Additive effect

FIX=1 - 2 Indifferent effect

FIX > 2 Antagonism

FIX= Fractional inhibitory index

$FIX = FIC_A + FIC_B$

4. REVERSAL OF MULTIDRUG RESISTANCE ON BACTERIAL STRAINS

These assays were carried out in collaboration with Prof. Leonard Amaral, at Instituto de Higiene e Medicina Tropical, Lisbon, Portugal.

4.1. Bacterial strains

The study was conducted with Gram-positive [methicillin-resistant *Staphylococcus aureus* (MRSA) COL_{OXA}, and *Enterococcus faecalis* ATCC 29212] and Gram-negative strains (*Escherichia coli* AG100, *Escherichia coli* $AG100_{TET8}$, *Salmonella enteritidis* 5408, and *Salmonella enteritidis* 5408_{CIP}). MRSA COL, gently provided by Prof. Hermínia de

Lencastre, Molecular Genetics Lab, Instituto de Tecnologia Química e Biológica da Universidade Nova de Lisboa (Crisostomo et al., 2001; Oliveira and de Lencastre, 2002; Oliveira et al., 2001), was adapted to 1600 mg/L of oxacillin, and named MRSA COL_{OXA} (Martins et al., 2007). *E. faecalis* ATCC 29212 was obtained from the American Type Culture Collection (ATCC). *E. coli* AG100 strain was exposed to increasing concentrations of tetracycline (TET) (Viveiros et al., 2005) leading to an efflux pump over-expressed strain, *Escherichia coli* $AG100_{TET8}$. *Salmonella enteritidis* 5408, and *Salmonella enteritidis* 5408 adapted to 16 mg/L of ciprofloxacin (CIP), named *Salmonella enteritidis* 5408_{CIP}, were gently provided by Professor Seamus Fanning, Centre for Food Safety, School of Agriculture, Food Science and Veterinary Medicine, University College Dublin, Ireland.

4.2. Growth conditions

The *E. coli* strains were grown in Luria Bertani broth media at 37ºC (components for this media were purchased from: peptone and Yeast E from Merck, Germany and NaCl from Panreac, Spain). Other bacteria strains were grown at 37ºC in Tryptic Soya broth (TSB) and Tryptic Soya agar (TSA), both purchased from Oxoid, England.

4.3. Determination of minimal inhibitory concentration (MIC) values

The MIC values of the compounds were determined by the broth micro dilution method in Muller-Hinton broth (MHB) (Oxoid, England), according to Clinical and Laboratory Standards Institute (CLSI) (Espinel-Ingroff et al., 2007) recommendations. Briefly, a stock solution of the compound to be tested was prepared and an aliquot added to MHB on the 96-well plates. Serial dilutions in the following wells were performed. Then, an over-night bacterial inoculum was diluted to McFarland 0.5 in MHB and added to wells. The MIC, defined as the lower concentration of compound at which the media does not present visible growth of the strain, was determined after 16 h and 18 h of incubation at 37ºC.

4.4. Ethidium bromide accumulation assay

The accumulation activity of some isolated compounds was assessed by the semiautomated ethidium bromide (EB) method using the Rotor-Gene 3000TM thermocycler with real-time analysis software (Corbett Research, Australia) (Viveiros et al., 2008), and the bacterial strains previously described. Briefly, strains were cultured in MHB medium until they reached an OD of 0.6 at 600 nm, centrifuged at 13.000 rpm for 3 minutes. The pellets were re-suspended in phosphate-buffered saline (PBS) pH 7.4, and the OD adjusted to 0.6. Aliquots of 1.0 mL were transferred to micro tubes, centrifuged, and the pellets re-suspended in PBS. The cell suspension was distributed in 45 μL aliquots into 0.2 mL tubes. The tested compounds were individually added at different concentrations (3 and 30 μM) in 5 μL volumes of their stock solutions, and finally 45 μL of EB (Sigma-Aldrich Química SA, Spain) were added (1 μg/mL or 0.5 μg/mL final concentration). The tubes were placed into a Rotor-Gene 3000^{TM} thermocycler with real-time analysis software (Corbett Research, Sidney, Australia) and the fluorescence monitored on a real-time basis (Viveiros et al., 2008).

CHAPTER 5

Conclusion

The main goal of this dissertation was to search for new antimalarials from plants used in traditional medicine, and also to contribute to the scientific validation of their use. Another objective was to evaluate the effect of isolated compounds as multidrug resistance modulators.

Screening for antimalarial activity

The claimed antimalarial properties of fifty eight extracts from fifteen plants, used in traditional medicine against malaria and/or fever, mainly from Mozambique, were evaluated against the chlroroquine-sensitive 3D7 *Plasmodium falciparum* strain. Plant parts used in traditional medicine, from selected species (*Acacia karroo*, *Aloe parvibracteata*, *Bridelia cathartica*, *Cassia abbreviata*, *Cassia occidentalis*, *Crossopteryx febrifuga*, *Leonotis leonurus*, *Momordica balsamina*, *Parkinsonia aculeata*, *Pittosporum tobira*, *Senna didymobotrya*, *Schefflera actinophylla*, *Tabernaemontana elegans* and *Trichilia emetica*) were extracted with apolar and polar solvents. The highest activity was found for ethyl acetate extracts of the aerial parts of *Momordica balsamina* (IC_{50} = 1.0 μg/mL and *Pittosporum tobira* (IC_{50} = 4.8 μg/mL). Significant IC_{50} values were also found for the *n*-hexane extract of *Cassia occidentalis* (IC_{50} = 19.3 μg/mL), and *n*-hexane and CH_2Cl_2 extracts of *Parkinsonia aculeata* (IC_{50} = 24.5 μg/mL). Based on the results obtained, *Momordica balsamina* L. (Cucurbitaceae) was selected for further phytochemical studies.

Phytochemical study of Momordica balsamina

A bioassay-guided fractionation of the methanol extract of *Momordica balsamina* led to the isolation of fourteen new cucurbitane-type triterpenoids (**3**, **26** - **36**, **38**, and **40**). The known cucurbitane triterpenoids **1**, **2**, **4**, **37**, **39**, and one megastigmane-type *nor*-isoprenoid (**25**) were also isolated.

In order to obtain a higher homologous series of compounds required for some structure-activity relationships, balsaminol F (**3**), and karavilagenin C (**1**), isolated in large amount, were derivatized. Balsaminol F yielded two new esters, triacetylbalsaminol F (**23**)

and tribenzoylbalsaminol F (**24**). On the other hand, karavilagenin C (**1**) was esterified, using several acylating agents, and eighteen new mono and diacyl derivatives (**5** - **22**) were obtained. The esters differ in the substitution pattern at C-3 and C-23.

Their chemical structures were deduced from their physical and spectroscopic data (IR, MS, HRMS, ^{1}H and ^{13}C NMR and 2D NMR experiments - COSY, HMQC, HMBC and NOESY experiments). Some of the new compounds feature unusual oxidation patterns, reported for the first time in cucurbitane triterpenoids from plant sources, such as at C-29 (balsaminagenins A, B, balsaminols A, B, C, D, and balsaminapentaol) and C-12 (cucurbalsaminols A - C). Moreover, balsaminapentaol (**36**) has a 23,24-diol system coupled with an exocyclic double bond in the side chain, found for the first time in compounds with the cucurbitane skeleton.

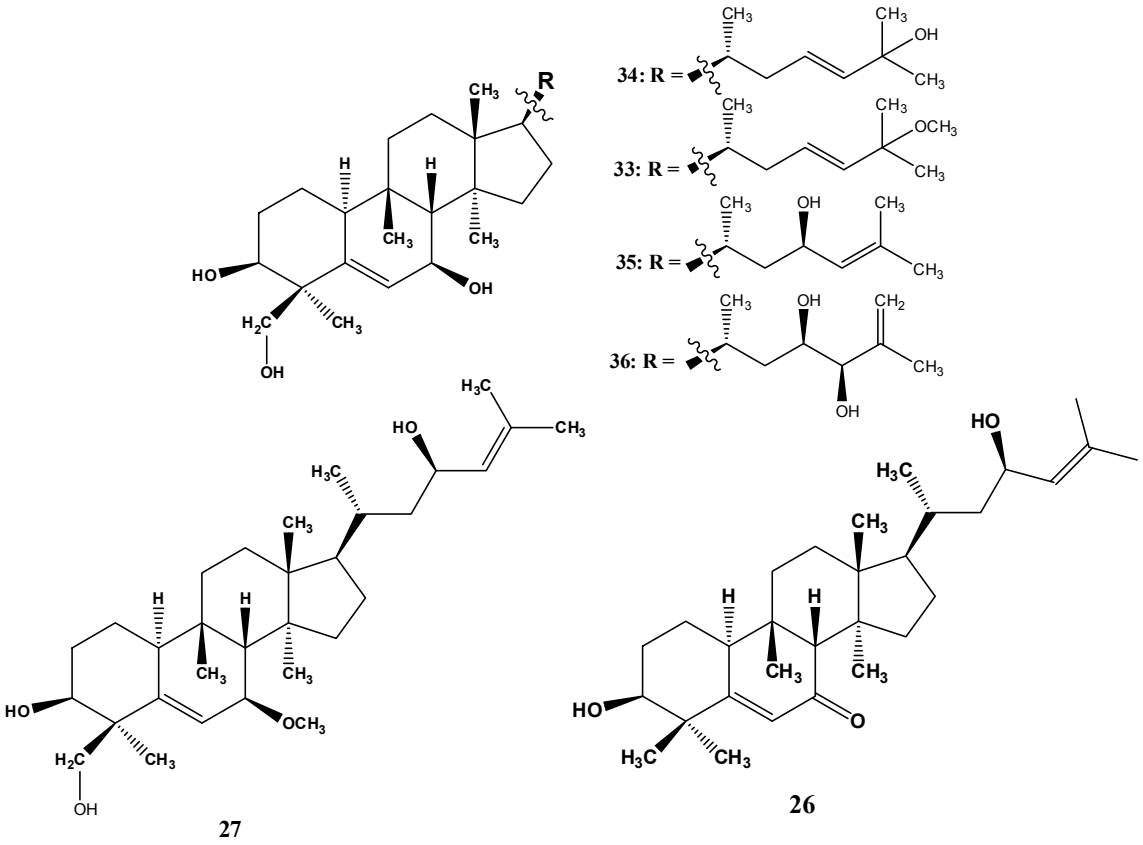

26: *Balsaminol E* [cucurbita-5,24-dien-7-one-3β,23(*R*)-diol

27: *Balsaminol B* [7β-methoxycucurbita-5,24-diene-3β,23(*R*),29-triol]

33: *Balsaminagenin B* [25-methoxycucurbita-5,23(*E*)-diene-3β,7β,29-triol]

34: *Balsaminagenin A* [cucurbita-5,23(*E*)-diene-3β,7β,25,29-tetraol]

35: *Balsaminol A* [cucurbita-5,24-diene-3β,7β,23(*R*),29-tetraol]

36: *Balsaminapentaol* [cucurbita-5,25-diene-3β,7β,23(*R*),24(*R*),29-pentaol]

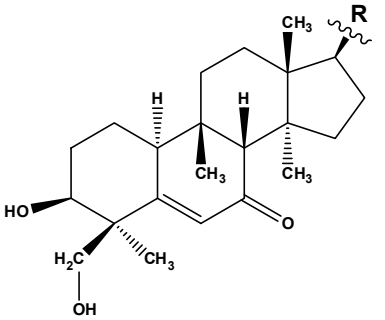

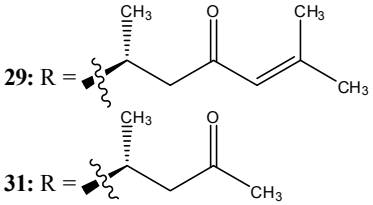

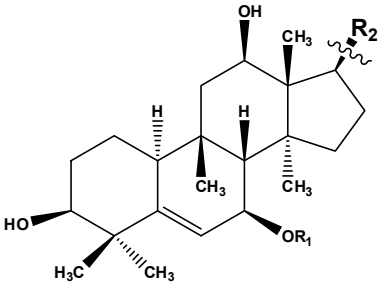

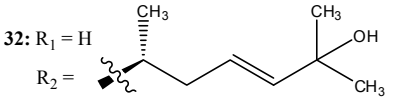

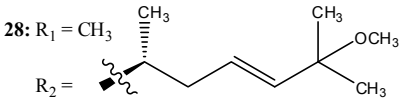

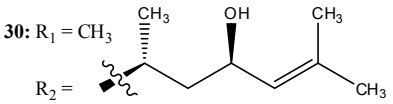

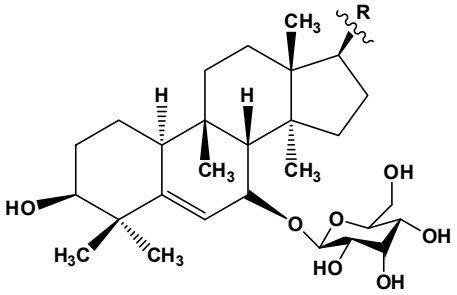

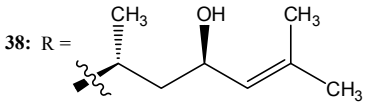

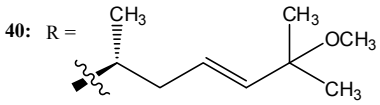

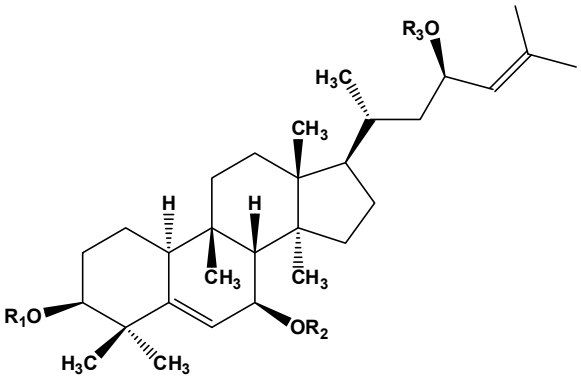

3: R_1 = H; R_2 = H; R_3 = H

23: R_1 = Ac; R_2 = Ac ; R_3 = Ac

24: R_1 = Bz; R_2 = Bz; R_3 = Bz

3: *Balsaminol F* [cucurbita-5,24-diene-3β,7β,23(*R*)-triol]

23: *Triacetilbalsaminol F* [3β,7β,23(*R*)-triacetoxycucurbita-5,24-diene]

24: *Tribenzoylbalsaminol F* [3β,7β,23(*R*)-triacetoxycucurbita-5,24-diene]

29: *Balsaminol C* [cucurbita-5,24-diene-7,23-dione-3*β*, 29-diol]

28: *Cucurbalsaminol B* [7β-methoxycucurbita-5,23(*E*)-diene-3*β*,12*β*,25-triol]

30: *Cucurbalsaminol A* [cucurbita-5,23(*E*)-diene-3*β*,7*β*,12*β*,25-tetraol]

31: *Balsaminol D* [25,26,27-*trinor*-cucurbit-5-ene-7,23-dione-3*β*, 29-diol]

32: *Cucurbalsaminol C* [7β-methoxycucurbita-5,24-diene-3β,12β,23(*R*)-triol]

38: *Balsaminoside B* [cucurbita-5,24-diene-3β,23(*R*)-diol-7-O-β-D-allopyranoside]

40: *Balsamioside A* [25-methoxycucurbita-5,23(*E*)-dien-3β-ol-7-O-β-D-allopyranoside]

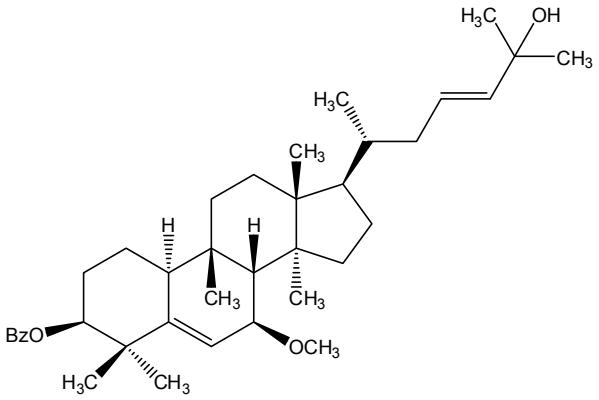

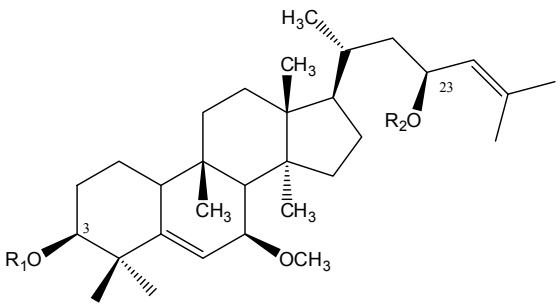

Karavoate G (**11**)

R_1	R_2	
5: H	Ac	*Karavoate A* [23(*R*)-acetoxy-7β-methoxycucurbita-5,24-dien-3*β*-ol]
6: Ac	Ac	*Karavoate B* [3β,23(*R*)-diacetoxy-7β-methoxycucurbita-5,24-diene]
7: H	Pr	*Karavoate C* [23(*R*)-propanoyloxy-7β-methoxycucurbita-5,24-dien-3*β*-ol]
8: Pr	Pr	*Karavoate D* [3β,23(*R*)-dipropanoyloxy-7β-methoxycucurbita-5,24-diene]
9: H	Bu	*Karavoate E* [23(*R*)-butanoyloxy-7β-methoxycucurbita-5,24-dien-3*β*-ol]
10: Bu	Bu	*Karavoate F* [3β,23(*R*)-dibutanoyloxy-7β-methoxycucurbita-5,24-diene]
11:		*Karavoate G* [3β-benzoyloxy-7β-methoxycucurbita-5,23-dien-25-ol]
12: Bz	Bz	*Karavoate H* [3β,23(*R*)-dibenzoyloxy-7β-methoxycucurbita-5,24-diene]
13: H	*p*-nitroBz	*Karavoate I* [23(*R*)-(*p*-nitrobenzoyloxy)-7β-methoxycucurbita-5,24-dien-3*β*-ol]
14: *p*-nitroBz	*p*-nitroBz	*Karavoate J* [3β,23(*R*)-di-(*p*-nitrobenzoyloxy)-7β-methoxycucurbita-5,24-diene]
15: H	*p*-chloroBz	*Karavoate K* [23(*R*)-(*p*-chlorobenzoyloxy)-7β-methoxycucurbita-5,24-dien-3*β*-ol]
16: *p*-chloroBz	*p*-chloroBz	*Karavoate L* [3β,23(*R*)-di-(*p*-chlorobenzoyloxy)-7β-methoxycucurbita-5,24-diene]
17: H	*p*-methoxyBz	*Karavoate M* [23(*R*)-(*p*-methoxybenzoyloxy)-7β-methoxycucurbita-5,24-dien-3*β*-ol]
18: *p*-methoxyBz	*p*-methoxyBz	*Karavoate N* [3β,23(*R*)-di-(*p*-methoxybenzoyloxy)-7β-methoxycucurbita-5,24-diene]
19: H	Cin	*Karavoate O*,[23(*R*)-cinnamoyloxy-7β-methoxycucurbita-5,24-dien-3*β*-ol]
20: Cin	Cin	*Karavoate P* [3β,23(*R*)-cinnamoyloxy-7β-methoxycucurbita-5,24-diene]
21: H	Suc	*Karavoate Q* [23(*R*)-succinoyloxy-7β-methoxycucurbita-5,24-dien-3*β*-ol]
22: Suc	Suc	*Karavoate R* [3*β*,23(*R*)-disuccinoyloxy-7β-methoxycucurbita-5,24-diene]

Antimalarial activity

The isolated compounds (**1** - **4** and **26** - **40**), together with the acyl derivatives **5** - **20** and **23** - **24** were evaluated for their antimalarial activity against the *Plasmodium falciparum* CQ-sensitive (3D7) and CQ-resistant (Dd2) strains. The cytotoxic activity of the compounds

against human breast cancer cell line (MCF-7) was evaluated in order to calculate the selectivity index (ratio between cytotoxic and parasitic activities).

Most of the compounds displayed antimalarial activity. Among the isolated compounds, the glycoside derivatives (**37 - 40**) and karavilagenin E (**4**) revealed the highest activity against both strains of *P. falciparum*, displaying IC_{50} < 9 μM. Significant antiplasmodial activity was also found for karavilagenin C (**1**, IC_{50} = 10.4 and 11.2 μM, for 3D7 and Dd2, respectively).

Regarding the esters of balsaminol F and karavilagenin C, a remarkable increase in the activity was found for most of the alkanoyl (mono and diacylated) and mono aroyl esters. The strongest antimalarial activity, against the resistant strain, was found for triacetylbalsaminol F (**23**), being 50-fold (IC_{50} = 0.4 μM, for Dd2) more active than balsaminol F (**3**, IC_{50} = 20.0 μM for Dd2). Similarly, a strong activity was also observed for the alkanoyl diesters, karavoates B (**6**, IC_{50} = 0.5 and 0.5 μM, for 3D7 and Dd2, respectively) and D (**8**, IC_{50} = 1.5 and 0.4 μM, for 3D7 and Dd2, respectively). In fact, when compared with karavilagenin C (**1**), karavoate B was approximately 20-fold more active against both strains. Regarding the aroyl mono-derivatives of karavilagenin C, karavoates I (**13**, IC_{50} = 2.6 and 0.5 μM, for 3D7 and Dd2, respectively) and M (**17**, IC_{50} = 1.3 and 0.6 μM, for 3D7 and Dd2, respectively), bearing a *p*-nitrobenzoyl and a *p*-methoxybenzoyl moiety at C-23, respectively, also displayed a strong activity against the Dd2 resistant strain. However, a decrease of activity was observed when both positions, C-3 and C-23, bear an aroyl or cinnamoyl moiety, as shown for karavoates H (**12**), J (**14**), L (**16**) and O (**20**), suggesting that molecular esteric effects may influence the antimalarial activity. In fact, esters with molecular volumes between 536.1 - 618.4 showed an excellent/good activity, and those with values between 682.3 - 739.9 showed a weak activity or were inactive. Moreover, for isolated compounds, it was observed that the substitution pattern at ring B may also play an important role in the antiplasmodial activity.

The compounds either were not cytotoxic or showed a weak cytotoxicity (IC_{50} > 13.5 μM) against the cell line tested. Most of the isolated compounds showed low SI values (SI < 7). Conversely, the majority of the ester derivatives displayed high SI values.

Reversal of multidrug resistance in cancer cells

The evaluation of MDR-reversal activity, of the isolated compounds (**1** - **4** and **26** - **40**), along with the acyl derivatives **5** - **24**, in a non-toxic concentration, was also carried out on L15178 mouse T-lymphoma cell line transfected with the human *mdr1* gene, by flow cytometry. A standard functional assay, which measures rhodamine-123 accumulation, was used. At the highest concentration (20 μM) most of the isolated compounds were found to be strong P-gp inhibitors. At this concentration, the highest effects were observed for balsaminol C (**29**, FAR = 2.9 and 198.9 at 2 and 20 μM, respectively) and balsaminagenin B (**33**, FAR = 6.0 and 104.2 at 2 and 20 μM, respectively), which showed a manifold activity when compared with that of the positive control verapamil (FAR = 7.4 - 9.6 at 22 μM). At the low concentration (2 μM), karavilagenin C (**1**, FAR = 42.1 at 2 μM), exhibited the highest effect in reversing MDR, being a very strong inhibitor of the efflux-pump activity of P-glycoprotein, even in a lower concentration (**1**, FAR = 1.5, 15.0 at 0.5, 1 μM, respectively). When comparing FAR values of karavilagenin C with its esters, lower values were found for the latters, suggesting that free hydroxyl groups at both C-3 and C-23 are crucial for reversing activity. On the other hand, the presence of methoxyl groups at C-7 and C-25 seems to increase MDR reversal activity. Furthermore, this work corroborates the importance of lipophilicity and H-bonding potential as general structural requirements for P-gp modulation. However, the most active compounds were not those with the highest log *P* values as exemplified by the decrease of activity found for the esters. Probably, some optimal lipophilicity needs to exist for an effective MDR reversal.

In the checkerboard model of combination chemotherapy, the interaction between doxorubicin and some compounds was also assayed. Most of the compounds synergistically enhanced the effect of the anticancer drug, doxorubicin.

Balsaminagenins A (**34**), B (**33**), karavilagenin C (**1**) and balsaminoside A (**40**), which showed a strong anti-MDR activity by the flow cytometric technique, were also investigated for their potential ability as MDR modulators, in the same cells, using a real-time fluorometry assay that employs ethidium bromide. The results obtained with this method were in accordance with those obtained in the flow cytometry assay. Similarly, karavilagenin C (**1**) showed the highest activity at the lower concentration tested.

Reversal of multidrug resistance on bacterial strains

Compounds **1**, **3**, **33** - **35**, and **40** were also evaluated for their ability to reverse the activity of bacterial efflux pumps of some Gram-positive [methicillin-resistant *Staphylococcus aureus* highly resistant to oxacillin (MRSA COL_{OXA}) and *Enterococcus faecalis* ATCC 29212] and Gram-negative (*Salmonella enteritidis* 5408, and *Salmonella enteritidis* 5408_{CIP}) resistant strains, using the same fluorometric assay. Furthermore, compounds **1**, **33**, and **40** were also tested on two resistant strains of *Escherichia coli* (*E. coli* AG100, *E. coli* $AG100_{TET8}$). Karavilagenin C (**1**), balsaminol F (**3**), and balsaminoside A (**40**) were able to inhibit, significantly, the efflux of ethidium bromide in $MRSA_{oxa}$, and *E. faecalis* ATCC29212. To the Gram-negative bacteria tested no significant activity was observed. A good correlation between $MRSA_{oxa}$ reversal activity and the topological polar surface area of compounds was found.

The study of *Momordica balsamina*, traditionally used to treat various diseases, mostly malaria and/or fever associated with malarial symptoms, infections, and diabetes in many African countries, was focused in this project. This work represents a contribution, not only to the phytochemical study of *M. balsamina*, but principally supports the biological importance of the main constituents of this species, cucurbitane-type triterpenoids. These compounds showed to be interesting leads for the development of new antimalarials, and also reversers of MDR in both cancer cells and bacteria strains. Further studies will be needed in order to improve their biological activities, and enhance the knowledge of their real targets.

Finally, it is important to emphasise that this study contributed to the scientific validation of the use of the *M. balsamina* against malaria in Mozambique. Although plants are widely used in the traditional medicine to treat several diseases, few data are available on their safety and effectiveness. This is the case of Mozambique, where medicinal plants are sold in markets or prescribed by traditional healers without any control whatsoever.

References

Agil, A., Miro, M., Jimenez, J., Aneiros, J., Caracuel, M.D., Garcia-Granados, A. and Navarro, M.C., 1999. Isolation of an anti-hepatotoxic principle from the juice of *Ecballium elaterium*. Planta Medica 65, 673-675.

Ajikumar, P.K., Tyo, K., Carlsen, S., Mucha, O., Phon, T.H. and Stephanopoulos, G., 2008. Terpenoids: Opportunities for biosynthesis of natural product drugs using engineered microorganisms. Molecular Pharmaceutics 5, 167-190.

Akihisa, T., Hayakawa, Y., Tokuda, H., Banno, N., Shimizu, N., Suzuki, T. and Kimura, Y., 2007a. Cucurbitane glycosides from the fruits of *Siraitia grosvenorii* and their inhibitory effects on Epstein-Barr virus activation. Journal of Natural Products 70, 783-788.

Akihisa, T., Higo, N., Tokuda, H., Ukiya, M., Akazawa, H., Tochigi, Y., Kimura, Y., Suzuki, T. and Nishino, H., 2007b. Cucurbitane-type triterpenoids from the fruits of *Momordica charantia* and their cancer chemopreventive effects. Journal of Natural Products 70, 1233-1239.

Aller, S.G., Yu, J., Ward, A., Weng, Y., Chittaboina, S., Zhuo, R.P., Harrell, P.M., Trinh, Y.T., Zhang, Q.H., Urbatsch, I.L. and Chang, G., 2009. Structure of P-glycoprotein reveals a molecular basis for poly-specific drug binding. Science 323, 1718-1722.

Amorim, C.Z., Marques, A.D. and Cordeiro, R.S.B., 1991. Screening of the antimalarial activity of plants of the Cucurbitaceae family. Memorias Do Instituto Oswaldo Cruz 86, 177-180.

Ansari, N.M., Houlihan, L., Hussain, B. and Pieroni, A., 2005. Antioxidant activity of five vegetables traditionally consumed by South-Asian migrants in Bradford, Yorkshire, UK. Phytotherapy Research 19, 907-911.

Asawamahasakda, W., Ittarat, I., Chang, C.C., McElroy, P. and Meshnick, S.R., 1994. Effects of antimalarials and protease inhibitors on plasmodial hemozoin production. Molecular and Biochemical Parasitology 67, 183-191.

Avendano, C. and Menendez, J.C., 2002. Inhibitors of multidrug resistance to antitumor agents (MDR). Current Medicinal Chemistry 9, 159-193.

Balliano, G., Caputo, O., Viola, F., Delprino, L. and Cattel, L., 1983a. Biosynthesis of cucurbitacins .1. The transformation of 10-alpha-cucurbita-5,24-dien-3-beta-ol into cucurbitacin C by seedlings of *Cucumis sativus*. Phytochemistry 22, 909-913.

Balliano, G., Caputo, O., Viola, F., Delprino, L. and Cattel, L., 1983b. Conversion of cyclolaudenol to 24 alpha-ethylsterol and 24 beta-ethylsterols in the Cucurbitaceae. Lipids 18, 302-305.

Bandeira, S.O., Gaspar, F. and Pagula, F.P., 2001. African ethnobotany and healthcare: Emphasis on Mozambique. Pharmaceutical Biology 39, 70-73.

Banzouzi, J.T., Soh, P.N., Mbatchi, B., Cave, A., Ramos, S., Retailleau, P., Rakotonandrasana, O., Berry, A. and Benoit-Vical, F., 2008. *Cogniauxia podolaena*: Bioassay-guided fractionation of defoliated stems, isolation of active compounds, antiplasmodial activity and cytotoxicity. Planta Medica 74, 1453-1456.

Basch, E., Gabardi, S. and Ulbricht, C., 2003. Bitter melon (*Momordica charantia*): A review of efficacy and safety. American Journal of Health-System Pharmacy 60, 356-359.

Bates, D.M., Robinson, R.W., Jeffrey, C., 1990. Biology and utilization of the Cucurbitaceae. In: C. Jeffrey (Ed.), Systematics of the Cucurbitaceae: an overview, Cornell University Press, Ithaca, NY, USA, pp. 3-9.

Batista, R., Silva, A.D. and de Oliveira, A.B., 2009. Plant-derived antimalarial agents: New leads and efficient phytomedicines. Part II. Non-alkaloidal natural products. Molecules 14, 3037-3072.

Belofsky, G., Percivill, D., Lewis, K., Tegos, G.P. and Ekart, J., 2004. Phenolic metabolites of *Dalea versicolor* that enhance antibiotic activity against model pathogenic bacteria. Journal of Natural Products 67, 481-484.

Beloin, N., Gbeassor, M., Akpagana, K., Hudson, J., de Soussa, K., Koumaglo, K. and Arnason, J.T., 2005. Ethnomedicinal uses of *Momordica charantia* (Cucurbitaceae) in Togo and relation to its phytochemistry and biological activity. Journal of Ethnopharmacology 96, 49-55.

Benoit-Vical, F., Grellier, P., Abdoulaye, A., Moussa, I., Ousmane, A., Berry, A., Ikhiri, K. and Poupat, C., 2006. *In vitro* and *in vivo* antiplasmodial activity of *Momordica balsamina* alone or in a traditional mixture. Chemotherapy 52, 288-292.

Bohlmann, J. and Keeling, C.I., 2008. Terpenoid biomaterials. Plant Journal 54, 656-669.

Bohlmann, J., Meyer-Gauen, G. and Croteau, R., 1998. Plant terpenoid synthases: Molecular biology and phylogenetic analysis. Proceedings of the National Academy of Sciences of the United States of America 95, 4126-4133.

Bot, Y.S., Mgbojikwe, L.O., Chika, N., Alash'le, A., Jelpe, D. and Demas, D., 2007. Screening of the fruit pulp extract of *Momordica balsamina* for anti HIV property. African Journal of Biotechnology 6, 47-52.

Cantrell, C.L., Lu, T.S., Fronczek, F.R., Fischer, N.H., Adams, L.B. and Franzblau, S.G., 1996. Antimycobacterial cycloartanes from *Borrichia frutescens*. Journal of Natural Products 59, 1131-1136.

Cappellini, M.D. and Fiorelli, G., 2008. Gluclose-6-phosphate dehydrogenase deficiency. Lancet 371, 64-74.

Chang, C.I., Chen, C.R., Liao, Y.W., Cheng, H.L., Chen, Y.C. and Chou, C.H., 2006. Cucurbitane-type triterpenoids from *Momordica charantia*. Journal of Natural Products 69, 1168-1171.

Chang, C.I., Chen, C.R., Liao, Y.W., Cheng, H.L., Chen, Y.C. and Chou, C.H., 2008. Cucurbitane-type triterpenoids from the stems of *Momordica charantia*. Journal of Natural Products 71, 1327-1330.

Chang, C.I., Chen, C.R., Liao, Y.W., Shih, W.L., Cheng, H.L., Tzeng, C.Y., Li, J.W. and Kung, M.T., 2010. Octanorcucurbitane triterpenoids protect against tert-butyl hydroperoxide-induced hepatotoxicity from the stems of *Momordica charantia*. Chemical & Pharmaceutical Bulletin 58, 225-229.

Chang, G. and Roth, C.B., 2001. Structure of MsbA from *E. coli*: A homolog of the multidrug resistance ATP binding cassette (ABC) transporters. Science 293, 1793-1800.

Chen, C., Qiang, S., Lou, L.G. and Zhao, W.M., 2009a. Cucurbitane-Type Triterpenoids from the Stems of *Cucumis melo*. Journal of Natural Products 72, 824-829.

Chen, J.C., Chiu, M.H., Nie, R.L., Cordell, G.A. and Qiu, S.X., 2005. Cucurbitacins and cucurbitane glycosides: Structures and biological activities. Natural Product Reports 22, 386-399.

Chen, J.C., Liu, W.Q., Lu, L., Qju, M.H., Zheng, Y.T., Yang, L.M., Zhang, X.M., Zhou, L. and Li, Z.R., 2009b. Kuguacins F-S, cucurbitane triterpenoids from *Momordica charantia*. Phytochemistry 70, 133-140.

Chen, J.C., Lu, L., Zhang, X.M., Zhou, L., Li, Z.R. and Qiu, M.H., 2008a. Eight new cucurbitane glycosides, kuguaglycosides A-H, from the root of *Momordica charantia* L. Helvetica Chimica Acta 91, 920-929.

Chen, J.C., Tian, R.R., Qiu, M.H., Lu, L., Zheng, Y.T. and Zhang, Z.Q., 2008b. Trinorcucurbitane and cucurbitane triterpenoids from the roots of *Momordica charantia*. Phytochemistry 69, 1043-1048.

Chen, W.J., Wang, J., Qi, X.Y. and Xie, B.J., 2007. The antioxidant activities of natural sweeteners, mogrosides, from fruits of *Siraitia grosvenorii*. International Journal of Food Sciences and Nutrition 58, 548-556.

Choi, K., Frommel, T.O., Stern, R.K., Perez, C.F., Kriegler, M., Tsuruo, T. and Roninson, I.B., 1991. Multidrug resistance after retroviral transfer of the human *mdr1* gene correlates with P-glycoprotein density in the plasma-membrane and is not affected by cytotoxic selection. Proceedings of the National Academy of Sciences of the United States of America 88, 7386-7390.

Clarkson, C., Maharaj, V.J., Crouch, N.R., Grace, W.M., Pillay, P., Matsabisa, M.G., Bhagwandin, N., Smith, P.J. and Folb, P.I., 2004. *In vitro* antiplasmodial activity of medicinal plants native to or naturalised in South Africa. Journal of Ethnopharmacology 92, 177-191.

Cooke, B.M., Wahlgren, M. and Coppel, R.L., 2000. Falciparum malaria: Sticking up, standing out and out-standing. Parasitology Today 16, 416-420.

Cooper, R.A., Ferdig, M.T., Su, X.Z., Ursos, L.M.B., Mu, J.B., Nomura, T., Fujioka, H., Fidock, D.A., Roepe, P.D. and Wellems, T.E., 2002. Alternative mutations at position 76 of the vacuolar transmembrane protein PfCRT are associated with chloroquine resistance and unique stereospecific quinine and quinidine responses in *Plasmodium falciparum*. Molecular Pharmacology 61, 35-42.

Cooper, R.A., Hartwig, C.L. and Ferdig, M.T., 2005. pfcrt is more than the *Plasmodium falciparum* chloroquine resistance gene: A functional and evolutionary perspective. Acta Tropica 94, 170-180.

Corea, G., Di Pietro, A., Dumontet, C., Fattorusso, E. and Lanzotti, V., 2009. Jatrophane diterpenes from *Euphorbia* spp. as modulators of multidrug resistance in cancer therapy. Phytochemistry Reviews 8, 431-447.

Cornwell, M.M., Pastan, I. and Gottesman, M.M., 1987. Certain calcium-channel blockers bind specifically to multidrug-resistant human-kb carcinoma membrane-vesicles and inhibit drug-binding to P-glycoprotein. Journal of Biological Chemistry 262, 2166-2170.

Cos, P., Vlietinck, A.J., Vanden Berghe, D. and Maes, L., 2006. Anti-infective potential of natural products: How to develop a stronger *in vitro* 'proof-of-concept'. Journal of Ethnopharmacology 106, 290-302.

Cowman, A.F., Karcz, S., Galatis, D. and Culvenor, J.G., 1991. A P-glycoprotein homolog of *Plasmodium falciparum* is localized on the digestive vacuole. Journal of Cell Biology 113, 1033-1042.

Cox-Singh, J., Hiu, J., Lucas, S.B., Divis, P.C., Zulkarnaen, M., Chandran, P., Wong, K.T., Adem, P., Zaki, S.R., Singh, B. and Krishna, S., 2010. Severe malaria - a case of fatal

Plasmodium knowlesi infection with post-mortem findings: a case report. Malaria Journal 9.

Crisostomo, M.I., Westh, H., Tomasz, A., Chung, M., Oliveira, D.C. and de Lencastre, H., 2001. The evolution of methicillin resistance in *Staphylococcus aureus*: Similarity of genetic backgrounds in historically early methicillin-susceptible and -resistant isolates and contemporary epidemic clones. Proceedings of the National Academy of Sciences of the United States of America 98, 9865-9870.

Cruz, A.K., de Toledo, J.S., Falade, M., Terrao, M.C., Kamchonwongpaisan, S., Kyle, D.E. and Uthaipibull, C., 2009. Current treatment and drug discovery against *Leishmania* spp. and *Plasmodium* spp.: A review. Current Drug Targets 10, 178-192.

Darzynkiewicz, Z., Bruno, S., Delbino, G., Gorczyca, W., Hotz, M.A., Lassota, P. and Traganos, F., 1992. Features of apoptotic cells measured by flow-cytometry. Cytometry 13, 795-808.

Dawson, R.J.P. and Locher, K.P., 2006. Structure of a bacterial multidrug ABC transporter. Nature 443, 180-185.

Demel, M.A., Kramer, O., Ettmayer, P., Haaksma, E.E.J. and Ecker, G.E., 2009. Predicting ligand interactions with ABC transporters in ADME. Chemistry & Biodiversity 6, 1960-1969.

Denis, M.B., Tsuyuoka, R., Lim, P., Lindegardh, N., Yi, P., Top, S.N., Socheat, D., Fandeur, T., Annerberg, A., Christophel, E.M. and Ringwald, P., 2006. Efficacy of artemether-lumefantrine for the treatment of uncomplicated falciparum malaria in northwest Cambodia. Tropical Medicine & International Health 11, 1800-1807.

Detommasi, N., Desimone, F., Defeo, V. and Pizza, C., 1991. Phenylpropanoid glycosides and rosmarinic acid from *Momordica balsamina*. Planta Medica 57, 201-201.

Detommasi, N., Desimone, F., Piacente, S., Pizza, C. and Mahmood, N., 1995. Diterpenes from *Momordica Balsamina*. Natural Product Letters 6, 261-268.

Dewick, P.M., 2002. The biosynthesis of C_5-C_{25} terpenoid compounds. Natural Product Reports 19, 181-222.

Duarte, N., Gyemant, N., Abreu, P.M., Molnar, J. and Ferreira, M.J.U., 2006. New macrocyclic lathyrane diterpenes, from *Euphorbia lagascae*, as inhibitors of multidrug resistance of tumour cells. Planta Medica 72, 162-168.

Duarte, N., Jardanhazy, A., Molnar, J., Hilgeroth, A. and Ferreira, M.J.U., 2008. Synergistic interaction between p-glycoprotein modulators and epirubicine on resistant cancer cells. Bioorganic & Medicinal Chemistry 16, 9323-9330.

Duarte, N., Varga, A., Cherepnev, G., Radics, R., Molnar, J. and Ferreira, M.J.U., 2007. Apoptosis induction and modulation of P-glycoprotein mediated multidrug resistance by new macrocyclic lathyrane-type diterpenoids. Bioorganic & Medicinal Chemistry 15, 546-554.

Duraisingh, M.T. and Cowman, A.F., 2005. Contribution of the *pfmdr1* gene to antimalarial drug-resistance. Acta Tropica 94, 181-190.

Eckstein-Ludwig, U., Webb, R.J., van Goethem, I.D.A., East, J.M., Lee, A.G., Kimura, M., O'Neill, P.M., Bray, P.G., Ward, S.A. and Krishna, S., 2003. Artemisinins target the SERCA of *Plasmodium falciparum*. Nature 424, 957-961.

Edstein, M.D., Bahr, S., Kotecka, B., Shanks, G.D. and Rieckmann, K.H., 1997. *In vitro* activities of the biguanide PS-15 and its metabolite, WR99210, against cycloguanil-resistant *Plasmodium falciparum* isolates from Thailand. Antimicrobial Agents and Chemotherapy 41, 2300-2301.

Egan, T.J., 2008. Haemozoin formation. Molecular and Biochemical Parasitology 157, 127-136.

Eisenreich, W., Bacher, A., Arigoni, D. and Rohdich, F., 2004. Biosynthesis of isoprenoids via the non-mevalonate pathway. Cellular and Molecular Life Sciences 61, 1401-1426.

Eliopoulos, M.M., Moellering, R. C., 1991. Antimicrobial Combinations. In: B. Williams and Wilkins (Ed.), Antibiotics in Laboratory Medicine.USA, pp. 434-441.

Engi, H., Vasas, A., Redei, D., Molnar, J. and Hohmann, J., 2007. New MDR modulators and apoptosis inducers from *Euphorbia* species. Anticancer Research 27, 3451-3458.

Escandell, J.M., Recio, M.C., Manez, S., Giner, R.M., Cerda-Nicolas, M. and Rios, J.L., 2007. Cucurbitacin R reduces the inflammation and bone damage associated with adjuvant arthritis in lewis rats by suppression of tumor necrosis factor-alpha in T lymphocytes and macrophages. Journal of Pharmacology and Experimental Therapeutics 320, 581-590.

Espinel-Ingroff, A., Fothergill, A., Ghannoum, M., Manavathu, E., Ostrosky-Zeichner, L., Pfaller, M.A., Rinaldi, M.G., Schell, W. and Walsh, T.J., 2007. Quality control and reference guidelines for CLSI broth microdilution method (M38-A document) for susceptibility testing of anidulafungin against molds. Journal of Clinical Microbiology 45, 2180-2182.

Evans, S.G., Butkow, N., Stilwell, C., Berk, M., Kirchmann, N. and Havlik, I., 1998. Citalopram enhances the activity of chloroquine in resistant *Plasmodium in vitro* and *in vivo*. Journal of Pharmacology and Experimental Therapeutics 286, 172-174.

Faiz, M.A., Bin Yunus, E., Rahman, M.R., Islam, F., Hoque, M.G., Hasan, M.U., Samad, R., Aung, S., Thein, S., Than, M., Thwe, Y., Ohn, K.M., Hla, S., Lwin, S., Htut, Y., Lin, K., Kyaw, M.P., Win, N., Aung, W.N., Win, M., Oo, A.Z., Aung, Z., Shein, O.M., Kyi, M.M., Myint, W.W., Pyar, K.P., Nyein, K., Win, K.K., Mishra, S.K., Mohanty, S., Pattnaik, R.B., Acharya, S.K., Mohanty, A., Mohapatra, D., Tijtra, E., Anstey, N., Price, R., Handoyo, T., Gampamola, D., Kenangalem, E., Takaendengan, D., Hardiyanto, Lampat, A., Harijanto, P., Dondorp, A.E., Nosten, F., Day, N., Stepniewska, K., Tipmanee, P., Douthwaite, S., Silamut, K., Proux, S., Pongsawat, K. and White, N., 2005. Artesunate versus quinine for treatment of severe falciparum malaria: a randomised trial. Lancet 366, 717-725.

Fatope, M.O., Takeda, Y., Yamashita, H., Okabe, H. and Yamauchi, T., 1990. New cucurbitane triterpenoids from *Momordica charantia*. Journal of Natural Products 53, 1491-1497.

Fernandes, J. and Gattass, C.R., 2009. Topological polar surface area defines substrate transport by multidrug resistance associated protein 1 (MRP1/ABCC1). Journal of Medicinal Chemistry 52, 1214-1218.

Fidock, D.A., Eastman, R.T., Ward, S.A. and Meshnick, S.R., 2008. Recent highlights in antimalarial drug resistance and chemotherapy research. Trends in Parasitology 24, 537-544.

Fidock, D.A., Nomura, T., Talley, A.K., Cooper, R.A., Dzekunov, S.M., Ferdig, M.T., Ursos, L.M.B., Sidhu, A.B.S., Naude, B., Deitsch, K.W., Su, X.Z., Wootton, J.C., Roepe, P.D.

and Wellems, T.E., 2000. Mutations in the *P. falciparum* digestive vacuole transmembrane protein PfCRT and evidence for their role in chloroquine resistance. Molecular Cell 6, 861-871.

Flyman, M.V. and Afolayan, A.J., 2007. Proximate and mineral composition of the leaves of *Momordica balsamina* L.: An under-utilized wild vegetable in Botswana. International Journal of Food Sciences and Nutrition 58, 419-423.

Foley, M. and Tilley, L., 1998. Quinoline antimalarials: Mechanisms of action and resistance and prospects for new agents. Pharmacology & Therapeutics 79, 55-87.

Foote, S.J., Thompson, J.K., Cowman, A.F. and Kemp, D.J., 1989. Amplification of the multidrug resistance gene in some chloroquine-resistant isolates of *P. falciparum*. Cell 57, 921-930.

Froelich, S., Onegi, B., Kakooko, A., Schubert, C., Jenett-Siems, K., 2007. Plants traditionally used against malaria: Phytochemical and pharmacological investigation of *Momordica foetida*. Brazilian Journal of Pharmognosy 17, 1-7.

Fusi, F., Saponara, S., Valoti, M., Dragoni, S., D'Elia, P., Sgaragli, T., Alderighi, D. and Sgaragli, G., 2006. Cancer cell permeability-glycoprotein as a target of MDR reverters: Possible role of novel dihydropyridine derivatives. Current Drug Targets 7, 949-959.

Garau, C., Phoenix, D.A., and Singh, J., 2003. Beneficial effect and mechanism of action of *Momordica charantia* in the treatment of diabetes mellitus: A mini review. International Journal of Diabetes & Metabolism 11, 46-55.

Gershenzon, J. and Dudareva, N., 2007. The function of terpene natural products in the natural world. Nature Chemical Biology 3, 408-414.

Gibbons, S., 2003. An overview of plant extracts as potential therapeutics. Expert Opinion on Therapeutic Patents 13, 489-497.

Gibbons, S., 2004. Anti-staphylococcal plant natural products. Natural Product Reports 21, 263-277.

Gibbons, S., 2008. Phytochemicals for bacterial resistance - Strengths, weaknesses and opportunities. Planta Medica 74, 594-602.

Gibbons, S., Moser, E. and Kaatz, G.W., 2004. Catechin gallates inhibit multidrug resistance (MDR) in *Staphylococcus aureus*. Planta Medica 70, 1240-1242.

Gibbons, S., Oluwatuyi, M., Veitch, N.C. and Gray, A.I., 2003. Bacterial resistance modifying agents from *Lycopus europaeus*. Phytochemistry 62, 83-87.

Ginsburg, H., Ward, S.A. and Bray, P.G., 1999. An integrated model of chloroquine action. Parasitology Today 15, 357-360.

Globisch, C., Pajeva, I.K. and Wiese, M., 2008. Identification of putative binding sites of P-glycoprotein based on its homology model. Chemmedchem 3, 280-295.

Gottesman, M.M., Fojo, T. and Bates, S.E., 2002. Multidrug resistance in cancer: Role of ATP-dependent transporters. Nature Reviews Cancer 2, 48-58.

Grover, J.K. and Yadav, S.P., 2004. Pharmacological actions and potential uses of *Momordica charantia*: A review. Journal of Ethnopharmacology 93, 123-132.

Guo, Z., Vangapandu, S., Nimrod, A., Walker, L.A., Sindelar, R.D., 2005. Synthesis of A/B-ring partial analogs of bruceantin as potential antimalarial agents. Medicinal Chemistry 1, 3-11.

Hallwirth, H.J., 2007. Composition for treatment of malaria, comprises cucurbitacin B and E to destroy malaria-causing parasite in liver. Sterolina Pte Ltd.

Hamilton-Miller, J.M.T. and Shah, S., 2000. Activity of the tea component epicatechin gallate and analogues against methicillin-resistant *Staphylococcus aureus*. Journal of Antimicrobial Chemotherapy 46, 852-853.

Harinantenaina, L., Tanaka, M., Takaoka, S., Oda, M., Mogami, O., Uchida, M. and Asakawa, Y., 2006. *Momordica charantia* constituents and antidiabetic screening of the isolated major compounds. Chemical & Pharmaceutical Bulletin 54, 1017-1021.

Haynes, R.K., 2006. From artemisinin to new artemisinin antimalarials: Biosynthesis, extraction, old and new derivatives, stereochemistry and medicinal chemistry requirements. Current Topics in Medicinal Chemistry 6, 509-537.

Hempelmann, E., 2007. Hemozoin biocrystallization in *Plasmodium falciparum* and the antimalarial activity of crystallization inhibitors. Parasitology Research 100, 671-676.

Hennessy, M. and Spiers, J.P., 2007. A primer on the mechanics of P-glycoprotein the multidrug transporter. Pharmacological Research 55, 1-15.

Henry, M., Alibert, S., Rogier, C., Barbe, J. and Pradines, B., 2008. Inhibition of efflux of quinolines as new therapeutic strategy in malaria. Current Topics in Medicinal Chemistry 8, 563-578.

Horgen, F.D., Sakamoto, B. and Scheuer, P.J., 2000. New triterpenoid sulfates from the red alga *Tricleocarpa fragilis*. Journal of Natural Products 63, 210-216.

Hout, S., Chea, A., Bun, S.S., Elias, R., Gasquet, M., Timon-David, P., Balansard, G. and Azas, N., 2006. Screening of selected indigenous plants of Cambodia for antiplasmodial activity. Journal of Ethnopharmacology 107, 12-18.

Ioset, J.R., 2008. Natural products for neglected diseases: A review. Current Organic Chemistry 12, 643-666.

Iwalokun, B.A., Ghenle, G.O., Adewole, T.A. and Akinsinde, K.A., 2001. Shigellocidal properties of three Nigerian medicinal plants: *Ocimum gratissimum*, *Terminalia avicennoides*, and *Momordica balsamina*. Journal of Health Population and Nutrition 19, 331-335.

Jambou, R., Legrand, E., Niang, M., Khim, N., Lim, P., Volney, B., Ekala, M.T., Bouchier, C., Esterre, P., Fandeur, T. and Mercereau-Puijalon, O., 2005. Resistance of *Plasmodium falciparum* field isolates to *in vitro* artemether and point mutations of the SERCA-type PfATPase6. Lancet 366, 1960-1963.

Jansen, P.C.M., Mendes, O., 1982. Plantas medicinais- Seu uso traditional em Moçambique. Maputo: Gabinete de Estudo da Medicina Tradicional, Maputo, Moçambique.

Jansen, P.C.M., Mendes, O., 1983. Plantas medicinais - Seu uso tradicional em Moçambique. Maputo: Gabinete de Estudo da Medicina Tradicional, Maputo, Moçambique.

Jansen, P.C.M., Mendes, O., 1990. Plantas medicinais - Seu uso tradicional em Moçambique. Maputo: Gabinete de Estudo da Medicina Tradicional., Maputo, Moçambique.

Jansen, P.C.M., Mendes, O., 1991. Plantas medicinais - Seu uso tradicional em Moçambique. Maputo: Gabinete de Estudo da Medicina Tradicional., Maputo, Moçambique.

Jodoin, J., Demeule, M. and Beliveau, R., 2002. Inhibition of the multidrug resistance P-glycoprotein activity by green tea polyphenols. Biochimica Et Biophysica Acta-Molecular Cell Research 1542, 149-159.

Johnson, J.D., Dennull, R.A., Gerena, L., Lopez-Sanchez, M., Roncal, N.E. and Waters, N.C., 2007. Assessment and continued validation of the malaria SYBR green I-based fluorescence assay for use in malaria drug screening. Antimicrobial Agents and Chemotherapy 51, 1926-1933.

Joseph, J.K. and Antony, V.T., 2008. Ethnobotanical investigations in the genus *Momordica* L. in the southern Western Ghats of India. Genetic Resources and Crop Evolution 55, 713-721.

Jurg, A., Tomas, T. and Pividal, J., 1991. Antimalarial activity of some plant remedies in use in Marracuene, Southern Mozambique. Journal of Ethnopharmacology 33, 79-83.

Kai, H., Baba, M. and Okuyama, T., 2007. Two new megastigmanes from the leaves of *Cucumis sativus*. Chemical & Pharmaceutical Bulletin 55, 133-136.

Kainyemi, K.O., Mendie, U.E., Smith, S.T., Oyefolu, A.O., Coker, A.O., 2005. Screening of some medicinal plants used in south-west Nigerian traditioal medicine for anti-*Salmonella typhi* activity. Journal of Herbal Pharmacotherapy 5, 45-60.

Kaou, A.M., Mahiou-Leddet, V., Hutter, S., Ainouddine, S., Hassani, S., Yahaya, I., Azas, N. and Ollivier, E., 2008. Antimalarial activity of crude extracts from nine African medicinal plants. Journal of Ethnopharmacology 116, 74-83.

Karumi, Y., Onyeeyili, P., Ogugbuaja, V.O., 2003. Anti-inflammatory and antinociceptive (analgesic) properties of *Momordica balsamina* L. (Balsam apple) leaves in rats. Pakistan Journal of Biological Sciences 6, 1515-1518.

Kashiwagi, T., Mekuria, D.B., Dekebo, A., Sato, K., Tebayashi, S.I. and Kim, C.S., 2007. A new oviposition deterrent to the leafminer, *Liriomyza trifolii*: Cucurbitane glucoside from *Momordica charantia*. Zeitschrift Fur Naturforschung C-a Journal of Biosciences 62, 603-607.

Kaur, K., Jain, M., Kaur, T. and Jain, R., 2009. Antimalarials from nature. Bioorganic & Medicinal Chemistry 17, 3229-3256.

Kim, I., Chin, Y.W., Lim, S.W., Kim, Y.C. and Kim, J., 2004. Norisoprenoids and hepatoprotective flavone glycosides from the aerial parts of *Beta vulgaris* var. cicla. Archives of Pharmacal Research 27, 600-603.

Kimura, Y., Akihisa, T., Yuasa, N., Ukiya, M., Suzuki, T., Toriyama, M., Motohashi, S. and Tokuda, H., 2005. Cucurbitane-type triterpenoids from the fruit of *Momordica charantia*. Journal of Natural Products 68, 807-809.

Kinyanjui, S.M., Mberu, E.K., Winstanley, P.A., Jacobus, D.P. and Watkins, W.M., 1999. The antimalarial triazine WR99210 and the prodrug PS-15: Folate reversal of *in vitro* activity against *Plasmodium falciparum* and a non-antifolate mode of action of the prodrug. American Journal of Tropical Medicine and Hygiene 60, 943-947.

Kirby, J. and Keasling, J.D., 2009. Biosynthesis of plant isoprenoids: Perspectives for microbial engineering. Annual Review of Plant Biology 60, 335-355.

Krettli, A.U., Adebayo, J.O. and Krettli, L.G., 2009. Testing of natural products and synthetic molecules aiming at new antimalarials. Current Drug Targets 10, 261-270.

Krishna, S., Bustamante, L., Haynes, R.K. and Staines, H.M., 2008. Artemisinins: Their growing importance in medicine. Trends in Pharmacological Sciences 29, 520-527.

Krishna, S., Uhlemann, A.C. and Haynes, R.K., 2004. Artemisinins: Mechanisms of action and potential for resistance. Drug Resistance Updates 7, 233-244.

Krudsood, S., Patel, S.N., Tangpukdee, N., Thanachartwet, W., Leowattana, W., Pornpininworakij, K., Boggild, A.K., Looareesuwan, S. and Kain, K.C., 2007. Efficacy of atovaquone-proguanil for treatment of acute multidrug-resistant *Plasmodium falciparum* malaria in Thailand. American Journal of Tropical Medicine and Hygiene 76, 655-658.

Kumar, A., Katiyar, S.B., Agarwal, A. and Chauhan, P.M.S., 2003. Perspective in antimalarial chemotherapy. Current Medicinal Chemistry 10, 1137-1150.

Kuzuyama, T. and Seto, H., 2003. Diversity of the biosynthesis of the isoprene units. Natural Product Reports 20, 171-183.

Lang, T. and Greenwood, B., 2003. The development of Lapdap, an affordable new treatment for malaria. Lancet Infectious Diseases 3, 162-168.

Lee, C.H., 2010. Reversing Agents for ATP-Binding Cassete Drug Transporters. In: J. Zhou (Ed.), Multi-Drug Resistance in Cancer, Methods in Molecular Biology, Human Press, pp. 325-340.

Lee, E.W., Huda, M.N., Kuroda, T., Mizushima, T. and Tsuchiya, T., 2003. EfrAB, an ABC multidrug efflux pump in *Enterococcus faecalis*. Antimicrobial Agents and Chemotherapy 47, 3733-3738.

Lewis, K., 2001. In search of natural substrates and inhibitors of MDR pumps. Journal of Molecular Microbiology and Biotechnology 3, 247-254.

Li, D.P., El-Aasr, M., Ikeda, T., Ogata, M., Miyashita, H., Yoshimitsu, H. and Nohara, T., 2009. Two new cucurbitane-type glycosides obtained from roots of *Siraitia grosvenorii* Swingle. Chemical & Pharmaceutical Bulletin 57, 870-872.

Li, D.P., Ikeda, T., Matsuoka, N., Nohara, T., Zhang, H.R., Sakamoto, T. and Nonaka, G.I., 2006a. Cucurbitane glycosides from unripe fruits of Lo Han Kuo (*Siraitia grosvenorii*). Chemical & Pharmaceutical Bulletin 54, 1425-1428.

Li, D.P., Ikeda, T., Matsuoka, N., Nohara, T., Zhang, H.R., Sakamoto, T. and Nonaka, G.I., 2006b. Cucurbitane glycosides from unripe fruits of Lo Han Kuo (*Siraitia grosvenorii*). Chemical & Pharmaceutical Bulletin 54, 1425-1428.

Li, D.P., Ikeda, T., Nohara, T., Liu, J.L., Wen, Y.X., Sakamoto, T. and Nonaka, G., 2007a. Cucurbitane glycosides from unripe fruits of *Siraitia grosvenorii*. Chemical & Pharmaceutical Bulletin 55, 1082-1086.

Li, Q.Y., Chen, H.B., Liu, Z.M., Wang, B. and Zhao, Y.Y., 2007b. Cucurbitane triterpenoids from *Momordica charantia*. Magnetic Resonance in Chemistry 45, 451-456.

Li, Q.Y., Liang, H., Chen, H.B., Wang, B. and Zhao, Y.Y., 2007c. A new cucurbitane triterpenoid from *Momordica charantia*. Chinese Chemical Letters 18, 843-845.

Li, Y., Yuan, H., Yang, K., Xu, W., Tang, W. and Li, X., 2010. The structure and functions of P-glycoprotein. Current Medicinal Chemistry 17, 786-800.

Limtrakul, P., 2007. Curcumin as chemosensitizer. Molecular Targets and Therapeutic Uses of Curcumin in Health and Disease 595, 269-300.

Limtrakul, P., Khantamat, O. and Pintha, K., 2004. Inhibition of P-glycoprotein activity and reversal of cancer multidrug resistance by *Momordica charantia* extract. Cancer Chemotherapy and Pharmacology 54, 525-530.

Liu, C.H., Yen, M.H., Tsang, S.F., Gan, K.H., Hsu, H.Y. and Lin, C.N., 2010. Antioxidant triterpenoids from the stems of *Momordica charantia*. Food Chemistry 118, 751-756.

Liu, J.Q., Chen, J.C., Wang, C.F., Qiu, M.H., 2010. New cucurbitane triterpenoids and steroidal glycoside from *Momordica charantia*. Molecules 14, 4804-4813.

Liu, T.Y., Zhang, M.X., Zhang, H.L., Sun, C.Y. and Deng, Y.H., 2008a. Inhibitory effects of cucurbitacin B on laryngeal squamous cell carcinoma. European Archives of Oto-Rhino-Laryngology 265, 1225-1232.

Liu, T.Y., Zhang, M.X., Zhang, H.L., Sun, C.Y., Yang, X.L., Deng, Y.H. and Ji, W.Y., 2008b. Combined antitumor activity of cucurbitacin B and docetaxel in laryngeal cancer. European Journal of Pharmacology 587, 78-84.

Liu, X., Cui, Y.X., Yu, Q. and Yu, B., 2005. Triterpenoids from *Sanguisorba officinalis*. Phytochemistry 66, 1671-1679.

Liu, Y., Ali, Z. and Khan, I.A., 2008c. Cucurbitane-type triterpene glycosides from the fruits of *Momordica charantia*. Planta Medica 74, 1291-1294.

Lomovskaya, O. and Bostian, K.A., 2006. Practical applications and feasibility of efflux pump inhibitors in the clinic - A vision for applied use. Biochemical Pharmacology 71, 910-918.

Longley, D.B. and Johnston, P.G., 2005. Molecular mechanisms of drug resistance. Journal of Pathology 205, 275-292.

Lubelski, J., de Jong, A., van Merkerk, R., Agustiandari, H., Kuipers, O.P., Kok, J. and Driessen, A.J.M., 2006. LmrCD is a major multidrug resistance transporter in *Lactococcus lactis*. Molecular Microbiology 61, 771-781.

Lubelski, J., Konings, W.N. and Driessen, A.J.M., 2007. Distribution and physiology of ABC-Type transporters contributing to multidrug resistance in bacteria. Microbiology and Molecular Biology Reviews 71, 463-474.

Mahato, S.B. and Kundu, A.P., 1994. ^{13}C NMR-Spectra of pentacyclic triterpenoids - A compilation and some salient features. Phytochemistry 37, 1517-1575.

Markham, P.N., Westhaus, E., Klyachko, K., Johnson, M.E. and Neyfakh, A.A., 1999. Multiple novel inhibitors of the NorA multidrug transporter of *Staphylococcus aureus*. Antimicrobial Agents and Chemotherapy 43, 2404-2408.

Marquez, B., 2005. Bacterial efflux systems and efflux pumps inhibitors. Biochimie 87, 1137-1147.

Martinelli, A., Moreira, R. and Cravo, P.V.L., 2008. Malaria combination therapies: Advantages and shortcomings. Mini-Reviews in Medicinal Chemistry 8, 201-212.

Martins, A., Couto, I., Aagaard, L., Martins, M., Viveiros, M., Kristiansen, J.E. and Amaral, L., 2007. Prolonged exposure of methicillin-resistant *Staphylococcus aureus* (MRSA) COL strain to increasing concentrations of oxacillin results in a multidrug-resistant phenotype. International Journal of Antimicrobial Agents 29, 302-305.

Matsuda, H., Nakamura, S., Murakami, T. and Yoshikawa, M., 2007. Structures of new cucurbitane-type triterpenes and glycosides, karavilagenins D and E, and karavilosides VI, VII, VIII, IX, X, and XI, from the fruit of *Momordica charantia*. Heterocycles 71, 331-341.

Mayur, Y.C., Peters, G.J., Prasad, V., Lemos, C. and Sathish, N.K., 2009. Design of new drug molecules to be used in reversing multidrug resistance in cancer cells. Current Cancer Drug Targets 9, 298-306.

Mekuria, D.B., Kashiwagi, T., Tebayashi, S. and Kim, C.S., 2006. Cucurbitane glycosides from *Momordica charantia* leaves as oviposition deterrents to the leafminer, *Liriomyza trifolii*. Zeitschrift Fur Naturforschung C-a Journal of Biosciences 61, 81-86.

Mekuria DB, K.T., Tebayashi S, Kim CS., 2005. Cucurbitane triterpenoid oviposition deterrent from *Momordica charantia* to the leafminer, *Liriomyza trifolii*. Biosci Biotechnol Biochem. 69, 1706-1710.

Menan, H., Banzouzi, J.T., Hocquette, A., Pelissier, Y., Blache, Y., Kone, M., Mallie, M., Assi, L.A. and Valentin, A., 2006. Antiplasmodial activity and cytotoxicity of plants used in West African traditional medicine for the treatment of malaria. Journal of Ethnopharmacology 105, 131-136.

Mita, T., Tanabe, K. and Kita, K., 2009. Spread and evolution of *Plasmodium falciparum* drug resistance. Parasitology International 58, 201-209.

Mohamad, K., Martin, M.T., Leroy, E., Tempete, C., Sevenet, T., Awang, K. and Pais, M., 1997. Argenteanones C-E and argenteanols B-E, cytotoxic cycloartanes from *Aglaia argentea*. Journal of Natural Products 60, 81-85.

Molnar, J., Gyemant, N., Tanaka, M., Hohmann, J., Bergmann-Leitner, E., Molnar, P., Deli, J., Didiziapetris, R. and Ferreira, M.J.U., 2006. Inhibition of multidrug resistance of cancer cells by natural diterpenes, triterpenes and carotenoids. Curr. Pharm. Design 12, 287-311.

Muñoz, V., Sauvain, M., Bourdy, G., Callapa, J., Rojas, I., Vargas, L., Tae, A., Deharo, E., 2000. The search for natural bioactive compounds through a multidisciplinary approach in Bolivia. Part II. Antimalarial activity of some plants used by Mosetene indians. Journal of Ethnopharmacology 69, 139-155.

Murakami, S., 2008. Multidrug efflux transporter, AcrB - the pumping mechanism. Current Opinion in Structural Biology 18, 459-465.

Murakami, S., Nakashima, R., Yamashita, E. and Yamaguchi, A., 2002. Crystal structure of bacterial multidrug efflux transporter AcrB. Nature 419, 587-593.

Muraleedharan, K.M. and Avery, M.A., 2009. Progress in the development of peroxide-based anti-parasitic agents. Drug Discovery Today 14, 793-803.

Na-Bangchang, K., Bray, P.G. and Ward, S.A., 2007. Study on the biochemical basis of mefloquine resistant *Plasmodium falciparum*. Experimental Parasitology 117, 141-148.

Na-Bangchang, K. and Karbwang, J., 2009. Current status of malaria chemotherapy and the role of pharmacology in antimalarial drug research and development. Fundamental & Clinical Pharmacology 23, 387-409.

Nakajima, Y., Satoh, Y., Ohtsuka, N., Tsujiyama, K., Mikoshiba, N., Ida, Y. and Shoji, J., 1994. Terpenoids of *Alisma orientale* rhizome and the crude drug Alismatis rhizoma. Phytochemistry 36, 119-127.

Nakamura, S., Murakami, T., Nakamura, J., Kobayashi, H., Matsuda, H. and Yoshikawa, M., 2006. Structures of new cucurbitane-type triterpenes and glycosides, karavilagenins and karavilosides, from the dried fruit of *Momordica charantia* L. in Sri Lanka. Chemical & Pharmaceutical Bulletin 54, 1545-1550.

Neuwinger, H.D., 1996. African Ethnobotany: Poisons and drugs. Wheinheim, Germany.

Neuwinger, H.D., 2000. African traditional medicine: A dictionary of plant use and applications. Medpharm Scientific Publ., Stuttgart, Germany.

Newton, C., Hien, T.T. and White, N., 2000. Cerebral malaria. Journal of Neurology Neurosurgery and Psychiatry 69, 433-441.

Neyfakh, A.A., 1992. The multidrug efflux transporter of *Bacillus subtilis* is a structural and functional homolog of the *Staphylococcus* nora protein. Antimicrobial Agents and Chemotherapy 36, 484-485.

Nhiem, N.X., Kiem, P.V., Minh, C.V., Ban, N.K., Cuong, N.X., Ha, L.M., Tai, B.H., Quang, T.H., Tung, N.H., Kim, Y.H., 2010. Cucurbitane-type triterpene glycosides from the fruits of *Momordica charantia*. Magnetic Ressonance Chemistry.

Nishino, K. and Yamaguchi, A., 2001. Analysis of a complete library of putative drug transporter genes in *Escherichia coli*. Journal of Bacteriology 183, 5803-5812.

Nobili, S., Landini, I., Giglioni, B. and Mini, E., 2006. Pharmacological strategies for overcoming multidrug resistance. Current Drug Targets 7, 861-879.

Oliveira, A.B., Dolabela, M.F., Braga, F.C., Jacome, R., Varotti, F.P. and Povoa, M.M., 2009. Plant-derived antimalarial agents: New leads and efficient phythomedicines. Part I. Alkaloids. Anais Da Academia Brasileira De Ciencias 81, 715-740.

Oliveira, D.C. and de Lencastre, H., 2002. Multiplex PCR strategy for rapid identification of structural types and variants of the mec element in methicillin-resistant *Staphylococcus aureus*. Antimicrobial Agents and Chemotherapy 46, 2155-2161.

Oliveira, D.C., Tomasz, A. and de Lencastre, H., 2001. The evolution of pandemic clones of methicillin-resistant *Staphylococcus aureus*: Identification of two ancestral genetic backgrounds and the associated *mec* elements. Microbial Drug Resistance-Mechanisms Epidemiology and Disease 7, 349-361.

Oluwatuyi, M., Kaatz, G.W. and Gibbons, S., 2004. Antibacterial and resistance modifying activity of *Rosmarinus officinalis*. Phytochemistry 65, 3249-3254.

Otimenyin, S.O., Uguru, M.O., Ogbonna, A., 2008. Antimicrobial and hypoglycemic effects of *Momordica balsamina* Linn. Journal of Natural Products 1, 3-9.

Ozben, T., 2006. Mechanisms and strategies to overcome multiple drug resistance in cancer. Febs Letters 580, 2903-2909.

Pages, J.M., James, C.E. and Winterhalter, M., 2008. The porin and the permeating antibiotic: A selective diffusion barrier in Gram-negative bacteria. Nature Reviews Microbiology 6, 893-903.

Pajeva, I., Globisch, C., Fleischer, R., Tsakovska, I. and Wiese, M., 2005. Molecular modeling of P-glycoprotein and related drugs. Medicinal Chemistry Research 14, 106-117.

Pajeva, I.K., Globisch, C. and Wiese, M., 2009. Combined pharmacophore modelling, docking, and 3D QSAR studies of ABCB1 and ABCC1 transporter inhibitors. Chemmedchem 4, 1883-1896.

Pajeva, I.K. and Wiese, M., 2009. Structure-activity relationships of tariquidar analogs as multidrug resistance modulators. Aaps Journal 11, 435-444.

Pastan, I., Gottesman, M.M., Ueda, K., Lovelace, E., Rutherford, A.V. and Willingham, M.C., 1988. A retrovirus carrying an mdr1 cdna confers multidrug resistance and polarized expression of P-glycoprotein in mdck cells. Proceedings of the National Academy of Sciences of the United States of America 85, 4486-4490.

Perez-Tomas, R., 2006. Multidrug resistance: Retrospect and prospects in anti-cancer drug treatment. Current Medicinal Chemistry 13, 1859-1876.

Pietras, Z., Bavro, V.N., Furnham, N., Pellegrini-Calace, M., Milner-White, E.J. and Luisi, B.F., 2008. Structure and mechanism of drug efflux machinery in Gram negative bacteria. Current Drug Targets 9, 719-728.

Poespoprodjo, J.R., Fobia, W., Kenangalem, E., Lampah, D.A., Hasanuddin, A., Warikar, N., Sugiarto, P., Tjitra, E., Anstey, N.M. and Price, R.N., 2009. Vivax malaria: A major cause of morbidity in early infancy. Clinical Infectious Diseases 48, 1704-1712.

Prasanna, S. and Doerksen, R.J., 2009. Topological polar surface area: A useful descriptor in 2D-QSAR. Current Medicinal Chemistry 16, 21-41.

Rafatro, H., Ramanitrahasimbola, D., Rasoanaivo, P., Ratsimamanga-Urverg, S., Rakoto-Ratsimamanga, A. and Frappier, F., 2000. Reversal activity of the naturally occurring chemosensitizer malagashanine in *Plasmodium* malaria. Biochemical Pharmacology 59, 1053-1061.

Ramanitrahasimbola, D., Rasoanaivo, P., Ratsimamanga, S. and Vial, H., 2006. Malagashanine potentiates chloroquine antimalarial activity in drug resistant *Plasmodium* malaria by modifying both its efflux and influx. Molecular and Biochemical Parasitology 146, 58-67.

Rathore, D., Jani, D., Nagarkatti, R., Kumar, S. , 2006. Heme detoxification and antimalarial drugs – Known mechanisms and future prospects. Drug Discovery Today: Therapeutic Strategies 3, 153-158

Rathore, D., McCutchan, T.F., Sullivan, M. and Kumar, S., 2005. Antimalarial drugs: current status and new developments. Expert Opinion on Investigational Drugs 14, 871-883.

Recio, M.C., Prieto, M., Bonucelli, M., Orsi, C., Manez, S., Giner, R.M., Cerda-Nicolas, M. and Rios, J.L., 2004. Anti-inflammatory activity of two cucurbitacins isolated from *Cayaponia tayuya* roots. Planta Medica 70, 414-420.

Reed, M.B., Saliba, K.J., Caruana, S.R., Kirk, K. and Cowman, A.F., 2000. Pgh1 modulates sensitivity and resistance to multiple antimalarials in *Plasmodium falciparum*. Nature 403, 906-909.

Ridley, R.G., 2003. Malaria - To kill a parasite. Nature 424, 887-889.

Rios, J.L., Escandell, J.M., Recio, M.C., 2005. New insights into bioactivity of cucurbitacins. In: Atta-ur-Rahman (Ed.), Studies in Natural Products Chemistry.Amsterdam, The Netherlands, pp. 429-469.

Roberts, S.C., 2007. Production and engineering of terpenoids in plant cell culture. Nature Chemical Biology 3, 387-395.

Rodriguez, N., Vasquez, Y., Hussein, A.A., Coley, P.D., Solis, P.N. and Gupta, M.P., 2003. Cytotoxic cucurbitacin constituents from *Sloanea zuliaensis*. Journal of Natural Products 66, 1515-1516.

Rohmer, M., 1999. The discovery of a mevalonate-independent pathway for isoprenoid biosynthesis in bacteria, algae and higher plants. Natural Product Reports 16, 565-574.

Rosengarten, F., 2004. The book of edible nuts. Dover Publication, Mineolo, New York, USA.

Rosenthal, P.J., 2003. Antimalarial drug discovery: old and new approaches. The Journal of Experimental Biology. 206, 3735-3744.

Ross, I.A., 2003. Medicinal Plants of the World: Chemical constituents, traditional and modern medicinal. Totowa, New Jersey.

Rowe, J., 1989. Natural Products of Woody Plants. Springer-Verlag, Berlin.

Sadzuka, Y., Hatakeyama, H. and Sonobe, T., 2010. Enhancement of doxorubicin concentration in the M5076 ovarian sarcoma cells by cucurbitacin E co-treatment. International Journal of Pharmaceutics 383, 186-191.

Sauna, Z.E., Smith, M.M., Muller, M., Kerr, K.M. and Ambudkar, S.V., 2001. The mechanism of action of multidrug-resistance-linked P-glycoprotein. Journal of Bioenergetics and Biomembranes 33, 481-491.

Sauvage, V., Aubert, D., Escotte-Binet, S. and Villena, I., 2009. The role of ATP-binding cassette (ABC) proteins in protozoan parasites. Molecular and Biochemical Parasitology 167, 81-94.

Savjani, J.K., Gajjar, A.K. and Savjani, K.T., 2009. Mechanisms of resistance: Useful tool to design antibacterial agents for drug - Resistant bacteria. Mini-Reviews in Medicinal Chemistry 9, 194-205.

Saxena, S., Pant, N., Jain, D.C. and Bhakuni, R.S., 2003. Antimalarial agents from plant sources. Current Science 85, 1314-1329.

Schmitt, L., 2002. The first view of an ABC transporter: The X-ray crystal structure of MsbA from *E. coli*. Chembiochem 3, 161-165.

Schottelius, J., Gilberger, T., Ehrhardt, S. and Burchard, G., 2010. *Plasmodium knowlesi*: cause of naturally acquired malaria in humans. Deutsche Medizinische Wochenschrift 135, 297-300.

Sennhauser, G., Bukowska, M.A., Briand, C. and Grutter, M.G., 2009. Crystal structure of the multidrug exporter MexB from *Pseudomonas aeruginosa*. Journal of Molecular Biology 389, 134-145.

Sharma, V., 2005. Therapeutic drugs for targeting chloroquine resistance in malaria. Mini-Reviews in Medicinal Chemistry 5, 337-351.

Shibuya, M., Adachi, S. and Ebizuka, Y., 2004. Cucurbitadienol synthase, the first committed enzyme for cucurbitacin biosynthesis, is a distinct enzyme from cycloartenol synthase for phytosterol biosynthesis. Tetrahedron 60, 6995-7003.

Shilling, R.A., Balakrishnan, L., Shahi, S., Venter, H. and van Veen, H.W., 2003. A new dimmer interface for an ABC transporter. International Journal of Antimicrobial Agents 22, 200-204.

Si, J.Y., Chen, D.H. and Tu, G.Z., 2005. Siraitic acid F, a new nor-cucurbitacin with novel skeleton, from the roots of *Siraitia grosvenorii*. Journal of Asian Natural Products Research 7, 37-41.

Sidhu, A.B.S., Uhlemann, A.C., Valderramos, S.G., Valderramos, J.C., Krishna, S. and Fidock, D.A., 2006. Decreasing *pfmdr1* copy number in *Plasmodium falciparum* malaria heightens susceptibility to mefloquine, lumefantrine, halofantrine, quinine, and artemisinin. Journal of Infectious Diseases 194, 528-535.

Siqueira, J.M., Peters, R.R., Gazola, A.C., Krepsky, P.B., Farias, M.R., Rae, G.A., de Brum-Fernandes, A.J. and Ribeiro-do-Valle, R.M., 2007. Anti-inflammatory effects of a triterpenoid isolated from *Wilbrandia ebracteata* Cogn. Life Sciences 80, 1382-1387.

Smilkstein, M., Sriwilaijaroen, N., Kelly, J.X., Wilairat, P. and Riscoe, M., 2004. Simple and inexpensive fluorescence-based technique for high-throughput antimalarial drug screening. Antimicrobial Agents and Chemotherapy 48, 1803-1806.

Spengler, G., Viveiros, M., Martins, M., Rodrigues, L., Martins, A., Molnar, J., Couto, I. and Amaral, L., 2009. Demonstration of the activity of P-glycoprotein by a semi-automated fluorometric method. Anticancer Research 29, 2173-2177.

Srinivas, E., Murthy, J.N., Rao, A.R.R. and Sastry, G.N., 2006. Recent advances in molecular modeling and medicinal chemistry aspects of phospho-glycoprotein. Current Drug Metabolism 7, 205-217.

Stavri, M., Piddock, L.J.V. and Gibbons, S., 2007. Bacterial efflux pump inhibitors from natural sources. Journal of Antimicrobial Chemotherapy 59, 1247-1260.

Su, Y.H., Li, G., Zhang, X.L., Gu, J.H., Zhang, C., Tian, Z.G. and Zhang, J., 2008. JSI-124 inhibits glioblastoma multiforme cell proliferation through G(2)/M cell cycle arrest and apoptosis augment. Cancer Biology & Therapy 7, 1243-1249.

Tabuti, J.R.S., 2008. Herbal medicines used in the treatment of malaria in Budiope county, Uganda. Journal of Ethnopharmacology 116, 33-42.

Takahashi, N., Yoshida, Y., Sugiura, T., Matsuno, K., Fujino, A. and Yamashita, U., 2009. Cucurbitacin D isolated from *Trichosanthes kirilowii* induces apoptosis in human hepatocellular carcinoma cells *in vitro*. International Immunopharmacology 9, 508-513.

Takahashi, S., Satoh, H., Hongo, Y. and Koshino, H., 2007. Structural revision of terpenoids with a (3*Z*)-2-methyl-3-penten-2-ol moiety by the synthesis of (23*E*)- and (23*Z*)-cycloart-23-ene-3 beta,25-diols. Journal of Organic Chemistry 72, 4578-4581.

Takasaki, M., Konoshima, T., Murata, Y., Sugiura, M., Nishino, H., Tokuda, H., Matsumoto, K., Kasai, R. and Yamasaki, K., 2003. Anticarcinogenic activity of natural sweeteners, cucurbitane glycosides, from *Momordica grosvenorii*. Cancer Letters 198, 37-42.

Tan, M.J., Ye, J.M., Turner, N., Hohnen-Behrens, C., Ke, C.Q., Tang, C.P., Chen, T., Weiss, H.C., Gesing, E.R., Rowland, A., James, D.E. and Yel, Y., 2008a. Antidiabetic activities of triterpenoids isolated from bitter melon associated with activation of the AMPK pathway. Chemistry & Biology 15, 263-273.

Tan, M.J., Ye, J.M., Turner, N., Ke, C.Q., Tang, C.P., Chen, T., Hohnen-Behrens, C., Rowland, A., James, D.E. and Ye, Y., 2008b. New Cucurbitane triterpenoids from bitter melon with potent antidiabetic properties associated with activation of AMPK. Planta Medica 74, 913-913.

Tannin-Spitz, T., Grossman, S., Dovrat, S., Gottlieb, H.E. and Bergman, M., 2007. Growth inhibitory activity of cucurbitacin glucosides isolated from *Citrullus colocynthis* on human breast cancer cells. Biochemical Pharmacology 73, 56-67.

Taylor, D., Walden, J.C., Robins, A.H. and Smith, P.J., 2000. Role of the neurotransmitter reuptake-blocking activity of antidepressants in reversing chloroquine resistance *in vitro* in *Plasmodium falciparum*. Antimicrobial Agents and Chemotherapy 44, 2689-2692.

Tegos, G., Stermitz, F.R., Lomovskaya, O. and Lewis, K., 2002. Multidrug pump inhibitors uncover remarkable activity of plant antimicrobials. Antimicrobial Agents and Chemotherapy 46, 3133-3141.

Teodori, E., Dei, S., Martelli, C., Scapecchi, S. and Gualtieri, F., 2006. The functions and structure of ABC transporters: Implications for the design of new inhibitors of Pgp and MRP1 to control multidrug resistance (MDR). Current Drug Targets 7, 893-909.

Thakur, G.S., Bag, M., Sanodiya, B.S., Bhadauriya, P., Debnath, M., Prasad, G. and Bisen, P.S., 2009. *Momordica balsamina*: A medicinal and neutraceutical plant for health care management. Current Pharmaceutical Biotechnology 10, 667-682.

Thomas, R., 2004. Biogenetic speculation and biosynthetic advances. Natural Product Reports 21, 224-248.

Torssell, K.B.G., 1997. Natural Product Chemistry - A Mechanistic, Biosynthetic and Ecological approach. Apotekarsocieteten, Swedish Pharmaceutical Society, Sweden.

Trager, W. and Jensen, J.B., 1976. Human malaria parasites in continuous culture. Science 193, 673-675.

Turschner, S. and Efferth, T., 2009. Drug resistance in *Plasmodium*: Natural products in the fight against malaria. Mini-Reviews in Medicinal Chemistry 9, 206-214.

Van Bambeke, F., Balzi, E. and Tulkens, P.M., 2000. Antibiotic efflux pumps - Commentary. Biochemical Pharmacology 60, 457-470.

van de Venter, M., Roux, S., Bungu, L.C., Louw, J., Crouch, N.R., Grace, O.M., Maharaj, V., Pillay, P., Sewnarian, P., Bhagwandin, N. and Folb, P., 2008. Antidiabetic screening and scoring of 11 plants traditionally used in South Africa. Journal of Ethnopharmacology 119, 81-86.

van Veen, H.W., Margolles, A., Muller, M., Higgins, C.F. and Konings, W.N., 2000. The homodimeric ATP-binding cassette transporter LmrA mediates multidrug transport by an alternating two-site (two-cylinder engine) mechanism. Embo Journal 19, 2503-2514.

van Veen, H.W., Putman, M., Margolles, A., Sakamoto, K. and Konings, W.N., 1999. Structure-function analysis of multidrug transporters in *Lactococcus lactis*. Biochimica Et Biophysica Acta-Biomembranes 1461, 201-206.

Van Wyk, B.E., de Wet, H. and Van Heerden, F.R., 2008. An ethnobotanical survey of medicinal plants in the southeastern Karoo, South Africa. South African Journal of Botany 74, 696-704.

VanVeen, H.W., Venema, K., Bolhuis, H., Oussenko, I., Kok, J., Poolman, B., Driessen, A.J.M. and Konings, W.N., 1996. Multidrug resistance mediated by a bacterial homolog of the human multidrug transporter MDR1. Proceedings of the National Academy of Sciences of the United States of America 93, 10668-10672.

Varma, M.V.S., Ashokraj, Y., Dey, C.S. and Panchagnula, R., 2003. P-glycoprotein inhibitors and their screening: a perspective from bioavailability enhancement. Pharmacological Research 48, 347-359.

Vicente, E., Lima, L.M., Bongard, E., Charnaud, S., Villar, R., Solano, B., Burguete, A., Perez-Silanes, S., Aldana, I., Vivas, L. and Monge, A., 2008. Synthesis and structure-activity relationship of 3-phenylquinoxaline 1,4-di-N-oxide derivatives as antimalarial agents. European Journal of Medicinal Chemistry 43, 1903-1910.

Viveiros, M., Jesus, A., Brito, M., Leandro, C., Martins, M., Ordway, D., Molnar, A.M., Molnar, J. and Amaral, L., 2005. Inducement and reversal of tetracycline resistance in *Escherichia coli* K-12 and expression of proton gradient-dependent multidrug efflux pump genes. Antimicrobial Agents and Chemotherapy 49, 3578-3582.

Viveiros, M., Martins, A., Paixao, L., Rodrigues, L., Martins, M., Couto, I., Fahnrich, E., Kern, W.V. and Amaral, L., 2008. Demonstration of intrinsic efflux activity of *Escherichia coli* K-12 AG100 by an automated ethidium bromide method. International Journal of Antimicrobial Agents 31, 458-462.

Voigt, B., Coburger, C., Monar, J. and Hilgeroth, A., 2007. Structure-activity relationships of novel N-acyloxy-1,4-dihydropyridines as P-glycoprotein inhibitors. Bioorganic & Medicinal Chemistry 15, 5110-5113.

Waako, P.J., Gumede, B., Smith, P. and Folb, P.I., 2005. The *in vitro* and *in vivo* antimalarial activity of *Cardiospermum halicacabum* L. and *Momordica foetida* Schumch. Et Thonn. Journal of Ethnopharmacology 99, 137-143.

Wakimoto, N., Yin, D., O'Kelly, J., Haritunians, T., Karlan, B., Said, J., Xing, H.T. and Koeffler, H.P., 2008. Cucurbitacin B has a potent antiproliferative effect on breast cancer cells *in vitro* and *in vivo*. Cancer Science 99, 1793-1797.

Wang, Y.-H., Joobeur, T., Dean, R.A., Staub, J., 2007. Cucurbits. In: C. Kole (Ed.), Genome Mapping and Molecular Breeding in Plants, Springer-Verlag, Berlin, Heidelberg, pp. 315-329.

Wells, T.N.C., Alonso, P.L. and Gutteridge, W.E., 2009. New medicines to improve control and contribute to the eradication of malaria. Nat. Rev. Drug Discov. 8, 879-891.

White, N.J., 2008. Qinghaosu (Artemisinin): The price of success. Science 320, 330-334.

WHO, 2008a. Traditional Medicines, Fact Sheet º 134. Geneve, Switzerland.

WHO, 2008b. World Malaria Report 2008. Geneve, Switzerland.

WHO, 2009. QUICK CANCER FACTS. Geneve, Switzerland.

WHO, 2010a. Fact sheet nº 94. Geneve, Switzerland.

WHO, 2010b. Guidelines for the treatment of malaria. Geneve, Switzerland.

Wiese, M. and Pajeva, I.K., 2001. Structure-activity relationships of multidrug resistance reversers. Current Medicinal Chemistry 8, 685-713.

Wilson, C.M., Serrano, A.E., Wasley, A., Bogenschutz, M.P., Shankar, A.H. and Wirth, D.F., 1989. Amplification of a gene related to mammalian *mdr* genes in drug-resistant *Plasmodium falciparum*. Science 244, 1184-1186.

Wirth, D.F., 2002. The parasite genome: Biological revelations. Nature 419, 495-496.

Wisedpanichkij, R., Chaijaroenkul, W., Sangsuwan, P., Tantisawat, J., Boonprasert, K. and Na-Bangchang, K., 2009. *In vitro* antimalarial interactions between mefloquine and cytochrome P450 inhibitors. Acta Tropica 112, 12-15.

Woodrow, C.J., Haynes, R.K. and Krishna, S., 2005. Artemisinins. Postgraduate Medical Journal 81, 71-78.

Wright, C.W., 2007. Recent developments in naturally derived antimalarials: Cryptolepine analogues. Journal of Pharmacy and Pharmacology 59, 899-904.

Wright, C.W., Addae-Kyereme, J., Breen, A.G., Brown, J.E., Cox, M.F., Croft, S.L., Gokcek, Y., Kendrick, H., Phillips, R.M. and Pollet, P.L., 2001. Synthesis and evaluation of cryptolepine analogues for their potential as new antimalarial agents. Journal of Medicinal Chemistry 44, 3187-3194.

Xu, R., Fazio, G.C. and Matsuda, S.P.T., 2004. On the origins of triterpenoid skeletal diversity. Phytochemistry 65, 261-291.

Yoshikawa, M., Hatakeyama, S., Tanaka, N., Fukuda, Y., Yamahara, J. and Murakami, N., 1993. Crude drugs from aquatic plants .1. On the constituents of Alismatis rhizoma .1. Absolute stereostructures of alisol-E 23-acetate, alisol-F, and alisol-G, 3 new protostane-

type triterpenes from chinese Alismatis rhizoma. Chemical & Pharmaceutical Bulletin 41, 1948-1954.

Yu, E.W., Aires, J.R. and Nikaido, H., 2003a. AcrB multidrug efflux pump of *Escherichia coli*: Composite substrate-binding cavity of exceptional flexibility generates its extremely wide substrate specificity. Journal of Bacteriology 185, 5657-5664.

Yu, E.W., McDermott, G., Zgurskaya, H.I., Nikaido, H. and Koshland, D.E., 2003b. Structural basis of multiple drug-binding capacity of the AcrB multidrug efflux pump. Science 300, 976-980.

Yuan, H.Y., Li, X., Wu, J.F., Li, J.P., Qu, X.J., Xu, W.F. and Tang, W., 2008. Strategies to overcome or circumvent P-glycoprotein mediated multidrug resistance. Current Medicinal Chemistry 15, 470-476.

Zhang, G.Q., Guan, Y.Y., Zheng, B., Wu, S. and Tang, L.H., 2008. No PfATPase6 S769N mutation found in *Plasmodium falciparum* isolates from China. Malaria Journal 7.

Zhang, M.X., Zhang, H.L., Sun, C.Y., Shan, X.L., Yang, X.L., Li-Ling, J. and Deng, Y.H., 2009. Targeted constitutive activation of signal transducer and activator of transcription 3 in human hepatocellular carcinoma cells by cucurbitacin B. Cancer Chemotherapy and Pharmacology 63, 635-642.

Zhou, S.F., Wang, L.L., Di, Y.M., Xue, C.C., Duan, W., Li, C.G. and Li, Y., 2008. Substrates and inhibitors of human multidrug resistance associated proteins and the implications in drug development. Current Medicinal Chemistry 15, 1981-2039.